Title

Stimulus-Cleavable Linkers for the Controlled Release of Bioactive Molecules: Therapeutic Proteins and Peptides

Author

Tan, Mikayla Ferrer

Publication Date

2023

Peer reviewed|Thesis/dissertation

UNIVERSITY OF CALIFORNIA

Los Angeles

Stimulus-Cleavable Linkers for the Controlled Release of Bioactive Molecules: Therapeutic Proteins and Peptides

A dissertation submitted in partial satisfaction of the

requirements for the Doctor of Philosophy

in Chemistry

by

Mikayla Ferrer Tan

2023

ABSTRACT OF THE DISSERTATION

Stimulus-Cleavable Linkers for the Controlled Release of Bioactive Molecules: Therapeutic Proteins and Peptides

by

Mikayla Ferrer Tan

Doctor of Philosophy in Chemistry

University of California, Los Angeles, 2023

Professor Heather Maynard, Chair

Proteins are ubiquitous in numerous pharmaceutical, technological, and industrial applications. However, these biomolecules are prone to stability issues due to internal and/or external stressors. One way to overcome such challenges is through the conjugation of polymers onto the surface of proteins. While protein-polymer conjugates have shown increased *in vivo* half-life and increased immunogenicity, reduction in activity has been observed due to either steric hindrance of polymers near the active site or changes to the protein's secondary structure. The use of traceless linkers to form protein-polymer conjugates allow for recovery of native protein, and thus restored protein activity upon exposure to a trigger. In this dissertation,

syntheses of protein-polymer conjugates and other drug systems incorporating such reversible linkages are presented.

Much work has been carried out over the years with the use of traceless linkages. In chapter 1, a mini literature review covering recent publications of the use of traceless linkages for protein and peptide applications is presented. These updates from the past few years will be incorporated into a comprehensive review the Maynard group plans to publish in *Bioconjugate Chemistry*. Chapters 2-4 will discuss the work carried out to synthesize protein-polymer conjugates *via* a heterobifunctional photocleavable linker, a type of traceless linker that responds to UV irradiation. In chapter 2, a new method to prepare noncovalent enzyme nanogels that utilizes a photocleavable monomer as a hybrid approach is reported. Photoirradiation cleaved the linkage between the polymer and protein to afford the poly((polyethylene glycol) methacrylate)-based noncovalent nanogels and enhanced enzyme activity. In chapter 3, the preparation of poly((polyethylene glycol) acrylate)-lysozyme (pPEGA-Lys) conjugates *via* a photocleavable linkage is presented. The conjugates were made by both *grafting-to* and *grafting-from* approaches. This work provided further evidence that reversing conjugation is successful for activity recovery for *ortho*-nitrobenzyl linked protein-polymer conjugates. Finally, in chapter 4, preliminary work towards the development of pNIPAM-based noncovalent enzyme nanogels and protein-polymer conjugates *via* a photocleavable linkage is discussed. This work aimed to demonstrate the versatility of the systems developed in Chapters 2 and 3.

The incorporation of traceless linkages has been applied to other applications beyond proteins and peptides. In chapter 5, the work towards scaling up an optimized abuse-deterrent opioid prodrug sequence is reported. Preparation of this material was carried out to allow for further biological studies.

The dissertation of Mikayla Ferrer Tan is approved.

Steven Clarke

Andrea Kasko

Paul Weiss

Heather D. Maynard, Committee Chair

University of California, Los Angeles

2023

This dissertation is dedicated to my family and friends,

especially my parents, Dennis and Bernadette Tan,

for their unwavering love and support.

TABLE OF CONTENTS

LIST OF ABBREVIATIONS

Abbreviation	Definition
AA	acrylic acid
ACN	acetonitrile
ACN	acetronitrile
AFM	atomic force microscopy
ANC	acrylamide-nitrobenzyl-carbonate
APS	tetramethylethylenediamine
ARGET	activator regenerated by electron transfer
ATRP	atom transfer radical polymerization
BCA	bicinchoninic acid
Cbz	carboxybenzyl
DAD	diode array detector
DCM	dichloromethane
DIPEA	diisopropylethylamine
DLS	dynamic light scattering
DMF	N-dimethylformamide
DMSO	dimethylsulfoxide
DSC	differential scanning calorimetry
EGDMA	ethylene glycol dimethacrylate
ENG	enzyme nanogels

ERT	enzyme replacement therapies
FDA	U.S. Department of Food and Administration
FPLC	fast protein liquid chromatography
GHR	growth-hormone receptor
HATU	hexafluorophosphate azabenzotriazole tetramethyl uronium
HBTU	hexafluorophosphate benzotriazole tetramethyl uronium
HPLC	high-performance liquid chromatography
IGF	insulin-growth factor
LCST	lower critical solution temperature
MALS	multiangle light scattering
MeOH	methanol
MWCO	molecular weight cut off
NHS	N-hydroxysuccinimide
NIPAM	N-isopropylacrylamide
NMR	nuclear magnetic resonance
PAL	phenylalanine ammonia lyase
PEG	polyethylene glycol
PEGMA	polyethylene glycol methacrylate
RAFT	reversible addition-fragmentation chain-transfer
RDRP	reversible-deactivation radical polymerization
ROMP	ring opening methathesis polymerization
SARA	supplemental activator and reducing agent
SDS PAGE	sodium dodecyl sulfate-polyacrylamide gel electrophoresis

SEC	size exclusion chromatography
TEM	transmission electron microscopy
TFA	trifluoroacetic acid
THF	tetrahydrofuran

LIST OF FIGURES

LIST OF TABLES

ACKNOWLEDGEMENTS

There are not enough words to express how truly grateful I am for all the support I have received over the years as I embarked on this journey.

First, I would like to thank Professor Heather Maynard for allowing me the opportunity to be a graduate student in her research group. She not only provided me with great scientific and professional mentorship; but, she has also taught me how to become more confident and to advocate for myself. I would also like to thank my doctoral committee members: Professor Steven Clarke, Professor Paul Weiss, and Professor Andrea Kasko for their advice and guidance during the major milestones of my graduate school studies. Although not directly involved in the development of my thesis, I would also like to thank Professor Ohyun Kwon for her mentorship during my summer rotation in 2018. It is through the work I did in her lab under Dr. Andy Smaligo that I was able to have my first publication (and in *Science!*). I would also like to thank Professor Jeffrey Sigman (Saint Mary's College of California), Professor Patricia Jackson (Saint Mary's College of California), and Professor Annaliese Franz (UC Davis) for their incredible mentorship over the years encouraging me to apply to UCLA for graduate school and celebrating with me all the accomplishments I have had since.

Next, I would like to thank all the Maynard group members that have been a part of my journey the past few years: Dr. Marco Messina, Dr. Kathryn Messina, Dr. Kyle Tamshen, Dr. Priera Panescu, Dr. Daniele Vinciguerra, Dr. Neil Forsythe, Dr. Doug Rose, Dr. Madeline Gelb, Dr. Jane Yang, Hayden Montgomery, Billy Treacy, Grace Kunkel, Ellie Puente, Haillie Lower, Felix Fu, Katie Snell, Elaine Chao, Brock Hosier, Dr. Pedro Salas, Dr. Theo Pesenti, Dr. Rajalakshmi Sivasankaran, Dr. Panos Georgiou, Nikolas Theopold, Arvind Bhattacharya, Kathleen Chen, Omar Ebrahim, and Jasper Aarts. All these individuals have been so supportive,

and I am so grateful to have worked alongside them. A very special thanks goes to Dr. Neil Forsythe for being an incredible mentor, role model, and friend.

During my time at UCLA, I have also had the great opportunity to be a part of the Organization for Cultural Diversity in the Sciences (OCDS). Thank you to my fellow OCDS members, past and present, for the amazing teamwork in our efforts to make the science community a more diverse, equitable, and inclusive environment. Thank you to my co-chair for the Outreach committee, Jordan Gonzalez, for helping me plan and hold our successful Fall and Spring showcases for undergraduate students.

As a graduate student at UCLA, I have also had to serve as a teaching assistant (TA) for several quarters. I would like to thank the instructors for the classes I taught: Dr. Amber Reilly, Dr. Daniel Nassrallah, Dr. Johnny Pang, and Dr. Laurence Lavelle. Thank you for helping me grow as a TA and reaffirm my passion for teaching.

Finally, I would like to thank all my family and friends who have shown nothing but endless love and support to me. Thank you to my freshmen year roommate at Saint Mary's, Vicky, for being a familiar face and piece of home down in SoCal as you embarked on your nursing degree in San Marcos. Thank you to my best friends Janelle and Kailey for visiting me and always finding time to listen to me rant about graduate school. Thank you to Madie and James for being great teammates on UCLA's Club Track team. As PhD students, you also understood the stresses I had over graduate school yet wanting to make sure I found time to maintain a healthy lifestyle and passion for running. A very special thanks to my boyfriend, Jon, who has been my rock and has taken care of me while I focused on school. Thank you for being my shoulder to cry on and making me laugh and smile, especially on days when research was taking a toll on me. Last, but not least, I would like to thank my sister, Megan, and my parents,

Dennis and Bernadette, for everything. I do not at all know how I would have been able to get through this PhD without the three of you. Thank you so much for always believing in me even when I doubted myself. Thank you for all the sacrifices you have made to help me pursue my graduate studies. I am eternally grateful.

For Chapter 1, I would like to thank the following publishers for the permission to reprint copyrighted material: Elsevier (reference 3a), American Chemical Society (references 7a, 25a, 26a, 36a), Royal Chemistry Society (references 17a, 32a, 33a), John Wiley and Sons (references 19a, 28a, 29a). Reprinted permission statements are detailed in the reference section of Chapter 1. Chapter 1 is a version of a review in preparation for publication: Rose, D., Tan, Mikayla F.., Vinciguerra, D., Panescu, P., Maynard, H. Traceless Linkers Used for Reversible Protein- and Peptide-Polymer Conjugates.

For Chapter 2, I would like to thank the UCLA Summer Mentored Research Fellowship for support. Chapter 2 is a version of the publication ‡Tan, M. F.; ‡Forsythe, N.L.; Vinciguerra, D.; Woodford, J.; Stieg, A. Z.; Maynard, H. D. “Noncovalent Enzyme Nanogels via a Photocleavable Linkage” *Macromolecules* **2022**, *55* (22), 9925-9933. Neil L. Forsythe. and I contributed equally to the manuscript. N.L.F., D.V., J.W., A.Z.S., and I conducted the experiments. H.D.M. oversaw the project and helped with data analysis. All authors contributed to writing of the paper. Only portions I contributed are herein presented.

For Chapter 3, I would like to thank the UCLA Dissertation Year Fellowship for support. Chapter 3 is a version of the publication ‡Tan, M. F.; Hosier, B.; Forsythe, N.L.; Maynard, H.D. “Enzyme-Polymer Conjugates via a Photocleavable Initiator for Control Over Protein Activity.” *Polymer Chemistry* xxxx, xx, xxxx-xxxx. Manuscript Submitted. Brock Hosier helped with the hydrolysis studies. Neil L. Forsythe helped with the development of the project. Heather D.

Maynard oversaw the project, helped with data analysis, and contributed to the writing of the paper.

For Chapter 5, I would like to thank Douglas Rose and Billy Treacy for the development of the synthesis. I would also like to thank Professors Chris Evans and Catherine Cahill and their undergraduate students for the work towards the biological studies.

The entirety of this dissertation was supported by the UCLA Dissertation Year Fellowship.

VITA

Education

University of California, Los Angeles, Los Angeles, CA — Expected: December 2023
Doctor of Philosophy in Chemistry
Area of Specialization: Chemical Biology

University of California, Los Angeles, Los Angeles, CA
Master of Science in Chemistry — Winter 2020
Candidate in Philosophy in Chemistry — Spring 2020

Saint Mary's College of California, Moraga, CA — Fall 2014 – Spring 2018
Bachelor of Science in Chemistry, Summa Cum Laude
Minor: Mathematics
Cumulative GPA: 3.959; Chemistry GPA: 3.973; Mathematics GPA: 4.000

Research Experience

PhD Researcher – University of California, Los Angeles — October 2018 – October 2023
Advisor: Professor Heather D. Maynard

- Prepared stimulus-responsive polymeric formulations and conjugates for the delivery of therapeutic proteins and peptides
- Designed new synthetic schemes for stimulus-responsive linkers with bioconjugation handles and carried out organic small molecule synthesis

Participant in NSF ChemEnergy REU Program – University of California, Davis — Summer 2017
Synthesis of a Model Compound for Lignin and Investigating Catalysts for Depolymerization

- Presented poster at the 225th ACS National Meeting in New Orleans Spring 2018

Participant in School of Science Summer Research Program – Saint Mary's College of California — Summer 2016
Evaluating the Importance of Salt Bridges in the Hinge-Bend Conformation of Neurolysin

- Presented at Saint Mary's School of Science Undergraduate Research Poster Session

Undergraduate Honors Research Projects – Saint Mary's College of California

- Honors Senior Thesis: *Undergraduate Lab Development: Emphasis on Green Chemistry* — Fall 2017
- Honors Contract: *Calibration of Pulsed-Field Gradient NMR with Network Polymer* — Spring 2017
- Honors Contract: *Synthesis and Spectroscopy of Conjugated Pi Systems* — Spring 2016

Publications

‡Tan, M. F.; Hosier, B.; Forsythe, N.L.; Maynard, H.D. "Enzyme-Polymer Conjugates via a Photocleavable Initiator for Control Over Protein Activity." *Polymer Chemistry* xxxx, xx, xxxx-xxxx. Manuscript Submitted.
‡Tan, M. F.; ‡Forsythe, N.L.; Vinciguerra, D.; Woodford, J.; Stieg, A. Z.; Maynard, H. D. "Noncovalent Enzyme Nanogels via a Photocleavable Linkage" *Macromolecules* **2022**, *55* (22), 9925-9933.
Forsythe, N. L.; Tan, M. F.; Maynard, H. D. "DiAzido Macrocyclic Sulfates as a Platform for the Synthesis of Hydrophilic, Sequence-Defined Oligomers for Antibody Drug Conjugates" *Chem. Sci.* **2022**, *13*, 3888-3893.
Smaligo, A. J.; Swain, M.; Quintana, J. C.; Tan, M. F.; Kim, D. A.; Kwon, O. "Hydrodealkenylative C(sp3)–C(sp2) bond fragmentation" *Science* **2019**, *364*, 681-685.

Conference and Symposium Presentations

1. "Noncovalent Enzyme Nanogels via a Photocleavable Linkage" (Talk) ‡**Tan, M. F**.; ‡Forsythe, N.L.; Vinciguerra, D.; Woodford, J.; Stieg, A. Z.; Maynard, H. D. University of California Chemical Symposium, April 2023.
2. "Noncovalent Enzyme Nanogels via a Photocleavable Linkage" (Poster) ‡**Tan, M. F**.; ‡Forsythe, N.L.; Vinciguerra, D.; Woodford, J.; Stieg, A. Z.; Maynard, H. D. UCLA Glenn T. Sigman Symposium, October 2022.
3. "Noncovalent Enzyme Nanogels via a Photocleavable Linkage" (Poster) ‡**Tan, M. F**.; ‡Forsythe, N.L.; Vinciguerra, D.; Woodford, J.; Stieg, A. Z.; Maynard, H. D. UCLA Glenn T. Seaborg Symposium, August 2022.

Teaching Experience

Middle School/High School Math and Science Teacher – A+ Tutoring Inc. Fall 2022 – Summer 2023

Graduate Student Teaching Assistant – University of California, Los Angeles Fall 2018 – Spring 2023

- Chemistry 30BL Organic Chemistry Laboratory I
- Chemistry 20L Introductory Organic Chemistry Laboratory
- 14A General Chemistry for Life Scientists

Leadership and Service

Co-outreach Coordinator for UCLA's Organization for Cultural Diversity in Science Fall 2020 – Spring 2023

- Organize a fall showcase for UCLA transfer students to familiarize with how to get undergraduate research positions
- Organize a spring showcase for community college applicants to learn about undergraduate research opportunities at UCLA
- Organizes smaller events throughout the school year for undergraduates to learn more about research and graduate school

Honors and Awards

Dissertation Year Fellowship Award Spring 2023
Summer Mentored Research Fellowship Fall 2021
Honorable Mention in NSF GFRP Spring 2020
Member of Phi Kappa Phi – Ranked in the top 10% of graduating class Spring 2017 – Spring 2018
Clare Boothe Luce Scholarship Fall 2016 – Spring 2018
RA Scholarship Award (LLC Science Mentor) Fall 2016 – Spring 2018
Robert W. and Beverly J. Summers Scholarship Summer 2016
Member of Saint Mary's College of California Honors Program Spring 2015 – Spring 2018

- Maintained 3.5 or higher GPA during first semester

Honors Entrance Scholarship Fall 2014 – Spring 2018
Presidential Scholars Program Fall 2014 – Spring 2018

Chapter 1 Updates on Traceless Linkers Used for Reversible Protein- or Peptide-Polymer Conjugates

1.1 Introduction

Proteins and peptides are ubiquitous in various pharmaceutical, technological, and industrial applications. Almost half of the 40 FDA novel drug approvals for 2023 are protein or peptide based.[1] THPdb is an online database that has been curated to list all FDA approved therapeutic protein and peptides.[2] While clearly becoming more popular, these biomolecules have had major challenges to overcome, such as stability issues due to several internal and external stressors that lead to short circulation times as well as a decrease in bioactivity. One of the best strategies that have been employed to overcome such challenges is through the conjugation of polymers onto the surface of the proteins and peptides. Fishburn *et al* wrote a review highlighting the effects that conjugation of polyethyleneglycol (PEG) has had on early FDA approved drugs.[3] Table 1 lists the pharmacokinetic and pharmacodynamic parameters of these conjugates.

Table 1.1 Comparative pharmacokinetic and pharmacodynamic parameters for PEGylated molecules and their parent unmodified drugs.[3a]

PEGylated Drug	**$t_{1/2}$ native (h)**	**$t_{1/2}$ PEGylated (h)**	**Activity Retained (%)**
Arginine deaminase	2.8	50	48
Superoxide dismutase	0.01	38	51
Granulocyte-colony stimulating factor (G-CSF)	1.8	7.0	41
Interferon alpha 2a (IFN-α2a)	0.7	51	7
Interleukin-6	0.05	48	51

Calcitonin	3.31	15.4	50
human Growth Hormone (hGH)	0.34	10	24

As shown above, the conjugation of PEG has drastically improved the half-lives of these proteins or peptides. However, a significant decrease in bioactivity was observed with these PEGylated drugs. Gauthier and coworkers wrote an excellent review discussing some of the challenges with the traditional conjugation of polymers onto proteins.[4] A common site of conjugation of PEG is the lysine residues of the proteins and peptides. Since there are an abundance of lysine residues on a protein or peptide, site-selective conjugation is quite challenging; topological control issues with the covalent attachment of the polymer can be observed leading to conformation changes and subsequent catalytic efficiency changes to the protein or peptide. Furthermore, conjugation of polymers may cause a steric hindrance near the active site of the protein or peptide leading to a decrease in catalytic turnover.

The use of traceless linkers, or linkers that cleave upon an internal or external stimulus such as changes in pH, redox properties, temperature, and light, is an effective strategy to increase the pharmacodynamics of proteins and peptides. The term "traceless" suggests that full or near full recovery of the native protein or peptide is recovered upon cleavage of the linker, which should therefore not cause much loss in bioactivity. We are currently in the process of submitting a review in *Bioconjugate Chemistry* to give an overview for the various types of traceless conjugation chemistries that can be applied in the development of protein-polymer or peptide-polymer drugs. The purpose of this short review is to highlight the work that has been done the past three years with regards to the incorporation of traceless linkers towards protein or peptide applications. These updates will be included in the ongoing review that is in preparation.

1.2. Lysine Modifications

As mentioned above, conjugation on lysine residues of a protein or peptide is a common site due to its abundance and ease in reactivity. For this reason, most traceless linker conjugation strategies have been developed for the modification and release of these groups. The different types of linkers are outlined below. It is important to note that there are other types of traceless lysine linkers that have been developed, but no new work on those have been reported based on my knowledge.

1.2.1 Anhydride Linkers

Recent work employing reversible anhydride linkers to drug delivery systems have been carried out to better target release in acidic conditions within the body. This has been studied extensively in the development of cancer treatments due to the acidic environments in and around tumors.[5] Liu and coworkers designed a pH-responsive hyaluronidase (HAse) delivery system that used a 3-(bromomethyl)-4-methyl-2,5-furadione linker in the formation of a dextran-based HAse nanoparticle. Upon entering areas of tumor accumulation, the protein would be released to degrade the extracellular matrix that is responsible for the irregular tumor microenvironment (TME). This hypothesis was supported when measuring the size of the nanoparticle and observing a rapid decrease in size when buffer exchanging the nanoparticles from pH 7.4 to pH 6.0. A measured increase in enzymatic activity upon buffer exchanging the nanoparticle in weakly acidic conditions *in vitro* further confirmed the controlled release of HAse. *In vivo* fluorescence images indicated a decrease in tumor vasculatures when treated with the Dex-HAse nanoparticles.[6] Overall, this work demonstrated the usefulness of the pH-responsive cleavable linker in the application of a therapeutic bioconjugate.

The same research group then applied the same methylmaleic anhydride linker in the preparation of blood-brain-barrier (BBB) crossing antibody-polymer conjugates that would release upon entering glioma tumors (Figure 1.1).[7] *In vivo* and *ex vivo* studies confirmed significant tumor damage upon treatment with such conjugates.

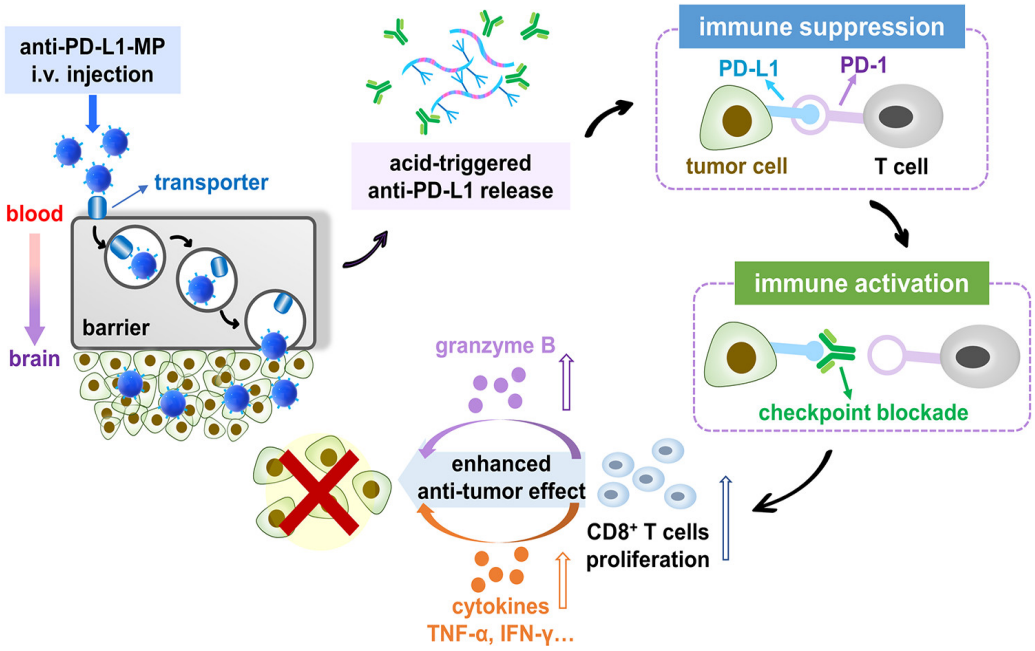

Figure 1.1 Schematic illustration of BBB-crossing anti-PD-L1 conjugates for enhanced glioma immunotherapy[7a].

Other types of therapies such as anticancer immunotherapy or enhanced cancer combination therapies have also been recently developed using the same reversible conjugation of biocompatible polymers or small molecule cancer drugs to various biologics.[8-11]

In addition to cancer treatment applications, the anhydride linkers have been applied to help in the design and improvement of other types of drug delivery vehicles. Kandil *et al*. have recently used a dimethylmaleic anhydride moiety to modify the peptide melittin in order to prepare an improved siRNA, polyethylenimine (PEI) delivery system with enhanced control of drug release in endosomal compartments.[12] Dynamic light scattering (DLS) and laser Doppler

anemometry analyses confirmed that in acidic conditions, the zeta potential of the polyplexes increased as a result of the unmasking of lysine residues on the peptide surface. This satisfies the hypothesis that there would be successful cleavage upon entering the endosome where the pH is in the range of 4.5-6.0.[13] Of particular interest is the synthesis of protein nanoparticles or nanogels utilizing a substituted maleic anhydride linker as therapeutic proteins are becoming more promising in medical applications.[14,15] In these final instances, model proteins myoglobin[14] and BSA[15] were employed to display potential in these drug delivery systems.

1.2.2 β-Mercaptocarbamate Linkers

Little work has been done the past couple years with the use of β-Mercaptocarbamate as a traceless linkage. However, this reversible linker has been used in reports of the synthesis of protein-polymer materials. The Nunh group used their previously developed work using the β-mercaptocarbamate linkage to redesign the synthesis of the amine reactive RAFT-polymer in a more efficient manner.[16] It was demonstrated by the group that protein-polymer hybrids with the self-immolative linker could still allow for the protein to be released upon exposure to reducing conditions with near full restoration. In another paper, stimuli-responsive protein nanogels were fabricated such that upon conjugation of the polymer to the protein, the traceless dithioethyl carbamate bonds were formed and cleaved when exposed to glutathione or dithiothreitol.[17]

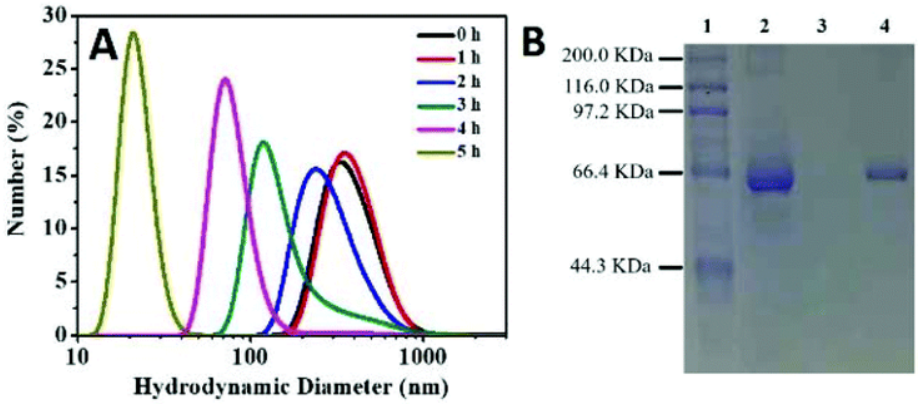

Figure 1.2 Nanogel characterization.

(A) Number-weighted size distribution of the BSA nanogel (N-B) after treatment in GSH solution at different times at 25 ℃. (B) SDS-PAGE results of the markers (lane 1), BSA + DTT (lane 2), N-B (lane 3), N-B + DTT (lane 4).[17a]

Upon introduction of the nanogel to a 10 mM solution of glutathione, DLS measurements of the nanogels were taken at regular time intervals. As can be seen in Figure 1.2A, the size of the nanogel decreased in size overtime indicating release of the protein. Additionally, SDS PAGE analysis indicates release of protein upon addition of DTT to the sample (Figure 1.2B). This work shows that while not the most popular choice for reversible conjugation, it has relevant use in the growing development for protein therapeutics.

1.2.3 1,6-Benzyl Carbamate Linkers

To date, this is still one of the most popular traceless linkers to incorporate in a system. The protecting group that is employed onto the phenol or aniline head group can easily be chosen according to what is most biologically relevant for the application. A recent example for the use of the reversible 1,6-benzyl carbamate linkage triggered by a disulfide reduction was reported by Ren *et al.*[18] Herein, they developed a vaccine nanoplatform using a block copolymer consisting

of the self-immolative linker and modifying it onto a micelle. Upon modification, the micelle self-assembled to capture short peptide antigens. In the presence of glutathione, the polymer disulfide bond was cleaved and thus, the antigens are released. Other triggers that can be integrated in the 1,6-benzyl carbamate linkers include ester hydrolysis and carbamate hydrolysis. However, no new work has been reported involving these types of triggers to the best of our knowledge.

Boronate reduction as a trigger for this type of self-immolative linker seems to be the most heavily explored particularly in the intracellular delivery for targeted cancer therapy. These types of traceless linkers are typically modified onto either proteins[19-22] r peptides[23,24] that will then be delivered into the cytosol of cancer cells. Upon entry, the biomolecule is released and restored as a result of the oxidation of the boronate groups from the reactive oxygen species, such as H_2O_2. For example, Zhao et al designed a carrier-free, cancer-selective protein delivery system in which proteins are first modified with a 4-nitrophenyl 4-(4,4,5,5-tetramethyl-1,3,2-dioxaborolan-2-yl) benzyl carbonate as an H_2O_2 responsive linker and then modified with a L-type amino acid transporter 1 (LAT1) substrate for direct transportation into cell membranes.[19] After *in vivo* antitumor efficacy studies with the conjugates, it was observed that tumor volume and size significantly decreased 12 days after the mice were treated with either the native protein

drug or the modified protein drug, thereby suggesting that this system improves the reduction in tumor growth (Figure 1.3).

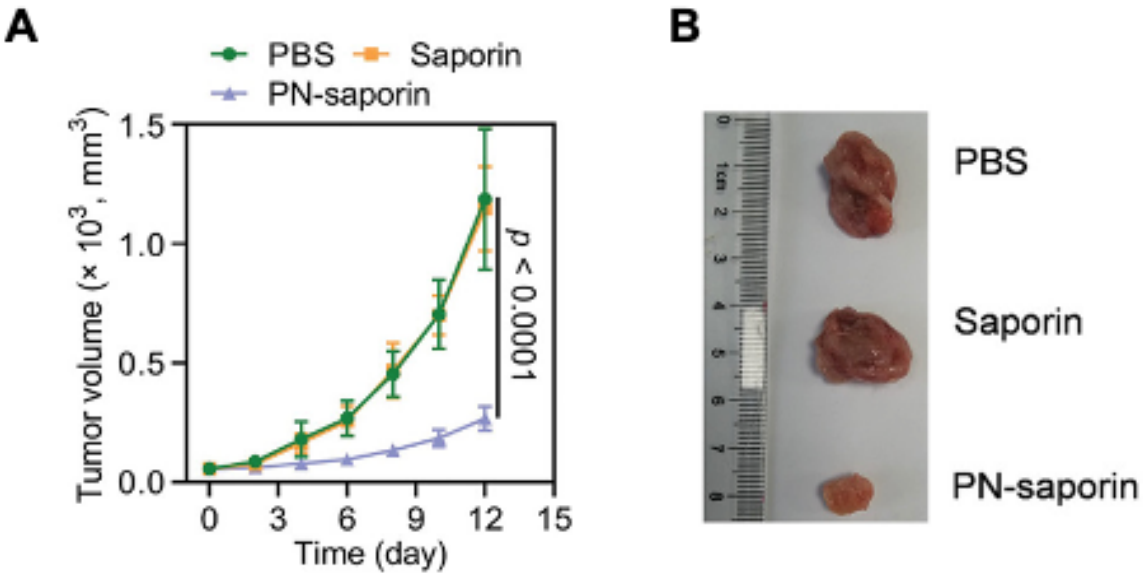

Figure 1.3 *In vivo* antitumor efficacy of PN-saporin against 4T1 xenograft tumors.

(A) Evolution of tumor volume (n = 10) (B) Representative images of tumors harvested on day 12.[19a]

Although this system is not polymer based, it does serve as a great proof-of-concept to incorporate this system into bioconjugates. For example, Rong et al utilized the same linker chemistry but in the development of polycatechol cargo peptide conjugates.[23]

Aside from cancer therapy, Xu *et al.* demonstrated the use of the 1,6-benzyl carbamate linker triggered by boronate reduction in the delivery of a polycaprolactone (PCL)-PEI insulin micelle for blood-glucose regulation in diabetes patients.[25] The general mechanism for the cleavage can be seen in Figure 1.4.

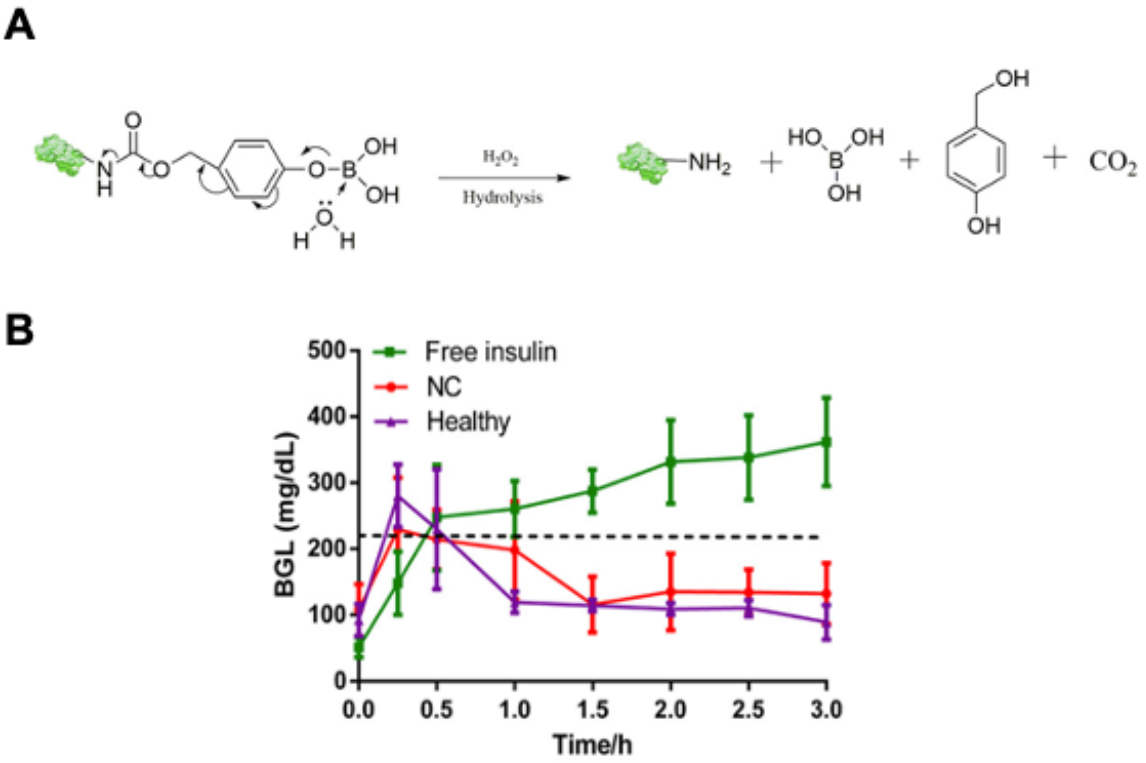

Figure 1.4 Redox-responsive insulin prodrug.

(A) Schematic Diagram of Insulin Prodrug in Response to H_2O_2 cleavage (B) IPGTT results in diabetic mice treated with free inulin and nanoconplex, using healthy rats as normal controls.

Intraperitoneal Glucose Tolerance Tests (IPGTT) were conducted on diabetic mice treated with either free insulin or the insulin conjugates and compared with healthy mice.[25a]

As is shown in the graph above (Figure 1.4B), blood glucose levels (BGL) seemed to decrease in a similar trend for the mice injected with the insulin conjugates as with the health mice, whereas the opposite trend in BGL was observed for the mice injected with free insulin. This confirms the glucose-responsive properties of the conjugate.

1.2.4 E1cB Linkers

Exciting work that has been done in the past few years using an E1cB linkers comes from our group reporting a new class of traceless linkers based on *ortho*- or *para*-hydroxybenzylamines. These linkers are stable in aqueous environments and can be conjugated to amines *via* reductive aminations on lysine and the N-terminal amine residue in a wide range of pH values. Compared to benzyl carbamate linkers, these linkers produce a secondary amine, thus maintaining the isoelectric point of the proteins. Once the protection group on the phenol is released (i.e. the pH is brought back to more neutral conditions in this scenario), the amine containing payload can be slowly released. (Figure 1.5). In this work, model enzyme lysozyme was used to demonstrate the usefulness of the self-immolative linker. It was determined that the protein conjugate loss approximately ~30% of its original activity; however, upon release of the linker, near full recovery of lysozyme activity is recovered.[26]

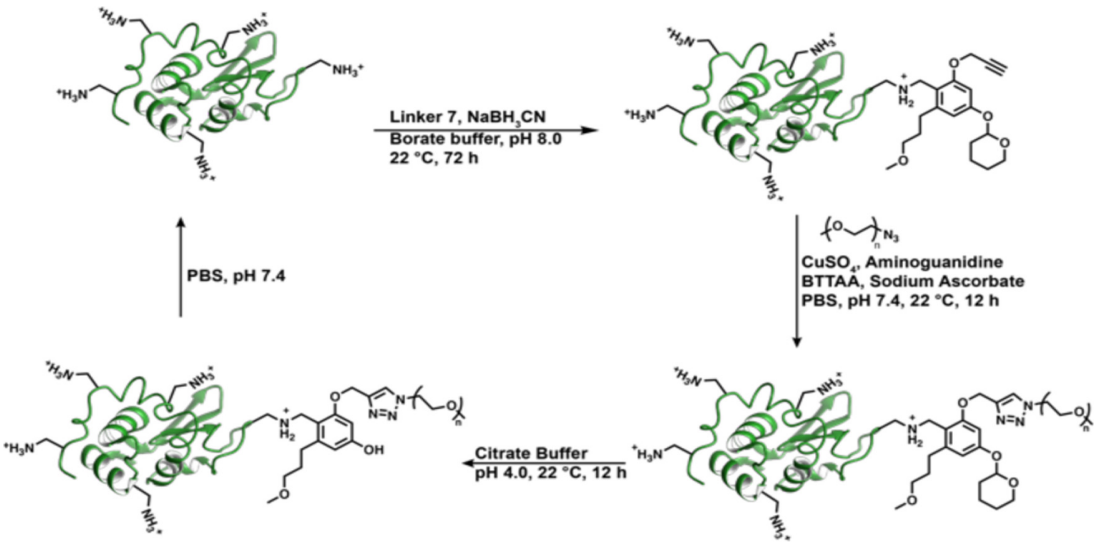

Figure 1.5 Representative stepwise protein conjugation scheme for the preparation of traceless mPEG-Lyz conjugate.[26a]

It is proposed that this strategy can have potential in future oral protein delivery or targeted drug delivery advancements. Our group is currently working on improving the system varying the electronics of the linker and the length of the attached polymer to tune the release rate of the payload.

1.2.5 Photocleavable Linkers

As will be shown in the later chapters of this dissertation, I have worked on traceless linker projects specifically incorporating a photocleavable linker for the development of protein-polymer conjugates. In my first paper published in *Macromolecules*, we synthesized noncovalent enzyme nanogels utilizing a heterobifunctional, photocleavable linker.[27] Herein it was demonstrated that upon irradiation of the protein nanogels with UV light enzymatic activity was restored as hypothesized. In a follow-up paper that is submitted for publication, I synthesized a photocleavable initiator that can be modified onto a protein of interest to prepare well-defined conjugates *via* a 'graft-to' or 'graft-from' approach. Both projects will be discussed more extensively in Chapters 2 and 3.

Yamaguchi and coworkers are another group that has been using photocleavable linkers but in the advancement of methods to study and control cellular functions. For example, they caged a cytotoxic protein saporin with biotin *via* a photocleavable, PEG-based linker and conjugated the modified protein with streptavidin to induce inactivation. Upon transduction into living cells and selective irradiation, they were able to introduce a spatio-temporal control of cell death (Figure 1.6)[28]

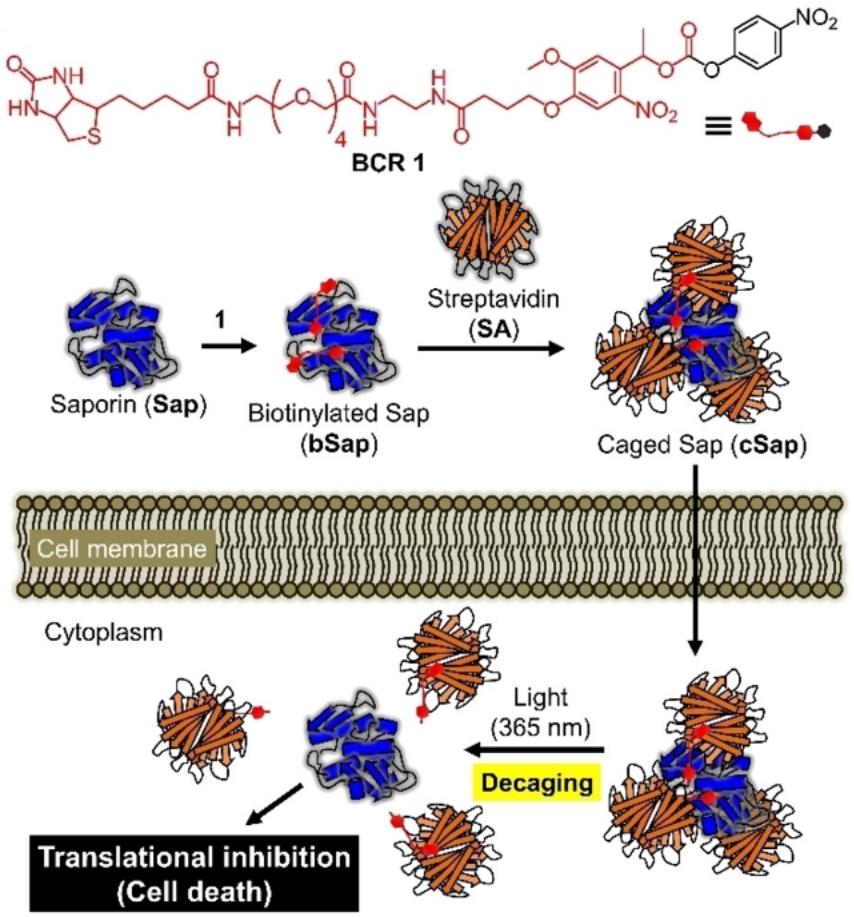

Figure 1.6 Schematic illustration of sterically bulky caged saporin and light-induced intracellular inactivation.[28a]

In another paper, Yamaguchi and coworkers prepared photodegradable protein-polymer hybrid shells and coated them onto mammalian cells to control their macrophage phagocytosis uptake and other cellular functions.[29] Phagocytosis experiments indicated that prior to light exposure, no cells seemed to be undergo any macrophage uptake as shown by the lack of green

fluorescence. However, after exposure to light, it was clear there was an uptake (Figure 1.7).

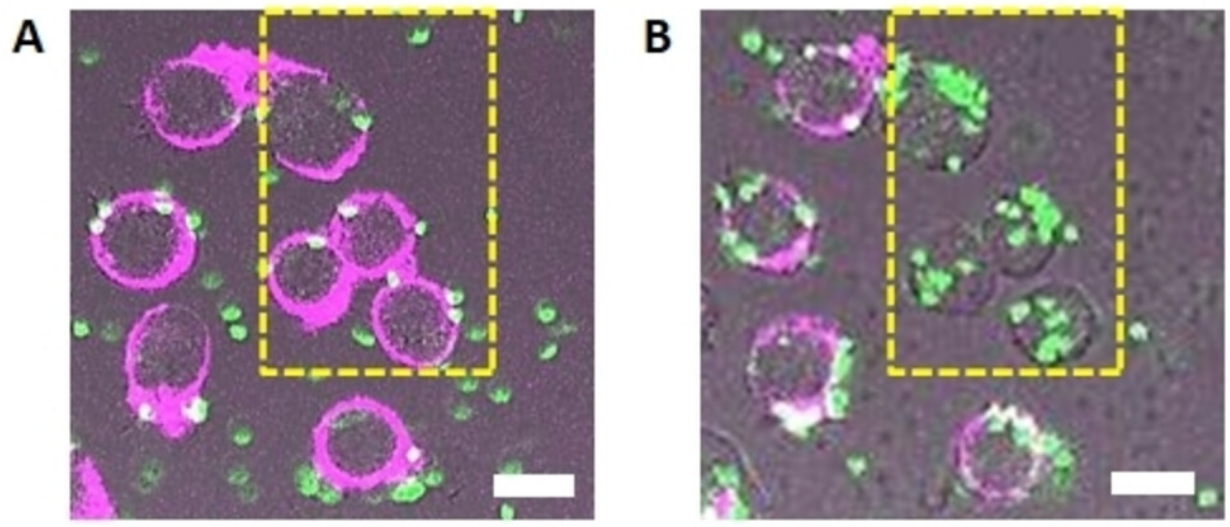

Figure 1.7 Light-induced control of cellular phagocytosis of the fluorescent beads**.**

Differential interference contrast images were taken (A) before and (B) after 20 minutes of light irradiation.[29a]

Certainly, this group has demonstrated that incorporation of photocleavable linkers in the development of bioconjugates can have a tremendous impact not only in a drug delivery setting but also in the studying complex biochemical processes.

1.3. Cysteine Modifications

Another common site of protein or peptide conjugation is the cysteine residue. Unlike lysine residues, cysteines are one of the least abundant residues found on proteins and peptides. This makes it an especially desirable site of modification to achieve higher site-selectivity. Below are listed recent reports in the development of traceless cysteine linkers in the past couple years. Due to the lack of variety in the cysteine linkers, no subcategories will be outlined in this section.

Retro-Michael addition linkers have been employed as traceless linkers for protein or peptide conjugates *via* both lysine modifications and cysteine modifications. However, no new work has been done with these linkers when modified to lysine residues. Herein, I will mention the current work being done with retro-Michael addition linkers when modified to the cysteine residues of biologics. One paper has been published in the past year using bromomaleimide derivatives for releasable conjugates. Chudasama and coworkers synthesized a trifunctional dibromomaleimide reagent for the modification of the disulfide bonds in trastuzumab. Two orthogonal clickable functional groups, one of which is PEG-based, were built into the reagent in order to increase drug-to-antibody ratios.[30] The same group reported the synthesis of other types of retro-Michael addition linkers, particularly dual-reactive reagents containing a 'stable-labile' design in which one side of the reagent can form a stable bond *via* a thioether with one cysteine residue and a labile bond *via* a thioester to another. This system was initially carried out to showcase a new opportunity to perform native chemical ligation (NCL) with N-terminal cysteines rather than the traditional use of C-terminal thioesters.[31] However, their approach was shown to also construct multifunctional antibody fragment conjugates which certainly can be of great interest for therapeutic applications.

Kalia and coworkers also explored the use of these type of linkers when developing a series of Michael addition elimination cyclization based turn-on fluorescence probes (MADELCY TOF) that selectively detect cysteine residues over other amino acids and biothiols (Figure 1.8).[32]

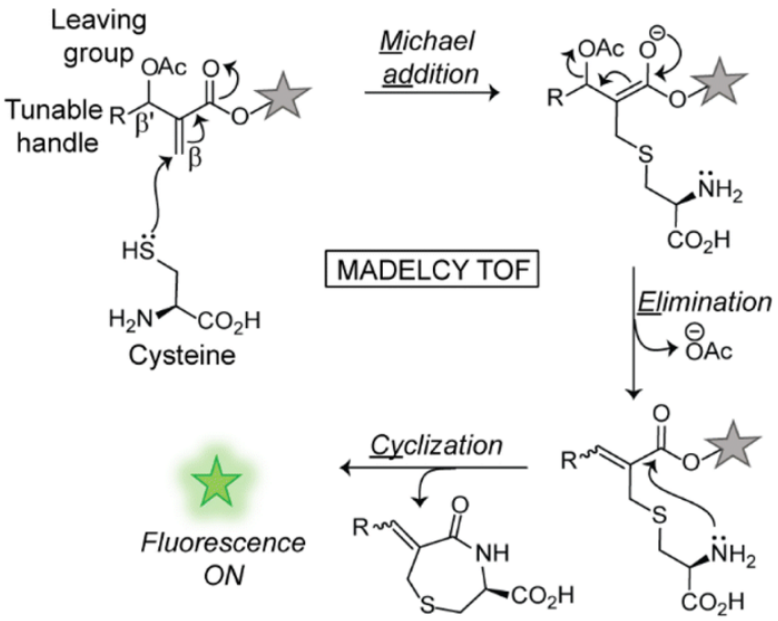

Figure 1.8 The Michael Addition-Elimination-Cyclization based Turn-On Fluorescence (MADELCY TOF) approach for selective Cys detection.[32a]

This was observed upon elimination of the leaving group and lactamization *via* the cysteinyl amine. The probe containing the 4-nitrophenyl group demonstrated rapid kinetics ($t_{1/2}$ = ~3 min) with excellent sensitivity with a detection limit of 8.2 nm towards Cys. Although no polymer is incorporated in this system, this work is promising for the study of oxidative stress levels for disease monitoring and new conjugates that can be developed in this application.

While cysteine modification with linkers *via* a Michael addition are generally irreversible, there are ways to tune the linkage such that reversible cleavage can occur. We previously mentioned the incorporation of leaving groups, such as bromine atoms, to maleimides as one popular method to induce a traceless release of the antibody. Maity *et al* very recently reported another strategy to reverse the modification of Michael addition-linkers to the cysteine residue of a protein. In their paper, human Cellular Retinol Binding Protein II (hCRBPII) was

labelled with a fluorescent ligand. Upon irradiation with UV light, the conjugation is reversed presumably through a retro-Michael addition process, yielding a fluorescent species (Figure 1.9).

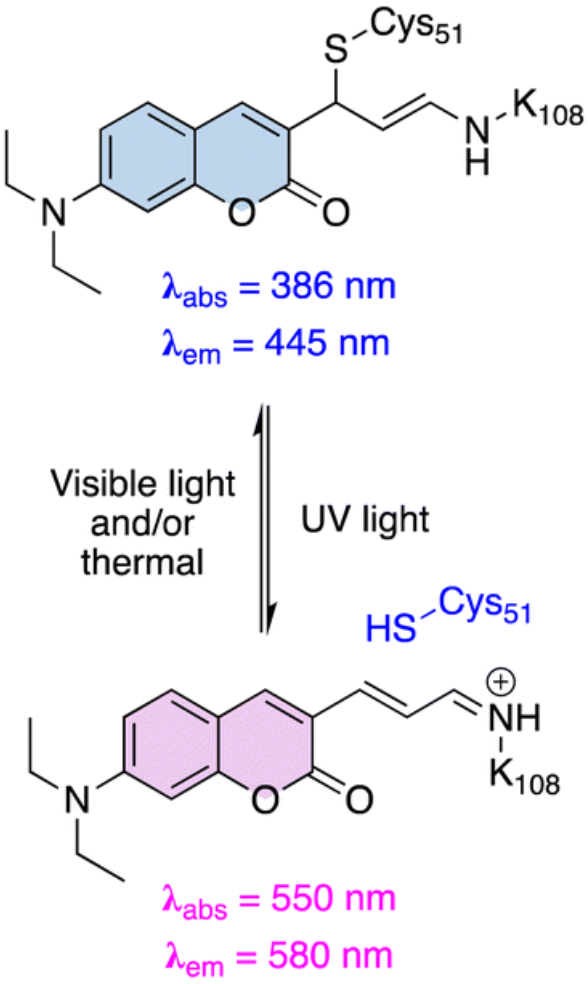

Figure 1.9 Reversible site-specific conjugation of cysteine.[33a]

This photoswitchable system enables better development of imaging and labeling of various proteins and can certainly be employed in future polymeric conjugates.[33]

1.4 Noncovalent Traceless Linkages

Most traceless linker strategies involve a temporary covalent linkage to the protein or peptide surface until cleaved upon a stimulus. These often require ambient reactions between the polymer and protein or peptide, followed by careful purification—all of which may lead to

inevitable loss in stability and activity of the biologic. For this reason, noncovalent conjugation strategies have also been developed for traceless linkage. These complexes are considered traceless if they can demonstrate reversibility upon an internal or external trigger.

1.4.1 Host-Guest Complexes

Webber and coworkers have continued to report of instances of using the host-guest complexation properties of curcubit[7]uril (CB) to proteins and peptides to prepare important biological conjugates. In collaboration with the Kramer group, it was demonstrated that instead of modification of PEG with CB zwitterionic polypeptide monofunctionalized with CB an inhibit aggregation when complexed to model peptides insulin and calcitonin.[34] Studies indicated that these conjugates were not cytotoxic. Furthermore, steady biodegradation was observed when conjugates were exposed to natural proteases, which is indicative of the eventual clearance of the protein additive unlike observed with PEG formulations. In another paper, Webber and coworkers synthesized multifunctional dendrimers in which one side of the molecule is modified with PEG-linked cholesterol to facilitate cell membrane integration and the other side of the molecule is modified with CB.[35] This demonstrates potential in increased control over cell imaging or cell-based therapies.

Other groups have also taken interest in the host-guest complexation. For example, Yang et al designed a new drug delivery system such that CB is coupled to a cyclic peptide that has a high binding affinity to low density lipoprotein receptors, which are more prevalent in cancer cells (Figure 1.10).[36]

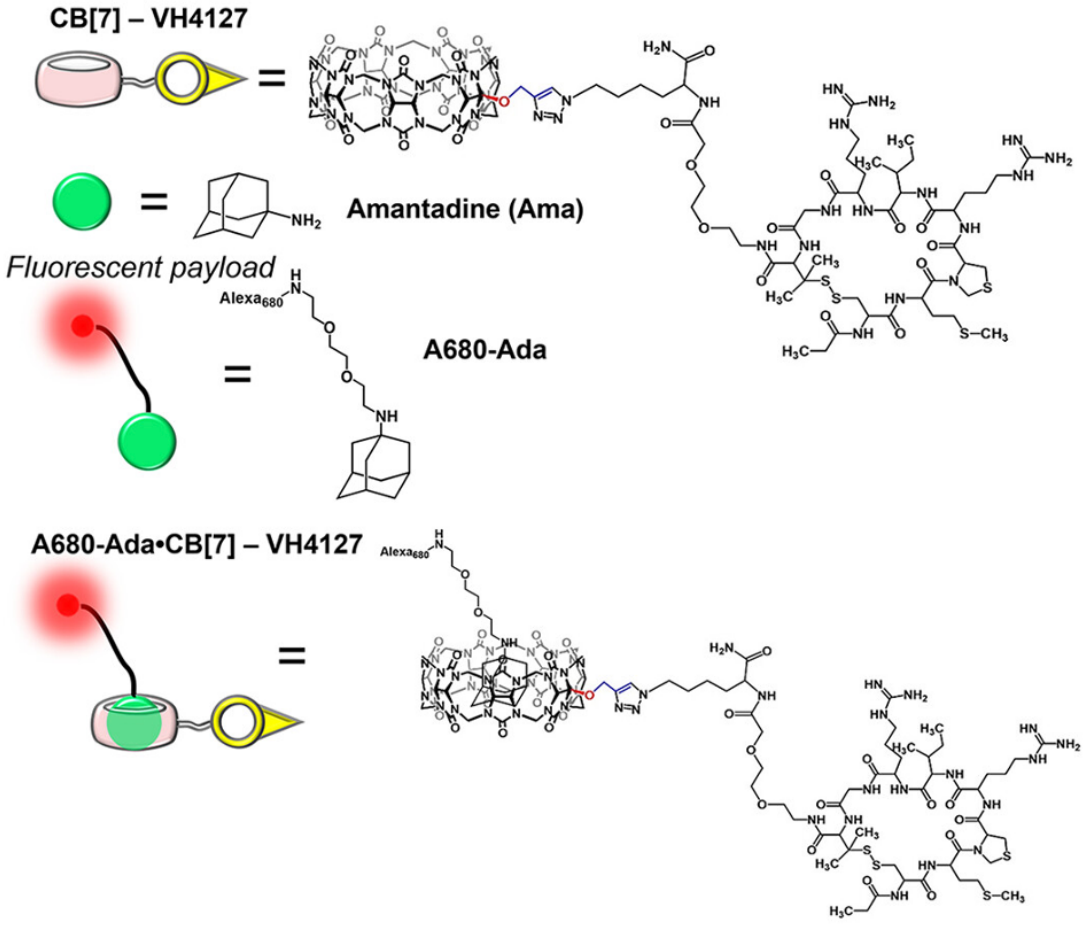

Figure 1.10 Illustration of the expected noncompetitive LDLR binding of CB vector conjugate allowing cell entry of different payloads by receptor-mediated transport.[36a]

Taking advantage of the host-guest complexations of CB may allow for another strategy to selectively deliver cargos of interests to the LDL proteins.

For a different application, Chen et al. utilized curcubit[8]uril to mediate the formation of heterodimers of different peptides. Herein, they demonstrated sufficient stabilization and on-demand release of insulin by complexing to a resin.[37]

While many groups have been interested in designing new types of conjugates with the host-guest complexation, recent work has been done to also improve the affinity in the

noncovalent interaction. More specifically, Meudom et al discovered that there would be a change in affinity between CB and peptides when introducing N-terminal substitutions to the peptide. Furthermore, it was determined that stimulus-responsive properties can be introduced to the host-guest interaction such as a pH-dependency or sugar concentration-dependency.[38] Overall, there seems to be a growing interest in the use of host-guest interactions for the formation of conjugates that can maintain similar bioactivity as the native counterparts.

1.4.2 Ionic Interactions

Not much work has been done with regards to other types of noncovalent linkages for traceless conjugation. However, there are a couple papers to note that have looked at better understanding the complexation properties between some polymers and proteins or peptides. For example, Simoncio et al sought to study the effects of co-solutes on complexation between BSA and sodium polystyrene sulfonates.[39] Vakili et al synthesized PEG analogs modified with different amino acids to study their interaction with hormone growth hormone and determine how physicochemical properties and protein stability are impacted by such groups.[40] These papers highlighting potential effects and mechanisms are crucial in the future development of novel traceless linkages based on any noncovalent interaction.

1.5 Future Outlook

This short review highlights the recent work that has been done regarding traceless linkers that are currently being used in reversible protein- or peptide-polymer conjugates. It is exciting to see these linkers being translated into research and products being developed at bigger pharmaceutical and biotechnological companies. For example, a couple months ago AbbVie published a preprint article reporting the use of a self-immolative carbamate linker in the development of antibody-drug conjugates that features a budesonide, a glucocorticoid receptor

agonist, payload.[41] We anticipate that as the field of bioconjugates continue to grow at such a rapid pace, the desire to include as well as advance traceless chemistries will become more prevalent.

References

(1) Research, C. for D. E. and. Novel Drug Approvals for 2023. *FDA* **2023**.

(2) Usmani, S. S.; Bedi, G.; Samuel, J. S.; Singh, S.; Kalra, S.; Kumar, P.; Ahuja, A. A.; Sharma, M.; Gautam, A.; Raghava, G. P. S. THPdb: Database of FDA-Approved Peptide and Protein Therapeutics. *PLOS ONE* **2017**, *12* (7), e0181748. https://doi.org/10.1371/journal.pone.0181748.

(3) Fishburn, C. S. The Pharmacology of PEGylation: Balancing PD with PK to Generate Novel Therapeutics. *J. Pharm. Sci.* **2008**, *97* (10), 4167–4183. https://doi.org/10.1002/jps.21278.

(3a) Reprinted from the Journal of Pharmaceutical Sciences, *97* (10), The Pharmacology of PEGylation: Balancing PD with PK to Generate Novel Therapeutics, 4167–4183, Copyright (2008), with permission from Elsevier.

(4) Gong, Y.; Leroux, J.-C.; Gauthier, M. A. Releasable Conjugation of Polymers to Proteins. *Bioconjug. Chem.* **2015**, *26* (7), 1172–1181. https://doi.org/10.1021/bc500611k.

(5) Zhang, X.; Lin, Y.; Gillies, R. J. Tumor pH and Its Measurement. *J. Nucl. Med.* **2010**, *51* (8), 1167–1170. https://doi.org/10.2967/jnumed.109.068981.

(6) Wang, H.; Han, X.; Dong, Z.; Xu, J.; Wang, J.; Liu, Z. Hyaluronidase with pH-Responsive Dextran Modification as an Adjuvant Nanomedicine for Enhanced Photodynamic-Immunotherapy of Cancer. *Adv. Funct. Mater.* **2019**, *29* (29), 1902440. https://doi.org/10.1002/adfm.201902440.

(7) Wang, H.; Chao, Y.; Zhao, H.; Zhou, X.; Zhang, F.; Zhang, Z.; Li, Z.; Pan, J.; Wang, J.; Chen, Q.; Liu, Z. Smart Nanomedicine to Enable Crossing Blood–Brain Barrier Delivery of Checkpoint Blockade Antibody for Immunotherapy of Glioma. *ACS Nano* **2022**, *16* (1), 664–674. https://doi.org/10.1021/acsnano.1c08120.

(7a) Reprinted (adapted) with permission from Wang, H.; Chao, Y.; Zhao, H.; Zhou, X.; Zhang, F.; Zhang, Z.; Li, Z.; Pan, J.; Wang, J.; Chen, Q.; Liu, Z. Smart Nanomedicine to Enable Crossing Blood–Brain Barrier Delivery of Checkpoint Blockade Antibody for Immunotherapy of Glioma. *ACS Nano* **2022**, *16* (1), 664–674. https://doi.org/10.1021/acsnano.1c08120. Copyright 2022 American Chemical Society.

(8) Zhao, Y.; Xie, Y.-Q.; Van Herck, S.; Nassiri, S.; Gao, M.; Guo, Y.; Tang, L. Switchable Immune Modulator for Tumor-Specific Activation of Anticancer Immunity. *Sci. Adv.* **2021**, *7* (37), eabg7291. https://doi.org/10.1126/sciadv.abg7291.

(9) Lyu, M.; Yazdi, M.; Lin, Y.; Höhn, M.; Lächelt, U.; Wagner, E. Receptor-Targeted Dual pH-Triggered Intracellular Protein Transfer. *ACS Biomater. Sci. Eng.* **2022**. https://doi.org/10.1021/acsbiomaterials.2c00476.

(10) Zhang, X.; Feng, L.; Dong, Z.; Xin, X.; Yang, Z.; Deng, D.; Wagner, E.; Liu, Z.; Liu, X. Protein-Drug Conjugate Programmed by pH-Reversible Linker for Tumor Hypoxia Relief and Enhanced Cancer Combination Therapy. *Int. J. Pharm.* **2020**, *582*, 119321. https://doi.org/10.1016/j.ijpharm.2020.119321.

(11) Melodia, D.; Di Pietro, Z.; Cao, C.; Stenzel, M. H.; Chapman, R. Traceless pH-Sensitive Antibody Conjugation Inspired by Citraconic Anhydride. *Biomacromolecules* **2022**, *23* (12), 5322–5329. https://doi.org/10.1021/acs.biomac.2c01125.

(12) Kandil, R.; Xie, Y.; Heermann, R.; Isert, L.; Jung, K.; Mehta, A.; Merkel, O. M. Coming in and Finding Out: Blending Receptor-Targeted Delivery and Efficient Endosomal Escape in a Novel Bio-Responsive siRNA Delivery System for Gene Knockdown in Pulmonary T Cells. *Adv. Ther.* **2019**, *2* (7), 1900047. https://doi.org/10.1002/adtp.201900047.

(13) Hu, Y.-B.; Dammer, E. B.; Ren, R.-J.; Wang, G. The Endosomal-Lysosomal System: From Acidification and Cargo Sorting to Neurodegeneration. *Transl. Neurodegener.* **2015**, *4* (1), 18. https://doi.org/10.1186/s40035-015-0041-1.

(14) Tao, A.; Huang, G. L.; Igarashi, K.; Hong, T.; Liao, S.; Stellacci, F.; Matsumoto, Y.; Yamasoba, T.; Kataoka, K.; Cabral, H. Polymeric Micelles Loading Proteins through Concurrent Ion Complexation and pH-Cleavable Covalent Bonding for In Vivo Delivery. *Macromol. Biosci.* **2020**, *20* (1), 1900161. https://doi.org/10.1002/mabi.201900161.

(15) Zhang, X.; Zhou, P.; Zhuo, S.; Zhang, F.; Yu, J.; Liu, X. Protein Nanogels with Enhanced pH-Responsive Dynamics Triggered by Remote NIR for Systemic Protein Delivery and Programmable Controlled Release. *Int. J. Pharm.* **2021**, *605*, 120833. https://doi.org/10.1016/j.ijpharm.2021.120833.

(16) Scherger, M.; Pilger, Y. A.; Komforth, P.; Räder, H.-J.; Nuhn, L. Reversible Polymer–Protein Functionalization by Stepwise Introduction of Amine-Reactive, Reductive-Responsive Self-Immolative End Groups onto RAFT-Derived Polymers. *ACS Biomater. Sci. Eng.* **2023**. https://doi.org/10.1021/acsbiomaterials.2c01106.

(17) Zhang, Y.; Zhang, D.; Wang, J.-T.; Zhang, X.; Yang, Y. Fabrication of Stimuli-Responsive Nanogels for Protein Encapsulation and Traceless Release without Introducing Organic Solvents, Surfactants, or Small-Molecule Cross-Linkers. *Polym. Chem.* **2021**, *12* (4), 554–563. https://doi.org/10.1039/D0PY01600D.

(17a) Used with permission of Royal Society of Chemistry, from Fabrication of Stimuli-Responsive Nanogels for Protein Encapsulation and Traceless Release without Introducing Organic Solvents, Surfactants, or Small-Molecule Cross-Linkers, Zhang, Y.; Zhang, D.; Wang,

J.-T.; Zhang, X.; Yang, Y., *12* (4), 2021; permission conveyed through Copyright Clearance Center, Inc.

(18) Ren, H.; Li, J.; Liu, G.; Sun, Y.; Yang, X.; Jiang, Z.; Zhang, J.; Lovell, J. F.; Zhang, Y. Anticancer Vaccination with Immunogenic Micelles That Capture and Release Pristine CD8+ T-Cell Epitopes and Adjuvants. *ACS Appl. Mater. Interfaces* **2022**, *14* (2), 2510–2521. https://doi.org/10.1021/acsami.1c18117.

(19) Zhao, Z.; Liu, X.; Hou, M.; Zhou, R.; Wu, F.; Yan, J.; Li, W.; Zheng, Y.; Zhong, Q.; Chen, Y.; Yin, L. Endocytosis-Independent and Cancer-Selective Cytosolic Protein Delivery via Reversible Tagging with LAT1 Substrate. *Adv. Mater.* **2022**, *34* (35), 2110560. https://doi.org/10.1002/adma.202110560.

(19a) Used with permission of John Wiley and Sons, from Endocytosis-Independent and Cancer-Selective Cytosolic Protein Delivery via Reversible Tagging with LAT1 Substrate, Zhao, Z.; Liu, X.; Hou, M.; Zhou, R.; Wu, F.; Yan, J.; Li, W.; Zheng, Y.; Zhong, Q.; Chen, Y.; Yin, L., *34* (35), 2022; permission conveyed through Copyright Clearance Center, Inc. © 2022 Wiley-VCH GmbH

(20) Liu, X.; Zhao, Z.; Wu, F.; Chen, Y.; Yin, L. Tailoring Hyperbranched Poly(β-Amino Ester) as a Robust and Universal Platform for Cytosolic Protein Delivery. *Adv. Mater.* **2022**, *34* (8), 2108116. https://doi.org/10.1002/adma.202108116.

(21) Tan, E.; Wan, T.; Yu, C.; Fan, Q.; Liu, W.; Chang, H.; Lv, J.; Wang, H.; Li, D.; Ping, Y.; Cheng, Y. ROS-Responsive Polypeptides for Intracellular Protein Delivery and CRISPR/Cas9 Gene Editing. *Nano Today* **2022**, *46*, 101617. https://doi.org/10.1016/j.nantod.2022.101617.

(22) Lu, R.; Zheng, Y.; Wang, M.; Lin, J.; Zhao, Z.; Chen, L.; Zhang, J.; Liu, X.; Yin, L.; Chen, Y. Reactive Oxygen Species-Responsive Branched Poly (β-Amino Ester) with Robust

Efficiency for Cytosolic Protein Delivery. *Acta Biomater.* **2022**, *152*, 355–366. https://doi.org/10.1016/j.actbio.2022.08.070.

(23) Rong, G.; Chen, L.; Zhu, F.; Tan, E.; Cheng, Y. Polycatechols with Robust Efficiency in Cytosolic Peptide Delivery via Catechol-Boronate Chemistry. *Nano Lett.* **2022**, *22* (15), 6245–6253. https://doi.org/10.1021/acs.nanolett.2c01810.

(24) Gao, X.; Yuan, C.; Tan, E.; Li, Z.; Cheng, Y.; Xiao, J.; Rong, G. Dual-Responsive Bioconjugates Bearing a Bifunctional Adaptor for Robust Cytosolic Peptide Delivery. *J. Controlled Release* **2023**, *355*, 675–684. https://doi.org/10.1016/j.jconrel.2023.02.014.

(25) Xu, X.; Ran, Y.; Huang, C.; Yin, Z. Glucose and H2O2 Dual-Responsive Nanocomplex Grafted with Insulin Prodrug for Blood Glucose Regulation. *Biomacromolecules* **2022**, *23* (4), 1765–1776. https://doi.org/10.1021/acs.biomac.2c00016.

(25a) Reprinted (adapted) with permission from Xu, X.; Ran, Y.; Huang, C.; Yin, Z. Glucose and H2O2 Dual-Responsive Nanocomplex Grafted with Insulin Prodrug for Blood Glucose Regulation. *Biomacromolecules* **2022**, *23* (4), 1765–1776. https://doi.org/10.1021/acs.biomac.2c00016. Copyright 2022 American Chemical Society.

(26) Rose, D. A.; Treacy, J. W.; Yang, Z. J.; Ko, J. H.; Houk, K. N.; Maynard, H. D. Self-Immolative Hydroxybenzylamine Linkers for Traceless Protein Modification. *J. Am. Chem. Soc.* **2022**, *144* (13), 6050–6058. https://doi.org/10.1021/jacs.2c01136.

(26a) Reprinted (adapted) with permission from Rose, D. A.; Treacy, J. W.; Yang, Z. J.; Ko, J. H.; Houk, K. N.; Maynard, H. D. Self-Immolative Hydroxybenzylamine Linkers for Traceless Protein Modification. *J. Am. Chem. Soc.* **2022**, *144* (13), 6050–6058. https://doi.org/10.1021/jacs.2c01136. Copyright 2022, American Chemical Society.

(27) Forsythe, N. L.; Tan, M. F.; Vinciguerra, D.; Woodford, J.; Stieg, A. Z.; Maynard, H. D. Noncovalent Enzyme Nanogels via a Photocleavable Linkage. *Macromolecules* **2022**, *55* (22), 9925–9933. https://doi.org/10.1021/acs.macromol.2c01334.

(28) Yamaguchi, S.; Yamamoto, K.; Yamamoto, R.; Takamori, S.; Ishiwatari, A.; Minamihata, K.; Nagamune, T.; Okamoto, A. Intracellular Protein Photoactivation Using Sterically Bulky Caging. *ChemBioChem* **2022**, *23* (22), e202200476. https://doi.org/10.1002/cbic.202200476.

(28a) Used with permission of John Wiley and Sons, from Intracellular Protein Photoactivation Using Sterically Bulky Caging. Yamaguchi, S.; Yamamoto, K.; Yamamoto, R.; Takamori, S.; Ishiwatari, A.; Minamihata, K.; Nagamune, T.; Okamoto, A. *23* (22), 2022, permission conveyed through Copyright Clearance Center, Inc. © 2022 Wiley-VCH GmbH

(29) Yamaguchi, S.; Chujo, K.; Ohashi, N.; Minamihata, K.; Nagamune, T. Photo-Degradable Protein-Polymer Hybrid Shells for Caging Living Cells. *Chem. – Eur. J.* **2022**, *28* (12), e202103941. https://doi.org/10.1002/chem.202103941.

(29a) Used with permission of John Wiley and Sons, from Photo-Degradable Protein-Polymer Hybrid Shells for Caging Living Cells., Yamaguchi, S.; Chujo, K.; Ohashi, N.; Minamihata, K.; Nagamune, T., *28* (12), 2022, permission conveyed through Copyright Clearance Center, Inc. © 2022 Wiley-VCH GmbH

(30) Zhao, Y.; Chudasama, V.; Baker, J. R. Trifunctional Dibromomaleimide Reagents Built Around A Lysine Scaffold Deliver Site-Selective Dual-Modality Antibody Conjugation. *ChemBioChem n/a* (n/a), e202300356. https://doi.org/10.1002/cbic.202300356.

(31) Chrzastek, A.; A. Thanasi, I.; A. Irving, J.; Chudasama, V.; R. Baker, J. Dual Reactivity Disulfide Bridging Reagents; Enabling New Approaches to Antibody Fragment Bioconjugation. *Chem. Sci.* **2022**, *13* (39), 11533–11539. https://doi.org/10.1039/D2SC04531A.

(32) Shakil Shaikh, D.; Parmar, S.; Kalia, D. Michael Addition–Elimination–Cyclization Based Turn-on Fluorescence (MADELCY TOF) Probes for Cellular Cysteine Imaging and Estimation of Blood Serum Cysteine and Aminoacylase-1. *Analyst* **2022**, *147* (17), 3876–3884. https://doi.org/10.1039/D2AN00713D.

(32a) Used with permission of Royal Society of Chemistry, from Michael Addition–Elimination–Cyclization Based Turn-on Fluorescence (MADELCY TOF) Probes for Cellular Cysteine Imaging and Estimation of Blood Serum Cysteine and Aminoacylase-1., Shakil Shaikh, D.; Parmar, S.; Kalia, D., *147* (17), 2022, permission conveyed through Copyright Clearance Center, Inc.

(33) Maity, S.; Bingham, C.; Sheng, W.; Ehyaei, N.; Chakraborty, D.; Tahmasebi-Nick, S.; E. Kimmel, T.; Vasileiou, C.; H. Geiger, J.; Borhan, B. Light Controlled Reversible Michael Addition of Cysteine: A New Tool for Dynamic Site-Specific Labeling of Proteins. *Analyst* **2023**, *148* (5), 1085–1092. https://doi.org/10.1039/D2AN01395A.

(33a) Used with permission of Royal Society of Chemistry, from Light Controlled Reversible Michael Addition of Cysteine: A New Tool for Dynamic Site-Specific Labeling of Proteins., Maity, S.; Bingham, C.; Sheng, W.; Ehyaei, N.; Chakraborty, D.; Tahmasebi-Nick, S.; E. Kimmel, T.; Vasileiou, C.; H. Geiger, J.; Borhan, B., *148* (5), 2023, permission conveyed through Copyright Clearance Center, Inc.

(34) Clauss, Z. S.; Meudom, R.; Su, B.; VandenBerg, M. A.; Saini, S. S.; Webber, M. J.; Chou, D. H.-C.; Kramer, J. R. Supramolecular Protein Stabilization with Zwitterionic Polypeptide–Cucurbit[7]Uril Conjugates. *Biomacromolecules* **2023**, *24* (1), 481–488. https://doi.org/10.1021/acs.biomac.2c01319.

(35) Gates, B. D.; Vyletel, J. B.; Zou, L.; Webber, M. J. Multivalent Cucurbituril Dendrons for Cell Membrane Engineering with Supramolecular Receptors. *Bioconjug. Chem.* **2022**, *33* (12), 2262–2268. https://doi.org/10.1021/acs.bioconjchem.2c00242.

(36) Yang, X.; Varini, K.; Godard, M.; Gassiot, F.; Sonnette, R.; Ferracci, G.; Pecqueux, B.; Monnier, V.; Charles, L.; Maria, S.; Hardy, M.; Ouari, O.; Khrestchatisky, M.; Lécorché, P.; Jacquot, G.; Bardelang, D. Preparation and In Vitro Validation of a Cucurbit[7]Uril-Peptide Conjugate Targeting the LDL Receptor. *J. Med. Chem.* **2023**, *66* (13), 8844–8857. https://doi.org/10.1021/acs.jmedchem.3c00423.

(36a) Reprinted (adapted) with permission from Yang, X.; Varini, K.; Godard, M.; Gassiot, F.; Sonnette, R.; Ferracci, G.; Pecqueux, B.; Monnier, V.; Charles, L.; Maria, S.; Hardy, M.; Ouari, O.; Khrestchatisky, M.; Lécorché, P.; Jacquot, G.; Bardelang, D. Preparation and In Vitro Validation of a Cucurbit[7]Uril-Peptide Conjugate Targeting the LDL Receptor. *J. Med. Chem.* **2023**, *66* (13), 8844–8857. https://doi.org/10.1021/acs.jmedchem.3c00423. Copyright 2023, American Chemical Society.

(37) Chen, X.; Huang, Z.; Sala, R. L.; McLean, A. M.; Wu, G.; Sokołowski, K.; King, K.; McCune, J. A.; Scherman, O. A. On-Resin Recognition of Aromatic Oligopeptides and Proteins through Host-Enhanced Heterodimerization. *J. Am. Chem. Soc.* **2022**, *144* (19), 8474–8479. https://doi.org/10.1021/jacs.2c02287.

(38) Meudom, R.; Zheng, N.; Zhu, S.; Jacobsen, M. T.; Cao, L.; Chou, D. H.-C. Expanding Peptide-Cucurbit[7]Uril Interactions through Selective N-Terminal Reductive Alkylation. *Curr. Res. Chem. Biol.* **2022**, *2*, 100013. https://doi.org/10.1016/j.crchbi.2021.100013.

(39) Simončič, M.; Lukšič, M. Modulating Role of Co-Solutes in Complexation between Bovine Serum Albumin and Sodium Polystyrene Sulfonate. *Polymers* **2022**, *14* (6), 1245. https://doi.org/10.3390/polym14061245.

(40) Vakili, S.; Chamani, J.; Amiri-Tehranizadeh, Z.; Hosseinzadeh, H.; Mosaffa, F.; Khatami, S.-M.; Khameneh, B.; Saberi, M. R. Amino Acid-mPEGs: Promising Excipients to Stabilize Human Growth Hormone against Aggregation. *Iran. J. Basic Med. Sci.* **2023**, *26* (6), 635–644. https://doi.org/10.22038/IJBMS.2023.67557.14804.

(41) Marvin, C.; Hobson, A.; McPherson, M.; Dunstan, T.; Vargo, T.; Hayes, M.; Fettis, M.; Bischoff, A.; Wang, L.; Wang, L.; Hernandez, Jr., A.; Jia, Y.; Oh, J.; Tian, Y. *Self-Immolative Carbamate Linkers for CD19-Budesonide Antibody-Drug Conjugates*; preprint; Chemistry, 2023. https://doi.org/10.26434/chemrxiv-2023-7lk43.

Chapter 2 Noncovalent Enzyme Nanogels via a Photocleavable Linkage

2.1 Introduction

Enzymes are utilized extensively in a scope of industries including the production of detergents, sensors, sweeteners, textiles, cosmetics, and pharmaceuticals.[1] For biocatalysis applications, the inherent specificity of enzymes along with their high turnover rates makes them attractive tools for the synthesis and production of structurally complex molecules. Furthermore, enzymes have also become increasingly important as therapeutics. For instance, enzyme replacement therapies (ERTs) are successful in treating a number of lysosomal storage diseases and immunodeficiencies.[2] While these enzymatic approaches to solving problems in both organic chemistry and medicine have many merits, the use of enzymes as such is not without their challenges.

Enzymes, like many proteins, are often unstable. External factors such as temperature, organic solvents, pH, mechanical agitation, proteases, and light can all lead to irreversible denaturation or inactivation of enzymes.[3] In both biocatalysis and ERT applications, these limitations are often prohibitive. Biocatalytic processes often require organic co-solvents, agitation, or temperature variation to support sufficient product formation, while in vivo application of therapeutic enzymes can suffer from immune-mediated clearance, protease degradation, and/or renal clearance. To combat this, a number of strategies have been developed to help increase enzyme stability. For instance, covalent attachment of functional polymers such as poly(ethylene glycol) (PEG), poly(N-(2-hydroxypropyl)methacrylamide), polysaccharide derivatives, and poly(N-isopropylacrylamide) have proved effective at increasing the stability of enzymes to stressors including heat, pH change, and protease degradation.[4,5] Beyond the direct conjugation of linear polymers, a variety of methods to increase enzyme stability have been

pursued, such as site-directed mutagenesis to remove degradation-prone regions from the protein structure,[6] covalent or noncovalent immobilization onto a matrix,[7,8] and direct encapsulation within nanoparticles, liposomes, or micelles.[9] Typically, immobilization and encapsulation favor larger complexes composed of multiple enzymes, which can constrain substrate diffusion and/or lead to protein aggregation. An approach that favors smaller sizes and individual encapsulation is enzyme nanogels (ENGs) that can offer greater colloidal stability for encapsulated proteins and controlled substrate diffusion.[10]

Fundamentally, the synthesis of ENGs involves the localization of monomers and crosslinkers around the surface of the protein followed by polymerization to yield a protective, polymeric shell.[11] First-generation nanogels involved covalent attachment of acryloyl groups to the lysine residues of the protein, followed by polymerization of acrylamide monomers.[12,13] This strategy has been effectively expanded to a number of enzymes including chymotrypsin,[14,15] carbonic anhydrase,[13,16] glucose oxidase,[17] green fluorescent protein,[18] and lipase.[19,20] While effective with all of these enzymes, this strategy does require the direct conjugation of monomers to surface residues of the protein, which can lead to a reduction in enzyme activity and even denaturation. To address these challenges, several approaches for noncovalent formation of ENGs have been developed. Gu et al. published a strategy wherein positively charged monomers are localized around a negatively charged protein.[21] Subsequent polymerization yielded nanogels without the need for covalent modification.[22-24] Beloqui et al. demonstrated an effective one-pot synthesis of noncovalent protein nanogels through the addition of sugar excipients such as sucrose.[25] While such noncovalent methods are effective, they rely on intramolecular/electrostatic interactions which inherently limit the pH range, proteins, or monomers that can be used in nanogel formation.

In this work, we present a method to form protein nanogels using a photocleavable monomer that temporarily takes advantages of covalent modification but ultimately allows the enzyme in the final ENG to be noncovalently bound. Conjugation of a bifunctional acrylamide-nitrobenzyl-carbonate (ANC) to lysine residues yields a polymerization handle on the protein surface linked through a photocleavable carbamate (Figure 2.1). Subsequent polymerization and photoirradiation with 365 nm produce the final noncovalent ENG.

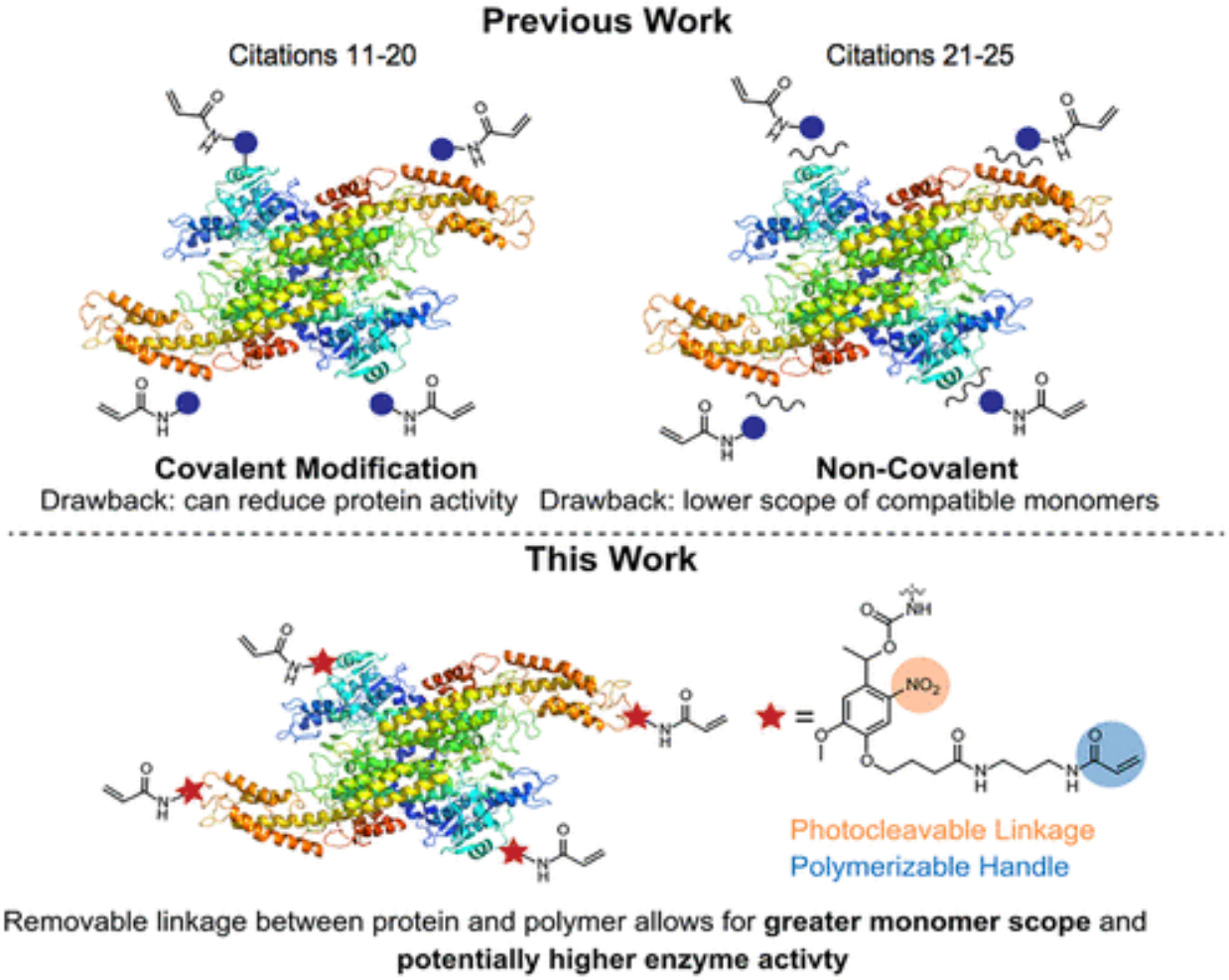

Figure 2.1 Comparison of strategies for the synthesis of ENGs.

To demonstrate the relevance and utility of this method, we encapsulated phenylalanine ammonia lyase (PAL), an enzyme used in the treatment of phenylketonuria. This disease is

characterized by the inability to process dietary phenylalanine, leading to an accumulation of the amino acid and resulting in cognitive impairment.[26] PAL has been shown to enzymatically transform phenylalanine into the natural metabolites *trans*-cinnamic acid and urea.[27] Studies have recently led to the development and FDA approval of a PEGylated variant of PAL, which is administered subcutaneously. While this drug is an excellent alternative to current treatments, its reliance on injection is inconvenient to patients. Further, this formulation presents added risk because it is bacterially derived and therefore can illicit an immune response.[28,29] Thus, a promising, alternative delivery of PAL is oral administration. However, the uniquely harsh environment of the digestive tract requires resistance to degradation at high concentrations of promiscuous proteases and low pH. Reported efforts to address these challenges include genetically engineered PAL via directed evolution[30] and encapsulation/adsorption of the enzyme onto membranes or other materials.[31-33] PAL also loses much of its activity when modified at its lysine residues.[34] As such, PAL represents a relevant model system to study because noncovalent encapsulation is required to maintain activity. Herein, we report the synthesis of non-covalently incorporated PAL nanogels with increased stability against the protease trypsin and low pH compared to the unencapsulated enzyme.

2.2 Results and Discussion

2.2.1 Synthesis and Characterization of Nanogels

Nanogel synthesis proceeded via polymerization followed by photocleavage (Figure 2.2A). Poly(ethylene glycol) methacrylate (PEGMA) was chosen as the monomer because of the known biocompatibility of the resulting polymer and its reported ability to protect proteins from protease degradation.[35,36] Free radical polymerization of PEGMA with ethylene glycol dimethacrylate (EGDMA) as a crosslinker was initiated by an ammonium persulfate (APS)/tetramethylethylenediamine initiator system. Complete incorporation of the acrylamide-modified PAL was confirmed by sodium dodecyl sulfate-polyacrylamide gel electrophoresis based on the absence of an unmodified protein band and a large molecular weight smear for the nanogels (Figure S2.1). Further validation of the polymerization was conducted via nuclear magnetic resonance (^{1}H NMR) wherein clearly identifiable peaks that correlate with the expected polymer backbone and side chains were observed (Figure S2.2). Fourier transform infrared analysis of the native enzyme and ENG confirmed the formation of the polymer by the appearance of a strong C–O–C stretch at 1079 cm^{-1} of the oligo(ethylene glycol) side chains and a C═O stretch at 1725 cm^{-1} (Figure S2.3) after polymerization. As expected, peaks distinct to the protein, for example, the C═O stretch at 1632 cm^{-1}, were also observed in the gel. The resulting nanogels were purified with spin desalting columns prior to analysis. The morphology of the synthesized nanogels appears to be principally spherical via transmission electron microscopy (TEM, Figure 2.2B).

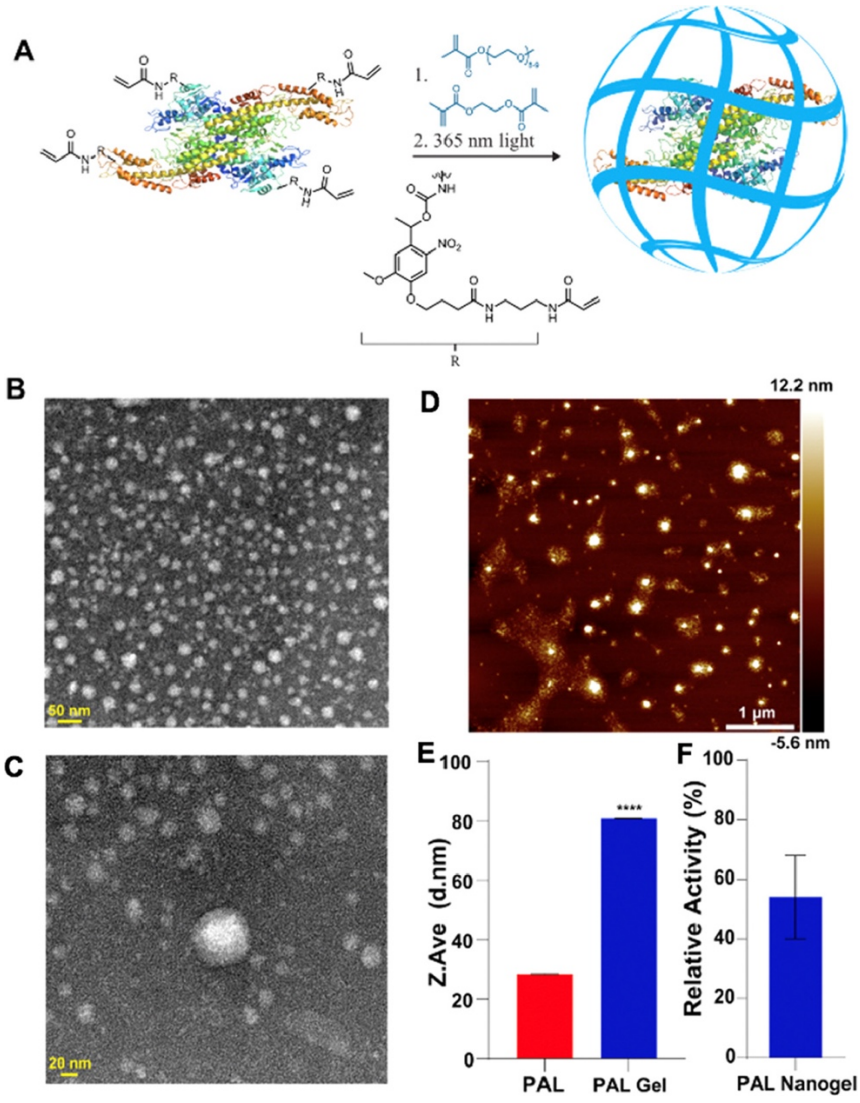

Figure 2.2 Synthesis of noncovalent PAL nanogels.

(A) Scheme for synthesis and photocleavage. Although the figure shows one PAL enzyme in the nanogel for simplicity, it is noted that multiple enzymes could possibly be encapsulated into a single nanogel. The synthesized nanogels post-irradiation were characterized by (B,C) TEM, (D) AFM, and (E) DLS. The activity of the nanogels (F) was measured via HPLC (n = 10).

Cross-sectional analysis of 70 independent particles by atomic force microscopy (AFM, Figure 2.2C) determined the particle size to be 76 nm (σ = 41 nm). Dynamic light scattering (DLS) showed an increase in size from a *Z*-average of 28 nm (unmodified PAL) to 80 nm (nanogel)

with PDIs of 0.53 and 0.46, respectively (Figure 2.2D), in agreement with size determination via AFM. It should be noted that both DLS and AFM characterization revealed larger clusters that likely include multiple enzymes within a single nanogel. As mentioned previously, following the polymerization, the nanogels were irradiated with 365 nm, 4 watt light for 15 min to remove the covalent linkage between the polymer and the enzyme. UV–vis analysis indicated that absorbance of the nanogel at this wavelength is negligible and would therefore not affect the photocleavage reaction (Figure S2.4). Given that it is possible that more than one PAL is encapsulated in a single gel, it was not possible to quantify the number of amines that were revealed upon exposure to 365 nm light. However, a fluorescamine assay was conducted to demonstrate a relative increase in fluorescence after irradiation of the PAL nanogels with UV light compared to that before irradiation, with UV light suggesting an expected recovery of lysine resides on the protein (Figure S2.5). Fluorescamine is a reagent that interacts with the primary amino groups of proteins to yield highly fluorescent derivatives.[37] Thus, we utilized this assay to qualitatively observe that functional amines increased after irradiation. The activity of the PAL in the nanogels was investigated by measuring change in absorbance at 290 nm after incubating with 4 mM phenylalanine for 2 h at 37 °C as adapted from McCallum and Walker.[38,39] It was not necessary to extend the length of the activity assay due to the enzyme reaching its steady state (Figure S2.6). The activity of the resulting noncovalent nanogels was 54 ± 14% compared to that of the unencapsulated PAL (Figure 2.2E). The activity of the nanogels before irradiation was considered negligible since no *trans*-cinnamic acid was detected.

2.2.2. Stabilization of Nanogels to Trypsin and pH

PEG nanogels are known to protect proteins from proteases.[40] In order to test this, the PAL nanogels were exposed to a range of trypsin concentrations that encompass the reported protease levels in the small intestine (0–40 μM).[41] Activity was measured by monitoring the increase in absorbance at 290 nm after 2 h of incubation; this corresponds to the concentration of *trans*-cinnamic acid and thus enzymatic activity. In this assay (Figure 2.3A), the PEG nanogel stabilizes PAL, as the activity is higher than PAL alone for trypsin concentrations equal to and above 0.25 μM. Furthermore, the nanogel maintained 34% of its original activity at a trypsin concentration of 52 μM, which is above the reported physiological concentration of trypsin. In contrast, unmodified PAL shows no measurable activity under identical conditions. Due to time-consuming nature of these experiments (where each single point represented a newly synthesized nanogel), this dose-response study could not feasibly be done in replicates. To compensate and verify results, we measured the PAL gel versus PAL activity at a single trypsin concentration against a *trans*-cinnamic acid standard via high-performance liquid chromatography (HPLC). In this assay, the nanogel achieved a statistically significant improvement in total enzymatic output over the 2 h exposure to 7.5 μM trypsin (Figure 2.3B).

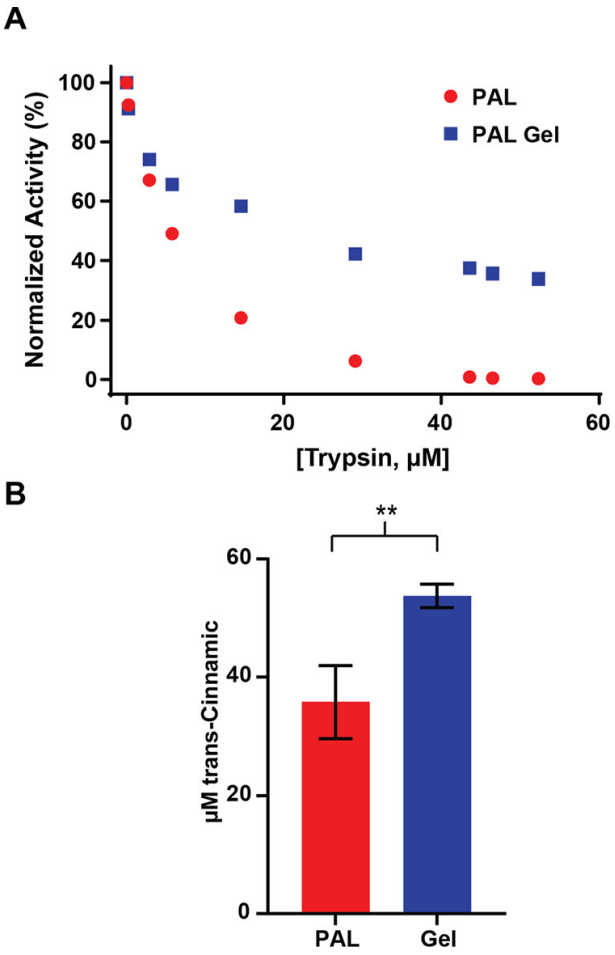

Figure 2.3 Trypsin stress test.

(A) Normalized dose response stabilization of nanogels against trypsin as measured by an increase in A290. Each blue data point represents an individually synthesized batch of nanogel. B) Total production of trans-cinnamic acid produced after 2 h in the presence of 7.5 µM trypsin. Concentration determination was determined via HPLC (n = 3).

The crosslinking density of the nanogel was then altered to determine its effect on protein stabilization to trypsin. We initially hypothesized that a greater molar equivalence ratio of crosslinker to monomer would increase the stability of PAL to trypsin as it would be more sterically protected from being degraded by the protease. To test this, PAL nanogels were synthesized with a range of crosslinking ratios starting from a 48:0 monomer to crosslinker

molar equivalence ratio to a 48:36 monomer to crosslinker molar equivalence ratio. The total concentration of monomer and crosslinker was maintained to allow for insignificant changes in polymerization kinetics. All nanogels were exposed to 6 μM trypsin, and activity was measured as done previously. As predicted, zero crosslinking density did not protect the protein from trypsin degradation (Figure S2.7). Stability was positively correlated with an increase in crosslinking molar equivalences until a 48:10 monomer to crosslinker ratio. Higher crosslinking density seemed to have no significant increase in protein stability, although further studies can be conducted to optimize the system toward other proteases such as pepsin.

Another major obstacle in the delivery of therapeutic enzymes by oral administration is the harsh conditions of the low pH in the stomach. The acidic environment can destabilize the protein due to hydrolysis. To test the ability of the nanogel to stabilize the protein, PAL nanogels were first buffer exchanged into a pH 3.5 buffer to mimic the stomach fluid (during eating) before introduction of phenylalanine to initiate the activity assay. After 0.5 h from the addition of phenylalanine, the nanogels were either maintained at pH 3.5 or allowed to be brought up to pH 7.8, which is the optimal pH for PAL activity. Activity was measured as described above monitoring an increase in absorbance at 290 nm. In this assay (Figure 2.4), the PAL nanogels subjected to a low pH maintained a higher activity percentage than PAL alone subjected to the

same pH of 3.5. This result supports that the nanogel stabilized the microenvironment for the enzyme, thereby increasing its tolerance to low pH.

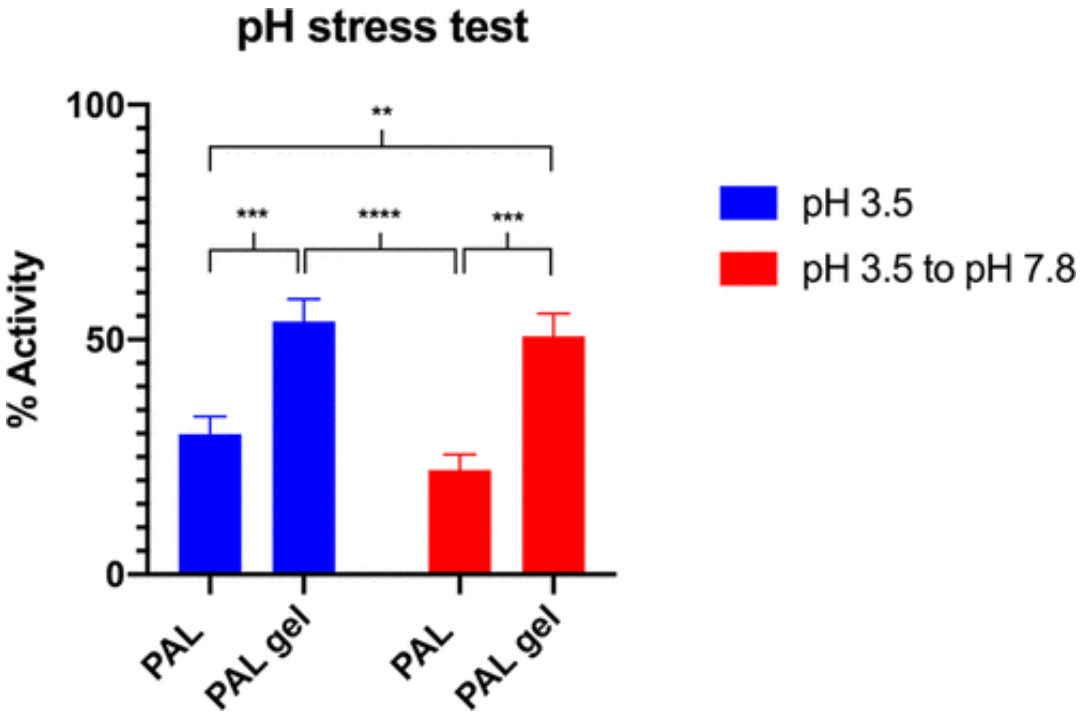

Figure 2.4 Low pH stress test.

Normalized stabilization of nanogels against low pH of 3.5 measured by an increase in A290. The activities of the PAL samples were measured via a plate reader assay. Each measurement was conducted in triplicate, and statistical significance was determined via a two-way ANOVA with multiple comparisons (** = $p \leq 0.001$, *** = $p \leq 0.0005$, **** = $p < 0.0001$). Normalization was done by comparing all samples against an unmodified PAL control measuring activity at pH 7.8.

2.3 Conclusions

Encapsulation of enzymes in nanogels is an excellent method to protect and deliver proteins for the treatment of metabolic diseases. Herein, we report a new strategy for synthesizing noncovalent ENGs that rely on a bifunctional ANC linkage between the lysine

residues of the enzyme and polymer. PEGMA was polymerized in the presence of the modified PAL enzyme and a crosslinker to form nanogels as determined by DLS, AFM, and TEM. Subsequent UV irradiation liberated PAL from covalent immobilization, allowing for enhanced enzyme activity.

The synthesized nanogels confer PAL the ability to resist trypsin and low pH degradation, indicating the potential utility of these PAL ENGs for oral administration. Since phenylalanine is a nonessential amino acid and is thus only introduced to the body by food, delivery of PAL ENGs could be useful by an oral route, taken at the same time as meal consumption. These ENGs may be further tuned to meet desired properties depending on the application. For example, other monomer systems such as *N*-isopropylacrylamide-*co*-acrylic acid could be used to prepare a nanogel that can control swelling of gel according to pH, temperature, or other stimuli. Furthermore, this proof-of-concept work could be potentially employed with a variety of other therapeutic enzymes for protein delivery applications.

2.4 References

(1) Gurung, N.; Ray, S.; Bose, S.; Rai, V. A Broader View: Microbial Enzymes and Their Relevance in Industries, Medicine, and Beyond. *BioMed Res. Int.* **2013**, *2013*, e329121. https://doi.org/10.1155/2013/329121.

(2) Desnick, R. J.; Schuchman, E. H. Enzyme Replacement and Enhancement Therapies: Lessons from Lysosomal Disorders. *Nat. Rev. Genet.* **2002**, *3* (12), 954–966. https://doi.org/10.1038/nrg963.

(3) Silva, C.; Martins, M.; Jing, S.; Fu, J.; Cavaco-Paulo, A. Practical Insights on Enzyme Stabilization. *Crit. Rev. Biotechnol.* **2018**, *38* (3), 335–350. https://doi.org/10.1080/07388551.2017.1355294.

(4) A. Gauthier, M.; Klok, H.-A. Polymer – Protein Conjugates: An Enzymatic Activity Perspective. *Polym. Chem.* **2010**, *1* (9), 1352–1373. https://doi.org/10.1039/C0PY90001J.

(5) A. Wright, T.; C. Page, R.; Konkolewicz, D. Polymer Conjugation of Proteins as a Synthetic Post-Translational Modification to Impact Their Stability and Activity. *Polym. Chem.* **2019**, *10* (4), 434–454. https://doi.org/10.1039/C8PY01399C.

(6) Nisthal, A.; Wang, C. Y.; Ary, M. L.; Mayo, S. L. Protein Stability Engineering Insights Revealed by Domain-Wide Comprehensive Mutagenesis. *Proc. Natl. Acad. Sci.* **2019**, *116* (33), 16367–16377. https://doi.org/10.1073/pnas.1903888116.

(7) Liu, Y.; Yu, J. Oriented Immobilization of Proteins on Solid Supports for Use in Biosensors and Biochips: A Review. *Microchim. Acta* **2016**, *183* (1), 1–19. https://doi.org/10.1007/s00604-015-1623-4.

(8) Mohamad, N. R.; Marzuki, N. H. C.; Buang, N. A.; Huyop, F.; Wahab, R. A. An Overview of Technologies for Immobilization of Enzymes and Surface Analysis Techniques for Immobilized Enzymes. *Biotechnol. Biotechnol. Equip.* **2015**, *29* (2), 205–220. https://doi.org/10.1080/13102818.2015.1008192.

(9) Chapman, R.; Stenzel, M. H. All Wrapped up: Stabilization of Enzymes within Single Enzyme Nanoparticles. *J. Am. Chem. Soc.* **2019**, *141* (7), 2754–2769. https://doi.org/10.1021/jacs.8b10338.

(10) Li, C.; Obireddy, S. R.; Lai, W.-F. Preparation and Use of Nanogels as Carriers of Drugs. *Drug Deliv.* **2021**, *28* (1), 1594–1602. https://doi.org/10.1080/10717544.2021.1955042.

(11) Jia, X.; Wang, L.; Du, J. In Situ Polymerization on Biomacromolecules for Nanomedicines. *Nano Res.* **2018**, *11* (10), 5028–5048. https://doi.org/10.1007/s12274-018-2080-2.

(12) Yan, M.; Ge, J.; Liu, Z.; Ouyang, P. Encapsulation of Single Enzyme in Nanogel with Enhanced Biocatalytic Activity and Stability. *J. Am. Chem. Soc.* **2006**, *128* (34), 11008–11009. https://doi.org/10.1021/ja064126t.

(13) Yan, M.; Liu, Z.; Lu, D.; Liu, Z. Fabrication of Single Carbonic Anhydrase Nanogel against Denaturation and Aggregation at High Temperature. *Biomacromolecules* **2007**, *8* (2), 560–565. https://doi.org/10.1021/bm060746a.

(14) Hegedűs, I.; Nagy, E. Improvement of Chymotrypsin Enzyme Stability as Single Enzyme Nanoparticles. *Chem. Eng. Sci.* **2009**, *64* (5), 1053–1060. https://doi.org/10.1016/j.ces.2008.10.063.

(15) Kim, J.; Jia, H.; Lee, C.; Chung, S.; Kwak, J. H.; Shin, Y.; Dohnalkova, A.; Kim, B.-G.; Wang, P.; Grate, J. W. Single Enzyme Nanoparticles in Nanoporous Silica: A Hierarchical Approach to Enzyme Stabilization and Immobilization. *Enzyme Microb. Technol.* **2006**, *39* (3), 474–480. https://doi.org/10.1016/j.enzmictec.2005.11.042.

(16) Yadav, R.; Labhsetwar, N.; Kotwal, S.; Rayalu, S. Single Enzyme Nanoparticle for Biomimetic CO2 Sequestration. *J. Nanoparticle Res.* **2011**, *13* (1), 263–271. https://doi.org/10.1007/s11051-010-0026-z.

(17) Liu, Y.; Du, J.; Yan, M.; Lau, M. Y.; Hu, J.; Han, H.; Yang, O. O.; Liang, S.; Wei, W.; Wang, H.; Li, J.; Zhu, X.; Shi, L.; Chen, W.; Ji, C.; Lu, Y. Biomimetic Enzyme Nanocomplexes and Their Use as Antidotes and Preventive Measures for Alcohol Intoxication. *Nat. Nanotechnol.* **2013**, *8* (3), 187–192. https://doi.org/10.1038/nnano.2012.264.

(18) Yan, M.; Du, J.; Gu, Z.; Liang, M.; Hu, Y.; Zhang, W.; Priceman, S.; Wu, L.; Zhou, Z. H.; Liu, Z.; Segura, T.; Tang, Y.; Lu, Y. A Novel Intracellular Protein Delivery Platform Based on

Single-Protein Nanocapsules. *Nat. Nanotechnol.* **2010**, *5* (1), 48–53. https://doi.org/10.1038/nnano.2009.341.

(19) Ge, J.; Lu, D.; Wang, J.; Yan, M.; Lu, Y.; Liu, Z. Molecular Fundamentals of Enzyme Nanogels. *J. Phys. Chem. B* **2008**, *112* (45), 14319–14324. https://doi.org/10.1021/jp8053923.

(20) Ge, J.; Lu, D.; Wang, J.; Liu, Z. Lipase Nanogel Catalyzed Transesterification in Anhydrous Dimethyl Sulfoxide. *Biomacromolecules* **2009**, *10* (6), 1612–1618. https://doi.org/10.1021/bm900205r.

(21) Gu, Z.; Yan, M.; Hu, B.; Joo, K.-I.; Biswas, A.; Huang, Y.; Lu, Y.; Wang, P.; Tang, Y. Protein Nanocapsule Weaved with Enzymatically Degradable Polymeric Network. *Nano Lett.* **2009**, *9* (12), 4533–4538. https://doi.org/10.1021/nl902935b.

(22) Zhao, M.; Biswas, A.; Hu, B.; Joo, K.-I.; Wang, P.; Gu, Z.; Tang, Y. Redox-Responsive Nanocapsules for Intracellular Protein Delivery. *Biomaterials* **2011**, *32* (22), 5223–5230. https://doi.org/10.1016/j.biomaterials.2011.03.060.

(23) Biswas, A.; Joo, K.-I.; Liu, J.; Zhao, M.; Fan, G.; Wang, P.; Gu, Z.; Tang, Y. Endoprotease-Mediated Intracellular Protein Delivery Using Nanocapsules. *ACS Nano* **2011**, *5* (2), 1385–1394. https://doi.org/10.1021/nn1031005.

(24) Wen, J.; Anderson, S. M.; Du, J.; Yan, M.; Wang, J.; Shen, M.; Lu, Y.; Segura, T. Controlled Protein Delivery Based on Enzyme-Responsive Nanocapsules. *Adv. Mater.* **2011**, *23* (39), 4549–4553. https://doi.org/10.1002/adma.201101771.

(25) Beloqui, A.; Yu Kobitski, A.; Ulrich Nienhaus, G.; Delaittre, G. A Simple Route to Highly Active Single-Enzyme Nanogels. *Chem. Sci.* **2018**, *9* (4), 1006–1013. https://doi.org/10.1039/C7SC04438K.

(26) Al Hafid, N.; Christodoulou, J. Phenylketonuria: A Review of Current and Future Treatments. *Transl. Pediatr.* **2015**, *4* (4), 304–317. https://doi.org/10.3978/j.issn.2224-4336.2015.10.07.

(27) Sarkissian, C. N.; Gámez, A. Phenylalanine Ammonia Lyase, Enzyme Substitution Therapy for Phenylketonuria, Where Are We Now? *Mol. Genet. Metab.* **2005**, *86*, 22–26. https://doi.org/10.1016/j.ymgme.2005.06.016.

(28) Rutsch, F. Antibodies against PEGylated Enzymes: Treat Them with Respect! *eBioMedicine* **2018**, *38*, 15–16. https://doi.org/10.1016/j.ebiom.2018.11.017.

(29) Gupta, S.; Lau, K.; Harding, C. O.; Shepherd, G.; Boyer, R.; Atkinson, J. P.; Knight, V.; Olbertz, J.; Larimore, K.; Gu, Z.; Li, M.; Rosen, O.; Zoog, S. J.; Weng, H. H.; Schweighardt, B. Association of Immune Response with Efficacy and Safety Outcomes in Adults with Phenylketonuria Administered Pegvaliase in Phase 3 Clinical Trials. *eBioMedicine* **2018**, *37*, 366–373. https://doi.org/10.1016/j.ebiom.2018.10.038.

(30) Huisman, G. W.; Agard, N. J.; Mijts, B.; Vroom, J.; Zhang, X. Engineered Phenylalanine Ammonia Lyase Polypeptides. US9611468B2, April 4, 2017. https://patents.google.com/patent/US9611468B2/en (accessed 2023-08-29).

(31) Pereira de Sousa, I.; Gourmel, C.; Berkovska, O.; Burger, M.; Leroux, J.-C. A Microparticulate Based Formulation to Protect Therapeutic Enzymes from Proteolytic Digestion: Phenylalanine Ammonia Lyase as Case Study. *Sci. Rep.* **2020**, *10* (1), 3651. https://doi.org/10.1038/s41598-020-60463-y.

(32) Cui, J. D.; Li, L. L.; Bian, H. J. Immobilization of Cross-Linked Phenylalanine Ammonia Lyase Aggregates in Microporous Silica Gel. *PLOS ONE* **2013**, *8* (11), e80581. https://doi.org/10.1371/journal.pone.0080581.

(33) *Phenylalanine Depletion for the Management of Phenylketonuria: Use of Enzyme Reactors with Immobilized Enzymes | Science*. https://www.science.org/doi/abs/10.1126/science.567372 (accessed 2023-08-29).

(34) Harris, J. M.; Chess, R. B. Effect of Pegylation on Pharmaceuticals. *Nat. Rev. Drug Discov.* **2003**, *2* (3), 214–221. https://doi.org/10.1038/nrd1033.

(35) Suk, J. S.; Xu, Q.; Kim, N.; Hanes, J.; Ensign, L. M. PEGylation as a Strategy for Improving Nanoparticle-Based Drug and Gene Delivery. *Adv. Drug Deliv. Rev.* **2016**, *99*, 28–51. https://doi.org/10.1016/j.addr.2015.09.012.

(36) Lutz, J.-F. Polymerization of Oligo(Ethylene Glycol) (Meth)Acrylates: Toward New Generations of Smart Biocompatible Materials. *J. Polym. Sci. Part Polym. Chem.* **2008**, *46* (11), 3459–3470. https://doi.org/10.1002/pola.22706.

(37) Udenfriend, S.; Stein, S.; Böhlen, P.; Dairman, W.; Leimgruber, W.; Weigele, M. Fluorescamine: A Reagent for Assay of Amino Acids, Peptides, Proteins, and Primary Amines in the Picomole Range. *Science* **1972**, *178* (4063), 871–872. https://doi.org/10.1126/science.178.4063.871.

(38) McCallum, J. A.; Walker, J. R. L. Phenolic Biosynthesis during Grain Development in Wheat: Changes in Phenylalanine Ammonia-Lyase Activity and Soluble Phenolic Content. *J. Cereal Sci.* **1990**, *11* (1), 35–49. https://doi.org/10.1016/S0733-5210(09)80179-3.

(39) Gordon, I. L. Selection against Sprouting Damage in Wheat. III.* Dormancy, Germinative Alpha-Amylase, Grain Redness and Flavanols. *Aust. J. Agric. Res.* **1979**, *30* (3), 387–402. https://doi.org/10.1071/ar9790387.

(40) Blackman, L. D.; Varlas, S.; Arno, M. C.; Houston, Z. H.; Fletcher, N. L.; Thurecht, K. J.; Hasan, M.; Gibson, M. I.; O'Reilly, R. K. Confinement of Therapeutic Enzymes in Selectively

Permeable Polymer Vesicles by Polymerization-Induced Self-Assembly (PISA) Reduces Antibody Binding and Proteolytic Susceptibility. *ACS Cent. Sci.* **2018**, *4* (6), 718–723. https://doi.org/10.1021/acscentsci.8b00168.

(41) Borgström, B.; Dahlqvist, A.; Lundh, G.; Sjövall, J. Studies of Intestinal Digestion and Absorption in the Human1. *J. Clin. Invest.* **1957**, *36* (10), 1521–1536. https://doi.org/10.1172/JCI103549.

2.5 Materials and Methods

All chemicals were purchased from Sigma-Aldrich and Fisher Scientific and were used without purification unless otherwise noted. For PEGMA, inhibitor was removed by passing through a plug of basic alumina. Plasmid for PAL expression was ordered from Twist Biosciences with the sequence cloned between Ndel_Xhol restriction sites in a pET-29b(+) vector. TEV protease was expressed following reported procedures and stored at -80 °C in 50% glycerol and thawed immediately before use.[1] For photocleavage experiments, a 4 watt, 365 nm lamp was used (brand: UVP).

2.6 Analytical Techniques

Nuclear Magnetic Resonance (NMR) spectra were recorded on a Bruker AV 500 MHz. Proton NMR spectra were acquired with a relaxation delay of 10 seconds for polymers.

For SDS PAGE, BioRad Any kD Mini-PROTEAN-TGXTM gels were used. SDS-PAGE protein standards were obtained from Bio-Rad (Precision Plus Protein Prestained Standards).

Small molecule purification was done via flash chromatography and conducted on a Biotage Isolera One auto-column system.

2.7 Appendix with Supplementary Figures

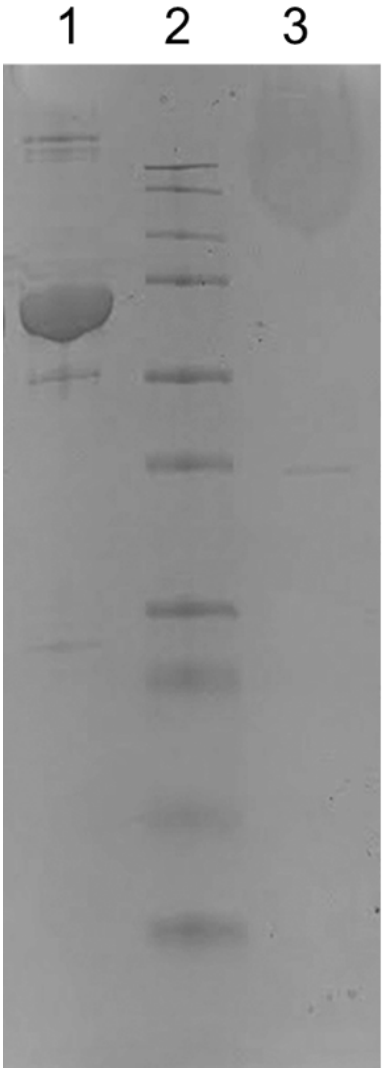

Figure S2.1 SDS-PAGE of unencapsulated PAL and purified nanogel mixture

stained with Coomassie. Lane 1: unencapsulated PAL, lane 2: ladder, lane 3: PAL nanogels (post-irradiation).

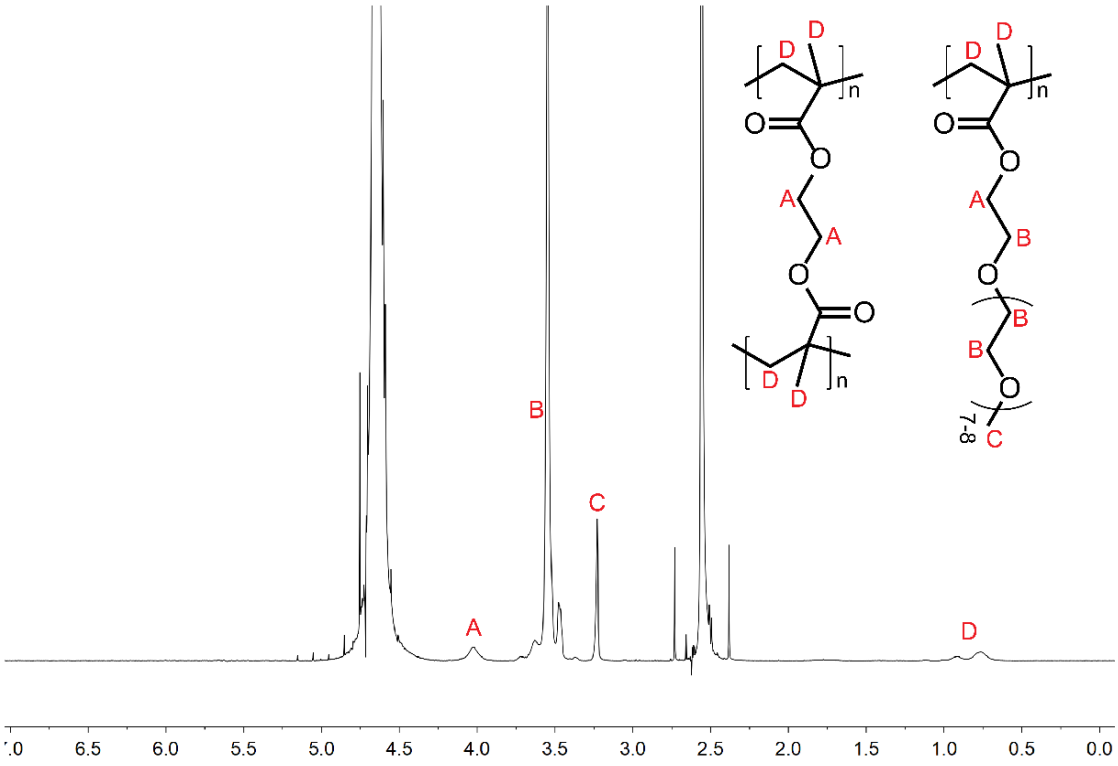

Figure S2.2 ^{1}H NMR (500 MHz, D_2O) of PAL nanogels (post-irradiation).

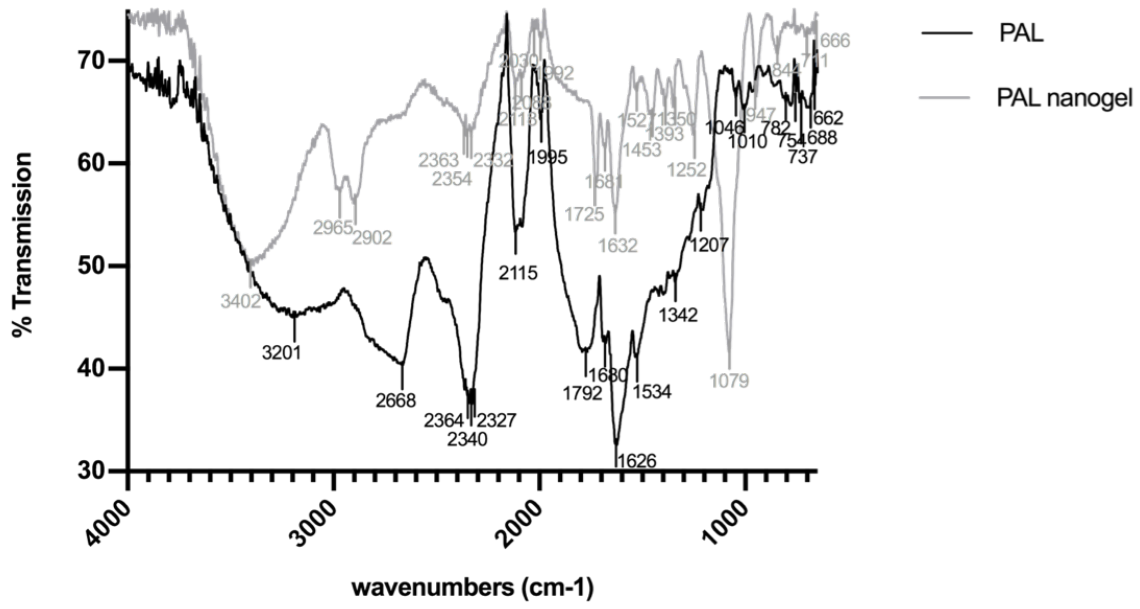

Figure S2.3 Fourier transform infrared spectrum of PAL and PAL nanogels (post-irradiation).

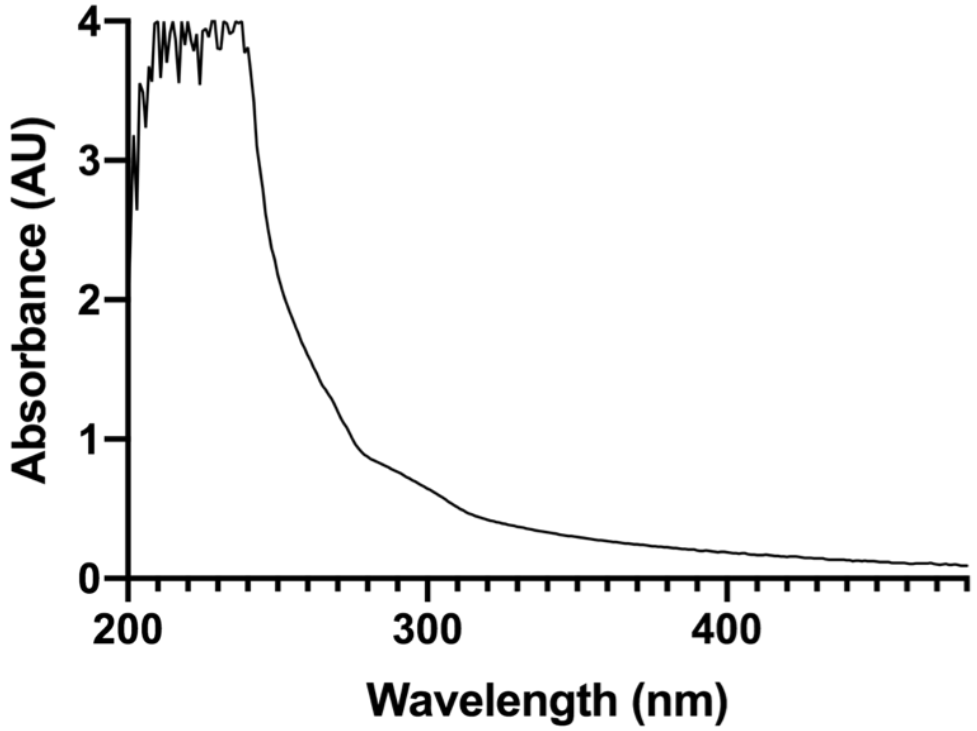

Figure S2.4 UV-Vis Spectrum of PAL nanogels.

Negligible absorbance at 365 nm, which is the wavelength used for photocleavage reaction.

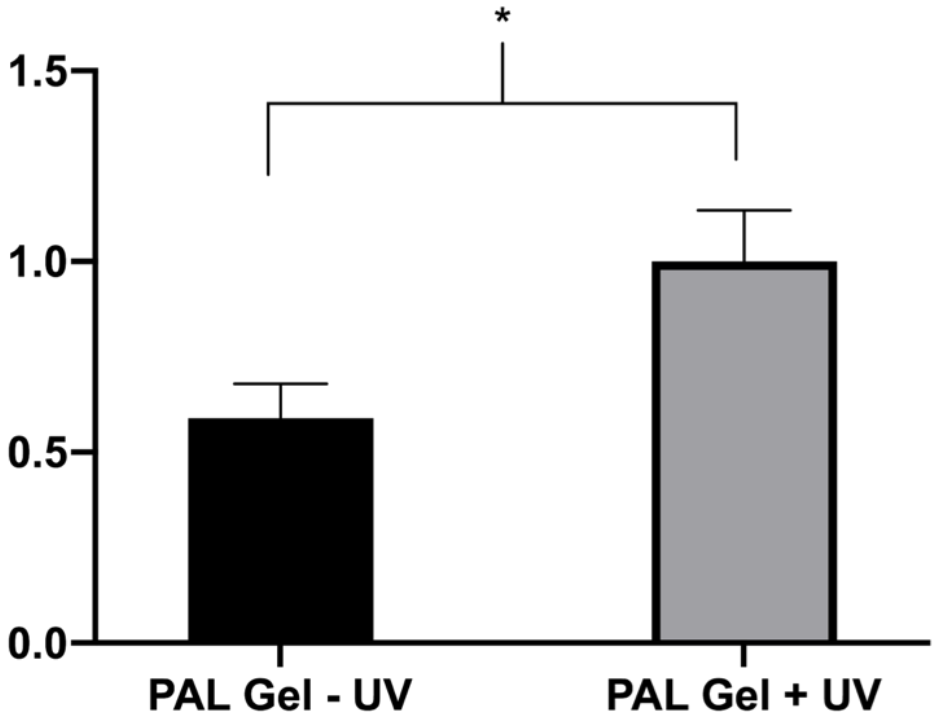

Figure S2.5 Fluorescamine assay to demonstrate a relative and statistically significant increase in fluorescence after PAL gel is irradiated with UV light.

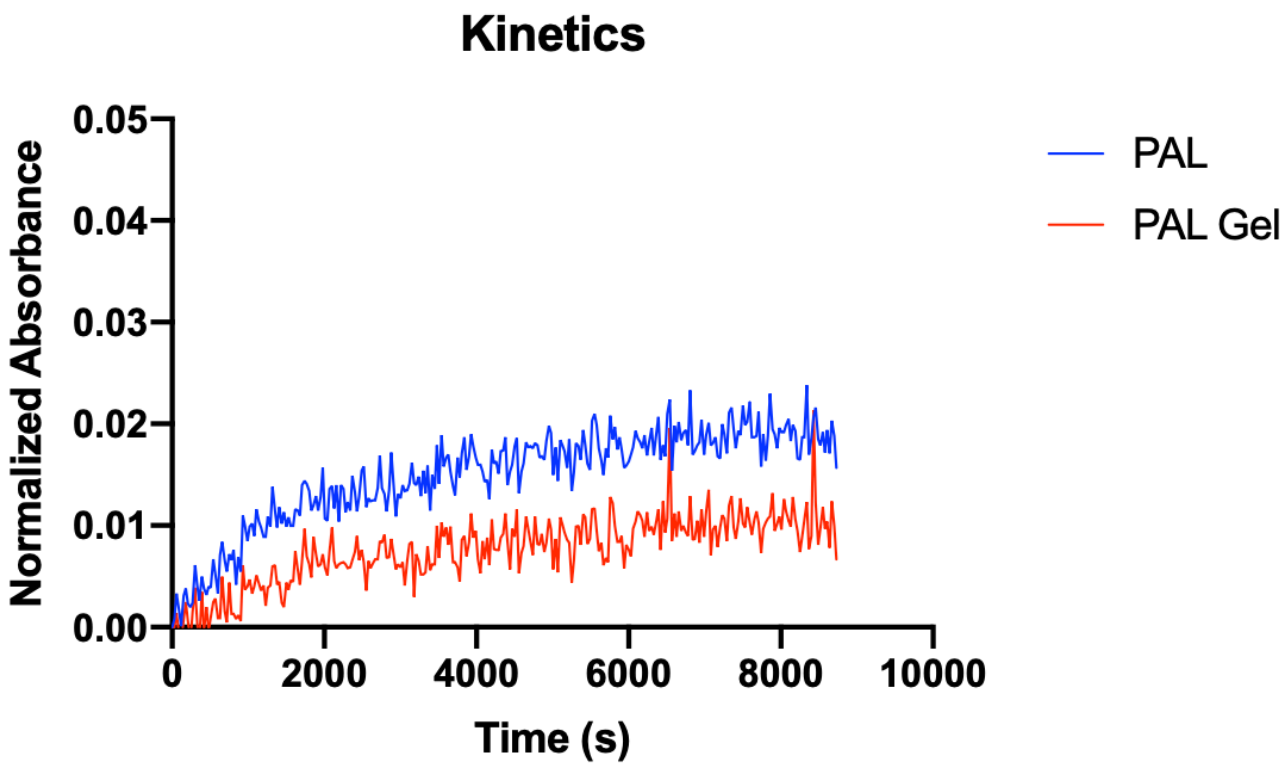

Figure S2.6 PAL activity kinetics indicate the enzyme reaches its steady state at 2 hours.

2 μg of PAL unencapsulated and freely encapsulated in PAL buffer (50 mM Tris base, 300 mM NaCl pH 7.8 buffer) was added, respectively, to a well in a UV-transparent 96 well plate and diluted up to 180 μL of PAL buffer. Then, 30 μL of 4 mM phenylalanine in PAL buffer was added to initiate the activity assay. Absorbance measurements at 290 nm were taken every 30 seconds and graphed in the figure above.

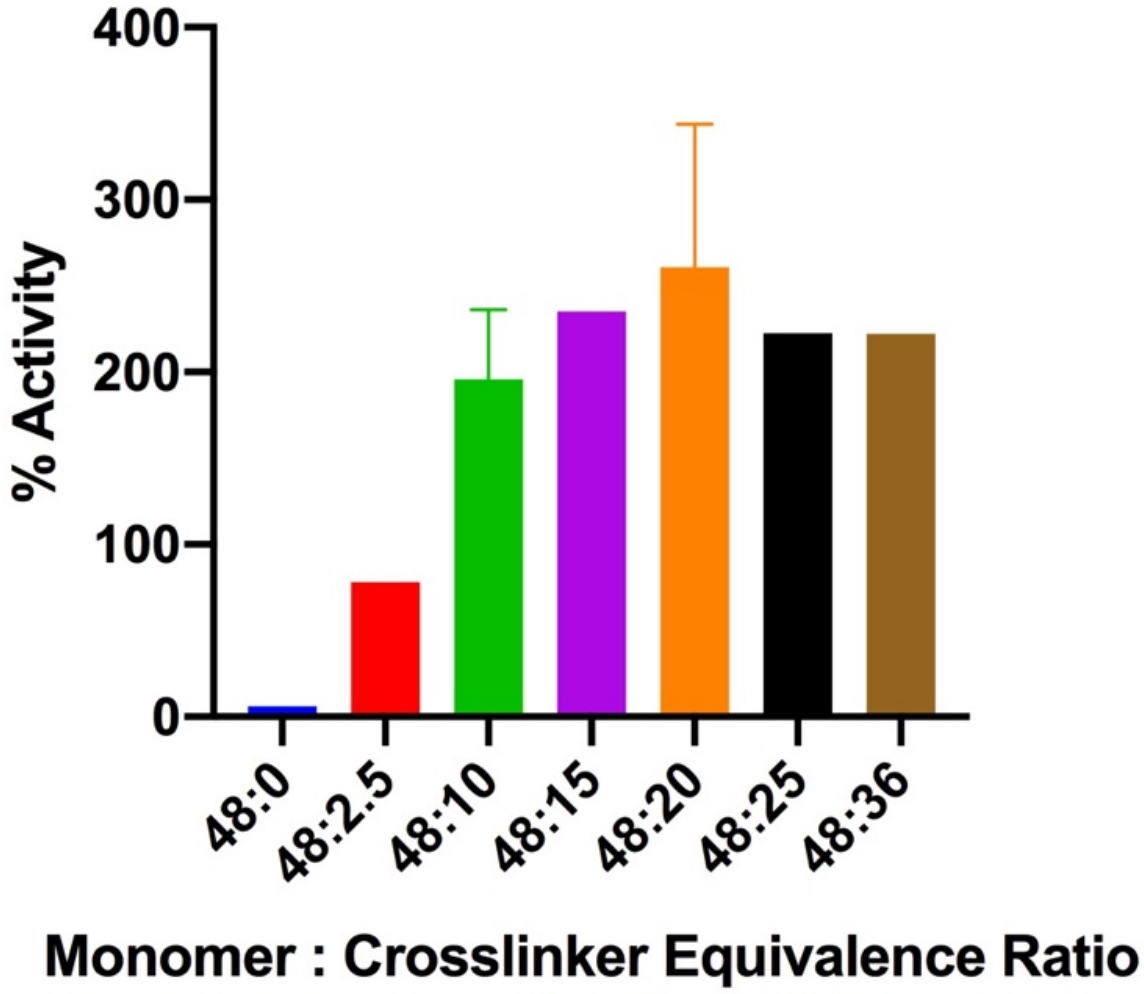

Figure S2.7 Experiment varying different monomer to crosslinker molar equivalence ratios for PAL nanogels

Eleven individual nanogels were prepared as described previously. All PAL nanogels were exposed to 6 μM trypsin. No significant increase in protein stability was observed for enzymes encapsulated by gels of higher crosslinking densities above a 48:10 monomer to crosslinker ratio.

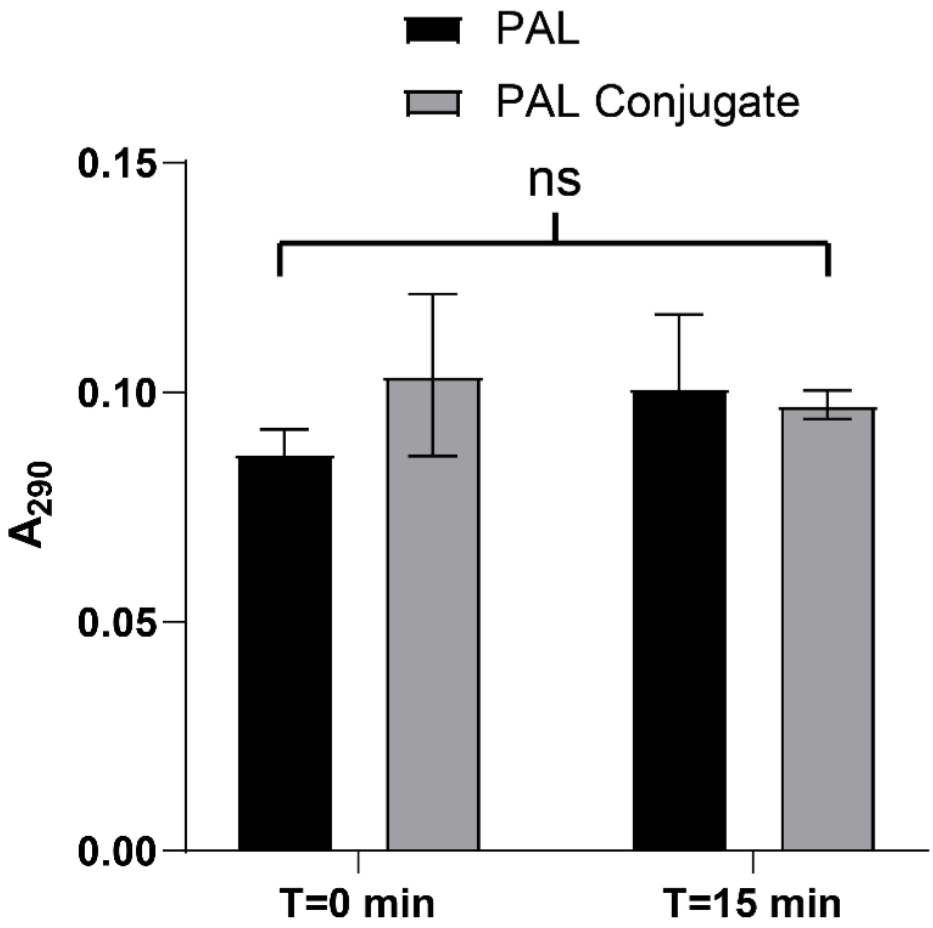

Figure S2.8 Control experiment verifying that the plate reader assay output is phenylalanine dependent.

No statistically significant increase in absorbance at 290 nm was observed over 15 minutes in the absence of phenylalanine.

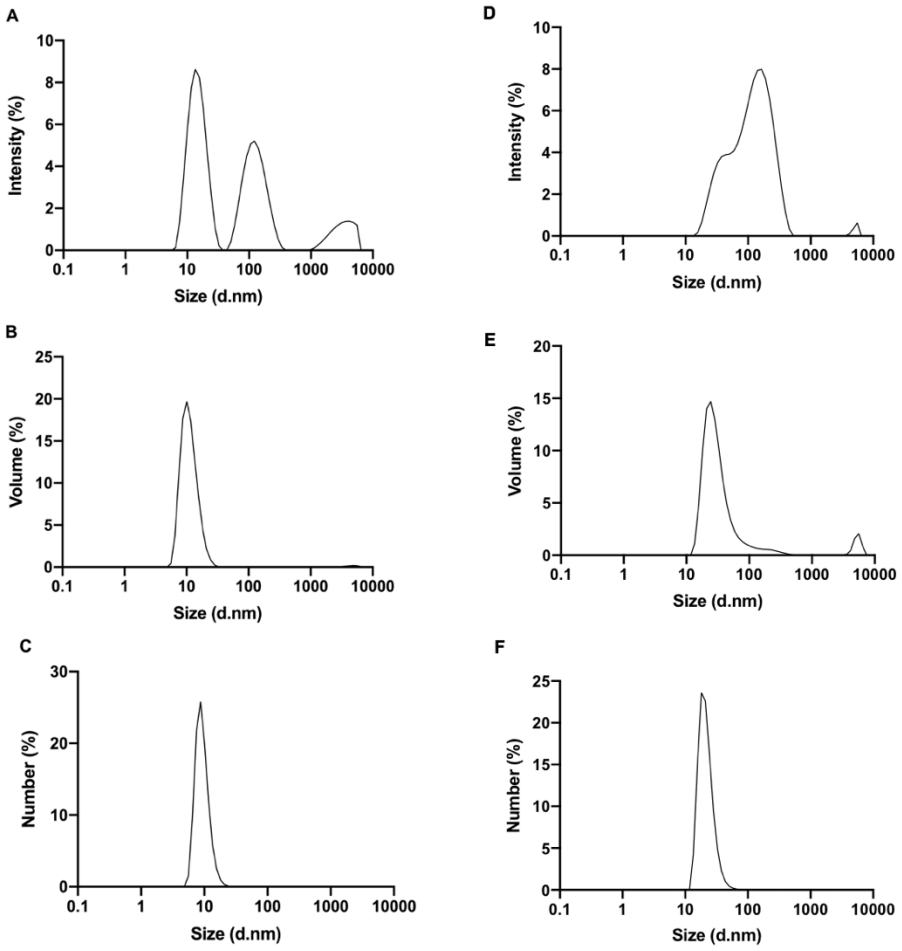

Figure S2.9 Dynamic Light Scattering (DLS) chromatograms of PAL.

A) Intensity Distribution: Peak 1 – 14.97 d.nm, 50.8%; Peak 2 – 131.8 d.nm, 38.2%; Peak 3 – 3374 d.nm, 10.9% (B) Volume Distribution: Peak 1 – 11.41 d.nm, 98.8%; Peak 2 – 105.0 d.nm, 0.2%; Peak 3 – 4229 d.nm, 0.9% , and (C) Number Distribution: Peak 1 – 9.410 d.nm, 100.0% and of irradiated PAL nanogels. (D) Intensity Distribution: Peak 1 – 142.5 d.nm, 98.9%; Peak 2 – 4968 d.nm, 1.1% (E) Volume Distribution: Peak 1 – 31.39 d.nm, 92.7%; Peak 2 – 273.0 d.nm, 3.1%; Peak 3 – 5161 d.nm, 4.3% (F) Number Distribution: Peak 1 – 20.00 d.nm; 100.0%.

2.8 Experimental and Appendix References

Conjugation

A 4 mg/mL solution of expressed PAL (stored at −80 °C) was thawed for 30 min at 4 °C. The protein was then buffer exchanged into pH 9, 50 mM sodium carbonate buffer via a 3 kDa MWCO Centriprep filter. After the protein concentration was determined via a BCA assay, a photocleavable linker (1.64 mg, 2.9 μmol, 4 equiv with respect to lysine residues) dissolved in dimethyl sulfoxide (DMSO) was added (final DMSO concentration of 5%). The conjugation reaction was allowed to proceed for 5 h at 25 °C. Excess linker was removed via 7 kDa MWCO Zeba desalting spin columns, and the modified PAL was buffer exchanged into PAL buffer via 3 kDa MWCO Centriprep filters.

Photocleavage Protocol

Samples were irradiated with UV light (365 nm, 4 watt) for 15 min at 4 °C to allow for photocleavage of the linker. Afterward, the samples were passed through a 7 kDa MWCO Zeba desalting spin column to remove excess monomer, photocleavage byproducts, and other small molecules. The desalting column was initially equilibrated with PAL buffer.

Fluorescamine Assay

Briefly, 100 μL of nanoparticle PAL (or modified PAL solution) was added to a 96 opaque well plate along with 30 μL of a 3 mg/mL fluorescamine solution (prepared in DMSO). The plate was incubated at 37 °C for 30 min. Fluorescence was then measured at an excitation wavelength of 380 nm and an emission wavelength of 460 nm.

Recovery of PAL Activity after Photocleavage

To determine percent recovery after photocleavage, each of the conjugated samples was compared against unmodified PAL. Conjugated samples underwent UV irradiation (365 nm, 4 watt) for 15 min at 4 °C as described previously. Afterward, the samples were passed through a 7 kDa MWCO Zeba desalting spin column to remove photocleavage byproducts and other small

molecules. The desalting column was equilibrated with PAL buffer. The remaining protein solutions were added to a 96-well plate and diluted to 200 μL with PAL buffer. The assay was initiated through the addition of 30 μL of 4 mM phenylalanine in PAL buffer, and kinetics were monitored by measuring absorbance values at 290 nm every 30 s for 2 h at 37 °C. Enzyme activity was determined by calculating the difference in absorbance values between the first and last time points. These values were normalized to that of the unmodified PAL.

Nanogel Synthesis

$PEGMA_{500}$ (20 μL, 0.05 mmol, 50 equiv), EGDMA (2 μL, 0.01 mmol, 10 equiv), tetramethylethylenediamine (0.6 μL, 0.004 mmol, 4 equiv), and conjugated PAL (12 μg) were added to a 4 mL dram vial with a stir bar and diluted up to 0.875 mL with PAL buffer. The mixture was allowed to degas under argon for 45–60 min. In a separate dram vial, APS stock solution in PAL buffer was prepared and also degassed under argon for 45–60 min. After degassing, 0.125 mL (0.2 mg, 1 μmol, 1 equiv) of the APS solution was added to the reaction mixture, and the polymerization was allowed to proceed for 2 h. To quench the reaction, samples were exposed to air.

Dose-Response Trypsin Challenge Assay

Ten individual PAL nanogels were prepared as described previously. For photocleavage, the gels were transferred to individual wells of a 48-well culture plate. The portion of the plate holding the samples was then irradiated with UV light (365 nm, 4 watt) for 15 min at 4 °C to allow for photocleavage of the linker. Afterward, the samples were passed through 7 kDa MWCO Zeba desalting spin columns to remove photocleavage byproducts and other small molecules. Buffer containing 50 mM Tris and 90 mM NaCl (pH 7.8) was used as equilibration buffer during this small-molecule cleanup.

The purified gel solutions were next split in half and added to individual wells on a UV transparent 96-well plate. One-half of the gel solution (20 μL) was added to a well consisting of a given concentration of trypsin (see below[a]), 95–195 μL PAL buffer, and 30 μL of 1% TFA 50/50 MeOH/ACN to immediately quench catalytic activity (these samples serve as t = 0 h). The second half of the gel solution was added to a well consisting of the same given concentration of trypsin as the first half of the gel solution in PAL buffer. All samples had a total volume of 275 μL. Lastly, 30 μL of 4 mM phenylalanine in 50 mM Tris base, 90 mM NaCl pH 7.8 buffer was added to all wells to initiate activity.

Absorbance measurements at 290 nm (37 °C) were taken every 30 s for 2 h. The catalytic activity was measured by calculating the difference between the absorbance measurements at t = 2 h and t = 0 h for each sample.

[a]The following concentrations of trypsin were used for this experiment: 0, 0.25, 2.9, 5.8, 14.5, 29.1, 43.6, 46.5, 52.4, and 58.2 μM." to here (after the Dose-Response Trypsin Challenge Assay.

Single Point HPLC Trypsin Challenge Assay

Six individual nanogels were prepared and photocleaved as described previously. Next, 150 μL of a 70 μM trypsin solution was added to the unencapsulated PAL and PAL nanogels (1200 μL) in 1.5 mL LoBind Eppendorf tubes. Lastly, 100 μL of 4 mM phenylalanine in PAL buffer was added to initiate the activity assay. The tubes were allowed to incubate in a thermoshaker for 2 h at (37 °C and 250 rpm). Afterward, samples were then passed through Centriprep 3 kDa MWCO filters to collect *trans*-cinnamic acid. Samples were filtered, and *trans*-cinnamic acid concentration was determined against a standard curve of a pure reference.

Low pH Assay

Six individual nanogels were prepared and photocleaved as described previously. Next, samples of unencapsulated PAL and PAL nanogels were buffer exchanged into a pH 3.5 citric acid buffer via Centriprep 30 kDa MWCO filters. The resulting volumes of the samples were 120 μL and added to individual wells on a UV transparent 96-well plate. Then, 30 μL of 4 mM phenylalanine in PAL buffer was added to each well to initiate the activity assay. Absorbance measurements at 290 nm (37 °C) were taken every 30 s for 2 h. At the 1 h mark, samples were either maintained at pH 3.5 or brought up to pH 7.8. The catalytic activity was measured by calculating the difference between the absorbance measurements at t = 2 h and t = 0 h for each sample. Normalization was done by comparing all samples against an unmodified PAL control measuring activity at pH 7.8.

References

(1) Tropea, J. E.; Cherry, S.; Waugh, D. S. Expression and Purification of Soluble His(6)- Tagged TEV Protease. *Methods Mol. Biol. Clifton NJ* **2009**, *498*, 297–307. https://doi.org/10.1007/978-1-59745-196-3_19.

Chapter 3 Enzyme-Polymer Conjugates with Photocleavable Linkers for Control Over Protein Activity

3.1 Introduction

Since the 1990s when the FDA approved the first poly(ethylene glycol) (PEG) modified protein, Adagen® (PEGylated form of adenosine deaminase), much work has been undertaken to develop protein-polymer conjugates for use in the pharmaceutical, technological, and industrial sectors.[1] Of particular interest is the incorporation of reversible linkers to control protein activity or binding.[2] Strategies include reliance on substituted maleic anhydride and succinate linkers for hydrolysis, thiol-disulfide or thiol-thioester exchange, 1,6-benzyl elimination linkers, β-eliminative or β-alanine linkers, bicin linkers, E1CB elimination linkers, biodegradation, proteolysis, host-guest interactions, ion complexation, and photo-immolation.[2]

Of the different types of triggers, light can be an advantageous tool for reversible conjugation of polymers due to its relatively non-invasive properties, as well as its proven safety in clinics and laboratories. A commonly used class of photolabile groups is *ortho*-nitrobenzyl (ONB) alcohol derivatives. This class was first described by Barltrop et al. in 1966; however, ONBs began to increase in popularity when Woodward and coworkers started utilizing them for modification of amino and carboxylic acid groups on peptides.[3,4] Since then ONBs have been used extensively in many areas of chemistry; there are several excellent reviews that discuss the work that has been accomplished with ONBs in polymer science, as well as in their applications to biomolecules.[5,6]

For example, we previously reported the use of an ONB photocleavable linkage for the synthesis of noncovalent enzyme nanogels.[7] Specifically, phenylalanine lyase caged in a nanogel recovered 54% of its catalytic activity when irradiated with UV light.

There is also interest in the application of ONBs to the synthesis of protein-polymer conjugates. Deiters and coworkers were the first to synthesize a photocleavable PEG that was installed onto an enzyme to demonstrate spatiotemporal control over protein activity.[8] Specifically, a lysine

reactive, PEG-alkyne derivative was coupled with a photocleavable ONB azide. Subsequent conjugation to lysozyme yielded a photocaged biological molecule that regained activity upon irradiation with UV light. Furthermore, Yamaguchi and coworkers designed a method in which photodegradable protein-polymer materials were used to remotely control the cell functions of mammalian cells.[9]

In both of these situations, the photodegradable polymers were synthesized prior to conjugation onto the protein of interest following the *grafting-to* technique. This approach involves first synthesizing well-defined polymers that retain a reactive handle for subsequent protein conjugation.[10,11] Another strategy that is commonly employed for the preparation of protein-polymer conjugates is a *grafting-from* approach in which the polymer is synthesized directly onto a protein that was previously modified with polymerizable initiating or chain transfer groups.[12-14] Our group has extensively reported the use of both strategies,[10,12,13,15-22] and there are advantages and disadvantages to both. In the research described in this paper, we sought to directly compare the *grafting-to* and *grafting-from* approaches for reversible protein conjugation of ONB linked polymers (Figure 3.1).

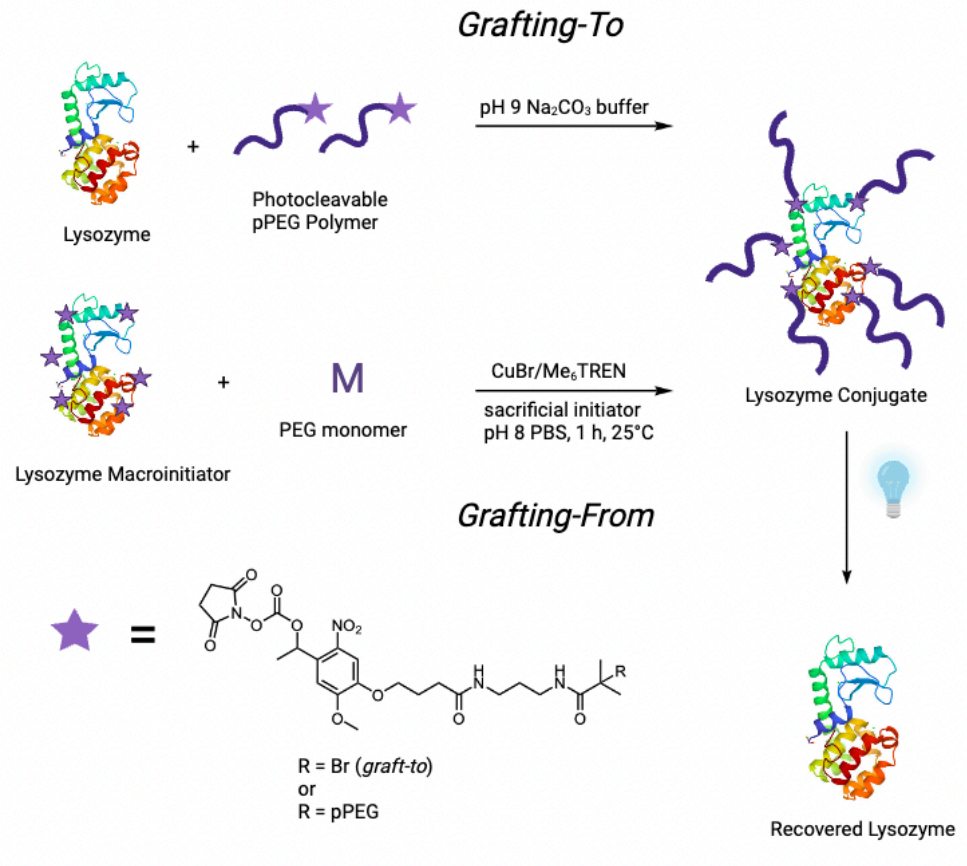

Figure 3.10 The two strategies explored in this study to synthesize photocleavable protein-polymer conjugates.

3.2 Results and Discussion

3.2.1. Design and Synthesis of Photocleavable Initiator

Acetovanillone (4-hydroxy-3-methoxyacetophenone) is a compound widely employed in the synthesis of *o*-nitrobenzyl linkers.[6] As in previous reports, alkylation of the phenol, *ortho*-nitration, coupling and subsequent deprotection of *N*-Boc-1,3-propanediamine were performed (Figure 3.2). [7,23] The ATRP initiating site was then installed by coupling the free amine with an N-hydroxysuccinimidyl (NHS)-activated bromoisobutyryl molecule to afford compound **1**. Subsequent reduction of the ketone using sodium borohydride afforded compound **2**, followed

by alkylation with *N,N*-disuccinimidyl carbonate resulted in the final, lysine-reaction photocleavable initiator **3**.

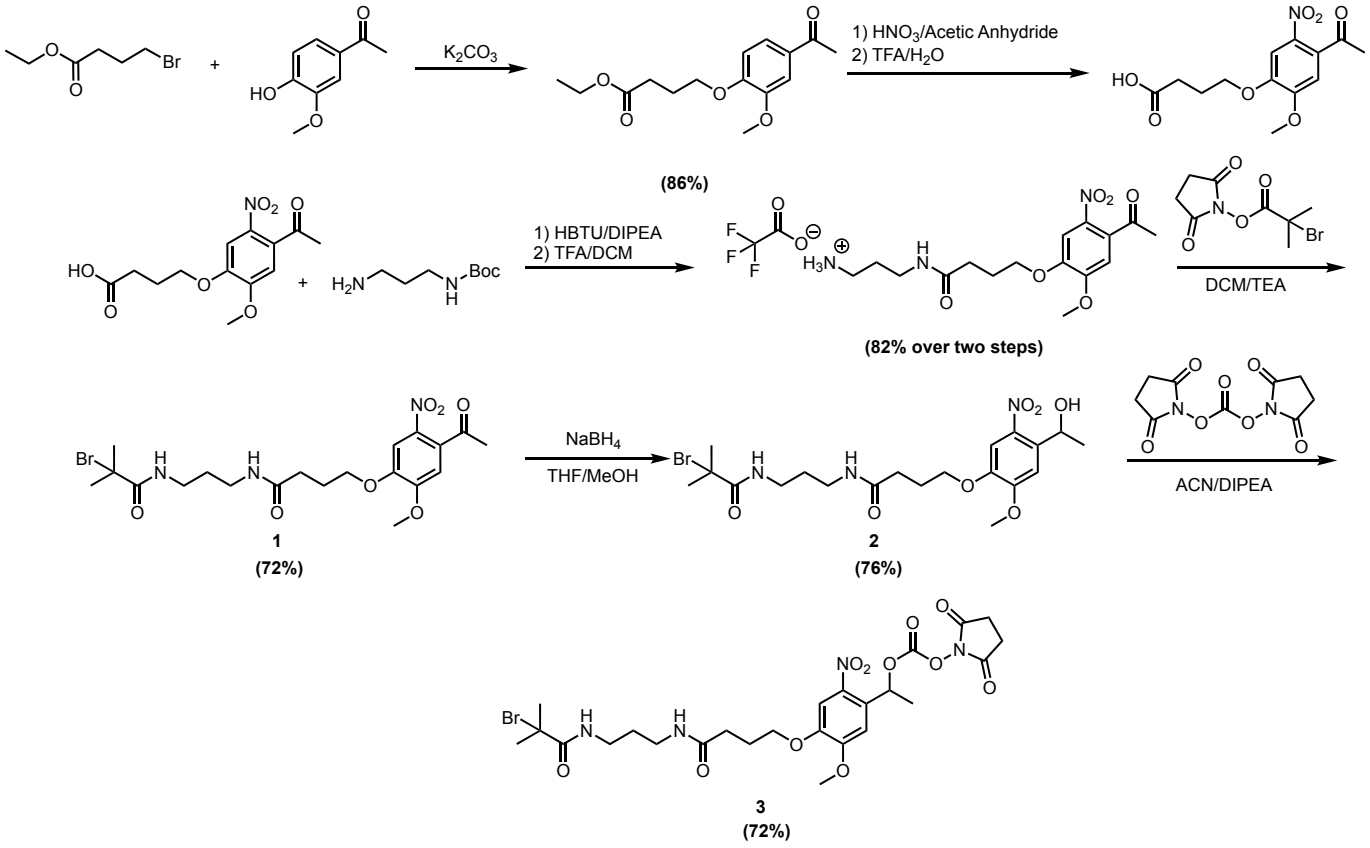

Figure 3.2 Scheme of synthesis of photocleavable initiator.

The following abbreviations are defined as follows: TFA = trifluoroacetic acid; HTBU = *N, N, N', N'*-Tetramethyl-*O*-(1*H*—benzotriazol-1-yl)uronium hexafluorophosphate; DIPEA = diisopropylethylamine; DCM = dichloromethane; TEA = triethylamine; THF = tetrahydrofuran; MeOH = methanol; ACN = acetonitrile

3.2.2. Preparation of Protein-Polymer Conjugates

3.2.2.1 Approach 1: *Grafting-To*

The main advantage for preparing protein-polymer conjugates *via grafting-to* is the ability to use traditional conditions to synthesize the polymers, such as reaction temperatures above 25 ℃ and in organic solvents, which are not typically suitable for proteins. In this report, we employed atom transfer radical polymerization (ATRP) as a controlled radical polymerization to synthesize polymers with relatively low polydispersity, i.e. < 1.4. More specifically, the type of ATRP chosen to prepare the photocleavable polymers herein generally followed an activated regeneration type of mechanism, which essentially consists of a constant reduction of copper (II) deactivator species to copper (I) activator species by a type of reducing agent or zero valent copper species.[24] We first attempted the controlled polymerization of PEGA using the activator regenerated by electron transfer (ARGET) ATRP mechanism, which was first demonstrated by Matyjaszewski and coworkers for polymerization of styrene.[25] Various conditions were screened for the polymerization of PEGA polymers by the photocleavable initiator to achieve a sufficient balance between end-group fidelity, monomer conversion, and low molecular weight dispersity (D) as listed in Table 1. Initially, the polymerization was attempted in dry DMSO with Sn_2Octoate (Entry 1) as the compatible reducing agent to avoid any hydrolysis of the photocleavable initiator at the lysine-reactive site. However, monomer conversion was only 8%, likely due to the slower disproportionation of the transition metal catalyst complex in DMSO.[26] Switching to water as the major solvent with 5% (v/v) DMSO to solubilize the initiator, and the use of ascorbic acid as the reducing agent (Entry 3), enabled slightly higher conversion of PEGA up to 37%. This was likely a result of improved solubility of the catalyst.[27]

Although the polymerization did not reach complete conversion, a number-average molecular weight (M_n) of 40 kDa polymer with a molecular weight dispersity less than 1.40 was obtained. We next investigated use of supplemental activator and reducing agent (SARA) ATRP polymerization (Table 1). This type of polymerization mediated by a zero-valent metal was first attempted by Matyjaszewski *et al.* for the synthesis of methyl acrylate, methyl methacrylate, and styrene polymers.[28] Similar to that of the ARGET approach, the SARA ATRP was initially attempted in DMSO to avoid hydrolysis of the initiator (Entry 4), which resulted in low monomer conversion. Switching the reaction in water yielded a polymer with a significantly higher conversion of 96% and a lower dispersity of 1.15 compared to that from ARGET which had a dispersity of 1.33 (Entry 5 versus 3). This polymer was close to the targeted molecular weight of 35,000 Da with a M_n by size exclusion chromatography (SEC) of 31,500 Da.

Table 3.1 Conditions for the synthesis of photocleavable pPEGA. Scheme of Polymerization above.

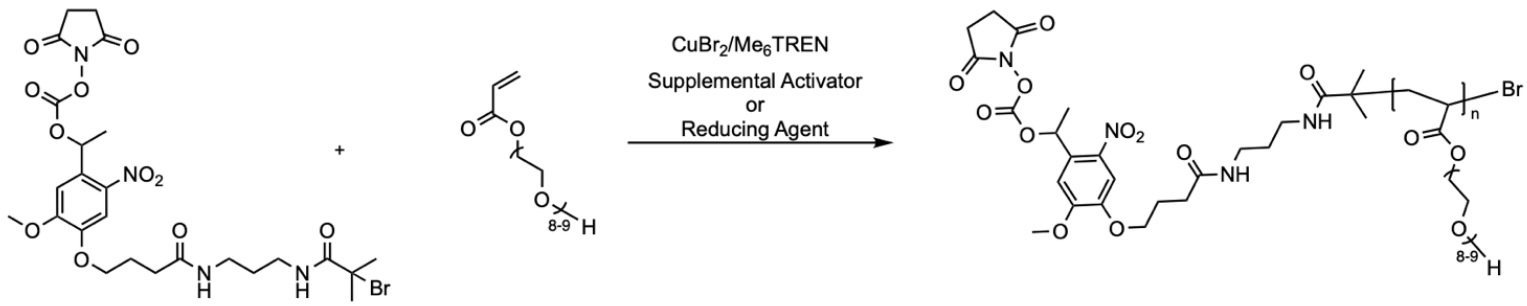

Entry	Supplemental Activator[a]/Reducing Agent[b]	Equiv. Ratios[c]	Solvent[d]	Conversion (%)	M_n[e] (targeted)	M_n[f] (NMR)	M_n[g] (SEC)	Đ
1	Sn_2Octoate	1: 50: 1: 4: 0.6	Dry DMSO	8	1.4	2	---	---
2	Ascorbic acid	1: 50: 1: 4: 0.6	DMSO	16	2.9	5	---	---
3	Ascorbic acid	1: 350: 1: 4: 0.6	H_2O	37	47	50	41.5	1.33
4	Cu^0	1: 200: 1: 4: 0.6	DMSO	5	3.6	4	---	---
5	Cu^0	1: 100: 1: 4: 0.6	H_2O	96	35	31	31.5	1.15
6	Cu^0	1: 500: 1: 4: 0.6	pH 6 PBS	57	103	115	90.4	1.29

[a]Cu^0 is used both as the supplemental activator and reducing agent following the mechanism of SARA ATRP

[b]Ascorbic acid or Sn_2Octoate is used as the reducing agent following the mechanism of ARGET ATRP

[c]Initiator/$PEGA_{(Mn=360)}$/$CuBr_2$/Me_6TREN/reducing agent

[d] 10% DMSO is added to the solvent conditions for the solubility of the photocleavable initiator in Entries 3, 5, and 6

[e, f, g] M_n values are reported in kDa

Hydrolysis of the initiator during conjugation in aqueous polymerization conditions was a concern. To investigate this, a kinetics study of the small molecule photocleavable initiator in water (and 10% DMSO for solubilization) was carried out by monitoring its conversion to hydrolyzed product by ^{1}H NMR spectroscopy over time (Figure S3.1). Since the end group of the photocleavable polymer was difficult to observe by NMR, the small molecule was used as a model system. Although, the hydrolysis rate could be different, we anticipated that this would provide a reasonable estimate. It was determined that at 1.5 hours, ~70% of the photocleavable initiator retained the NHS group. This indicated that while hydrolysis was occurring, it proceeded at a slow enough rate such that aqueous polymerization could be conducted. Interestingly, Haddleton and coworkers carried out a similar small molecule hydrolysis study of a NHS-functionalized initiator. They reported fast cleavage of the end group in pH 9 buffer but nearly negligible hydrolysis in pH 6 PBS buffer.[11] To study this with our initiator, It was determined by ^{1}H NMR that the hydrolysis rate was in fact slowed by 10% in pH 6.0 PBS buffer in comparison to the initiator in pH 7 (Figure S3.1). Therefore, the next polymerization was carried out at pH 6.0 resulting in a M_n of 90 kDa and D of 1.29.

Lysozyme (Lys) is a well-studied, small (~14 kDa) enzyme with a straight forward activity assay, and thus this protein was used as a model enzyme for conjugation. The largest polymer (entry 6, Table 1) was utilized for the *grafting to* approach, because it was anticipated that this polymer would have the greatest effect on protein activity. After conjugation, FPLC was utilized with a

cation exchange column to purify the product (chromatogram Figure 3.3A).[21]

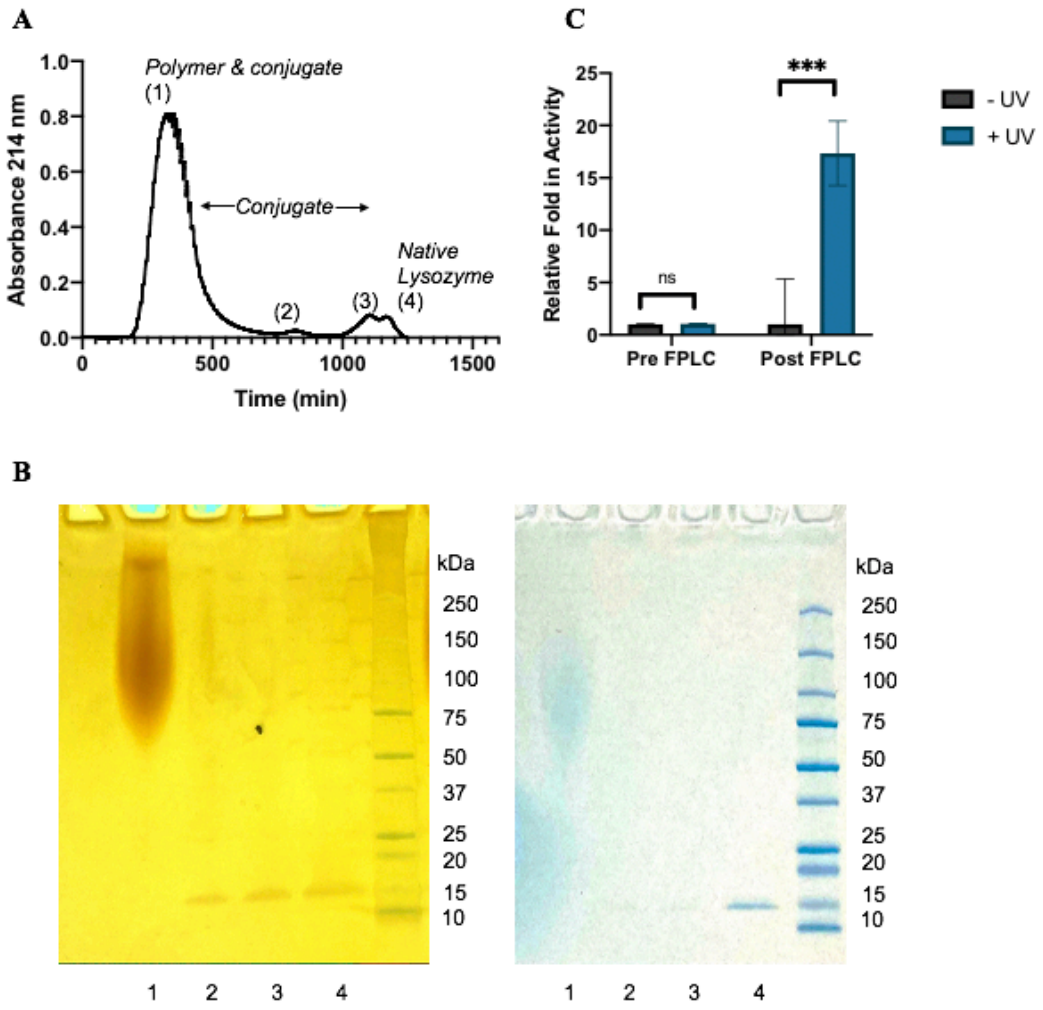

Figure 3.3 Characterization of *grafting-to* photocleavable PEGA lysozyme conjugate

A) FPLC chromatogram of crude conjugate. B) SDS PAGE analysis of FPLC fractions by iodine stain (left) and Coomassie stain (right). C) Activity test of photocleavable PEGA lysozyme conjugate before and after UV irradiation pre- and post- FPLC Purification. Each measurement was conducted in triplicate and statistical significance was determined *via* a two-way ANOVA with multiple comparisons (*** = $p \leq 0.0001$ compared against the sample before UV irradiation post-FPLC).

It was observed by FPLC that unreacted lysozyme was still in solution. Fortunately, this was readily removed as shown by SDS PAGE analysis (Figure 3.3B). Specifically, the conjugate without any unmodified Lys (Lane 1) was observed by both iodine and Coomassie staining. Activity assays were carried out before and after irradiation with UV light. In order to accurately measure the activity of the conjugated enzyme it was crucial to remove any unmodified enzyme. Before FPLC purification of the conjugate, the unmodified enzyme swamped the single and no difference was observed (Figure 3C Pre FPLC). However, after the purified lysozyme-photocleavable conjugate was irradiated with UV light, the released lysozyme was 20 times more active compared to conjugated lysozyme (Figure 3C, Post FPLC). These results confirmed that removal of the polymer with light resulted in significant increased enzyme activity.

Control experiments such as impact of UV irradiation on protein (365 nm used for removal of the polymer) as well as background photocleavage at 450 nm (the wavelength utilized for the activity assay) were conducted because it is known that light, especially UV irradiation, can damage some proteins.[29] Fortunately, it was determined that the UV irradiation had no significant impact on the activity of lysozyme even after 2 hours (Figure S3.2). Furthermore, no increase in absorbance was observed when the protein-polymer conjugate was irradiated with 450 nm over time (Figure S3.3).

3.2.2.2 Approach 2: *Grafting-From*

Protein-polymer conjugates were next synthesized *via* a 'graft-from' approach. Lysozyme was modified with the photocleavable initiator (Figure 3.4A) by allowing the protein to react with the NHS-activated carbonate **3** at room temperature in pH 9 sodium carbonate buffer for 5 hours. Fluorescamine assay, that interacts with the primary amino groups of proteins yielding highly fluorescent derivatives,

Confirmed that 89% of the lysine residues on lysozyme were modified (Figure 3.4B).[30] This was compared to a control sample modified with NHS-bromoisobutyrate as a non-cleavable initiator, which showed the same degree of lysine modification. LCMS of the lysozyme photocleavable macroinitiator further confirmed modification of five lysine residues on the protein (Figures 3.4C). LCMS of lysozyme non-cleavable macroinitiator (Figure S3.4), which showed similar modification.

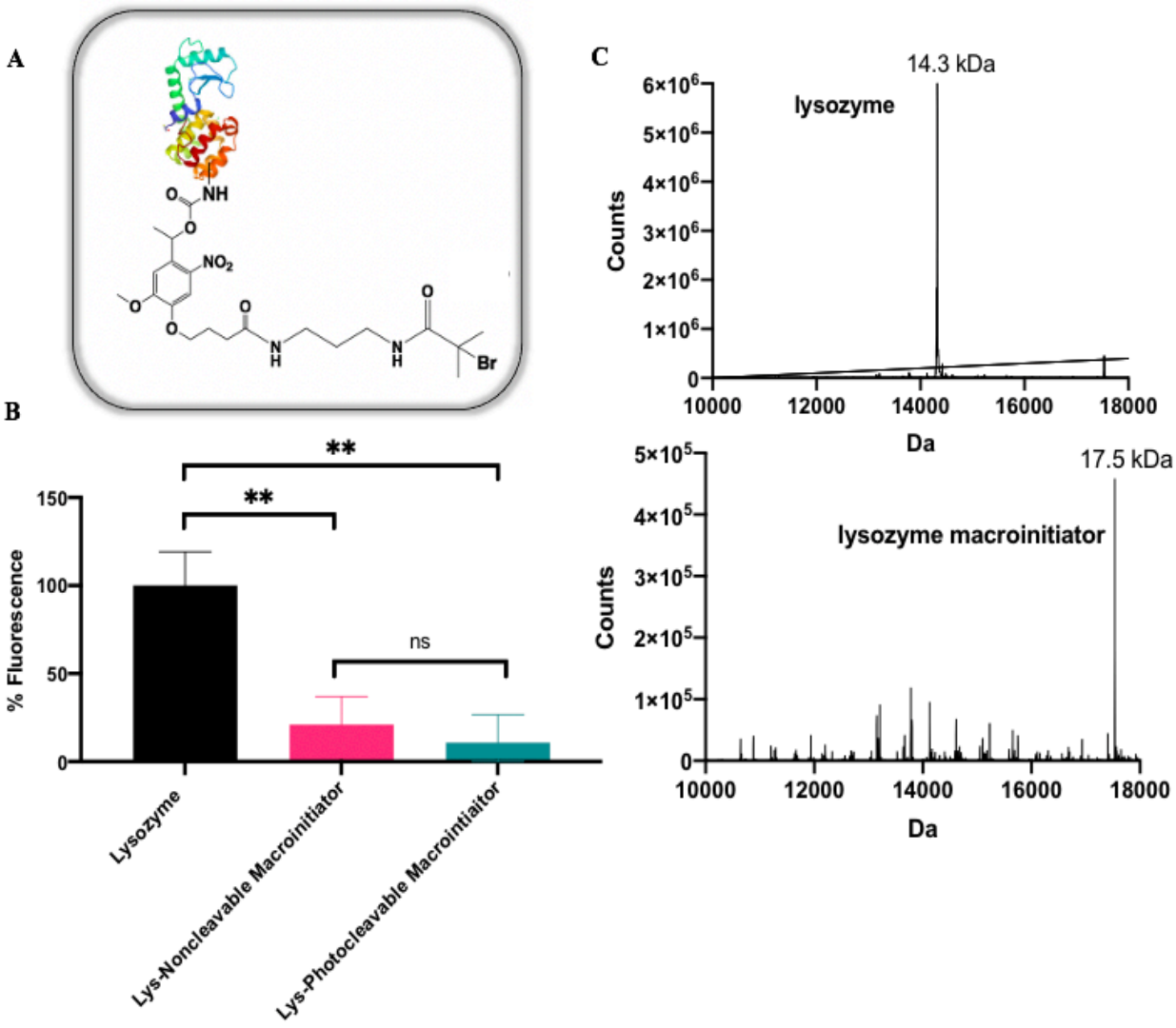

Figure 3.4 Characterization of photocleavable lysozyme macroinitiator

A) Photocleavable macroinitiator. Only one modification is shown for simplicity purposes, Lysozyme PDB: 253L. B) Fluorescence for conjugates and Lys after subjection to fluorescamine. Each measurement was conducted in triplicate and statistical significance was determined *via* an ordinary one-way ANOVA with multiple comparison. (** = $p \leq 0.001$ compared against the native lysozyme). C) LCMS Spectrum of native lysozyme (top) and photocleavable lysozyme macroinitiator (bottom).

Polymerization from the lysozyme macroinitiator by an ATRP mechanism using PEGA monomer was then attempted to form the protein-polymer conjugate. Briefly, CuBr and Me_6TREN in buffer was employed. Based on a previous report, incorporation of a sacrificial initiator was also utilized to promote polymerization from the protein due to the increased number of initiating sites in solution.[22] To match the size of the polymer chosen for the *grafting*-to approach, a M_n 90.0 kDa was targeted. To characterize the polymer size after polymerization, the Lys was digested using Proteinase K.[22] By SEC analysis, the polymer was 117.1 kDa with a dispersity of 1.16 (Figure S3.5).

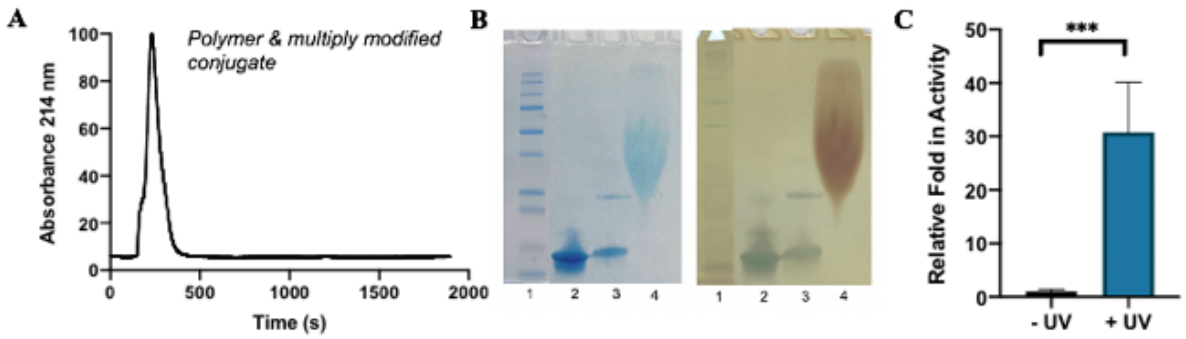

Figure 3.5 Characterization of *grafting-to* photocleavable PEGA lysozyme conjugate

A) FPLC chromatogram of crude product. B) SDS PAGE analysis of FPLC fractions by Coomassie stain (left) and iodine stain (right) Lane 1: Protein Ladder, Lane 2: Native Lysozyme, Lane 3: Lysozyme Macroinitiator, Lane 4: Lysozyme PEGA Conjugate. C) Activity Test of photocleavable PEGA lysozyme conjugate before and after UV irradiation. Each measurement was conducted in triplicate and statistical

significance was determined *via* a 2way ANOVA with multiple comparisons (* = $p \leq 0.01$ compared against the sample before UV irradiation.)

Analysis of the conjugate solution by FPLC (Figure 3.5A) and SDS PAGE (Figure 3.5B) revealed no unreacted lysozyme macroinitiator. The FPLC chromatogram did not have multiple peaks, indicating uniformity. As for the *grafting-to* approach, an activity assay of the conjugate was conducted before and after irradiation with UV light on the crude conjugate. It was observed that the lysozyme-photocleavable conjugate irradiated with UV light was 30 times more active compared to pre-irradiation conjugate (Figure 3.5C). Unlike *grafting to,* the product did not need to be purified first to observe activity. The purified *grafting from* conjugate was also studied and compared to pristine Lys. It was determined that the Lys released from the conjugate after exposure to UV light was 82.9 ± 6.8% active relative to native lysozyme (Figure 3.6B). These results indicate good restoration of native protein activity. To further investigate the photocleavage, a fluorescamine assay was conducted on the conjugate before and after irradiation. A 60% recovery of primary amine residues was observed (Figure 3.6C). This suggests that not all the native lysine residues were restored after irradiation. However, SDS PAGE analysis (Figure 6D), as well as MALDI (Figure 3.6E) demonstrated complete recovery of protein without modification. SDS PAGE before and after irradiation confirmed recovery of protein. By MALDI, it appears that the difference in mass between the native lysozyme (14.4 kDa) and irradiated conjugate (14.9 kDa) is small enough that there should not be any polymer fragments remaining on the protein. Potential reasons for the difference in mass may be attributed to photochemical side reactions or impurities due to the copper chelation to the

enzyme.[31] This could also be the reason for the discrepancy between the fluorescamine and SDS PAGE/MALDI results.

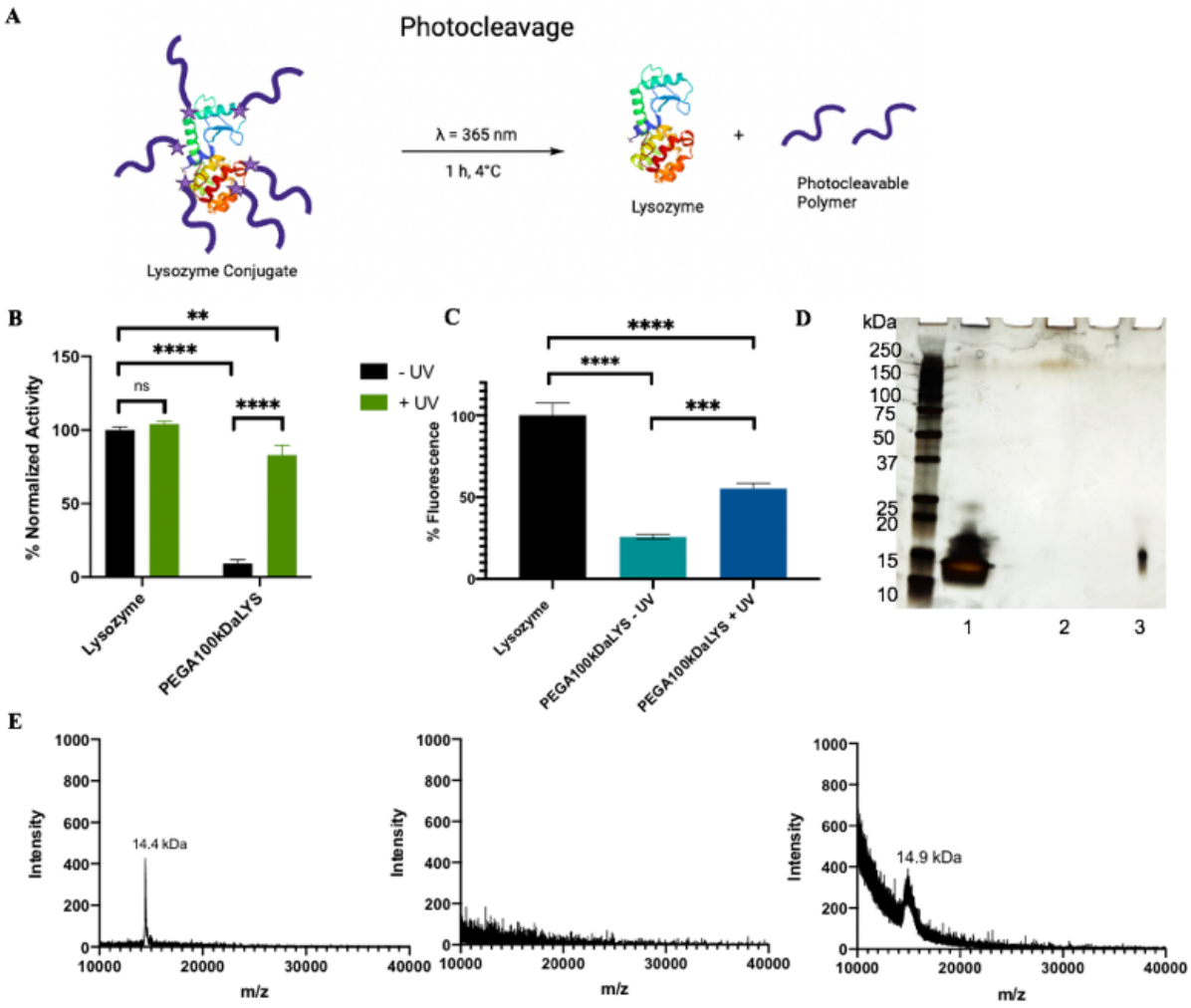

Figure 3.6 Scheme of photocleavage of grafting-from conjugate to recover protein

B) Activity assay of purified conjugate compared to native enzyme before and after irradiation with UV light. Each measurement was conducted in triplicate and statistical significance was determined *via* a 2-way ANOVA with multiple comparisons. (** = $p \leq 0.01$, **** = $p < 0.0001$ compared against the native lysozyme before UV irradiation). C) Fluorescamine assay results of conjugate before and after irradiation with UV light compared to native enzyme. Each measurement was conducted in triplicate and statistical significance was determined *via* an ordinary one-way ANOVA with multiple comparisons. (*** = $p \leq 0.001$, **** = $p \leq 0.0001$ compared against the native lysozyme). D) SDS PAGE analysis of conjugate before and

after irradiation with UV light by silver stain. Lane 1: Lysozyme macroinitiator, Lane 2: PEGA-Lysozyme conjugate before irradiation, Lane 3: PEGA-Lysozyme conjugate after irradiation. E) MALDI analysis of native lysozyme (left), PEGA-Lysozyme conjugate before irradiation (middle), PEGA-Lysozyme conjugate after irradiation (right).

3.2.3. Advantages & Disadvantages of *Grafting-To and Grafting-From*

Our group, as well as many others, have written extensive reviews discussing the *grafting-to* and *grafting-from* strategies to prepare protein-polymer conjugates.[15,16] A summary of the advantages and disadvantages observed for the system described herein are summarized in Table 2.

There was one advantage of the *grafting-to* approach. Monitoring the molecular weight of the polymer was faster and easier in the *grafting-to* approach. The *grafting-from* polymerization was performed with sacrificial initiator added in excess in order to be able to use only a few milligrams of protein sample. The polymer formed by the sacrificial initiator must first be removed before cleaving the polymer from the conjugate in order to accurately determine the molecular weight of the polymer on the conjugate. Thus, it is not as straightforward to quickly monitor the polymer size.

More advantages were observed with the *grafting-from* approach. First, concern over hydrolysis of the NHS-activated carbonate was reduced in the *grafting-from* approach because the initiator was added in excess and prior to polymer formation. In the *grafting-to* approach, it was possible to retain the NHS group during synthesis and application of the photocleavable polymer, but the conditions had to be carefully considered. Small molecule hydrolysis studies needed to be conducted at various pHs to determine the percent loss of end group. While we were able to identify conditions that allowed for polymer conjugation, some proteins are not stable to changes

in pH. Second, the *grafting-from* conjugate was easier to purify. The FPLC chromatogram demonstrated that the *grafting-from* conjugate had no residual Lys or polymer; these needed to be removed for the *grafting-to* strategy. Purification by centriprep *via* ultracentrifugation was not sufficient in removing excess unmodified protein in the latter. This led to the conjugate being subjected to further FPLC purification steps. FPLC often leads to lower yields and can destabilize some biomolecules. Consequently, this is problematic if the protein of interest is expensive or prepared in small quantity. Third, due to the unmodified enzyme in the first case, the conjugate needed to be purified prior to performing the activity assay in order to obtain accurate results (Figure 3.3C), which was not necessary in the case of the *grafting from* strategy (Figure 3.6C).

While not explored for the scope of this paper, potential advantages for the *grafting-to* approach would be an easy expansion of the polymer structure with fewer restrictions; the *grafting-from* approach has a narrow set of acceptable conditions (aqueous solutions, temperatures, pHs, etc.) that can be used for the polymerization directly off the protein. For example, this can be especially difficult when attempting to prepare water-insoluble polymers; although this has been achieved by Velonia et al[32]. Furthermore, depending on the protein being used for the system, *grafting-from* may not be ideal if the protein is not stable enough to withstand the polymerization conditions.

Table 3.2 Summary of advantages and disadvantages of two strategies.

Grafting-To	*Grafting-From*
☑ Targeting MW	☒ Targeting MW
☒ Hydrolysis of End-Group	☑ Hydrolysis of End-Group
☒ Ease of Purification	☑ Ease of Purification
☑ Versatility of Polymer Prepared	☒ Versatility of Polymer Prepared
☑ Protein Employed	☒ Protein Employed

3.3 Conclusions

In summary, protein-polymer conjugates containing a photocleavable linkage were successfully prepared by both *grafting-to* and *grafting-to* strategies. It was determined that the latter approach was more favourable for synthesizing the conjugates due to ease in purification and avoidance of hydrolysis of the end-group. Furthermore, it was shown that the photocleavable linkage serves as an effective method for the controlled release of polymers after conjugation and modulation of enzyme activity. This system can be easily adapted to other proteins and polymers, which expands the tool box for reversible bioconjugation development

3.4 References

(1) JevsÌ□evar, S.; Kunstelj, M.; Porekar, V. G. PEGylation of Therapeutic Proteins. *Biotechnol. J.* **2010**, *5* (1), 113–128. https://doi.org/10.1002/biot.200900218.

(2) Gong, Y.; Leroux, J.-C.; Gauthier, M. A. Releasable Conjugation of Polymers to Proteins. *Bioconjug. Chem.* **2015**, *26* (7), 1172–1181. https://doi.org/10.1021/bc500611k.

(3) Barltrop, J. A.; Plant, P. J.; Schofield, P. Photosensitive Protective Groups. *Chem. Commun. Lond.* **1966**, No. 22, 822–823. https://doi.org/10.1039/C19660000822.

(4) Patchornik, A.; Amit, B.; Woodward, R. B. Photosensitive Protecting Groups. *J. Am. Chem. Soc.* **1970**, *92* (21), 6333–6335. https://doi.org/10.1021/ja00724a041.

(5) Romano, A.; Roppolo, I.; Rossegger, E.; Schlögl, S.; Sangermano, M. Recent Trends in Applying Ortho-Nitrobenzyl Esters for the Design of Photo-Responsive Polymer Networks. *Materials* **2020**, *13* (12), 2777. https://doi.org/10.3390/ma13122777.

(6) Shen, W.; Zheng, J.; Zhou, Z.; Zhang, D. Approaches for the Synthesis of O-Nitrobenzyl and Coumarin Linkers for Use in Photocleavable Biomaterials and Bioconjugates and Their Biomedical Applications. *Acta Biomater.* **2020**, *115*, 75–91. https://doi.org/10.1016/j.actbio.2020.08.024.

(7) Forsythe, N. L.; Tan, M. F.; Vinciguerra, D.; Woodford, J.; Stieg, A. Z.; Maynard, H. D. Noncovalent Enzyme Nanogels via a Photocleavable Linkage. *Macromolecules* **2022**, *55* (22), 9925–9933. https://doi.org/10.1021/acs.macromol.2c01334.

(8) Georgianna, W. E.; Lusic, H.; McIver, A. L.; Deiters, A. Photocleavable Polyethylene Glycol for the Light-Regulation of Protein Function. *Bioconjug. Chem.* **2010**, *21* (8), 1404–1407. https://doi.org/10.1021/bc100084n.

(9) Yamaguchi, S.; Chujo, K.; Ohashi, N.; Minamihata, K.; Nagamune, T. Photo-Degradable Protein-Polymer Hybrid Shells for Caging Living Cells. *Chem. – Eur. J.* **2022**, *28* (12), e202103941. https://doi.org/10.1002/chem.202103941.

(10) Bontempo, D.; Heredia, K. L.; Fish, B. A.; Maynard, H. D. Cysteine-Reactive Polymers Synthesized by Atom Transfer Radical Polymerization for Conjugation to Proteins. *J. Am. Chem. Soc.* **2004**, *126* (47), 15372–15373. https://doi.org/10.1021/ja045063m.

(11) Lecolley, F.; Tao, L.; Mantovani, G.; Durkin, I.; Lautru, S.; Haddleton, D. M. A New Approach to Bioconjugates for Proteins and Peptides ("Pegylation") Utilising Living Radical Polymerisation. *Chem. Commun.* **2004**, No. 18, 2026–2027. https://doi.org/10.1039/B407712A.

(12) Bontempo, D.; Maynard, H. D. Streptavidin as a Macroinitiator for Polymerization: In Situ Protein−Polymer Conjugate Formation. *J. Am. Chem. Soc.* **2005**, *127* (18), 6508–6509. https://doi.org/10.1021/ja042230+.

(13) Heredia, K. L.; Bontempo, D.; Ly, T.; Byers, J. T.; Halstenberg, S.; Maynard, H. D. In Situ Preparation of Protein−"Smart" Polymer Conjugates with Retention of Bioactivity. *J. Am. Chem. Soc.* **2005**, *127* (48), 16955–16960. https://doi.org/10.1021/ja054482w.

(14) Lele, B. S.; Murata, H.; Matyjaszewski, K.; Russell, A. J. Synthesis of Uniform Protein−Polymer Conjugates. *Biomacromolecules* **2005**, *6* (6), 3380–3387. https://doi.org/10.1021/bm050428w.

(15) Grover, G. N.; Maynard, H. D. Protein–Polymer Conjugates: Synthetic Approaches by Controlled Radical Polymerizations and Interesting Applications. *Curr. Opin. Chem. Biol.* **2010**, *14* (6), 818–827. https://doi.org/10.1016/j.cbpa.2010.10.008.

(16) Pelegri-O'Day, E. M.; Maynard, H. D. Controlled Radical Polymerization as an Enabling Approach for the Next Generation of Protein–Polymer Conjugates. *Acc. Chem. Res.* **2016**, *49* (9), 1777–1785. https://doi.org/10.1021/acs.accounts.6b00258.

(17) Messina, M. S.; Messina, K. M. M.; Bhattacharya, A.; Montgomery, H. R.; Maynard, H. D. Preparation of Biomolecule-Polymer Conjugates by Grafting-from Using ATRP, RAFT, or ROMP. *Prog. Polym. Sci.* **2020**, *100*, 101186. https://doi.org/10.1016/j.progpolymsci.2019.101186.

(18) Bontempo, D.; Li, R. C.; Ly, T.; Brubaker, C. E.; Maynard, H. D. One-Step Synthesis of Low Polydispersity, Biotinylated Poly(N-Isopropylacrylamide) by ATRP. *Chem. Commun.* **2005**, No. 37, 4702–4704. https://doi.org/10.1039/B507912H.

(19) Ko, J. H.; Forsythe, N. L.; Gelb, M. B.; Messina, K. M. M.; Lau, U. Y.; Bhattacharya, A.; Olafsen, T.; Lee, J. T.; Kelly, K. A.; Maynard, H. D. Safety and Biodistribution Profile of Poly(Styrenyl Acetal Trehalose) and Its Granulocyte Colony Stimulating Factor Conjugate. *Biomacromolecules* **2022**, *23* (8), 3383–3395. https://doi.org/10.1021/acs.biomac.2c00511.

(20) Forsythe, N. L.; Maynard, H. D. Synthesis of Disulfide-Bridging Trehalose Polymers for Antibody and Fab Conjugation Using a Bis-Sulfone ATRP Initiator. *Polym. Chem.* **2021**, *12* (9), 1217–1223. https://doi.org/10.1039/D0PY01579B.

(21) Pelegri-O'Day, E. M.; Matsumoto, N. M.; Tamshen, K.; Raftery, E. D.; Lau, U. Y.; Maynard, H. D. PEG Analogs Synthesized by Ring-Opening Metathesis Polymerization for Reversible Bioconjugation. *Bioconjug. Chem.* **2018**, *29* (11), 3739–3745. https://doi.org/10.1021/acs.bioconjchem.8b00635.

(22) Mansfield, K. M.; Maynard, H. D. Site-Specific Insulin-Trehalose Glycopolymer Conjugate by Grafting from Strategy Improves Bioactivity. *ACS Macro Lett.* **2018**, *7* (3), 324–329. https://doi.org/10.1021/acsmacrolett.7b00974.

(23) Griffin, D. R.; Schlosser, J. L.; Lam, S. F.; Nguyen, T. H.; Maynard, H. D.; Kasko, A. M. Synthesis of Photodegradable Macromers for Conjugation and Release of Bioactive Molecules. *Biomacromolecules* **2013**, *14* (4), 1199–1207. https://doi.org/10.1021/bm400169d.

(24) Szczepaniak, G.; Fu, L.; Jafari, H.; Kapil, K.; Matyjaszewski, K. Making ATRP More Practical: Oxygen Tolerance. *Acc. Chem. Res.* **2021**, *54* (7), 1779–1790. https://doi.org/10.1021/acs.accounts.1c00032.

(25) Jakubowski, W.; Min, K.; Matyjaszewski, K. Activators Regenerated by Electron Transfer for Atom Transfer Radical Polymerization of Styrene. *Macromolecules* **2006**, *39* (1), 39–45. https://doi.org/10.1021/ma0522716.

(26) H. Nguyen, N.; Kulis, J.; Sun, H.-J.; Jia, Z.; Beusekom, B. van; E. Levere, M.; A. Wilson, D.; J. Monteiro, M.; Percec, V. A Comparative Study of the SET-LRP of Oligo(Ethylene Oxide) Methyl Ether Acrylate in DMSO and in H2O. *Polym. Chem.* **2013**, *4* (1), 144–155. https://doi.org/10.1039/C2PY20782F.

(27) Rademacher, J. T.; Baum, M.; Pallack, M. E.; Brittain, W. J.; Simonsick, W. J. Atom Transfer Radical Polymerization of N,N-Dimethylacrylamide. *Macromolecules* **2000**, *33* (2), 284–288. https://doi.org/10.1021/ma991550o.

(28) Matyjaszewski, K.; Coca, S.; Gaynor, S. G.; Wei, M.; Woodworth, B. E. Zerovalent Metals in Controlled/"Living" Radical Polymerization. *Macromolecules* **1997**, *30* (23), 7348–7350. https://doi.org/10.1021/ma9712581.

(29) Schöneich, C. Photo-Degradation of Therapeutic Proteins: Mechanistic Aspects. *Pharm. Res.* **2020**, *37* (3), 45. https://doi.org/10.1007/s11095-020-2763-8.

(30) Udenfriend, S.; Stein, S.; Böhlen, P.; Dairman, W.; Leimgruber, W.; Weigele, M. Fluorescamine: A Reagent for Assay of Amino Acids, Peptides, Proteins, and Primary Amines in the Picomole Range. *Science* **1972**, *178* (4063), 871–872. https://doi.org/10.1126/science.178.4063.871.

(31) Jing, M.; Song, W.; Liu, R. Binding of Copper to Lysozyme: Spectroscopic, Isothermal Titration Calorimetry and Molecular Docking Studies. *Spectrochim. Acta. A. Mol. Biomol. Spectrosc.* **2016**, *164*, 103–109. https://doi.org/10.1016/j.saa.2016.04.008.

(32) Velonia, K.; Rowan, A. E.; Nolte, R. J. M. Lipase Polystyrene Giant Amphiphiles. *J. Am. Chem. Soc.* **2002**, *124* (16), 4224–4225. https://doi.org/10.1021/ja017809b.

3.5 Materials and Methods

Acetovanillone was purchased from Oakwood Chemicals. O-(Benzotriazol-1-yl)-N,N,N',N'-tetramethyluronium hexafluorophosphate (HBTU) and N,N'-disuccinimidyl carbonate (DSC) were purchased from Chem-Impex International. Tin(II) 2-ethylhexanoate, fluorescamine, and tris(2-dimethylaminoethyl)amine, were purchased from Alfa Aesar. All other chemicals were purchased from Sigma-Aldrich and Fisher Scientific and were used without purification unless otherwise noted. For PEGA, 100 ppm BHT and 100 ppm MEHQ inhibitors were removed by passing through a plug of basic alumina. Copper bromide (Cu(I)Br) was purified by stirring in glacial acetic acid for 16 hours, filtering and rinsing with ethanol and diethyl ether twice and storing in a desiccator. Lysozyme from chicken egg white, Catalog No. J60701.06, Lot: V041520 was purchased from Sigma Aldrich. Lyophilized cells from Micrococcus Lysodeikticus ATCC No. 4698 were purchased from Sigma Aldrich. For photocleavage experiments, a 4 watt, 365 nm lamp was used (brand: UVP).

3.6 Analytical Techniques

Nuclear Magnetic Resonance (NMR) spectra were recorded on a Bruker AV 400 MHz and Bruker AV 500 MHz spectrometer. Proton NMR spectra were acquired with a relaxation delay for 2 s for small molecules. Abbreviations are s = singlet, d = doublet, t = triplet, q = quartet, p = pentet, m = multiplet. Mass spectrometry for small molecules and lysozyme macroinitiators was obtained on an Agilent Q-TOF 6530 Liquid Chromatography/Mass Spectrometry (LC/MS) using a 10-95% acetonitrile gradient over 15 minutes. Mass spectrometry for lysozyme conjugates was

obtained on a Bruker Ultraflex MALDI-TOF using sinapinic acid as the matrix. The matrix solution was prepared with a final concentration of 10 mg/mL sinapinic acid in 50/50 acetonitrile/water with 0.1% TFA. For SDS PAGE, BioRad Any kDa Mini-PROTEAN-TGX™ gels were used. SDS-PAGE protein standards were obtained from Bio-Rad (Precision Plus Protein Prestained Standards). Small molecule purification was done *via* flash chromatography and conducted on a Biotage Isolera One auto-column system. Size exclusion chromatography (SEC) measurements in N,N-dimethylformamide (DMF) were performed on an Infinity 1260 II HPLC system from Agilent equipped with a diode array detector DAD from Wyatt technology. The system also included a multiangle light scattering detector MALS and differential refractive index detector dRI from Wyatt technology. Polymers were separated on two PLgel Mixed-D gel columns PL1110-6504 (300 x 7.5 mm) (exclusion limits from 200 to 400 000 Da) at a flow rate of 0.6 mL min^{-1}. Column temperatures were held at 40°C in DMF with LiBr (0.1 M). Molar masses were calculated from PMMA standards. Conjugates were purified and analyzed by Fast Protein Liquid Chromatography on a Bio-Rad BioLogic DuoFlow chromatography system equipped with a HiTrap SP HP column employing a method of 0 to 1 M NaCl in 10 mM PB, pH 6.0 (Buffer A: 10 mM PB, pH 6.0; Buffer B: 10 mM PB, pH 6.0 + 1 M NaCl; 0.4 mL/min; 1 x 0.10 mL injections; 2 CV 0% Buffer B, then 8 CV 0- 100% Buffer B, then 2 CV 100% Buffer B). Plate reader assays for protein quantification by BSA standard assay, fluorescamine, and lysozyme activity assays were run on a Molecular Devices Spectramax iD3 instrument and data analysis was conducted on SoftMax Pro 7.1 software. Infrared spectroscopy (IR) data was collected using a Perkin Elmer University ATR Sampling Accessor Spectrum One FT-IR Spectrometer with 80 scans.

3.7. Appendix with Supplemental Figures

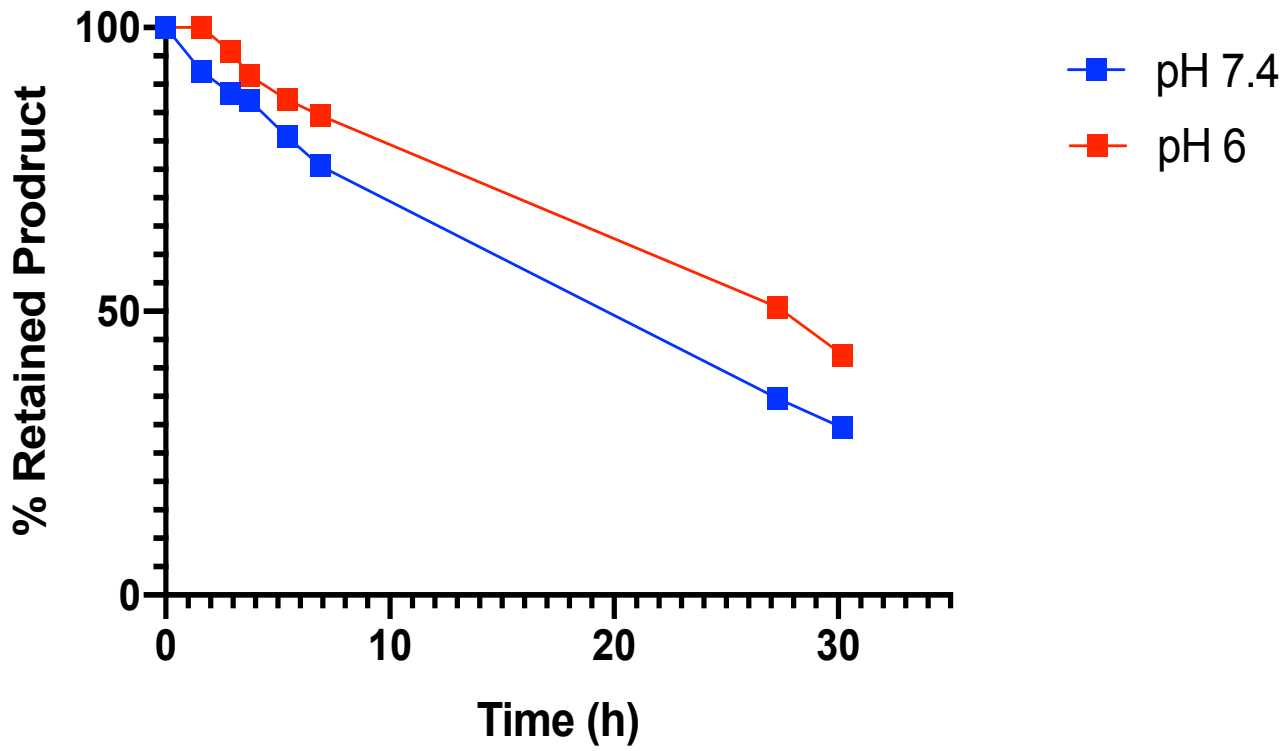

Figure S3.1 Hydrolysis studies of photocleavable initiator

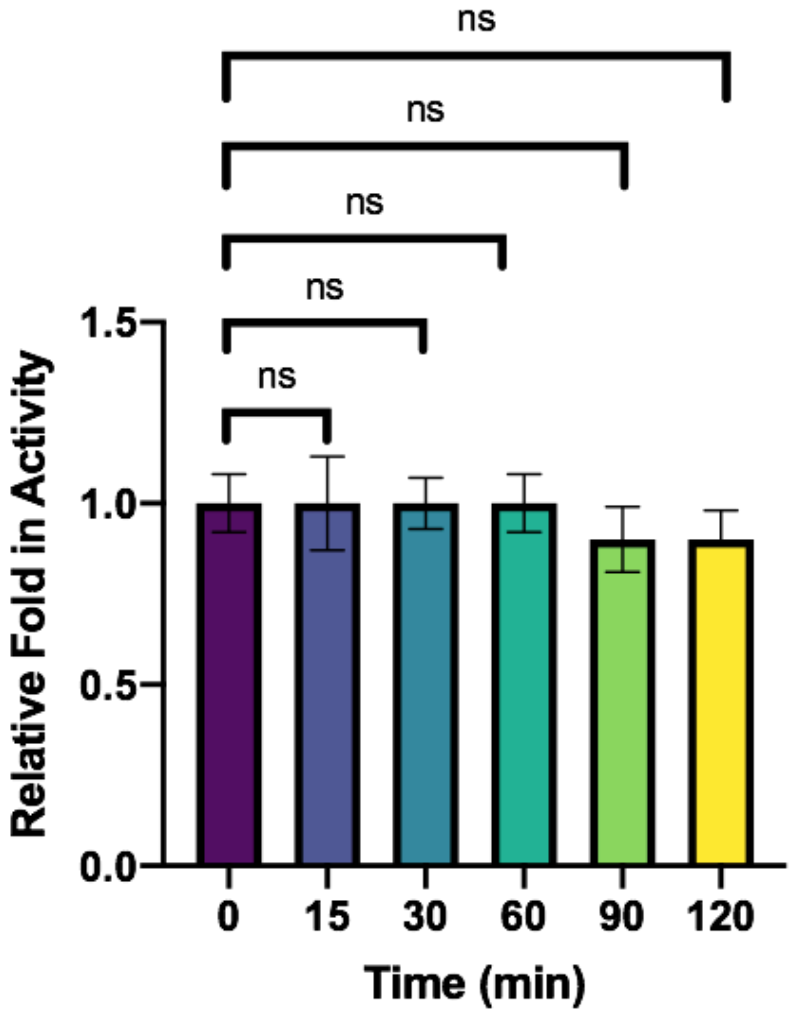

Figure S3.2 Impact of native lysozyme activity upon exposure to UV irradiation.

Each measurement was conducted in triplicate and statistical significance was determined via a one-way ANOVA with multiple comparisons (ns = $p \geq 0.05$ compared against the sample at t = 0 min).

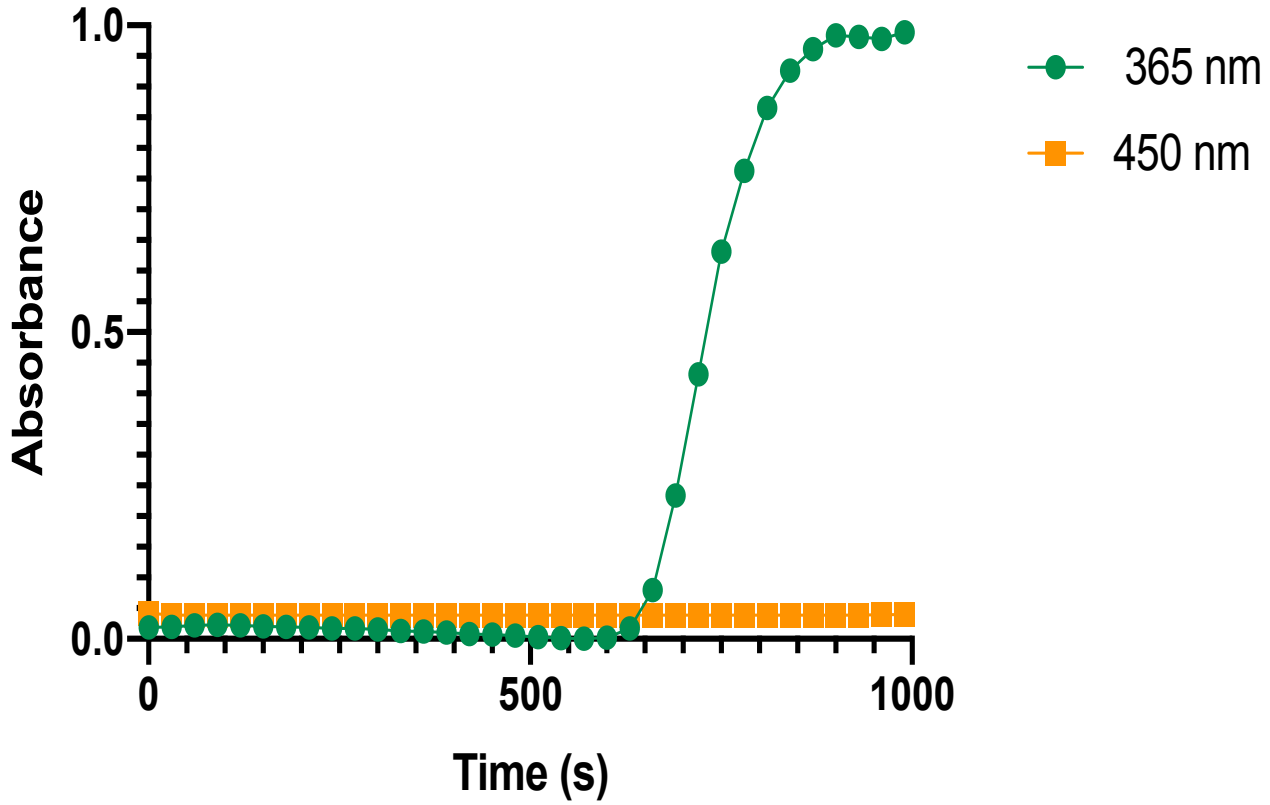

Figure S3.3 Absorbance measurements of conjugate after exposure to different wavelengths over time.

Measurements were taken at 365 nm and 450 nm, respectively, over the course of 16 minutes at 30 second intervals. The result shows that 450 nm utilized in the activity assay does not change protein absorbance, while 365 does, due to cleavage of the polymer.

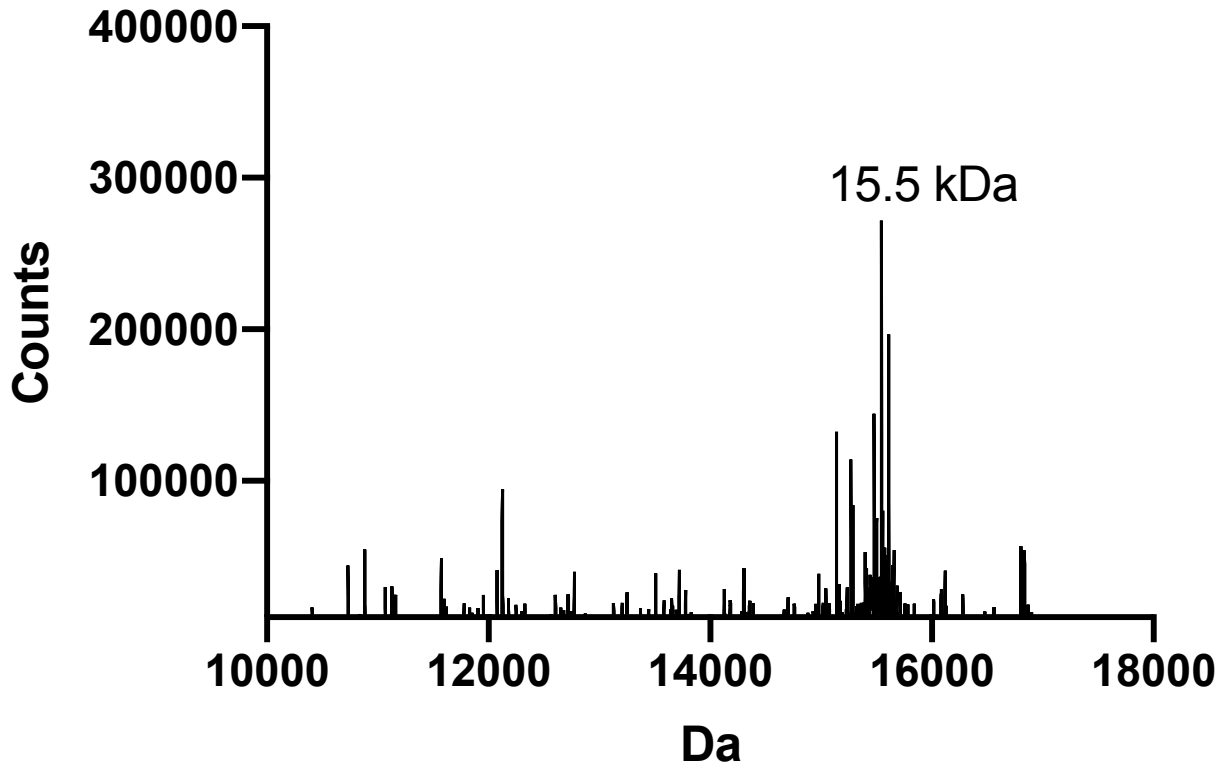

Figure S3.4 LCMS spectrum of non-cleavable lysozyme macroinitiator.

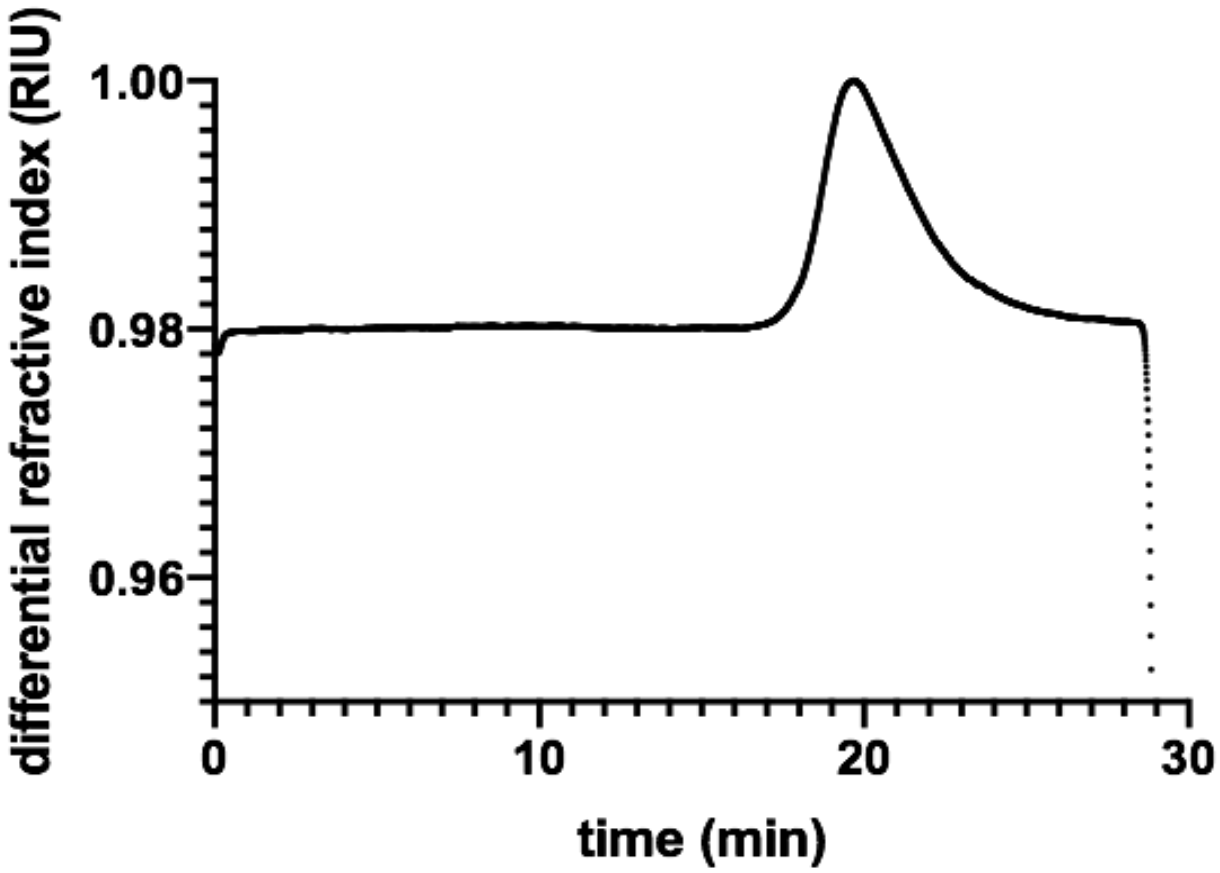

Figure S3.5 DMF SEC trace of polymer from *grafting-from.*

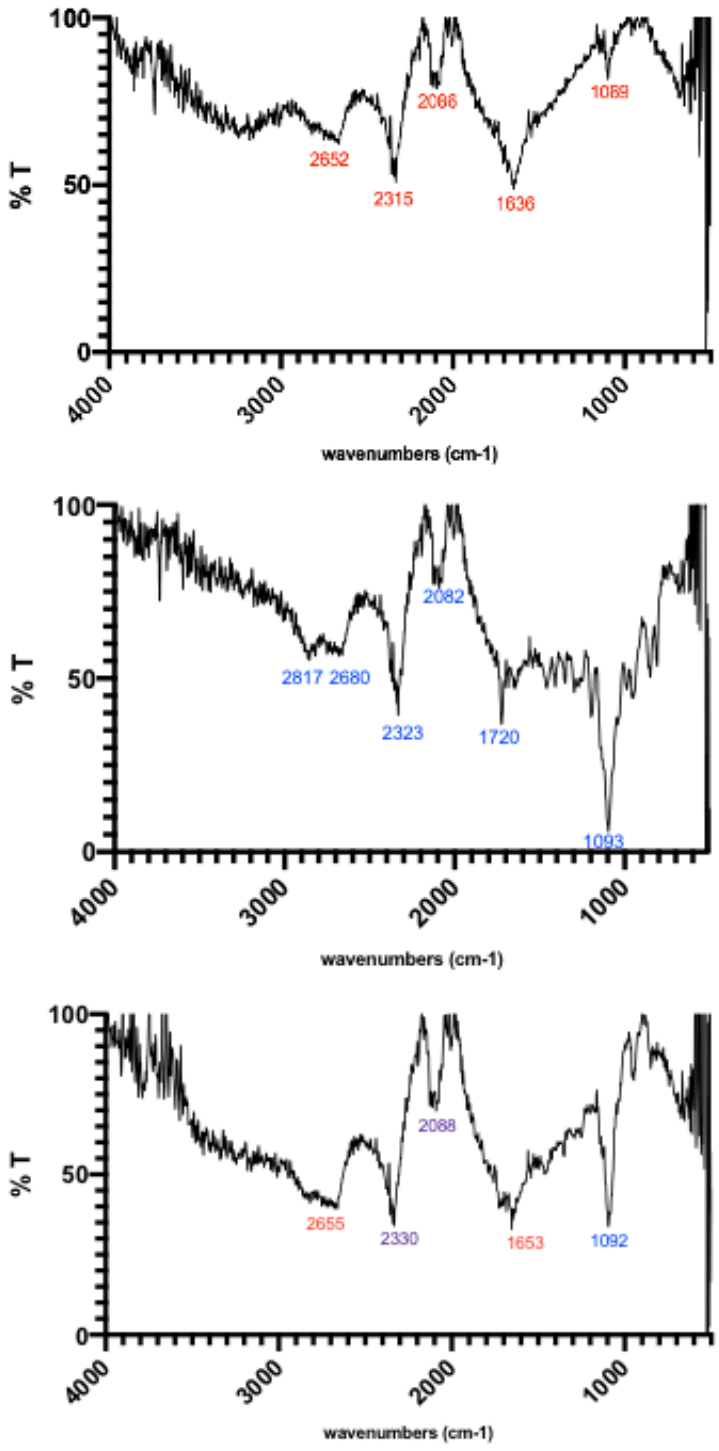

Figure S3.6 IR analysis of *grafting-from* conjugate.

Lysozyme macroinitiator (top), PEGA monomer (middle), lysozyme polymer conjugate (bottom).

Other DMF SEC Traces

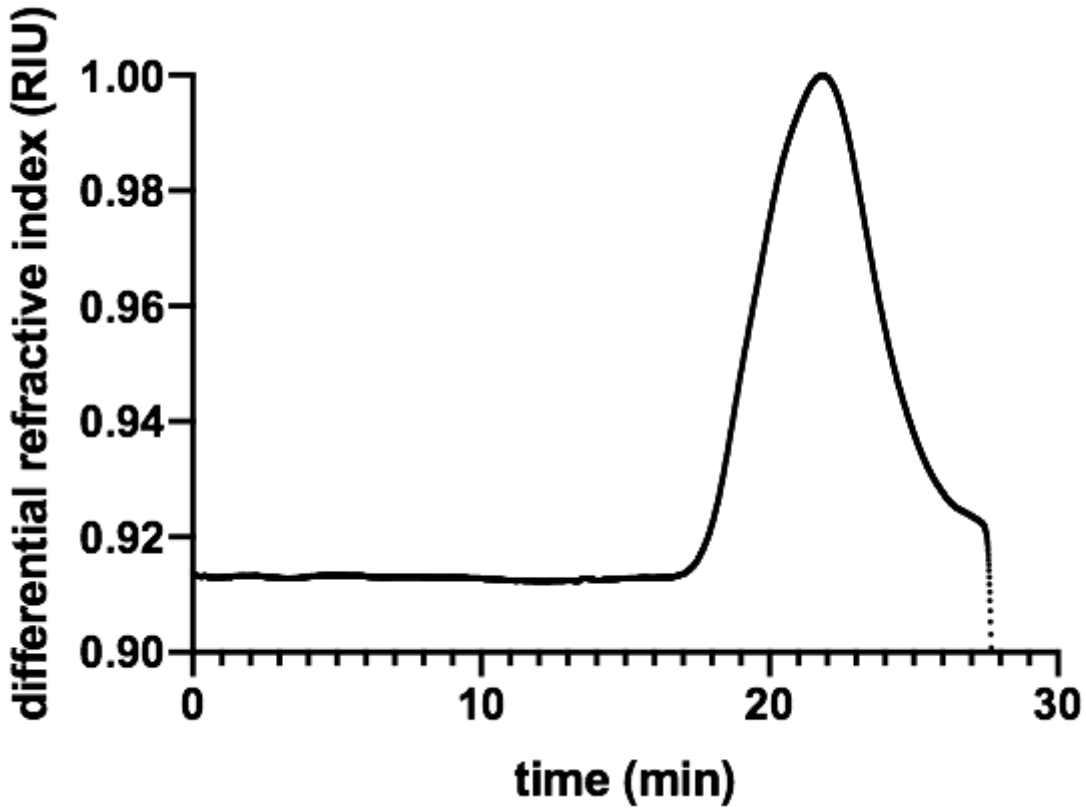

Figure S3.7 DMF SEC trace of polymer entry 3 (Table 1).

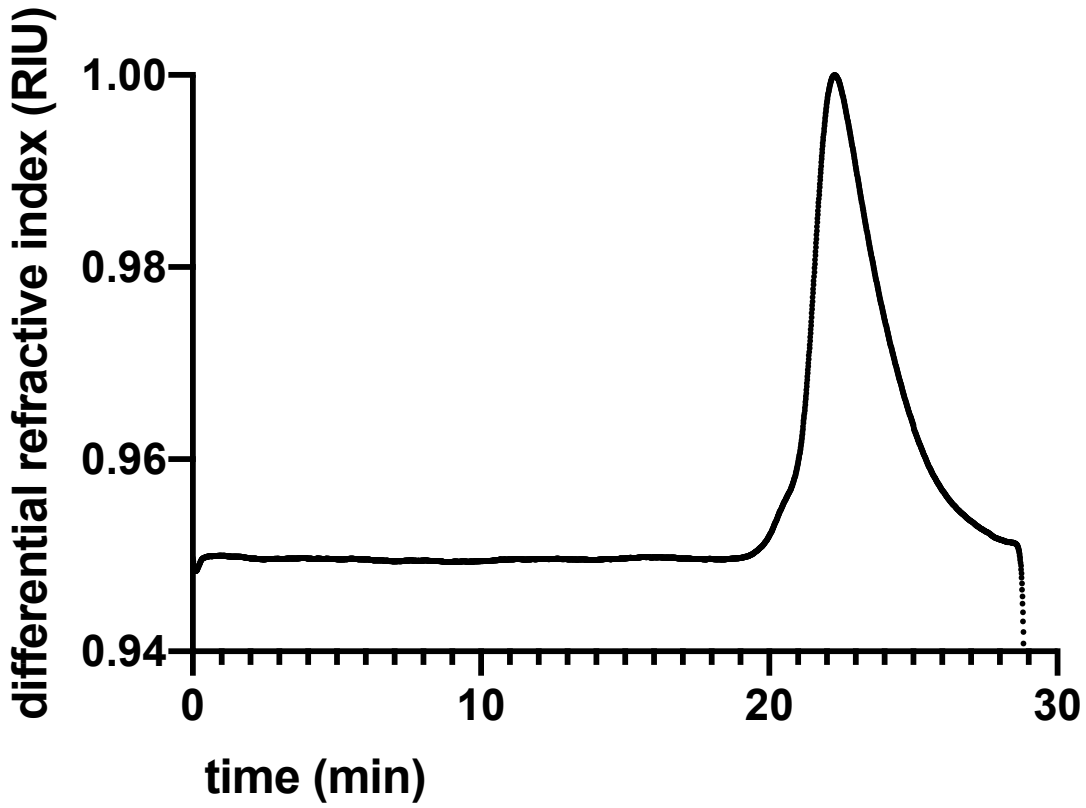

Figure S3.8 DMF SEC trace of polymer entry 5 (Table 1).

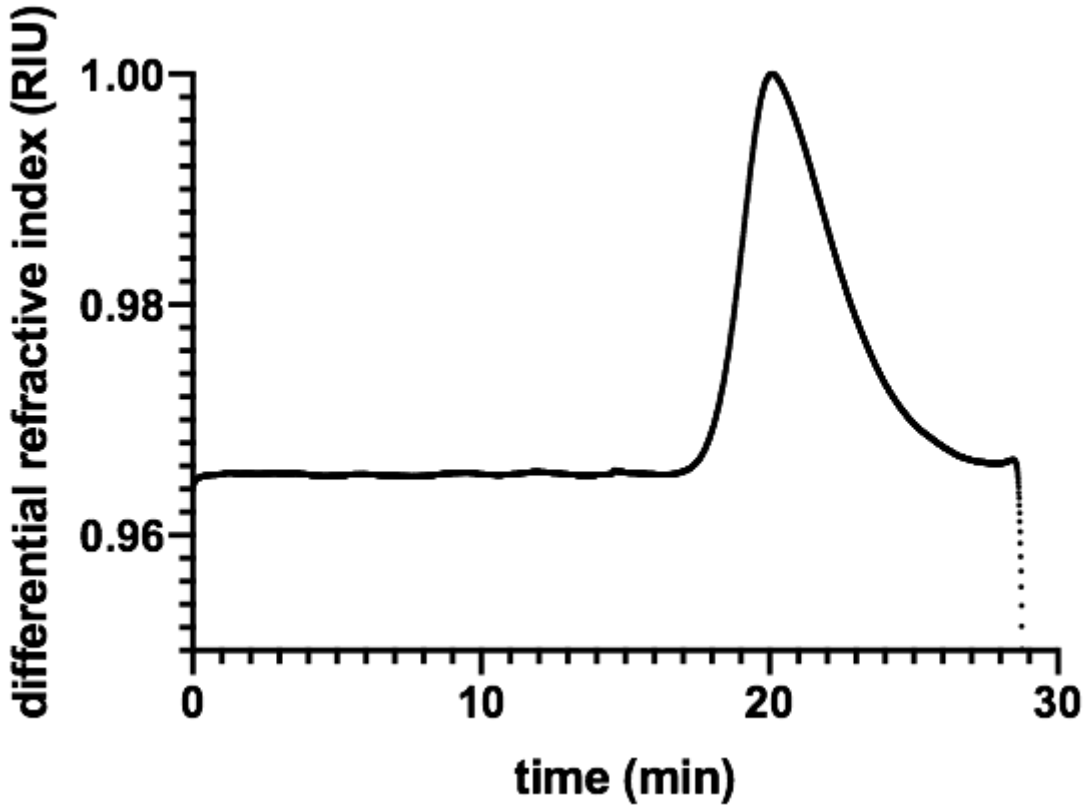

Figure S3.9 DMF SEC trace of polymer entry 6 (Table 1).

^{1}H NMR and ^{13}C NMR Spectrum for Photocleavable Initiator Synthesis

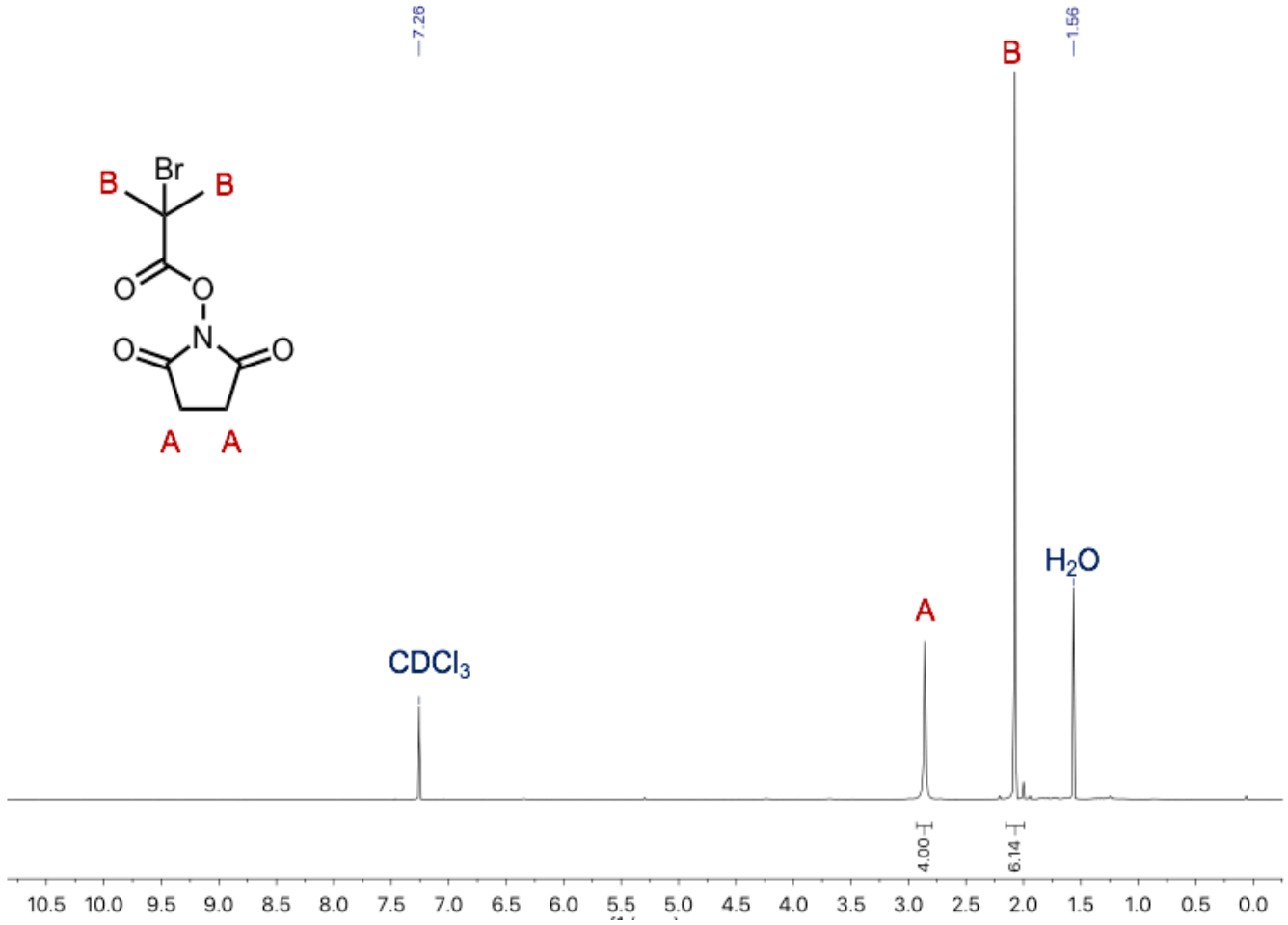

Figure S3.10 ^{1}H NMR spectrum of NHS-activated isobromobutyryl molecule in $CDCl_3$.

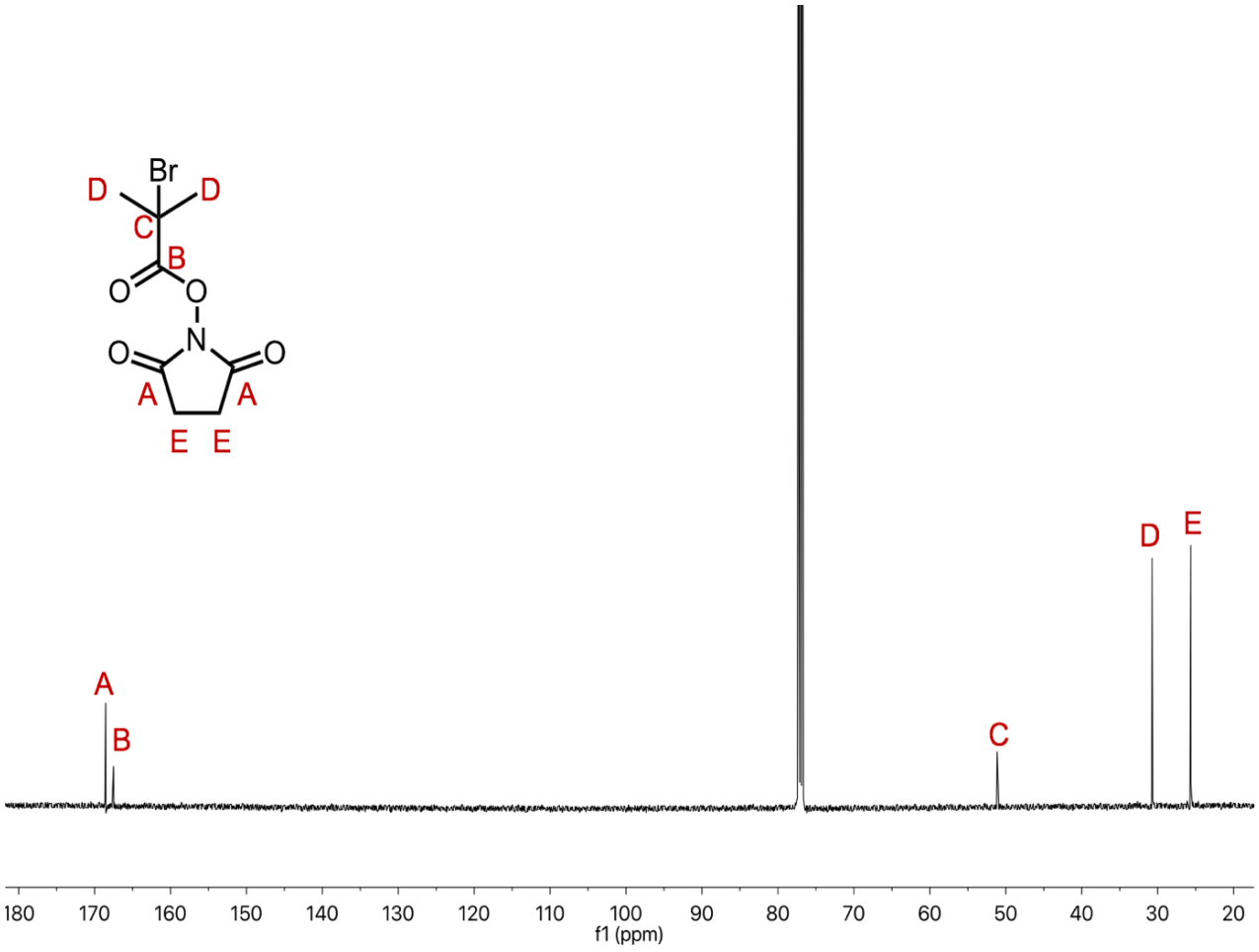

Figure S3.11 ^{13}C NMR spectrum of NHS-activated isobromobutyryl molecule in $CDCl_3$.

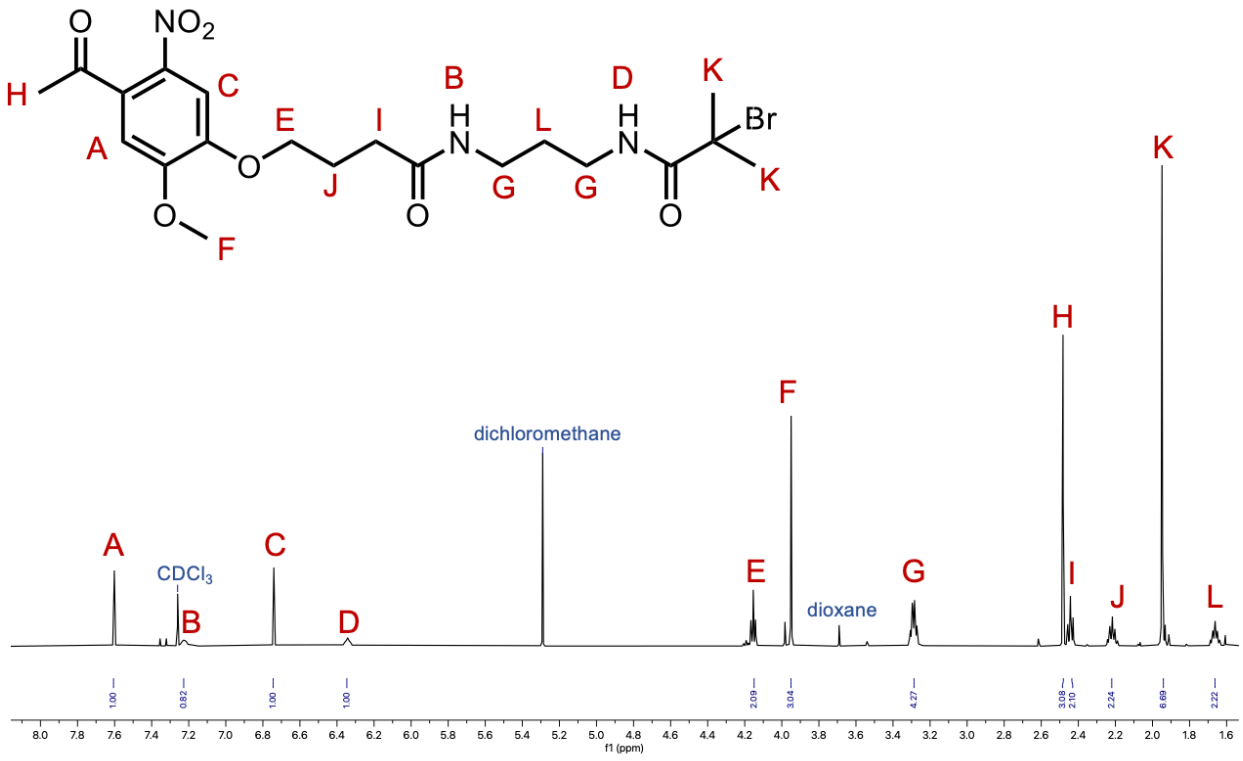

Figure S3.12 ^{1}H NMR spectrum of **1** in $CDCl_3$.

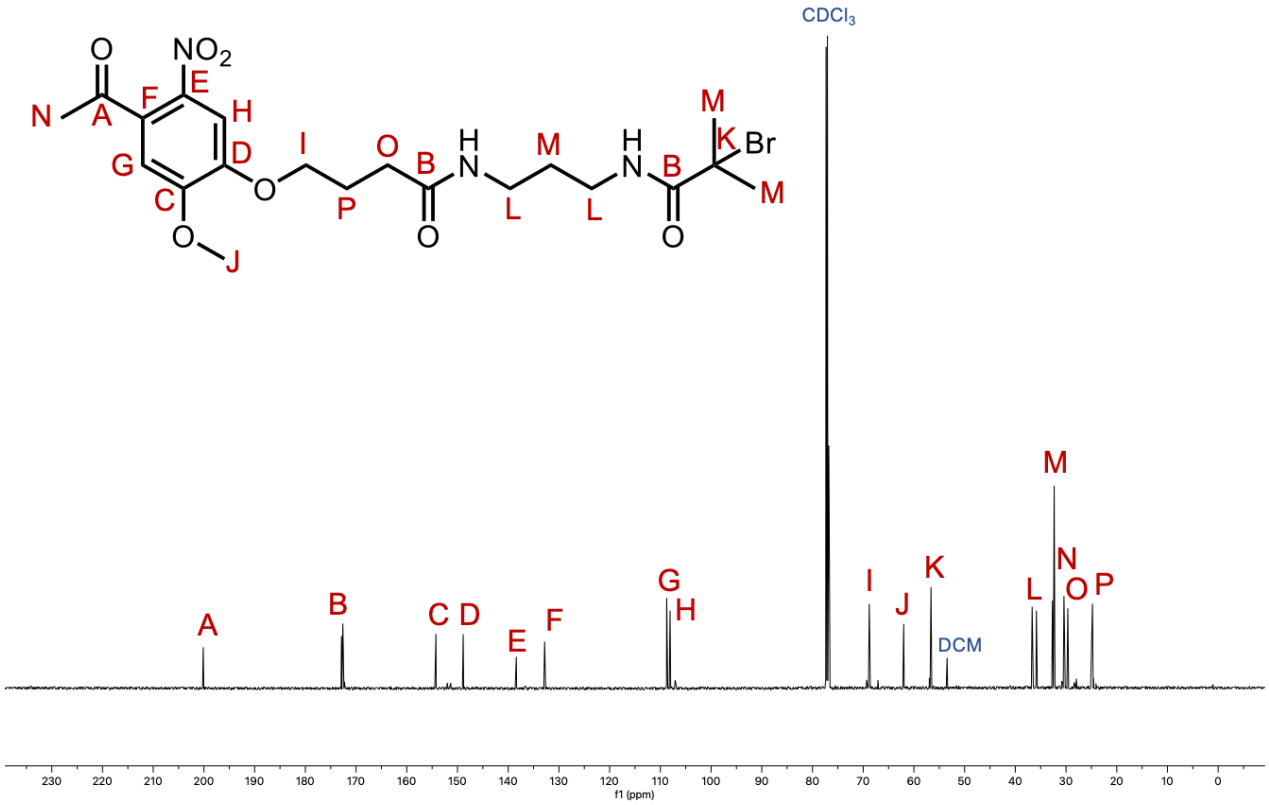

Figure S3.13 ^{13}C NMR spectrum of **1** in $CDCl_3$.

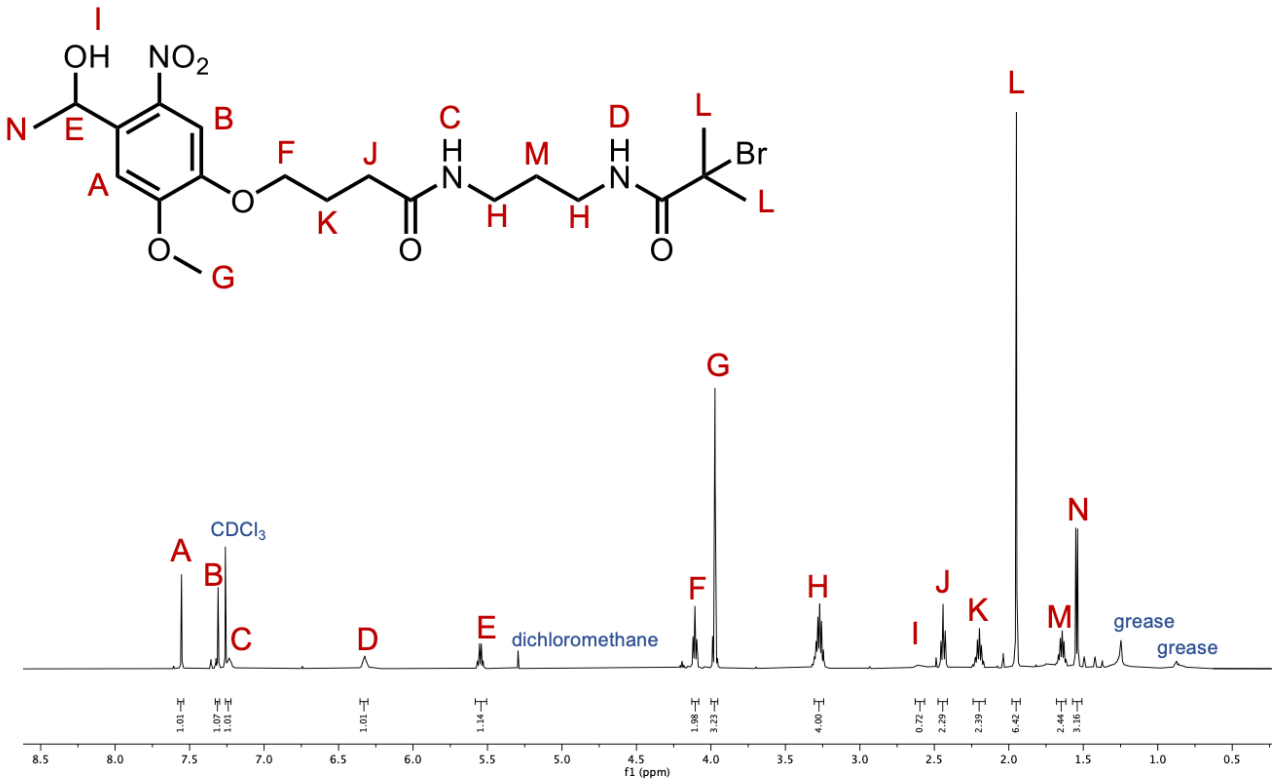

Figure S3.14 ^{1}H NMR spectrum of **2** in $CDCl_3$.

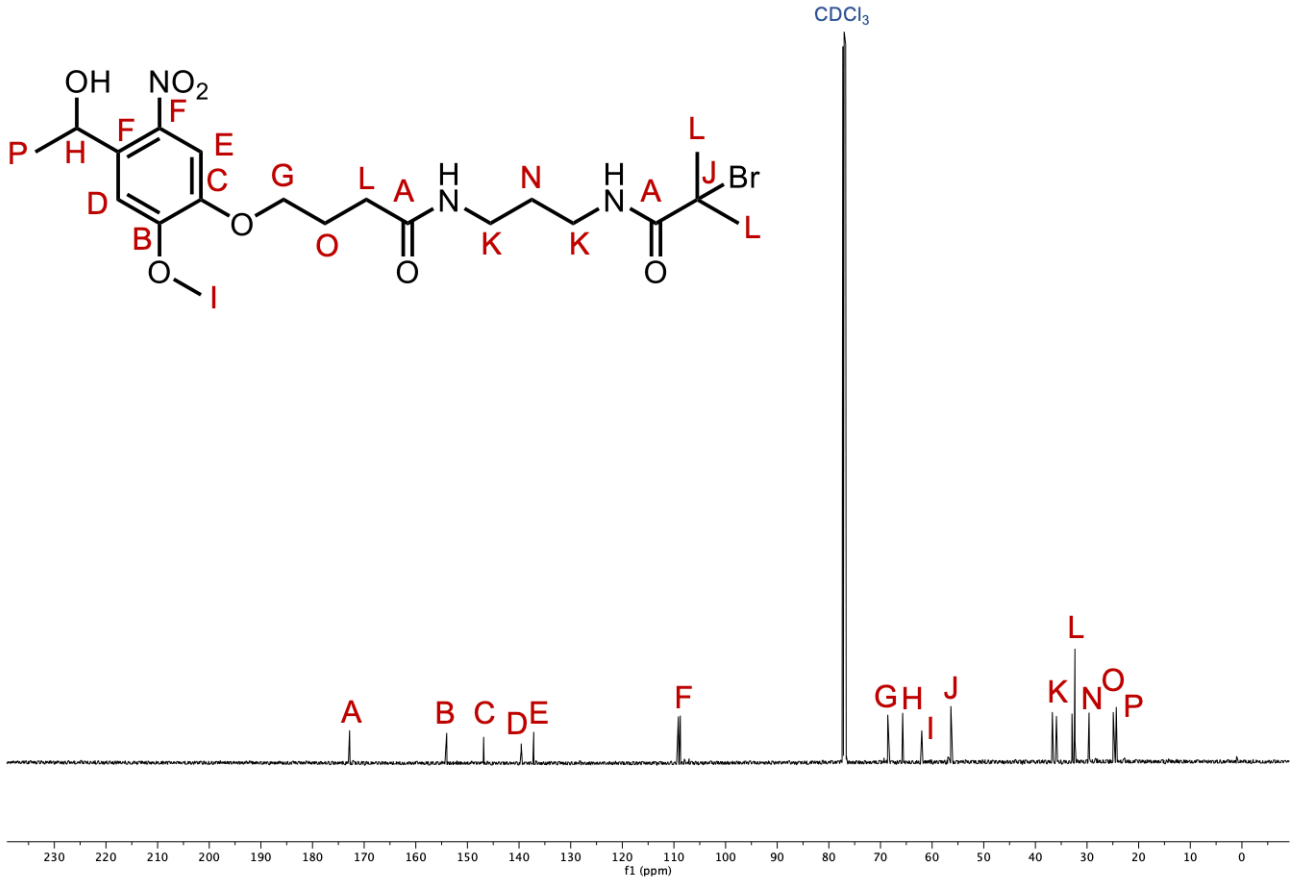

Figure S3.15 ^{13}C NMR spectrum of **2** in $CDCl_3$

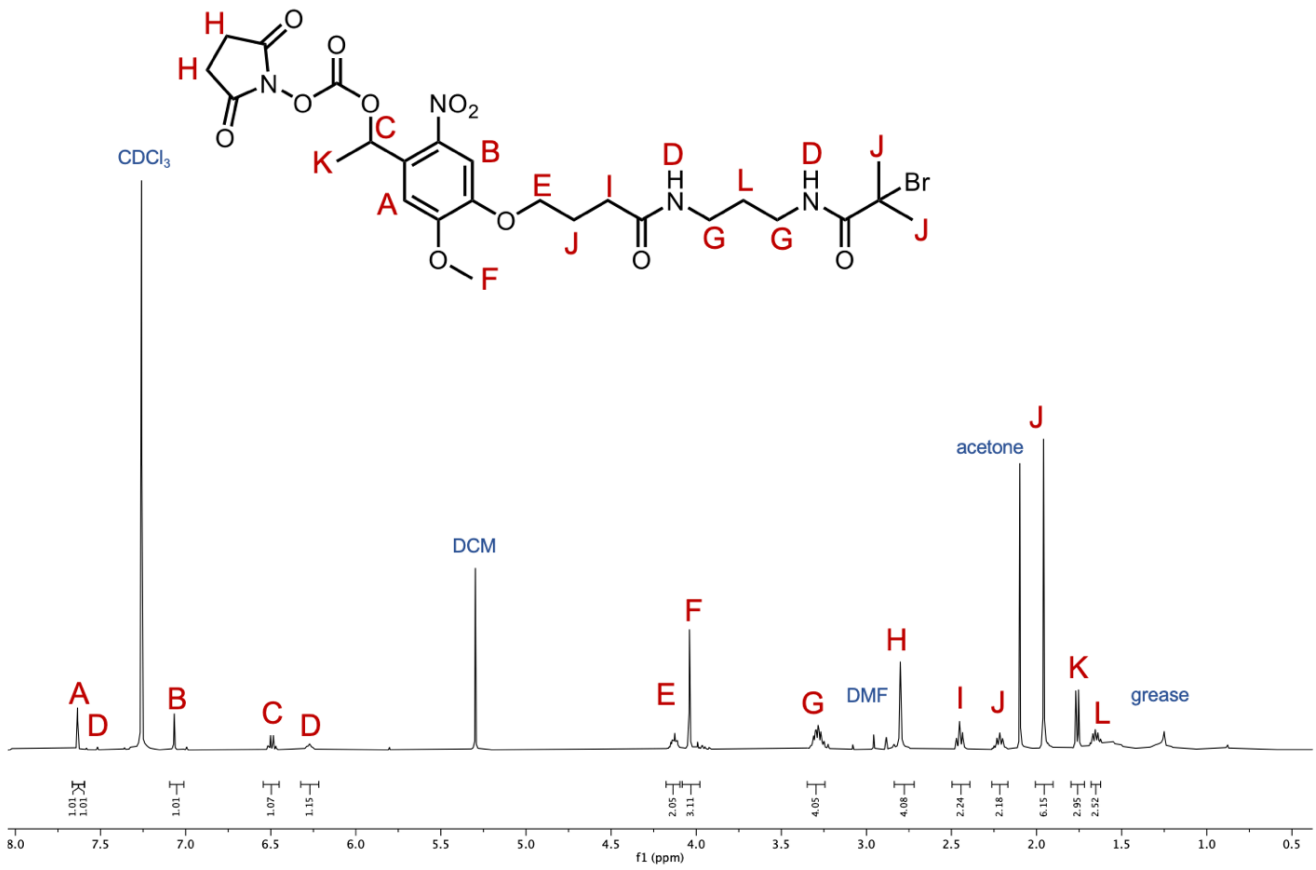

Figure S3.16 ^{1}H NMR spectrum of **3** in $CDCl_3$.

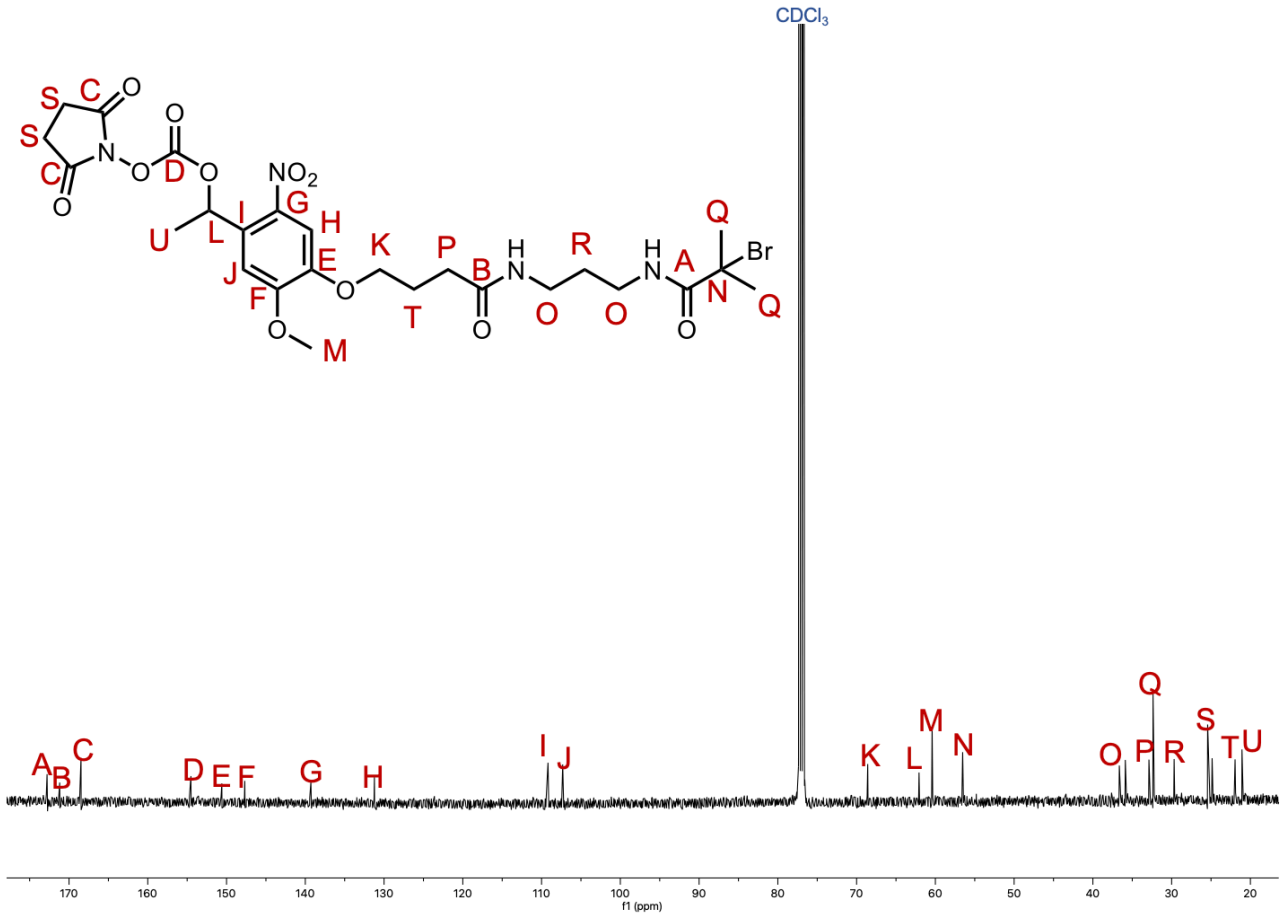

Figure S3.17 ^{13}C NMR spectrum of **3** in $CDCl_3$.

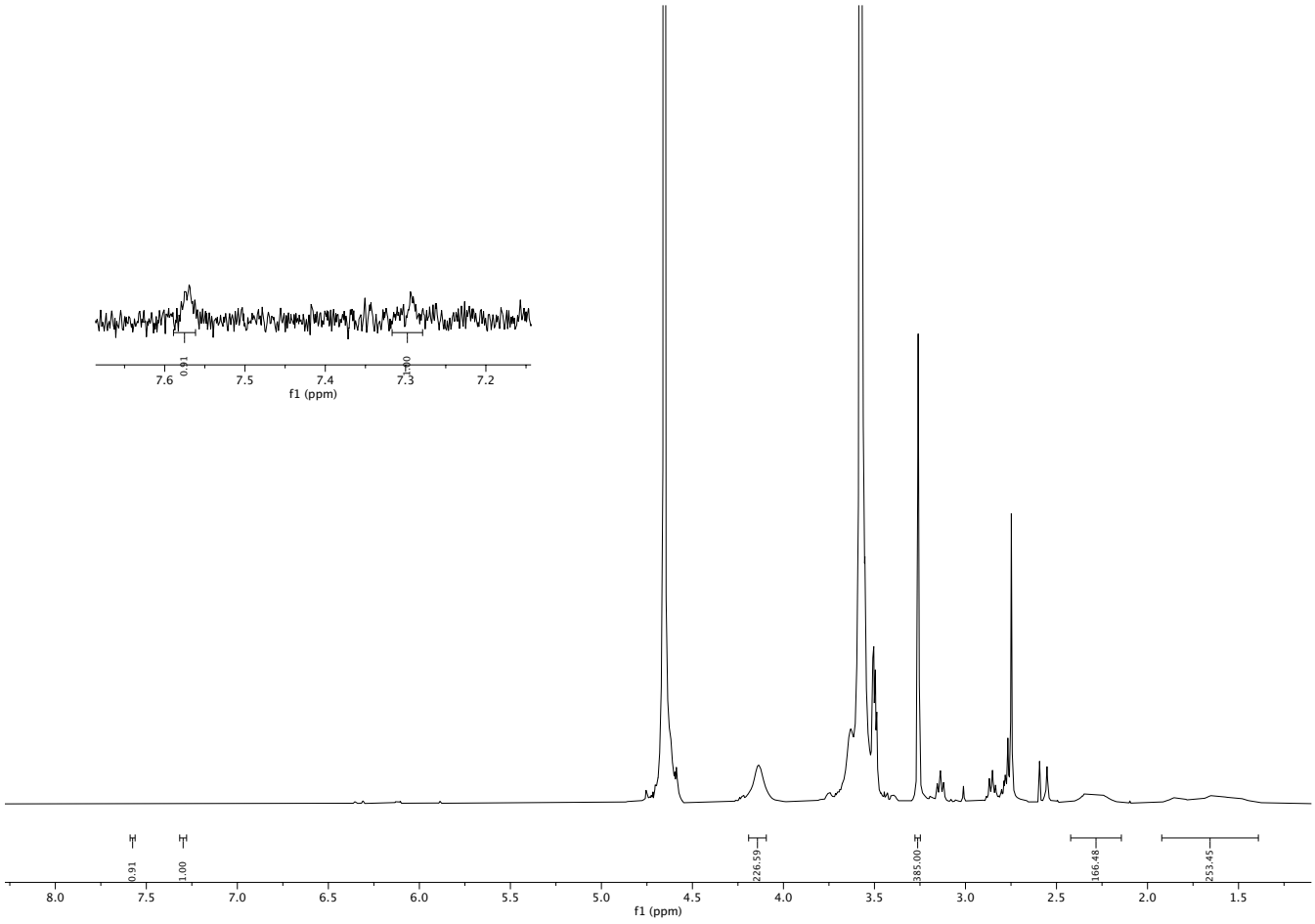

Figure S3.18 ^{1}H NMR spectrum of Entry 3 in D_2O.

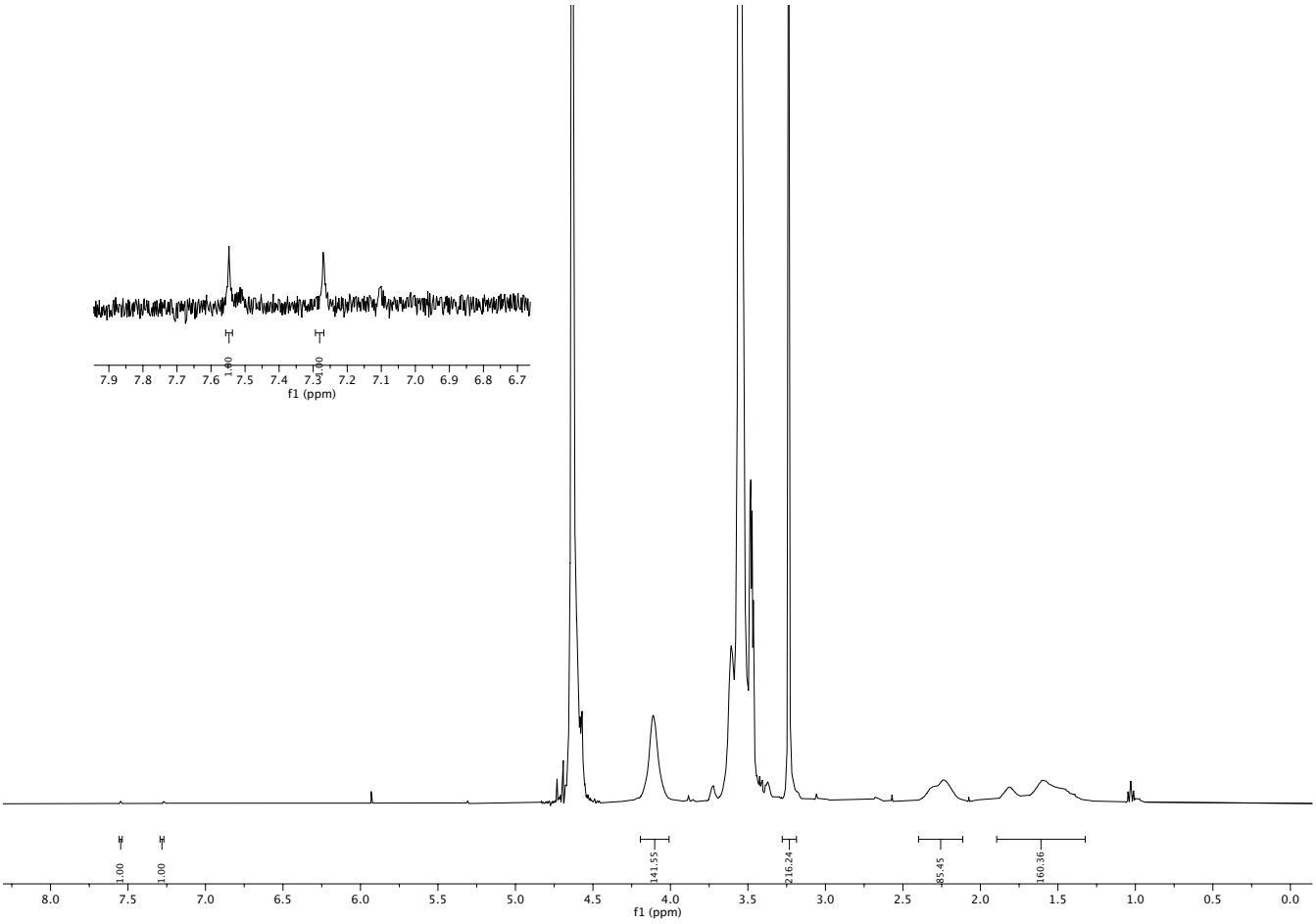

Figure S3.19 ^{1}H NMR spectrum of Entry 5 in D_2O.

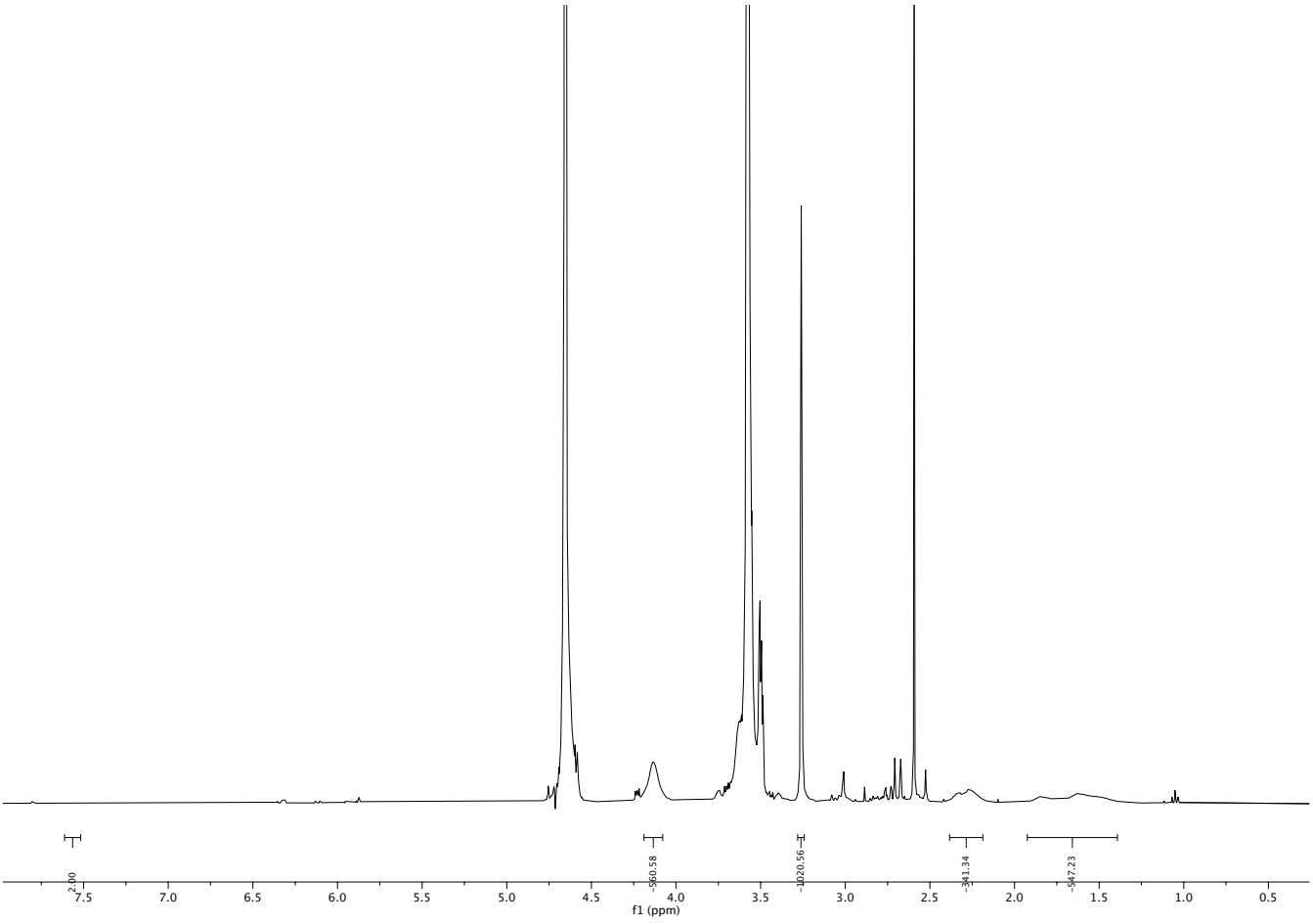

Figure S3.20 ^{1}H NMR spectrum of Entry 6 in D_2O.

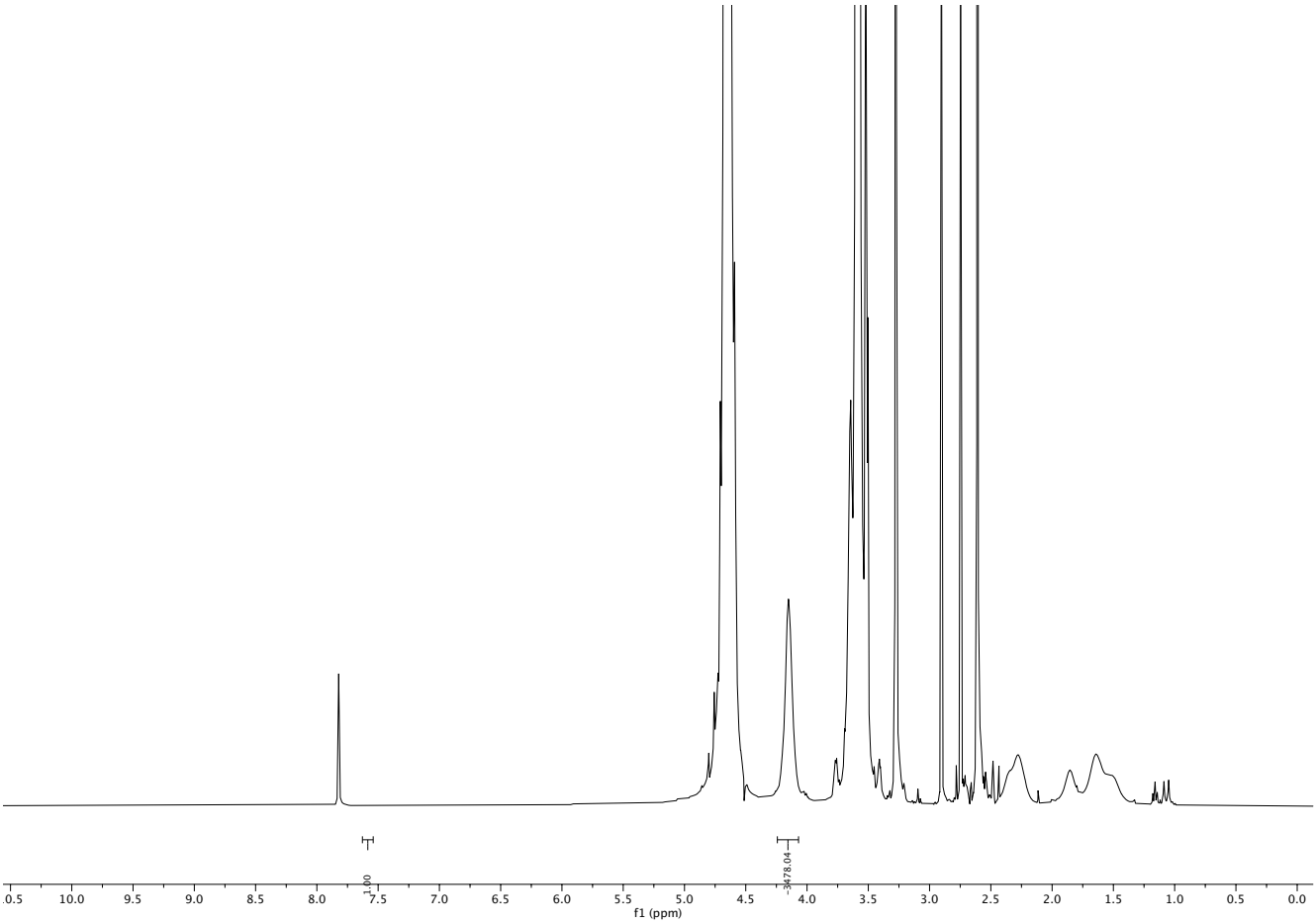

Figure S3.21 ^{1}H NMR spectrum of *grafting-from* polymer after protein digestion in D_2O.

3.8. Experimental and Appendix References

Photocleavable Initiator Synthesis.

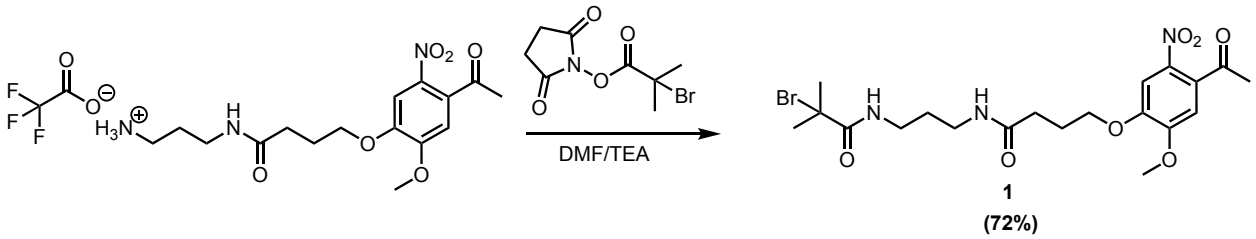

Synthesis of 1.

This reagent was prepared as previously reported.[1] 4-(4-Acetyl-2-methoxy-5-nitrophenoxy)-N-(3-aminopropyl)butanamide (1.16 g, 1 Eq, 3.28 mmol) was dissolved in 10 mL of dry DMF. Anhydrous triethylamine (TEA) (352 mg, 458 µL, 1 Eq, 3.28 mmol) and 2,5-dioxopyrrolidin-1-yl 2-bromo-2-methylpropanoate (1.73 g, 2 Eq, 6.57 mmol) were then added. Reaction proceeded for 16 hours at 25 °C. After reaction, the crude mixture was then precipitated into dry diethyl ether three times. 1.18 g (72% yield) product was collected as a yellow wax.

^{1}H NMR (500 MHz, chloroform-*d*) δ 7.60 (s, 1H), 7.23 (s, 1H), 6.74 (s, 1H), 6.34 (s, 1H), 4.15 (t, *J* = 6.2 Hz, 2H), 3.95 (s, 3H), 3.29 (m, *J* = 6.2, 1.7Hz, 4H), 2.46 (s, 2H), 2.26 – 2.16 (m, 2H), 1.94 (d, *J* = 1.8 Hz, 6H), 1.66 (m, *J* = 7.7, 5.5, 4.0, 2H). ^{13}C NMR (126 MHz, chloroform-*d*) δ 200.11, 172.97, 172.87, 154.23, 148.86, 138.39, 132.81, 108.74, 107.07, 77.24, 62.00, 56.62, 53.45, 36.71, 35.85, 32.69, 32.34, 30.84, 30.41, 24.10. IR: ν = 2155, 1967, 1964, 1706, 1645, 1517, 1363, 1278, 1205, 1036, 649 cm^{-1}. ESI-MS calculated for $C_{20}H_{28}BrN_3O_7$ $[M+H]^+$ Expected: 502.11 Observed: 502.13

^{1}H and ^{13}C NMR results are similar to what was previously published.[1]

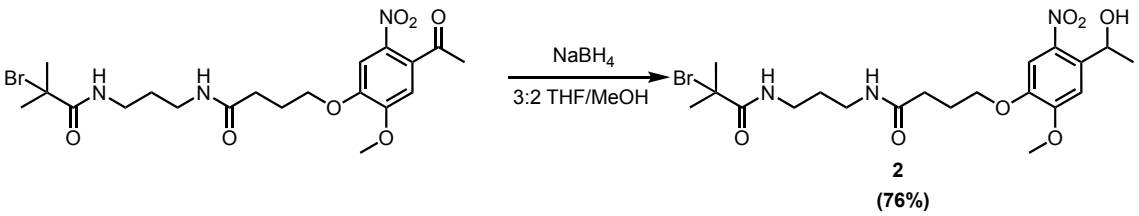

Synthesis of 2.

4-(4-Acetyl-2-methoxy-5-nitrophenoxy)-N-(3-(2-bromo-2-methylpropanamido)propyl)-butanamide (809 mg, 1 Eq, 1.61 mmol) was dissolved in 10 mL of 3:2 tetrahydrofuran/methanol (THF/MeOH) with a stir bar in a glass scintillation vial. Sodium borohydride (243 mg, 4 Eq, 6.44 mmol) was then added in portions, resulting in the evolution of H_2. Reaction was allowed to proceed at 25 °C for 3 h. Saturated NH_4Cl was then added to quench the reaction, and the organic layer was collected. The aqueous layer was then extracted three times with ethyl acetate. The organic layers were combined and dried with $MgSO_4$ to yield and concentrated. 620 mg (76%) of product was collected as a yellow wax.

^{1}H NMR (500 MHz, chloroform-*d*) δ 7.55 (s, 1H), 7.30 (s, 1H), 7.22 (d, *J* = 7.2 Hz, 1H), 6.32 (t, *J* = 6.4 Hz, 1H), 5.54 (q, *J* = 6.3 Hz, 1H), 4.10 (t, *J* = 6.2 Hz, 2H), 3.97 (s, 3H), 3.34 – 3.21 (m, 4H), 2.56 (s, 1H), 2.44 (t, *J* = 7.2 Hz, 2H), 2.27 – 2.15 (m, 2H), 1.94 (s, 6H), 1.70 – 1.59 (m, 2H), 1.54 (d, *J* = 6.3 Hz, 3H) ^{13}C NMR (126 MHz, Chloroform-*d*) δ 172.82, 172.80, 154.01, 146.86, 139.59, 137.15, 109.15, 108.77, 68.59, 65.71, 62.00, 56.37, 36.71, 35.92, 32.38, 32.34, 29.71, 24.92. IR: ν = 2659, 2330, 1629, 1507, 1262, 1093, 731 cm^{-1}. ESI-MS calculated for $C_{20}H_{30}BrN_3O_7$ $[M+H]^+$ Expected: 504.13 Observed: 504.14

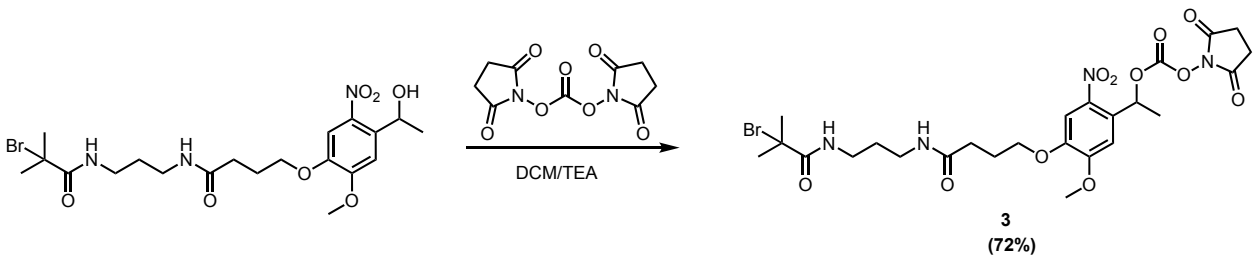

Synthesis of 3.

N-(3-(2-Bromo-2-methylpropanamido)propyl)-4-(4-(1-hydroxyethyl)-2-methoxy-5-nitrophenoxy)butanamide (732 mg, 1 Eq, 1.45mmol) was dissolved in 20 mL dry dichloromethane (DCM). N.N'-disuccinimidyl carbonate (1.86 g, 5 Eq, 7.26 mmol) and anhydrous TEA (0.147 g, 202 µL, 1 Eq, 1.45 mmol) were then added to the flask. Reaction was allowed to stir at 25 °C for 16 h. Afterwards, reaction mixture was quenched and washed three times with $NaHCO_3$ solution, dried over $MgSO_4$, and concentrated. Product was purified by gradient column chromatography (90% DCM, 10% MeOH). 685 mg (73%) of product was collected as an orange-yellow wax.

^{1}H NMR (500 MHz, chloroform-*d*) δ 7.63 (s, 1H), 7.07 (s, 1H), 6.49 (q, *J* = 6.3 Hz, 1H), 6.27 (s, 1H), 4.11 (q, *J* = 7.2 Hz, 2H), 4.04 (s, 3H), 3.28 (m, *J* = 12.2, 8.2, 6.9, 4H), 2.80 (s, 4H), 2.45 (t, *J* = 7.2 Hz, 2H), 2.21 (p, *J* = 6.8 Hz, 2H), 1.95 (s, 6H), 1.65 (p, *J* = 6.1 Hz, 2H), 1.59 (m, 3H). ^{13}C NMR (126 MHz, chloroform-*d*)) δ 172.77, 172.72, 171.16, 168.46, 154.50, 150.58, 147.66, 139.27, 131.21, 109.17, 107.30, 68.58, 62.06, 60.41, 56.53, 36.64, 32.88, 32.36, 29.68, 25.43, 24.86, 21.07. IR: ν = 2658, 2330, 1697, 1628, 1508, 1197, 1070, 636 cm^{-1}.

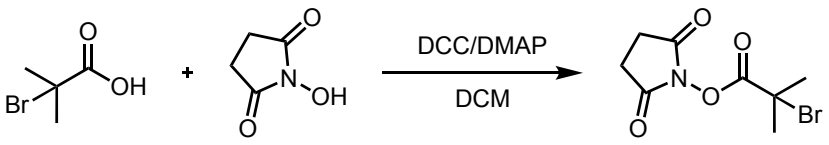

Synthesis of NHS-activated bromoisobutyryl initiator .

This procedure was adapted from Zhang, A. et al.[2] To a 250 mL round bottom flask were added 2-bromo-2-methylpropanoic acid (10 g, 1 Eq, 60 mmol), N-hydroxysuccinimide (NHS) (10 g, 1.5 Eq, 90 mmol), N,N'-dicydclohexylcarbodiimide (DCC) (19 g, 1.5 Eq, 90 mmol), and 4-dimethylaminopyridine (DMAP) (1.5 g, 0.2 Eq, 12 mmol). These reagents were suspended in 60 mL of DCM. Reaction was allowed to stir for 16 hours at 25 ℃. The crude reaction was then filtered and purified by gradient column chromatography (85% DCM, 15% MeOH). 12.2 g (77%) of product was collected as a white solid.

1H NMR (500 MHz, chloroform-*d*) δ 2.86 (s, 2H), 2.08 (d, J = 1.2 Hz, 3H). 13C NMR (126 MHz, chloroform-*d*) δ 168.53, 167.49, 51.14, 30.73, 25.64. IR: ν = 2661, 2331, 1078 cm-1. 1H and 13C NMR results are similar to what was previously published.[2]

General Procedure for the AGET ATRP of PEGA with 3.

To a 10 mL Schlenk flask was added Me_6TREN (33 μL, 0.12 mmol, 4 Equiv.), which was diluted with 0.1 mL of solvent. This solution was allowed to deoxygenate via sparging with argon for 15 minutes. To a second 10 mL Schlenk flask was added $PEGA_{Mn = 480}$ (0.68 mL, 1.5 mmol, 50 Equiv.), **3** (20 mg, 0.031 mmol, 1 Equiv.) and DMF as an internal standard. The monomer-initiator solution was diluted with 0.1 mL of solvent and 10 μL of dimethylsulfoxide (DMSO) to fully dissolve the initiator. The solution was also deoxygenated via sparging with argon for 30 minutes. Meanwhile, $CuBr_2$ (6.9 mg, 0.031 mmol, 1 Equiv.) was added to the first

Schlenk flask under a positive argon flow. Upon addition of $CuBr_2$, the catalyst complex solution became blue. Sparging with argon was continued for an additional 15 minutes. A stock solution of ascorbic acid dissolved in solvent was prepared and deoxygenated via sparging for 30 minutes. After 30 minutes, the monomer-initiator solution was first transferred via an argon-flushed syringe into the catalyst complex solution. Then, ascorbic acid (3.3 mg, 0.05 mL, 0.019 mmol, 0.6 Equiv.) was fed slowly into the reaction solution via an argon-flushed syringe. Upon complete addition of the ascorbic acid, the reaction mixture turned olive green in color. Reaction was allowed to stir for 15 hours at 30 ℃ under a closed argon atmosphere. Reaction was quenched by exposing solution to air and diluting with THF. To purify polymer, the crude solution was passed through a neutral alumina oxide column and precipitated into cold diethyl ether. Wash with cold diethyl ether was carried out three times. After drying under high vacuum, the final polymer was then characterized by ^{1}H NMR and DMF SEC analysis (with PMMA standards).

Polymer Entry 3 (Table 1):

^{1}H NMR (400 MHz, D_2O) δ 7.57 (s, 1H), 7.29 (s, 1H), 4.14 (s, 280H), 3.26 (s, 385H), 2.29 (s, 166H), 1.73 (m, 253H).

M_n (kDa): 41.5 (± 3.60%)

$Đ$: 1.33

This procedure was followed for other entries, but no characterization was obtained for those entries due to unsuccessful monomer conversion.

General Procedure for the SARA ATRP of PEGA with 3.

To a 20 mL Schlenk flask was added Me_6TREN (87 μL, 0.34 mmol, 3 Equiv.), which was diluted with 3 mL of solvent. This solution was allowed to deoxygenate via sparging with argon for 15 minutes. To a second Schlenk flask was added PEGA (1.3 g, 11 mmol, 100 Equiv.), initiator (30 mg, 0.11 mmol, 1 Equiv.) and DMF as an internal standard. The monomer-initiator solution was diluted with 1 mL of isopropanol (IPA) to dissolve the monomer and 100 μL of DMSO to fully dissolve the initiator. After 15 minutes, copper nanopowder (4.3 mg, 0.068 mmol, 0.6 Equiv.) was added to the first Schlenk flask under a positive argon flow, and then finally $CuBr_2$ (10 mg, 0.045 mmol, 0.4 Equiv.) was added. Upon addition of $CuBr_2$, the catalyst complex solution became blue in color with black specs of copper nanopowder at the bottom. The catalyst complex solution was allowed to deoxygenate for another 15 minutes *via* sparging with argon. Finally, to initiate the polymerization, the monomer-initiator solution was transferred via an argon-flushed syringe into the catalyst complex solution. Reaction was allowed to stir for 1 hour at 25 ℃ under a closed argon atmosphere. Reaction was quenched by exposing the solution to air and diluting with THF. To purify polymer, the crude solution was passed through a neutral alumina oxide column and precipitated into cold diethyl ether. Washing with cold diethyl ether was carried out three times. After drying under high vacuum, the final polymer was then characterized by ^{1}H NMR and DMF SEC analysis (with PMMA standards).

Polymer Entry 5 (Table 1):

^{1}H NMR (400 MHz, D_2O) δ 7.55 (s, 1H), 7.27 (s, 1H), 4.11 (s, 143H), 3.24 (s, 218H), 2.24 (s, 86H), 1.70 (m, 162H).

M_n (kDa): 31.3 (± 4.90%)

$Đ$: 1.15

Polymer Entry 6 (Table 1):

^{1}H NMR (400 MHz, D_2O) δ 7.57 (s, 1H), 4.13 (s, 565H), 3.26 (d, J = 2.7 Hz, 1029H), 2.30 (m, 344H), 1.73 (m, 552H).

M_n (kDa): 90.4 (± 3.60%)

$Đ$: 1.293

General Procedure for Hydrolysis Studies of Photocleavable Initiator:

A sample of the photocleavable initiator was dissolved in 10% (v/v) deuterated acetonitrile (acetonitrile-*d*) and diluted with either pH 6 PBS buffer or pH 7.4 deuterated water. ^{1}H NMR analysis was used to quantify retainment of the NHS end-group in comparison to the hydrolyzed product. The following time points were taken: 0, 1.6, 2.9, 3.8, 5.4, 6.9, 27.3, and 30.2 hours. Percent retainment was determined based on the ratio of photocleavable initiator to hydrolyzed product at the first ^{1}H NMR measurement of t = 0.

General Procedure for Conjugation of 90 kDa Photocleavable Polymer to Lysozyme:

A 1 mg/mL solution of lysozyme was prepared in pH 9, 50 mM sodium carbonate buffer. After the protein concentration was determined via a BCA assay, the 90 kDa photocleavable polymer (Table 1 Entry 6) (2.9 μmol, 4 equiv with respect to lysine residues) dissolved in dimethyl sulfoxide (DMSO) was added to the protein solution (final DMSO concentration of 5%). The conjugation reaction was allowed to proceed for 5 h at 25 °C.

Procedure for the Preparation of Lysozyme Macroinitiators:

A stock solution of 10.53 mg/mL lysozyme was prepared in pH 8 carbonate buffer. 1 mg of lysozyme (95 µL) was diluted up to 200 µL with pH 8 carbonate buffer. Then, 50 equivalents of initiator (dissolved in 10 µL of DMSO) was added to the 1 mg solution of lysozyme. Conjugation was allowed to proceed for 16 hours at 25 °C. Afterwards, lysozyme samples (modified and unmodified) were purified via the use of 3 kDa molecular weight cut off (MWCO) centriprep filters. Three washes with MilliQ H_2O for 15 minutes, 13.2 rpm were carried out during this purification process. Finally, purified samples were rediluted to a total volume of 1 mL using pH 8 carbonate buffer. % Modification was determined by a fluorescamine assay.

Procedure for the Polymerization of Lysozyme Macroinitiators:

To a 10 mL Schlenk flask is added Me_6TREN (7.4 mg, 8.7 µL, 1.26 Eq, 0.032 mmol), copper (I) bromide (4.6 mg, 0.98 µL, 1.26 Eq, 0.032 mmol), and 0.1 mL of pH 8 phosphate buffer. This was allowed to stir at 0 °C using an ice bath. Upon addition of the copper bromide, the appearance of the blue deactivating Cu^{2+} species in solution was observed. Meanwhile, to another 10 mL Schlenk flask was added PEGA (3.13 g, 3.13 mL, 250 Eq, 6.5 mmol), lysozyme macroinitiator (200 µg, 5.0 x 10^{-3} Eq, 0.0140 µL), ethyl 2-bromo-2-methyl-propanoate (5.0 mg, 3.8 µL, 1 Eq, 26 µmol) as sacrificial initiator, and DMF (5.6 mg, 6.0 µL, 3 Eq, 77 µmol) which was used as an internal standard). Deoxygenation via sparging with argon was undertaken for 15 minutes. To initiate the polymerization, the monomer and initiator solution was transferred by a syringe argon-flushed needle to the copper catalyst complex flask. Polymerization was allowed to proceed for 1 hour at 25 °C.

Procedure for the Characterization of Polymer by 'Graft-From':

This experiment was carried out as we previously reported.[3] Briefly, protein-polymer conjugate was buffer exchanged by centriprep ultracentrifugation (MWCO 3kDa) to digestion buffer (10 mM Tris HCl, 2 mM $CaCl_2$, pH 7.4). 100 µL of this sample was then added to 100 µL Proteinase K at 2 mg/mL in digestion buffer. The solution was incubated in a 50 ℃ water bath for 24 hours. Peptide fragments were removed by centriprep ultracentrifugation (MWCO 3 kDa) before analysis by SEC.

^{1}H NMR (400 MHz, D_2O) δ 7.57 (s, 1H), 7.31 (s, 1H), 4.15 (s, 3506H), 3.78 – 3.37 (m, 60714H), 3.28 (s, 5744H), 2.28 (s, 1646H), 1.75 (m, 3252H).

M_n (kDa): 117.1 kDa

$Đ$: 1.16

General Procedure for Photocleavage of Protein-Polymer Conjugates:

Samples, diluted up to 100 µL of pH 8 phosphate buffer, were irradiated with UV light (365 nm, 4 watt) for 1 hour at 4 ℃ to allow for photocleavage of the polymer from the protein. Afterwards, samples were immediately used for activity assay or further characterization.

General Procedure for Activity Assay of Protein-Polymer Conjugates:

Samples were added to a transparent 96-well plate. All samples were mixed with 200 µL of a suspension of lyophilized Micrococcus Lysodeikticus cells (0.15 mg/mL in 50 mM potassium phosphate buffer, pH 6.24). Absorbance measurements were taken at 450 nm for 30 minutes

over 30 second intervals. The change in absorbance over 120 minutes was determined and used to determine protein activity.

Control Experiment on Native Lysozyme Activity Upon Exposure to UV Irradiation:
5 μg of native lysozyme was diluted up to 100 μL of MilliQ H_2O in a 96 well-plate. These samples were allowed to be exposed to UV irradiation for a given amount of time. The following exposure time points were carried out: 0 minutes, 15 minutes, 30 minutes, 60 minutes, 90 minutes, and 120 minutes. Each time point was done in triplicate. After the final exposure time point of 120 minutes all samples were mixed with 200 μL of a suspension of lyophilized Micrococcus Lysodeikticus cells (0.15 mg/mL in 50 mM potassium phosphate buffer, pH 6.24). Absorbance measurements were taken at 450 nm for 120 minutes over 30 second intervals. The change in absorbance over 120 minutes was determined and used to determine protein activity.

References:

(1) Forsythe, N. L.; Tan, M. F.; Vinciguerra, D.; Woodford, J.; Stieg, A. Z.; Maynard, H. D. Noncovalent Enzyme Nanogels via a Photocleavable Linkage. *Macromolecules* **2022**, *55* (22), 9925–9933. https://doi.org/10.1021/acs.macromol.2c01334.

(2) Zhang, A.; Barner, J.; Göessl, I.; Rabe, J. P.; Schlüter, A. D. A Covalent-Chemistry Approach to Giant Macromolecules and Their Wetting Behavior on Solid Substrates. *Angew. Chem. Int. Ed.* **2004**, *43* (39), 5185–5188. https://doi.org/10.1002/anie.200460390.

(3) Mansfield, K. M.; Maynard, H. D. Site-Specific Insulin-Trehalose Glycopolymer Conjugate by Grafting from Strategy Improves Bioactivity. *ACS Macro Lett.* **2018**, *7* (3), 324–329. https://doi.org/10.1021/acsmacrolett.7b00974.

Chapter 4 Alternatives to PEG: pNIPAM-based Enzyme Nanogels and Protein-Polymer Conjugates *via* a Photocleavable Linkage

4.1 Introduction

Synthetic polymers have been employed in a wide range of biotechnological and pharmaceutical applications. Poly(ethylene glycol), or PEG, has been the gold standard due to its high solubility in aqueous media and its biocompatibility.[1] The U.S. Food and Drug Administration (FDA) has approved the use of PEG in medical devices, sealants, wound dressing, bone fillers, dyes, drugs, and other therapeutic options.[2] Our research group has extensively studied PEG towards the preparation of protein-polymer conjugates, also known as PEGylated proteins. For example, we previously reported the site-specific conjugation of PEG to mutated growth-hormone receptor (GHR) antagonists and demonstrated substantially improved *in vitro* bioactivity and *in vivo* reduction in serum insulin-growth factor (IGF).[3,4] It was determined that after substituting tyrosine 35 in a GHR antagonist with unnatural amino acid propargyl tyrosine (pgIY) and conjugating site-specifically with a 20 kDa PEG azide there was a 12.5-fold improvement of *in vitro* bioactivity compared to that of multi-PEGylated native GHR.[3] In other work, we prepared PEG polymers by ring opening metathesis polymerization (ROMP) to conjugate to a protein and demonstrated that the conjugate is nontoxic up to 1 mg/mL in human dermal fibroblasts.[5] While PEG is a popular polymer in drug delivery development, limitations such as immunogenicity have prompted researchers to seek out alternatives. Multiple excellent reviews discussing the issues that arise with the use of PEG in drug delivery and biotechnology have been reported.[1,6-9] Several reported cases of patients encountering adverse reactions were likely due to PEG, such as symptoms of anaphylaxis, rapid-onset sneezing, rhinorrhea (runny nose), urticaria (hives), and angioedema (swelling).[10] To alleviate these concerns and bolster patient compliance, it is crucial that other types of polymers are explored.

One PEG alternative is poly(*N*-isopropylacrylamide) (pNIPAM), which is a water-soluble polymer that has been employed in the preparation of protein-polymer conjugates. pNIPAM in water exhibits a lower critical solution temperature (LCST) around 32 °C, and this value can easily be tuned to match a more biologically relevant temperature, such as the physiological temperature of 37 °C. Conjugates utilizing pNIPAM also possess thermoresponsivity, which is highly useful for enzyme and protein purification, controlling biomolecular activity, biosensing, and other emerging applications. The first pNIPAM conjugates were developed by Hoffman and coworkers to be utilized as a novel separation method for an immunoassay.[11] Our research group previously prepared a glutathione-pNIPAM conjugate by a reversible addition-fragmentation chain-transfer (RAFT) polymerization and purified the enzyme in a scalable manner that can be useful in industry.[12] In another report, we synthesized aminooxy end-functionalized pNIPAM by RAFT and demonstrated potential application towards stabilization and storage of growth factors on surfaces or coating of medical devices.[13] With growing interest in the field of protein-polymer conjugates, it is critical to continue research towards a multitude of synthetic polymers and develop their use in new and advancing biotechnology. In this chapter, noncovalent pNIPAM-enzyme nanogels and linear pNIPAM-enzyme conjugates have been synthesized *via* the photocleavable linkages developed in **Chapters 2 and 3** to demonstrate potential for thermoresponsive applications**.**

4.2 Noncovalent Enzyme Nanogels *via* a Photocleavable Linkage – pNIPAM-*co*-acrylic acid-based

4.2.1 Results and Discussion

4.2.1.1 Synthesis and Characterization of Nanogels

As mentioned previously, pNIPAM is a popular choice for nanogel synthesis due to its thermoresponsive properties. The reversible lower critical solution temperature (LCST) of homopolymer pNIPAM is approximately 32 °C.[14] Below the LCST, pNIPAM exists as a flexible random coil. However, above the LCST, pNIPAM will collapse to globular state. Incorporation of acrylic acid into the copolymerization of pNIPAM will yield a polymer with a higher LCST in basic conditions due to the increased number of deprotonated, hydrophilic units allowing for the polymer to be more soluble in water.[15] Alternatively, in acidic conditions the polymer will have a lower LCST due to the protonated acrylic acid units thereby making the polymer more hydrophobic. The molar feed ratio of NIPAM monomer and acrylic acid can be tuned accordingly to impart a specific LCST on the polymer system. This unique property can be beneficial in the development of drug delivery systems for intracellular drug delivery where endosome and lysosomal pH levels are known to be 5-6 and 4-5, respectively. Our research group previously reported the synthesis of dual pH- and temperature-responsive protein nanoparticles based on the conjugation of pNIPAM-*co*-AA to human vaults. UV-Vis, dynamic light scattering, and electron microscopy measurements demonstrated that the vault nanoparticles reversibly aggregated at pH 6 when reaching 45 °C from 25 °C, whereas at pH 7 did not aggregate until temperatures reached above 60 °C.[16] The pH- and temperature-responsiveness of pNIPAM conjugates could also be applied in the development of drug delivery methods *via* oral route administrations by facilitating the polymer to de-swell and swell as it passes through the

stomach and small intestine, respectively. Gao, X. et al prepared pNIPAM-*co*-AA copolymers and hydrogels containing insulin and evaluated them for their applicability to oral protein delivery. It was confirmed that the *in vitro* release of insulin from the hydrogel was suppressed in artificial gastric fluid (pH 1.5-2.0) but was markedly enhanced in artificial intestinal fluid (pH 6.6-7.6).[17] Thus, it was hypothesized that the synthesis of pNIPAM-*co*-AA noncovalent nanogels using our previously reported photocleavage system would enable the materials to have enhanced stabilization properties to multiple triggers.

Nanogel synthesis proceeded *via* polymerization followed by photocleavage (Figure 4.1).

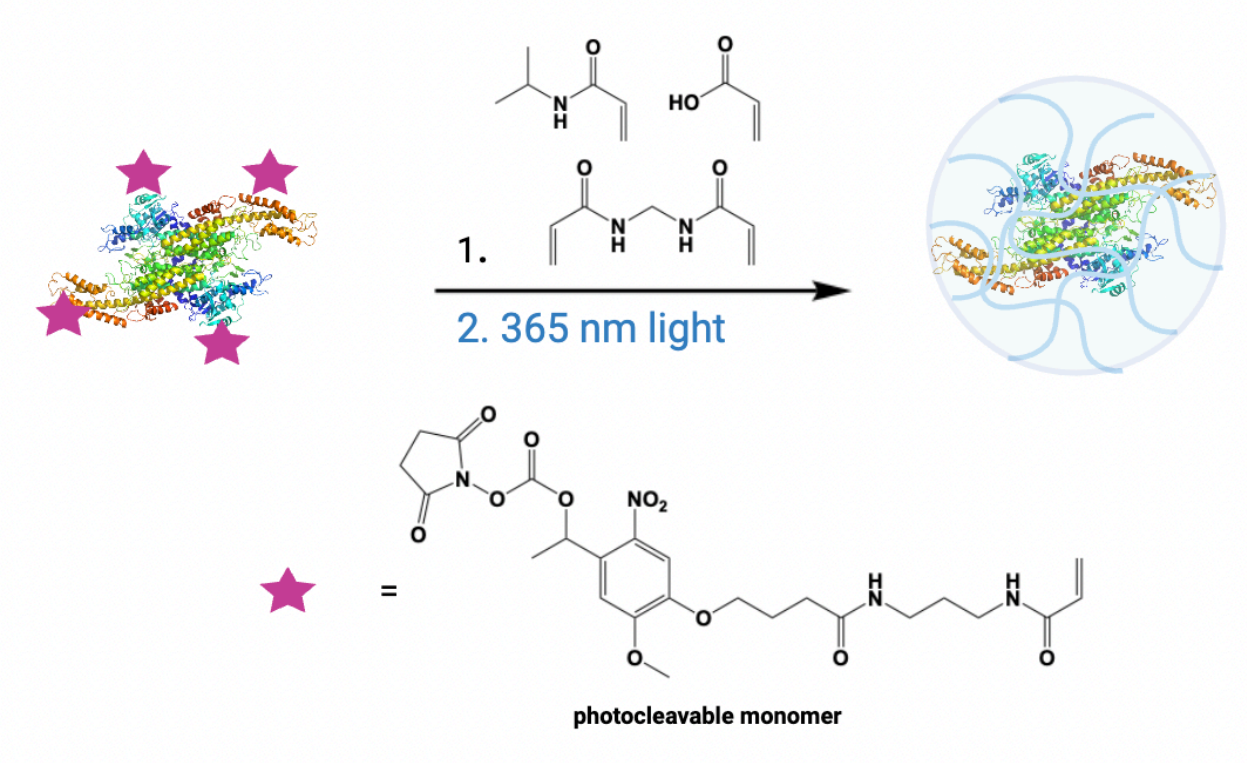

Figure 4.1 Scheme for synthesis and photocleavage of noncovalent pNIPAM-PAL nanogels.

Free radical polymerization of NIPAM monomer and acrylic acid with bisdimethylacrylamide as a crosslinker was initiated by an ammonium persulfate (APS)/tetramethylethylenediamine initiator system. Complete incorporation of the acrylamide-modified PAL was confirmed by

sodium dodecyl sulfate-polyacrylamide gel electrophoresis based on the absence of an unmodified protein band and a large molecular weight band (Figure S4.1). Further validation of the polymerization was conducted *via* nuclear magnetic resonance (^{1}H NMR) wherein clearly identifiable peaks that correlate with the expected polymer backbone and side chains were observed (Figure S4.2). The resulting nanogels were purified with spin desalting columns prior to analysis to remove initiator and photodegradation byproducts. Dynamic light scattering (DLS) showed an increase in size of approximately 200 nm compared to PAL alone. (Figure 4.2). It should be noted that DLS characterization also revealed larger clusters that likely include multiple enzymes within a single nanogel.

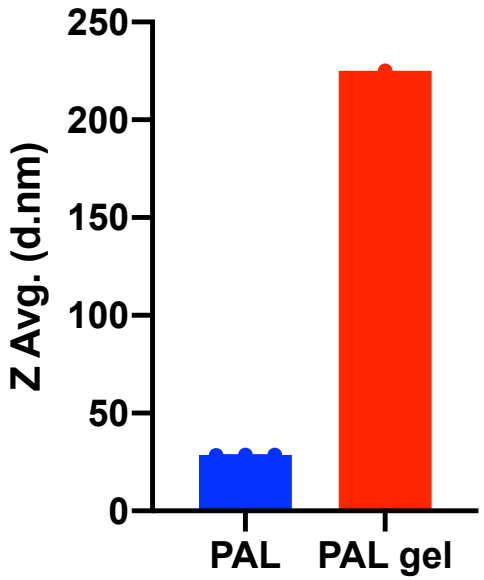

Figure 4.2 Dynamic light scattering (DLS) results of PAL and PAL gel.

The activity of the PAL in the nanogels was investigated similarly to our previous report by measuring change in absorbance at 290 nm after incubating with 4 mM phenylalanine for 2 hours at 37 °C as adapted from McCallum and Walker.[18,19] The activity of the resulting noncovalent nanogels was 25% compared to that of the unencapsulated PAL (Figure 4.3). The

activity of the nanogels before irradiation was considered negligible since no *trans*-cinnamic acid was detected.

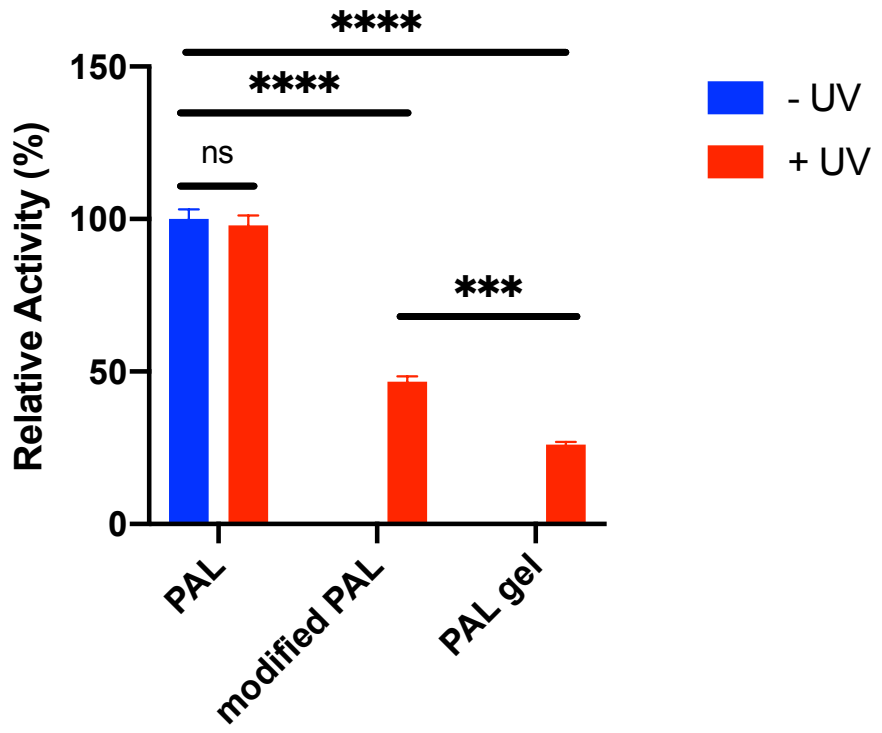

Figure 4.3 Activity of native PAL, modified PAL, and PAL nanogels measured *via* HPLC before and after irradiation.

Each measurement was conducted in triplicate and statistical significance was conducted in triplicate and statistical significance was determined via a 2way ANOVA with multiple comparisons. (*** = $p \leq 0.001$, **** = $p \leq 0.0001$, and ns = $p \geq 0.05$ compared against native PAL before irradiation).

4.2.1.2 Preliminary Stabilization of Trypsin and pH

Our previously reported noncovalent enzyme nanogels demonstrated stabilization to proteases (Chapter 2). It was thus necessary to confirm this with our new pNIPAM-*co*-AA nanogel. In order to test this, the PAL nanogels were exposed to a range of trypsin concentrations. Activity was measured by monitoring the increase in absorbance at 290 nm after 2 hours of incubation; this

corresponds to the concentration of *trans*-cinnamic acid and thus enzymatic activity. In this assay, the pNIPAM-*co*-AA nanogel did not achieve any significant improvement in total enzymatic activity output over 2 hours of exposure to substrate (Figure 4.4) unlike in our previous PEG-based nanogel. We attribute this result to the difference in steric hindrance of the NIPAM and acrylic acid side chains compared to that of the PEGA side chains. Optimization in crosslinking densities will need to be explored.

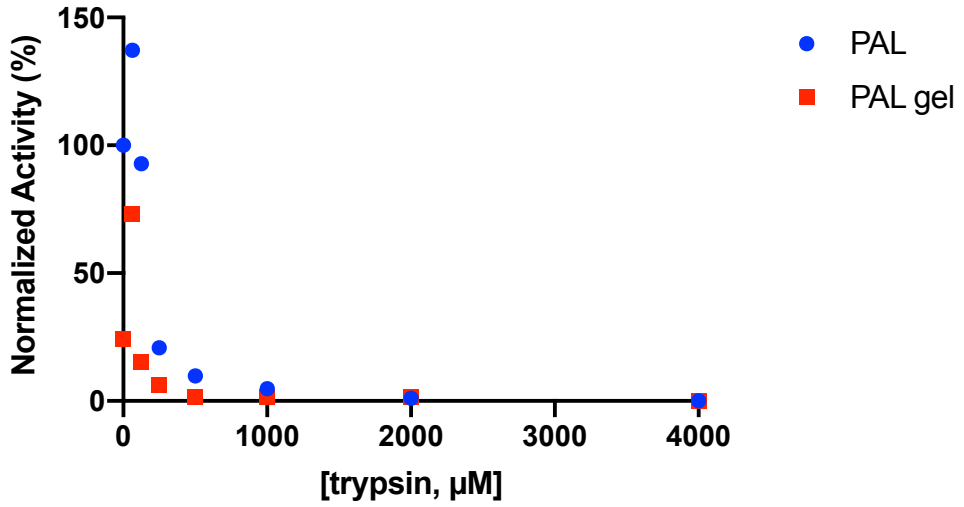

Figure 4.4 Normalized dose response stabilization of nanogels against trypsin.

Each red data point represents an individually synthesized batch of nanogel.

4.2.2 Outlook and Future Directions

Herein, it has been shown that noncovalent PAL nanogels can be synthesized with pNIPAM and acrylic acid utilizing a photocleavable linkage. We expect that this will allow for the enzyme to have enhanced bioactivity upon irradiation with UV light, but much work will need to be carried out to confirm this hypothesis. As in our report of PEG-based noncovalent PAL nanogels, we have characterized the pNIPAM-based nanogels by DLS. Further

characterization by AFM and TEM may be carried out in the future to confirm the size of the nanogels.

The preliminary dose-response assay did not support the hypothesis that the pNIPAM – based nanogel can stabilize the enzyme to trypsin. This may be due to the crosslinking density of the nanogel prepared in these experiments; it will be necessary to optimize polymerization conditions in future studies.

To move forward with this system, it is also necessary that the thermoresponsive properties of the nanogel are measured. The LCST of the nanogel needs to be determined by either DLS or differential scanning calorimetry (DSC). DLS measurements of the nanogels in various pH environments must also be carried out to determine if the nanogel collapses as hypothesized in simulated gastric fluid. Once these experiments are completed, we would then want to subject the enzyme nanogels to a low pH stress test by measuring enzymatic activity to confirm that the thermoresponsive properties of the gel does in fact protect the enzyme to the low pH conditions found in the oral route of administration. Overall, this work demonstrates potential in applying this strategy for the development of oral protein delivery systems.

4.2.3 Materials and Methods

All chemicals were purchased from Sigma-Aldrich and Fisher Scientific and were used without purification unless otherwise noted. NIPAM was purified by repeated recrystallization in hexanes and dried in vacuum at 40 ℃. Plasmid for PAL expression was ordered from Twist Biosciences with the sequence cloned between Ndel_Xhol restriction sites in a pET-29b(+) vector. TEV protease was expressed following reported procedures and stored at -80 °C in 50% glycerol and thawed immediately before use.[1] For photocleavage experiments, a 4 watt, 365 nm lamp was used (brand: UVP).

4.2.4 Analytical Techniques

Nuclear Magnetic Resonance (NMR) spectra were recorded on a Bruker AV 500 MHz. Proton NMR spectra were acquired with a relaxation delay of 10 seconds for polymers.

For SDS PAGE, BioRad Any kD Mini-PROTEAN-TGXTM gels were used. SDS-PAGE protein standards were obtained from Bio-Rad (Precision Plus Protein Prestained Standards). Small molecule purification was done via flash chromatography and conducted on a Biotage Isolera One auto-column system.

4.2.5 Appendix with Supplemental Figures

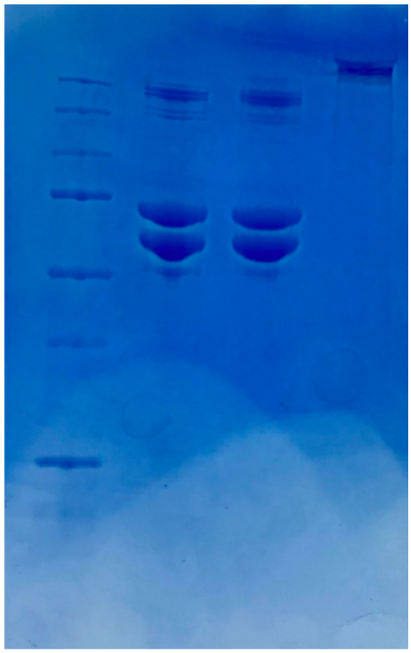

Figure S4.1 SDS-PAGE of PAL, modified PAL, and PAL nanogel stained with Coomassie blue.

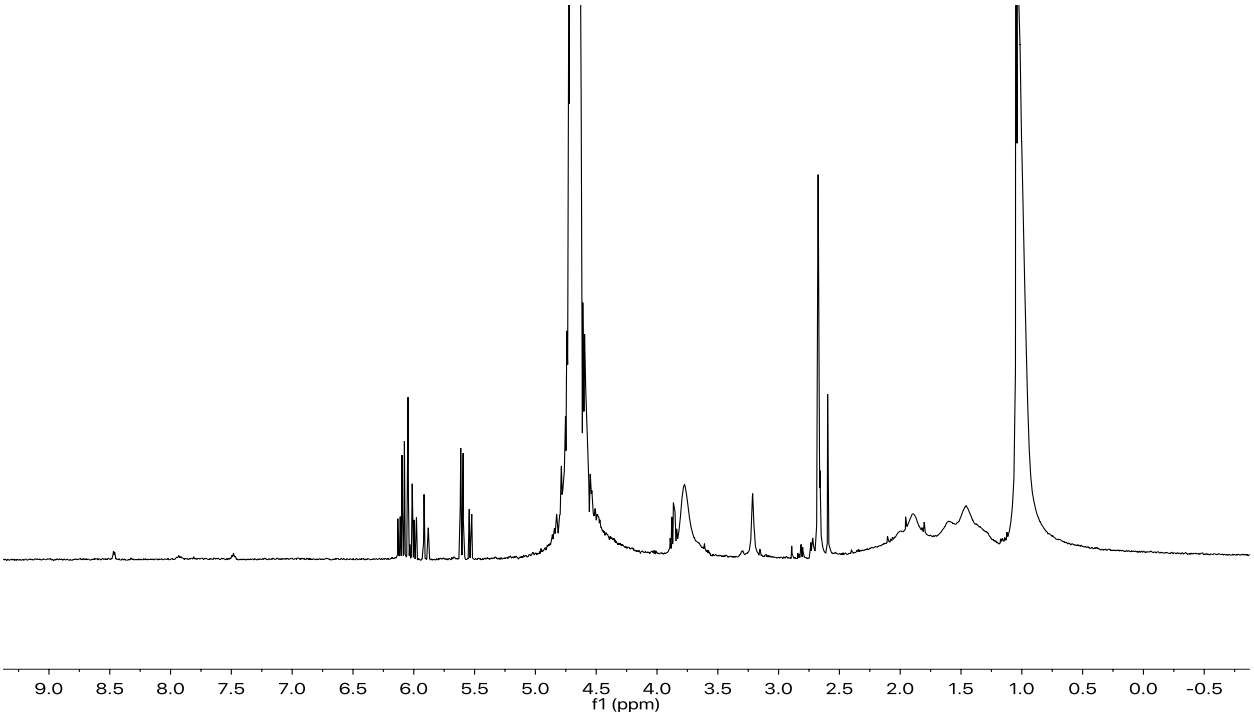

Figure S4.2 ^{1}H NMR (500 MHz, D_2O) of crude PAL nanogels (post-irradiation).

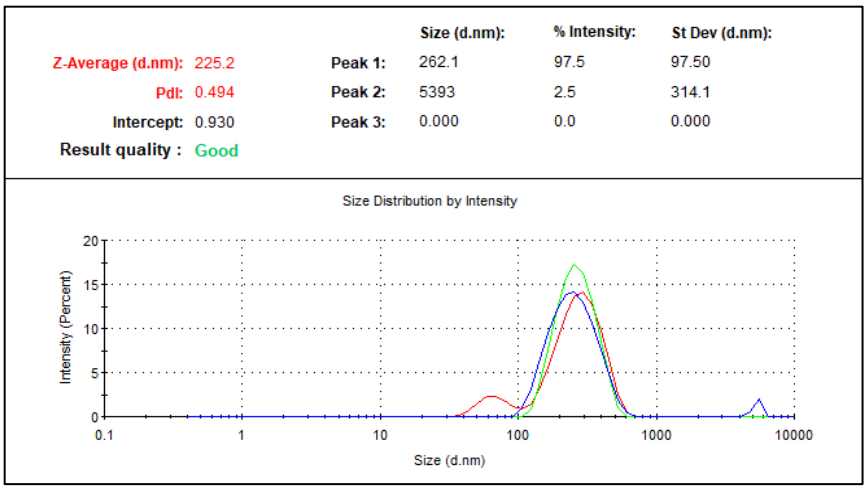

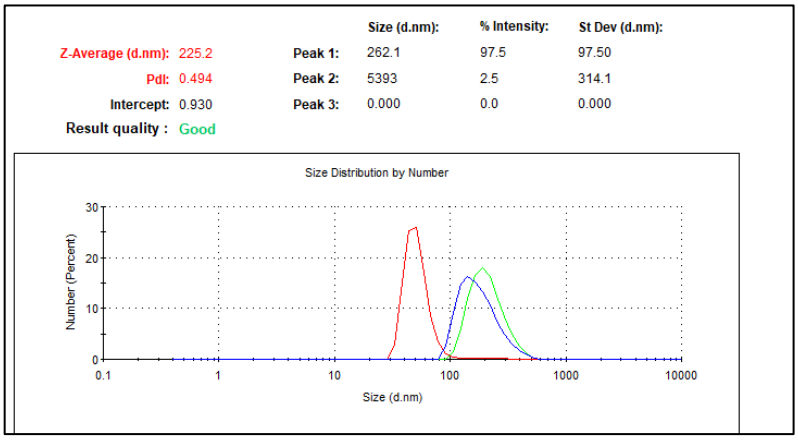

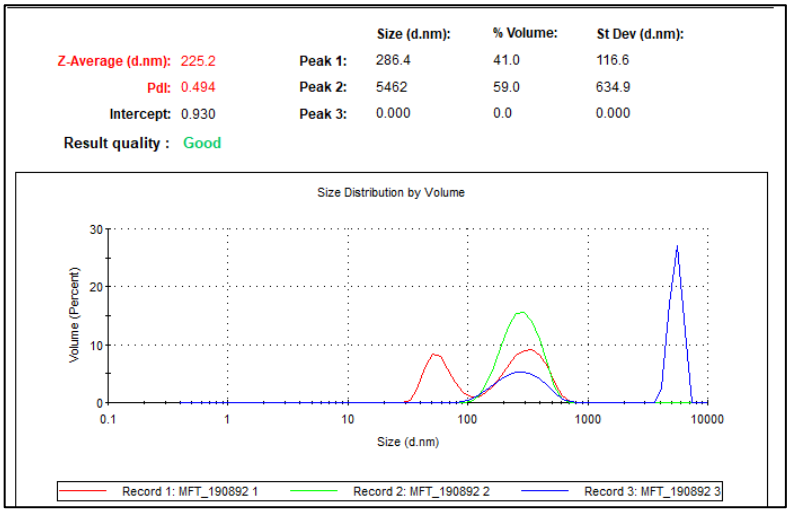

Figure S4.3 DLS size distribution by intensity (top), number (middle), and volume (bottom).

4.2.6 Experimental and Appendix References

Conjugation:

A 4 mg/mL solution of expressed PAL (stored at -80 ℃) was thawed for 30 min at 4 ℃. The protein was then buffer exchanged into pH 9, 50 mM sodium carbonate buffer *via* a 3 kDa MWCO Centriprep filter. After the protein concentration was determined *via* a BCA assay, a photocleavable linker (1.64 mg, 2.9 μmol, 4 equiv with respect to lysine residues) dissolved in dimethyl sulfoxide (DMSO) was added (final DMSO concentration of 5%). The conjugation reaction was allowed to proceed for 5 h at 25 ℃. Excess linker was removed via 7 kDa MWCO Zeba desalting spin columns, and the modified PAL was buffer exchanged into PAL buffer via 3 kDa MWCO centriprep filters.

Photocleavage Protocol:

Samples were irradiated with UV light (365 nm, 4 watt) for 15 min at 4 ℃ to allow for photocleavage of the linker. Afterward, the samples were passed through a 7 kDa MWCO Zeba desalting spin column to remove excess monomer, photocleavage byproducts, and other small molecules. The desalting column was initially equilibrated with PAL buffer.

Recovery of PAL Activity after Photocleavage:

To determine percent recovery after photocleavage, each of the conjugated samples was compared against unmodified PAL. Conjugated samples underwent UV irradiation (365 nm, 4 watt) for 15 min at 4 ℃ as described previously. Afterward, the samples were passed through a 7 kDa MWCO Zeba desalting spin column to remove photocleavage byproducts and other small molecules. The desalting column was equilibrated with PAL buffer. The remaining protein solutions were added to a 96-well plate and diluted to 200 μL with PAL buffer. The assay was

initiated through the addition of 30 μL of 4 mM phenylalanine in PAL buffer, and kinetics were monitored by measuring absorbance values at 290 nm every 30 s for 2 h at 37 ℃. Enzyme activity was determined by calculating the difference in absorbance values between the first and last time points. These values were normalized to that of the unmodified PAL.

Nanogel Synthesis:

NIPAM (1.98 mg, 17.5 μmol, 50 Eq.), acrylic acid (0.140 mg, 0.145 μL, 2.03 μmol, 6 Eq.), N, N' Methylenebis(acrylamide) (0.502 mg, 3.26 μmol, 9 Eq.), tetramethylethylenediamine (0.186 mg, 0.143 μL, 1.60 μmol, 4.5 Eq.), and conjugated PAL (1 mg) were added to a 4 mL dram vial with a stir bar and diluted up to 175 μL with PAL buffer. The mixture was allowed to degas under argon for 45-60 min. In a separate dram vial, APS stock solution in PAL buffer was prepared and also degassed under argon for 45-60 min. After degassing, 175 μL (93.0 μg, 0.407 μL, 1.2 Eq.) of the APS solution was added to the reaction mixture, and the polymerization was allowed to proceed for 2 h. To quench the reaction, samples were exposed to air.

Dose-Response Trypsin Challenge Assay:

The PAL nanogels were prepared as described previously. For photocleavage, the gels were transferred to individual wells of a 48-well culture plate. The portion of the plate holding the samples was then irradiated with UV light (365 nm, 4 watt) for 15 min at 4 ℃ to allow for photocleavage of the linker. Afterward, the samples were passed through 7 kDa MWCO Zeba desalting spin columns to remove photocleavage byproducts and other small molecules. Buffer containing 50 mM Tris and 90 mM NaCl (pH 7.8) was used as equilibration buffer during this small-molecule cleanup.

The purified gel solutions were next split into 16 parts and added to individual wells on a UV transparent 96-well plate. Eight (20 μL) was added to a well consisting of a given concentration

of trypsin (see below[a]), 95-195 μL PAL buffer, and 30 μL of 1% TFA 50/50 MeOH/ACN to immediately quench catalytic activity (these samples serve as $t = 0$ h). The second half of the gel solution was added to a well consisting of the same given concentration of trypsin as the first half of the gel solution in PAL buffer. All samples had a total volume of 275 μL. Lastly, 30 μL of 4 mM phenylalanine in 50 mM Tris base, 90 mM NaCl pH 7.8 buffer was added to all wells to initiate activity.

Absorbance measurements at 290 nm (37 °C) were taken every 30 s for 2 h. The catalytic activity was measured by calculating the difference between the absorbance measurements at $t =$ 2 h and $t = 0$ h for each sample.

[a]The following concentrations of trypsin were used for this experiment: 0, 62.5, 125, 250, 500, 1000, 2000, and 4000 μM.

4.3 Enzyme-Polymer Conjugates *via* a Photocleavable Initiator – pNIPAM-based

4.3.1 Results and Discussion

4.3.1.1 Optimization of Polymerization Conditions

In a previous report, lysozyme-PEG conjugates were synthesized *via* a photocleavable initiator for control over the recovery of protein activity. These conjugates were prepared by both a *grafting-to* and *grafting-from* approach. As previously mentioned, there has been growing interest in developing other types of protein-polymer conjugates using alternatives to PEG due to the higher immunogenicity. Furthermore, employing other types of polymers allows for the ability to tune properties according to the desired application. For preliminary studies, I have chosen to synthesize pNIPAM conjugates.

To determine the best conditions to prepare photocleavable pNIPAM polymers, I optimized the polymerization reaction with a noncleavable initiator. First, 2-bromoisobutanoic acid *N*-hydroxysuccinimide ester was synthesized as adapted by Zhang et al.[20] Table 1 outlines the conditions that were screened for the synthesis of the noncleavable polymers.

Table 4.1 Conditions for the synthesis of non-cleavable pNIPAM.

Entry	Supplemental Activator[a]/Reducing Agent[b]	Equiv. Ratios[c]	Solvent[d]	Conversion (%)	M_n [e] (targeted)	M_n [f] (NMR)	M_n [g] (SEC)	Đ
1	n/a	1: 250: 1: 3: n/a	DMSO	0	0	n/a	n/a	n/a
2	Sn_2Octoate	1: 250: 0.4: 3: 0.6	DMSO	0	0	n/a	n/a	n/a
3	Ascorbic acid	1: 250: 0.4: 3: 0.6	DMSO	0	0	n/a	n/a	n/a
4	Ascorbic acid	1: 250: 0.4: 3: 0.6	H_2O	---	---	---	---	---
5	Ascorbic acid	1: 250: 0.4: 3: 0.6	pH 6 PBS	---	---	---	---	---
6	Cu^0	1: 250: 0.4: 3: 0.6	3:1 IPA/DMSO	0	0	n/a	n/a	n/a
7	Cu^0	1: 250: 0.4: 3: 0.6	3:1 IPA/ H_2O	---	---	---	---	---
8	Cu^0	1: 250: 0.4: 3: 0.6	3:1 IPA/ pH 6 PBS	63	17.8	19	19.9	1.23

[a]Cu^0 is used both as the supplemental activator and reducing agent following the mechanism of SARA ATRP
[b]Ascorbic acid or Sn_2Octoate is used as the reducing agent following the mechanism of ARGET ATRP
[c]Initiator/NIPAM$_y$/$CuBr_2$/Me_6TREN/reducing agent.
[d] 10% DMSO is added to the solvent conditions for the solubility of the photocleavable initiator in Entries 3, 5, & 6
[e, f, g] M_n values are reported in kDa.

Due to the susceptibility of the NHS end-group to hydrolysis, it would be ideal for the polymerization to be conducted in anhydrous aprotic solvents. For this reason, I first attempted to perform atom transfer radical polymerization (ATRP) of NIPAM monomer in DMSO (Entry 1); however, no conversion of monomer was observed. It had been found by Narain et al. that the polymerization of NIPAM monomer proceeds to higher conversion in aqueous conditions with a mixture of alcoholic solvents to ensure monomer and subsequent polymer solubility.[21] Matyjaszewski and coworkers also disclosed that a potential major challenge of the ATRP of acrylamides include the deactivation of the transition metal catalyst due to chelation to the amide groups on the monomer, which is mitigated by protic solvents that compete with hydrogen bonding.[22]

Therefore, polymerizations by reversible-deactivation radical polymerization (RDRP) mechanisms, were then explored; namely, an activator regenerated by electron transfer (ARGET) ATRP mechanism (Entries 2 through 5) and a supplemental activator and reducing agent (SARA) ATRP mechanism (Entries 6 through 8) were conducted in protic conditions whilst maintaining control over dispersity. It was found that polymerization by SARA ATRP was more successful at achieving monomer conversion and narrow dispersity within a short reaction time of 1-2 hours at 25 °C. The same outcome was observed in my previous report synthesizing photocleavable PEGA polymers. While it is possible to further optimize both mechanisms, such as performing ARGET ATRP in water (Entry 4), it is beyond the scope of this project to synthesize pNIPAM by multiple types of polymerization reactions. Thus, the SARA ATRP reaction was used as the preferred polymerization technique in the following experiments.

As in my previous report, the polymerization of NIPAM monomer was attempted at a ratio of 3:1 isopropanol/pH 6 buffer, instead of 3:1 isopropanol/water, to slow down the rate of hydrolysis of the NHS end-group (Entry 8). Matyjaszewski and coworkers were the first to report a successful ATRP in a strongly acidic environment.[23] Haddleton and coworkers specifically observed that the living polymerization of NIPAM monomer by a copper-mediated mechanism could be done in pH 6 PBS buffer. [24] Therefore, polymerization of NIPAM monomer was done with the adapted conditions, and it was determined that pNIPAM can be synthesized with sufficient conversion and low dispersity in pH 6 PBS buffer. These optimized conditions were then applied for the polymerization of photocleavable pNIPAM. Table 2 outlines the photocleavable pNIPAM polymers that were synthesized.

Table 4.2 Results of photocleavable pNIPAM

Entry	Supplemental Activator[a]/Reducing Agent[b]	Equiv. Ratios[c]	Solvent[d]	Conversion (%)	M_n [e] (targeted)	M_n [f] (NMR)	M_n [g] (SEC)	Đ
1	Cu^0	1: 450: 0.4: 3: 0.6	3:1 IPA/ pH 6 PBS	91	46	35	33.9	1.21
2	Cu^0	1: 900: 0.4: 3: 0.6	3:1 IPA/ pH 6 PBS	48	49	---	48.5	1.42
3	Cu^0	1: 1350: 0.4: 3: 0.6	3:1 IPA/ pH 6 PBS	53	81	---	66.9	1.89

[a]Cu^0 is used both as the supplemental activator and reducing agent following the mechanism of SARA ATRP
[b]Ascorbic acid or Sn_2Octoate is used as the reducing agent following the mechanism of ARGET ATRP
[c]Initiator/NIPAM/$CuBr_2$/Me_6TREN/reducing agent.
[d] 10% DMSO is added to the solvent conditions for the solubility of the photocleavable initiator in Entries 3, 5, & 6
[e, f, g] M_n values are reported in kDa.

As shown in the above table, photocleavable pNIPAM polymers were synthesized and characterized by NMR and SEC. Unsurprisingly, the dispersity of the polymers increase as higher molecular weight polymers are targeted even though monomer concentration, reaction time, and reaction temperature remained consistent throughout. Further optimization of the reaction can be carried out in the future to achieve lower dispersity for all sizes of the polymers, but it is beyond the scope of this study.

4.3.1.2 Preparation of Conjugates and Activity Assay

Conjugation of the noncleavable and photocleavable polymers to a model protein was then carried out to prepare conjugates *via* a *grafting-to* approach. To serve as a control for the proof-of-concept, a ~19 kDa noncleavable pNIPAM polymer (Table 1 entry 18) was first conjugated onto lysozyme, a 14.3 kDa model enzyme that had been used in Chapter 3. After purification of the conjugate by fast protein liquid chromatography (FPLC), an activity assay was carried out as described in a previous report in which protein samples were incubated with Micrococcus Lysodeikticus cells and a decrease in absorbance at 450 nm was monitored over time.[25] Interestingly, the lysozyme conjugate demonstrated no significant reduction in activity compared to that of a native lysozyme sample (Figure 4.5).

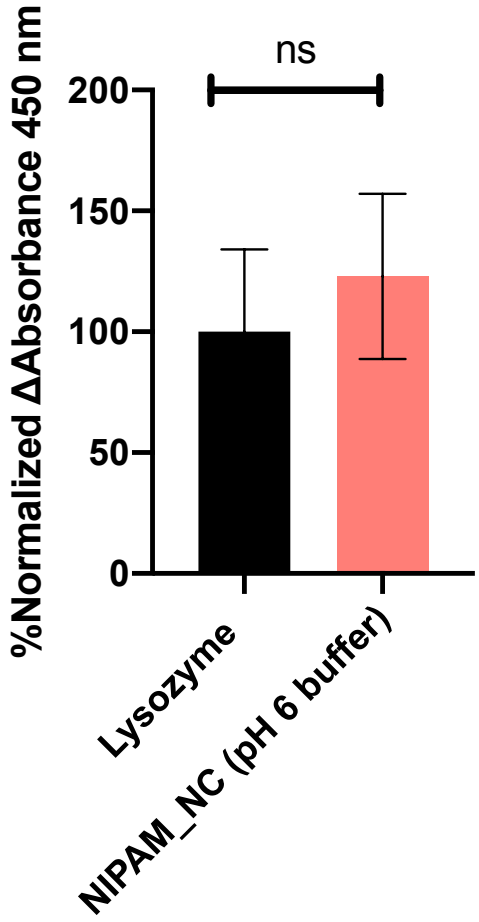

Figure 4.5 Activity test of noncleavable pNIPAM lysozyme conjugate to lysozyme control post-purification.

Each measurement was conducted in triplicate and statistical significance was determined *via* a Welch's t-test (ns = $p > 0.5$).

FPLC analysis and SDS PAGE of the conjugates were conducted to confirm successful conjugation of the polymer onto the protein (Figure S4.4 and Figure S4.5). Other forms of characterization such as a fluorescamine assay or mass spectrometry analysis could be done in the future for additional characterization, but it was beyond the scope of this preliminary work.

Nevertheless, it was ensured that the activity of the noncleavable conjugate was not a result of the lack of conjugation of the polymer onto the protein.

While we previously observed the reduction in protein activity when covalently attaching PEGA polymers to lysozyme; it is possible that the conjugation of a different polymer could retain enzymatic activity. Beloqui and coworkers wrote a review recently that highlights the challenges of predicting an impact a polymer has on biocatalytic activity.[26] Specifically in relation to pNIPAM and lysozyme, Vaidya et al reported that homopolymer pNIPAM did not inhibit lysozyme binding activity unlike its derivates with acetoamido groups.[27] Thus, it is reasonable that the activity of lysozyme was unchanged after conjugation of the pNIPAM onto the protein. Another possibility is that the pNIPAM conjugates to different residues compared to that of PEGA polymers, and such sites may be far from the active site of the enzyme. It will be necessary to determine in future studies where and how many sites are conjugated by the pNIPAM we prepared.

To determine whether protein activity was affected by UV irradiation of the protein conjugated with the photocleavable pNIPAM, an activity assay was conducted on samples before

and after exposure to UV light for 1 hour (Figure 4.6).

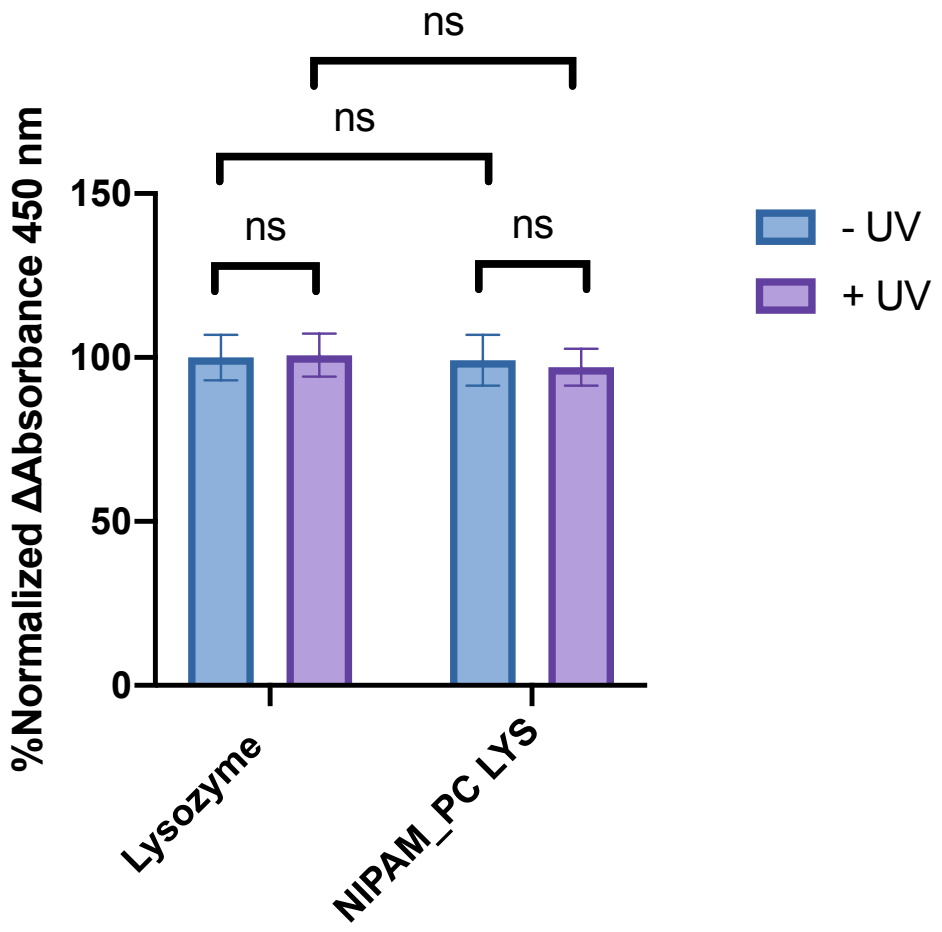

Figure 4.6 Activity test of photocleavable pNIPAM lysozyme conjugate before and after UV irradiation post-purification.

Each measurement was conducted in triplicate and statistical significance was determined via a 2-way ANOVA (ns = $p \geq 0.5$).

As observed in the assay conducted with the noncleavable polymer protein conjugate, there was no significant difference found in catalytic activity between native lysozyme and the lysozyme-pNIPAM conjugates. Furthermore, there was no significant change in activity between the lysozyme conjugate before and after exposed to UV irradiation. This confirmed that the covalent attachment of pNIPAM onto the lysozyme enzyme does not inhibit protein activity,

unlike the covalent attachment of PEGA polymers onto lysozyme, in which we previously observed near complete loss in activity.

4.3.2 Outlook and Future Directions

We prepared pNIPAM-protein conjugates *via* a photocleavable linkage by a *grafting-to* strategy. We did not demonstrate synthesis of the conjugates via a *grafting-from* strategy. However, we believe that this approach should be possible given the success that was observed for the PEGA system as described in Chapter 3. Furthermore, we hypothesize that the *grafting-from* strategy will be a more favorable approach for the preparation of these conjugates due to ease in purification and avoidance of hydrolysis of end-group.

We did not observe that photocleavable linkage between the pNIPAM and lysozyme allowed for enhanced bioactivity upon irradiation with UV light. We strongly suspect that these results are due to the fact the lysozyme activity is not inhibited by pNIPAM as was previously reported.[22.]Future work may involve observation of protein activity when pNIPAM is conjugated to another enzyme, such as PAL. Overall, we have shown that this system has been adapted to another polymer beyond PEG, which is promising for future bioconjugation development.

4.3.3 Materials and Methods

Acetovanillone was purchased from Oakwood Chemicals. O-(Benzotriazol-1-yl)-N,N,N',N'-tetramethyluronium hexafluorophosphate (HBTU) and N,N'-Disuccinimidyl carbonate (DSC) were purchased from Chem-Impex International. Tin(II) 2-ethylhexanoate, fluorescamine, and tris(2-dimethylaminoethyl)amine, were purchased from Alfa Aesar. All other chemicals were purchased from Sigma-Aldrich and Fisher Scientific and were used without purification unless otherwise noted. NIPAM was purified by repeated recrystallization in hexanes and dried in

vacuum at 40 °C. Copper bromide (Cu(I)Br) was purified by stirring in glacial acetic acid for 16 hours, filtration and rinsing with ethanol and diethyl ether twice and storing in a desiccator. Lysozyme from chicken egg white, Catalog No. J60701.06, Lot: V041520 was purchased from Sigma Aldrich. Lyophilized cells from Micrococcus Lysodeikticus ATCC No. 4698 were purchased from Sigma Aldrich.

For photocleavage experiments, a 4 watt, 365 nm lamp was used (brand: UVP).

4.3.4 Analytical Techniques

Bruker AV 500 MHz spectrometer. Proton NMR spectra were acquired with a relaxation delay for 2 s for small molecules. Abbreviations are s = singlet, d = doublet, t = triplet, q = quartet, p = pentet, m = multiplet. For SDS PAGE, BioRad Any kDa Mini-PROTEAN-TGX™ gels were used. SDS-PAGE protein standards were obtained from Bio-Rad (Precision Plus Protein Prestained Standards). Small molecule purification was done *via* flash chromatography and conducted on a Biotage Isolera One auto-column system. Size exclusion chromatography (SEC) measurements in DMF were performed on an Infinity 1260 II HPLC system from Agilent equipped with a diode array detector DAD from Wyatt technology. The system also included a multiangle light scattering detector MALS and differential refractive index detector dRI from Wyatt technology. Polymers were separated on two PLgel Mixed-D gel columns PL1110-6504 (300 x 7.5 mm) (exclusion limits from 200 to 400000 Da) at a flow rate of 0.6 mL min^{-1}. Column temperatures were held at 40 °C in DMF with LiBr (0.1 M). Molar masses were calculated from PMMA standards. Conjugates were purified and analyzed by Fast Protein Liquid Chromatography on a Bio-Rad BioLogic DuoFlow chromatography system equipped with a HiTrap SP HP column employing a method of 0 to 1 M NaCl in 10 mM PB, pH 6.0 (Buffer A: 10 mM PB, pH 6.0; Buffer B: 10 mM PB, pH 6.0 + 1 M NaCl; 0.4 mL/min; 1 x 0.10 mL

injections; 2 CV 0% Buffer B, then 8 CV 0- 100% Buffer B, then 2 CV 100% Buffer B). Plate reader assays for protein quantification by BSA standard assay, Fluorescamine, and lysozyme activity assay were run on a Molecular Devices Spectramax iD3 instrument and data analysis was conducted on SoftMax Pro 7.1 software.

4.3.5 Appendix with Supplemental Figures

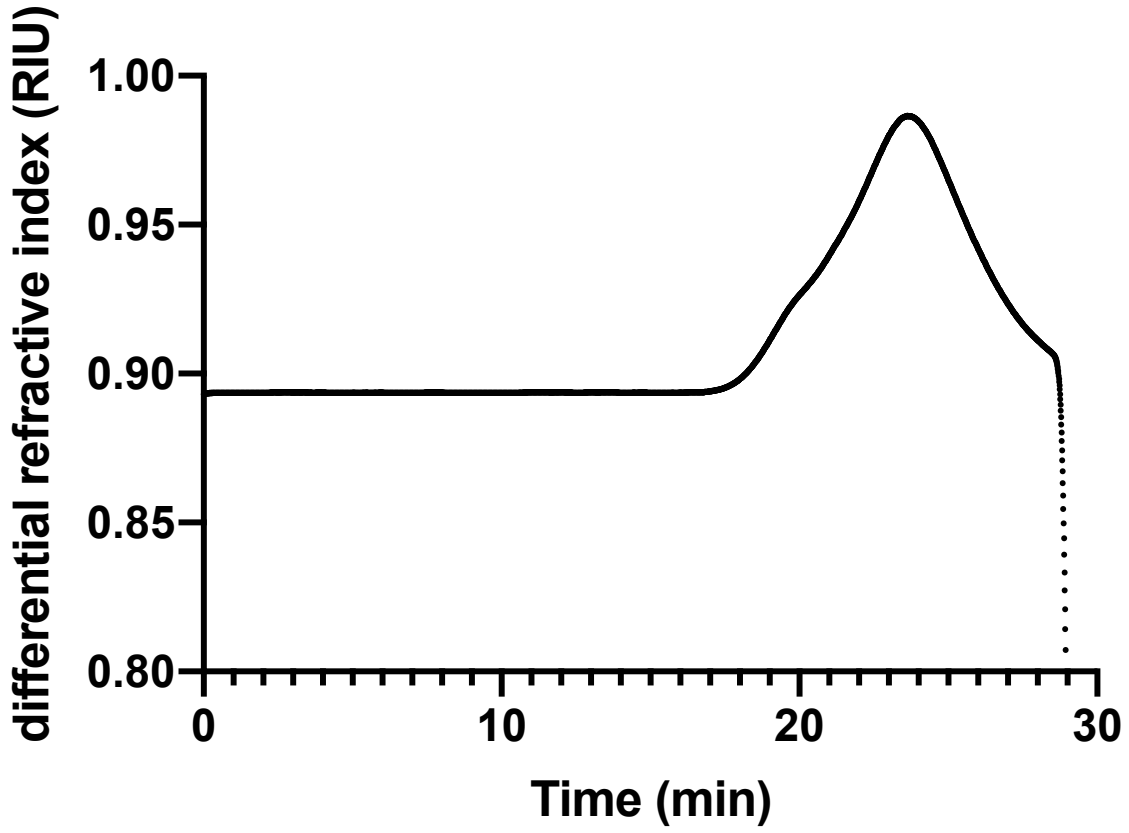

Figure S4.4 DMF SEC trace of noncleavable pNIPAM (Table 1 Entry 7).

M_n (kDa): 22.6
$Đ$: 1.51

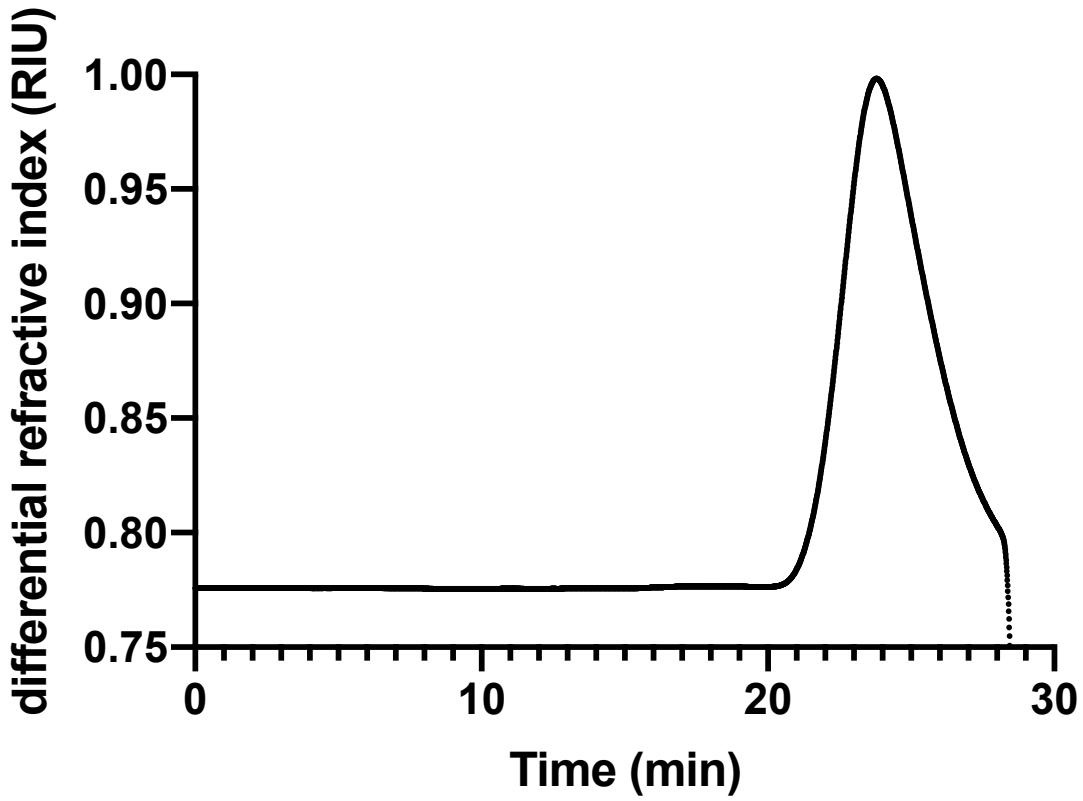

Figure S4.5 DMF SEC trace of noncleavable pNIPAM (Table 1 Entry 8).

M_n (kDa): 19.9
$Đ$: 1.23

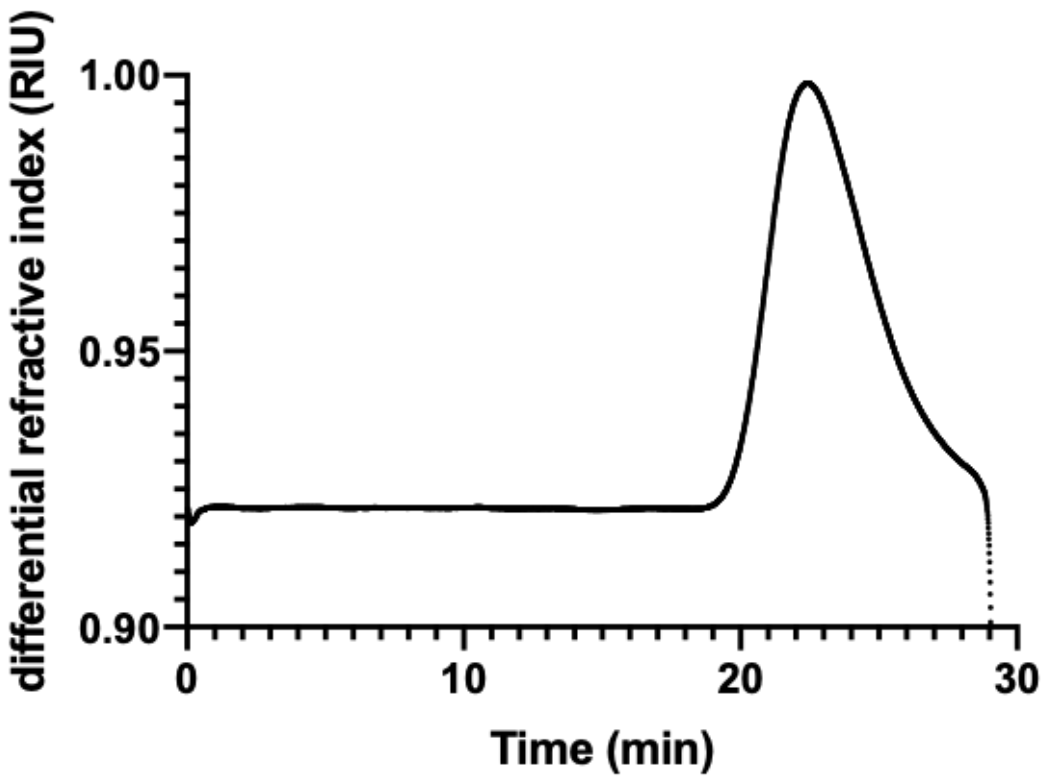

Figure S4.6 DMF SEC trace of photocleavable pNIPAM (Table 2 Entry 1).

M_n (kDa): 33.9
$Đ$: 1.21

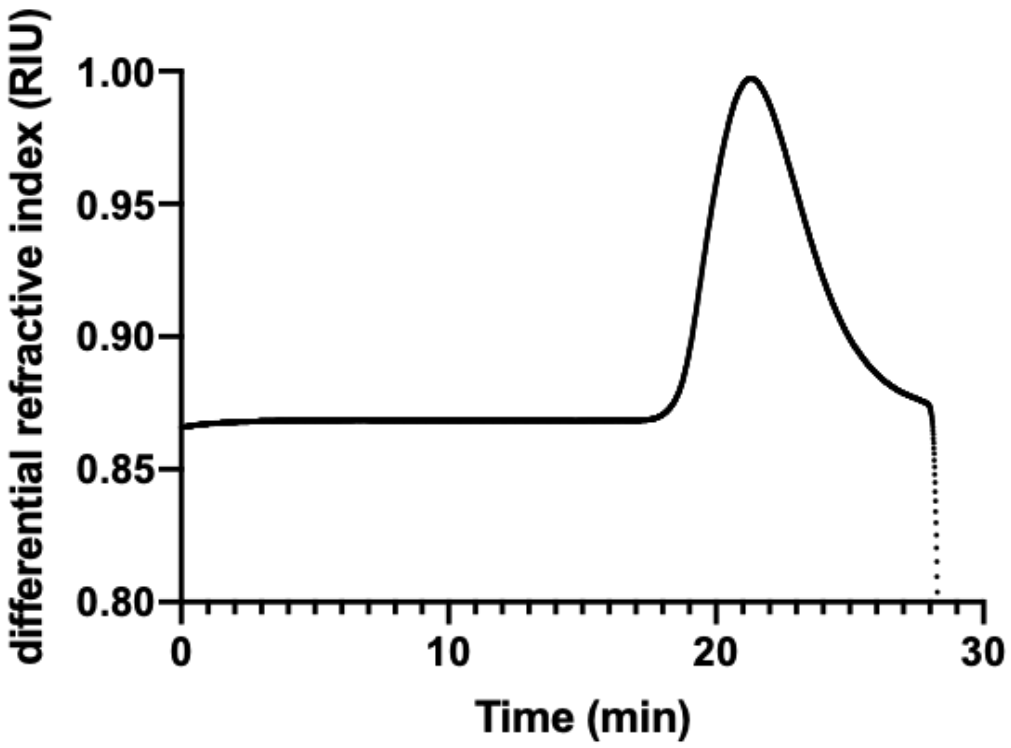

Figure S4.7 DMF SEC trace photocleavable pNIPAM (Table 1 Entry 2).

M_n (kDa): 48.5
$Đ$: 1.42

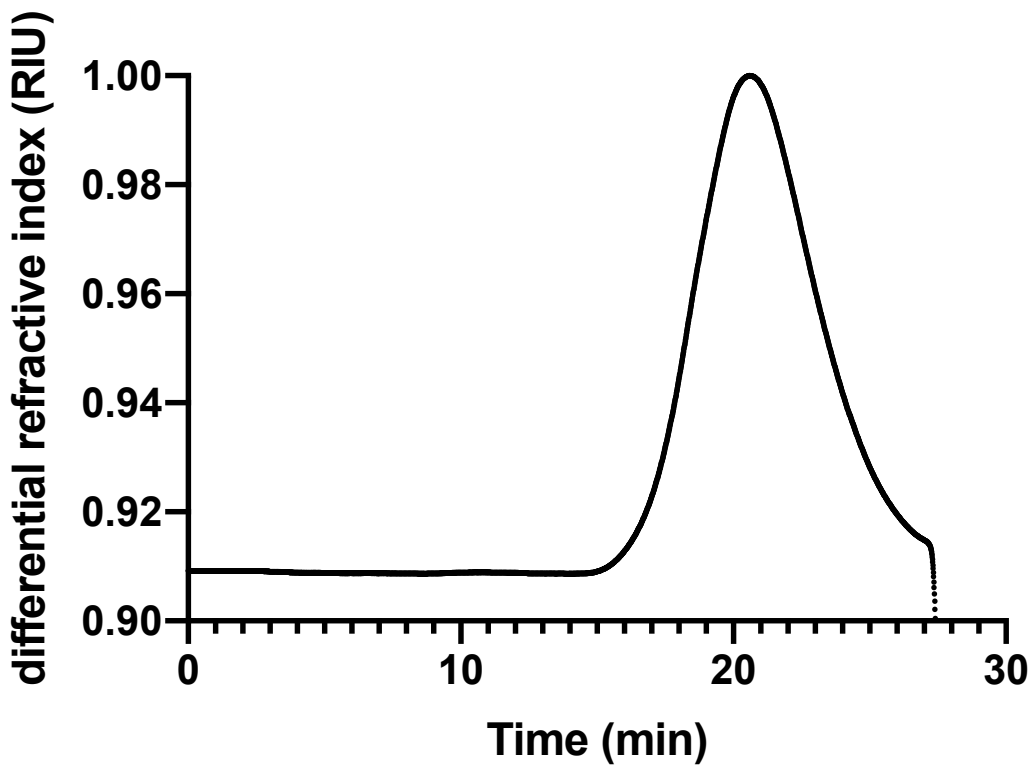

Figure S4.8 DMF SEC trace of photocleavable pNIPAM (Table 2 Entry 3).

M_n (kDa): 66.8
$Đ$: 1.89

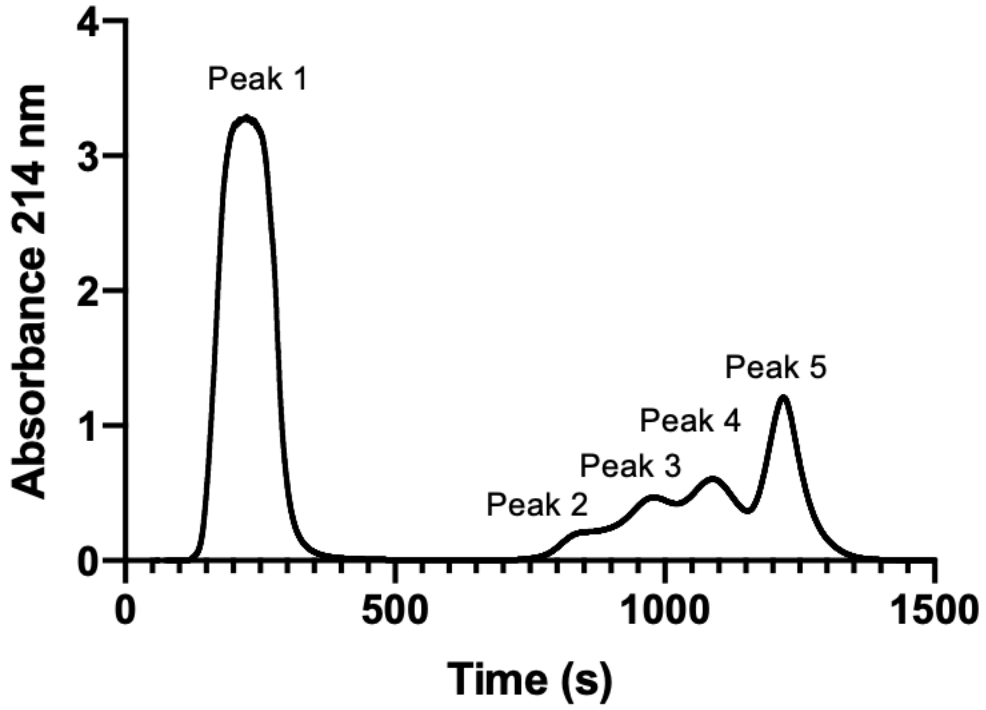

Figure S4.9 FPLC chromatogram of noncleavable NIPAM lysozyme conjugate.

Peak 1 represents unreacted noncleavable pNIPAM; Peak 2-4 represents different number-modified lysozyme conjugates; Peak 5 represent unreacted lysozyme. Note: FPLC may not have fully separated polymer, conjugate, and native enzyme as will be observed below in Figure S4.10.

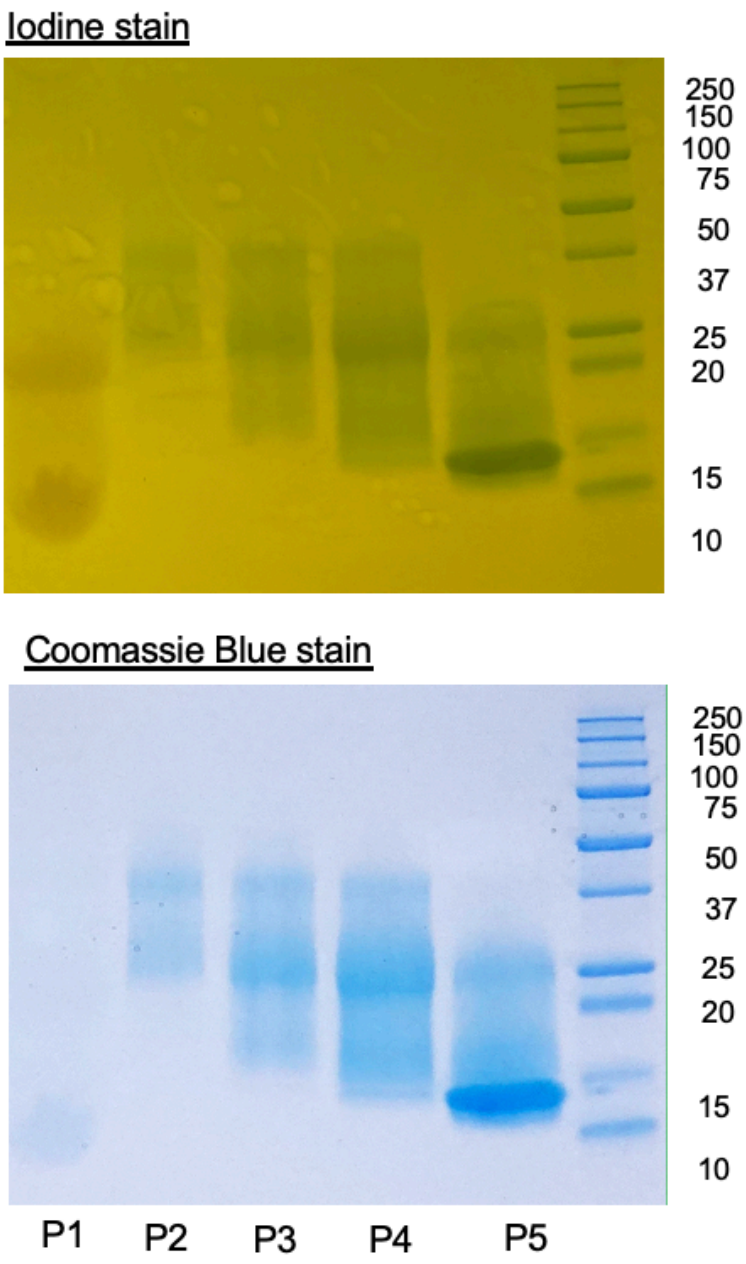

Figure S4.10: SDS PAGE analysis of FPLC fractions of noncleavable pNIPAM lysozyme conjugates

P1 represents unreacted noncleavable pNIPAM (and possible degraded protein); P2-4 represents different number-modified lysozyme conjugates; P5 represent unreacted lysozyme (P = peak from FPLC Chromatogram).

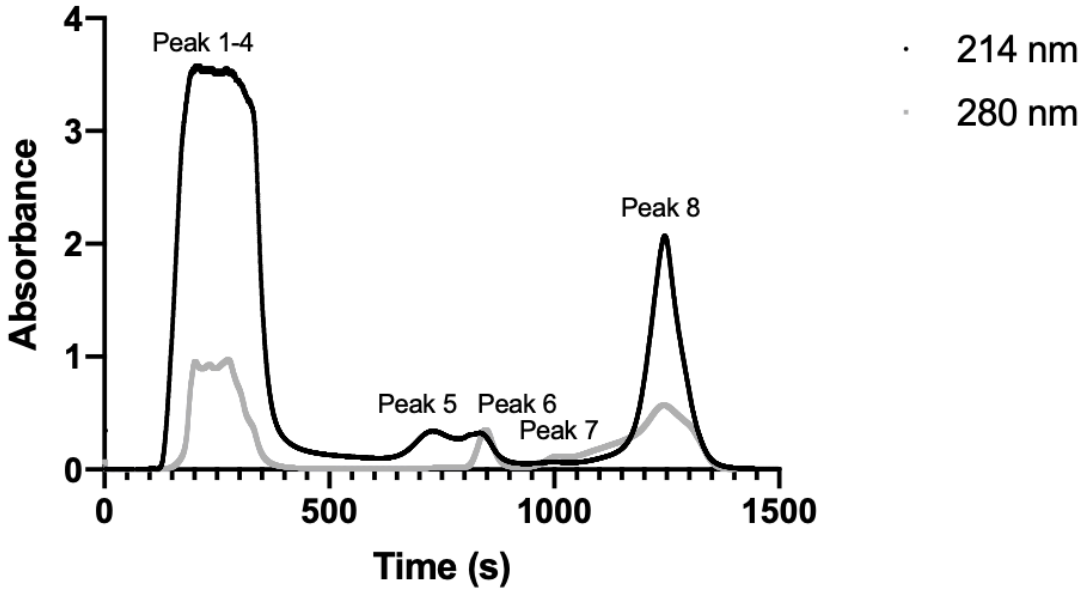

Figure S4.11 FPLC chromatogram of photocleavable NIPAM lysozyme conjugate.

Peak 1-4 represents unreacted noncleavable pNIPAM; Peak 5-7 represents different number-modified lysozyme conjugates; Peak 8 represent unreacted lysozyme. Note: FPLC may not have fully separated polymer, conjugate, and native enzyme as will be observed below in Figure S4.12.

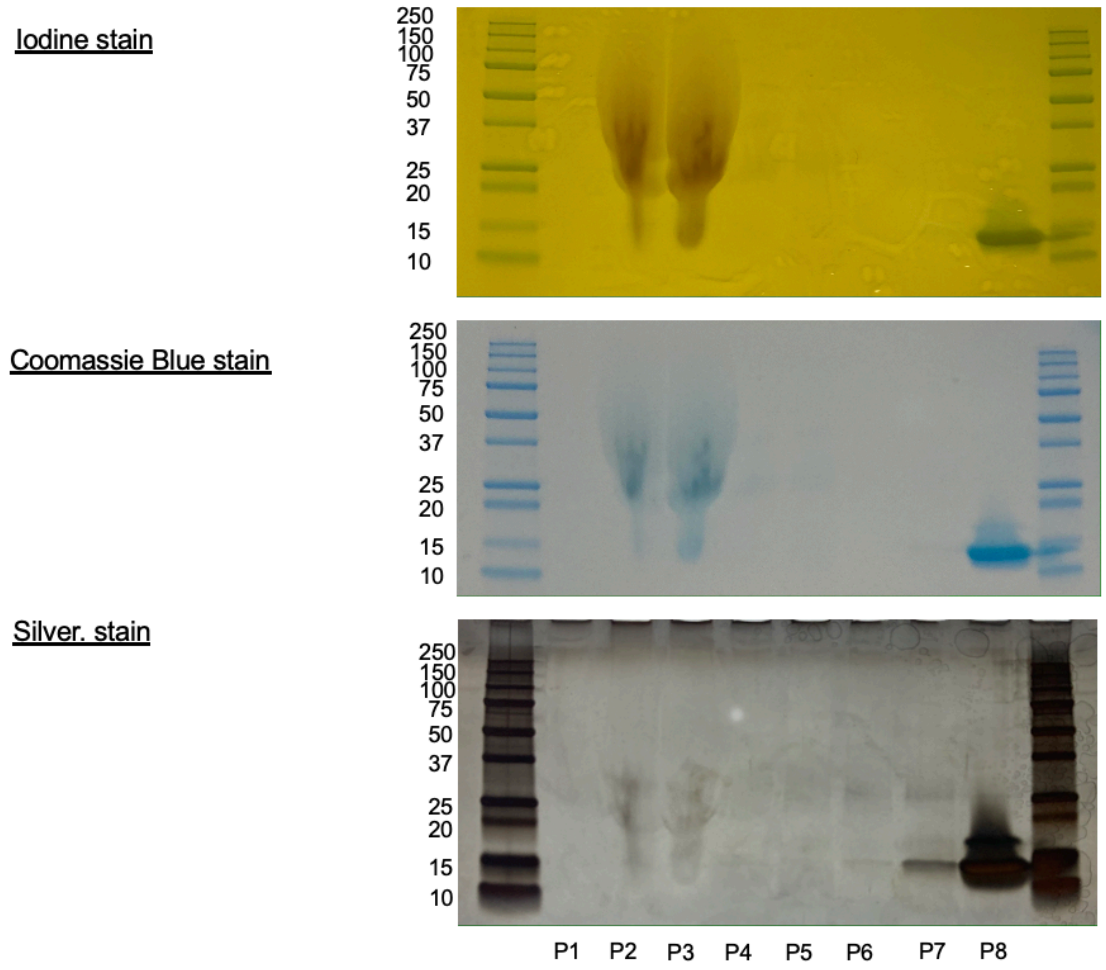

Figure S4.12 SDS PAGE analysis of FPLC fractions of noncleavable pNIPAM lysozyme conjugates.

P1-4 represents unreacted noncleavable pNIPAM; P5-7 represents different number-modified lysozyme conjugates; P8 represent unreacted lysozyme (P = peak from FPLC Chromatogram).

4.3.6 Experimental and Appendix References

General Procedure for the AGET ATRP of NIPAM with Initiator.

To a 20 mL Schlenk flask was added Me_6TREN (33 µL, 0.12 mmol, 4 Equiv.), which was diluted with 0.1 mL of solvent. This solution was allowed to deoxygenate *via* sparging with argon for 15 minutes. To a second 20 mL Schlenk flask was added NIPAM (876 mg, 7.75 mmol,

250 Equiv.), initiator (20 mg, 0.031 mmol, 1 Equiv.) and DMF as an internal standard. The monomer-initiator solution was diluted with 7 mL of solvent and 700 µL of DMSO to fully dissolve the initiator. The solution was also deoxygenated *via* sparging with argon for 30 minutes. Meanwhile, $CuBr_2$ (6.9 mg, 0.031 mmol, 1 Equiv.) was added to the first Schlenk flask under a positive argon flow. Upon addition of $CuBr_2$, the catalyst complex solution became blue as expected. This solution was continued to deoxygenate *via* sparging with argon for an additional 30 minutes. A stock solution of ascorbic acid dissolved in solvent was prepared and deoxygenated *via* sparging for 30 minutes. After 30 minutes, the monomer-initiator solution was transferred *via* an argon-flushed syringe into the catalyst complex solution. Then, ascorbic acid (3.3 mg, 0.05 mL, 0.019 mmol, 0.6 Equiv.) was fed slowly into the reaction solution *via* an argon-flushed syringe. Upon complete addition of the ascorbic acid, the reaction mixture turned into an olive-green color. The reaction was allowed to stir for 15 hours at 30 ℃ under a closed argon atmosphere. Reaction was quenched by exposing solution to air and diluting with THF. To purify polymer, the crude solution was passed through a neutral alumina oxide column and precipitated into cold diethyl ether. A wash with cold diethyl ether was carried out three times. The final polymer was dried under high vacuum.

General Procedure for the SARA ATRP of NIPAM with Initiator.

To a 20 mL Schlenk flask was added Me_6TREN (87 µL, 0.34 mmol, 3 Equiv.), which was diluted with 3 mL of solvent. This solution was allowed to deoxygenate *via* sparging with argon for 15 minutes. To a second Schlenk flask was added NIPAM (1.2 g, 10 mmol, 90 Equiv.), initiator (30 mg, 0.11 mmol, 1 Equiv.), and DMF as an internal standard. The monomer-initiator solution was diluted with 1 mL of IPA to dissolve the monomer and 100 µL of DMSO to fully

dissolve the initiator. After 15 minutes, copper nanopowder (4.3 mg, 0.068 mmol, 0.6 Equiv.) was added to the first Schlenk flask under a positive argon flow, and then finally $CuBr_2$ (10 mg, 0.045 mmol, 0.4 Equiv.) was added. Upon addition of $CuBr_2$, the catalyst complex solution became blue in color with black specs of copper nanopowder at the bottom. The catalyst complex solution was allowed to deoxygenate for another 15 minutes *via* sparging with argon. Finally, to initiate the polymerization, the monomer-initiator solution was transferred *via* an argon-flushed syringe into the catalyst complex solution. Reaction was allowed to stir for 1 hour at 30 °C under a closed argon atmosphere. Reaction was quenched by exposing solution to air and diluting with THF. To purify polymer, the crude solution was passed through a neutral alumina oxide column and precipitated into cold diethyl ether. A wash with cold diethyl ether was carried out three times. After drying under high vacuum, final polymer was then characterized by ^1H NMR and DMF SEC analysis (with PMMA standards).

General Procedure for Conjugation of Photocleavable Polymers to Lysozyme:

A 1 mg/mL solution of lysozyme was prepared in pH 9, 50 mM sodium carbonate buffer. After the protein concentration was determined *via* a BCA assay, a photocleavable polymer (2.9 μmol, 4 equiv. with respect to lysine residues) dissolved in DMSO was added to the protein solution (final DMSO concentration of 5% (v/v)). The conjugation reaction was allowed to proceed for 5 h at 25 °C.

General Procedure for Photocleavage of Protein-Polymer Conjugates:

Samples, diluted up to 100 μL of pH 8 phosphate buffer, were irradiated with UV light (365 nm, 4 watt) for 1 hour at 4 ℃ to allow for photocleavage of the polymer from the protein. Afterwards, samples were immediately used for activity assay for further characterization.

General Procedure for Activity Assay of Protein-Polymer Conjugates:

Samples were added to a transparent 96-well plate. All samples were mixed with 200 μL of a suspension of lyophilized Micrococcus Lysodeikticus cells (0.15 mg/mL in 50 mM potassium phosphate buffer, pH 6.24). Absorbance measurements were taken at 450 nm for 30 minutes over 30 second intervals. The change in absorbance over 120 minutes was determined and used to determine protein activity.

4.4 Conclusion

Although further studies need to be conducted to confirm our hypotheses that the pNIPAM versions of the noncovalent enzyme nanogels and protein-polymer conjugates are just as successful in providing protein stabilization while protecting protein activity, these initial results are quite promising. This work demonstrates potential in advancing current drug delivery systems and other biotechnology products by incorporating polymeric alternatives to PEG. While the industry may be slow to adapt to other polymer types beyond PEG, these PEG alternatives undeniably allow for conjugates to possess increased efficacy for their intended applications. This work further demonstrates the versatility of the systems reported herein.

4.5 References

(1) Hoang Thi, T. T.; Pilkington, E. H.; Nguyen, D. H.; Lee, J. S.; Park, K. D.; Truong, N. P. The Importance of Poly(Ethylene Glycol) Alternatives for Overcoming PEG Immunogenicity in Drug Delivery and Bioconjugation. *Polymers* **2020**, *12* (2), 298. https://doi.org/10.3390/polym12020298.

(2) Argentieri, M.; Schabowsky, C. N.; Kommala, D. ECRI Corporate Governance.

(3) Tamshen, K.; Wang, Y.; Jamieson, S. M. F.; Perry, J. K.; Maynard, H. D. Genetic Code Expansion Enables Site-Specific PEGylation of a Human Growth Hormone Receptor Antagonist through Click Chemistry. *Bioconjug. Chem.* **2020**, *31* (9), 2179–2190. https://doi.org/10.1021/acs.bioconjchem.0c00365.

(4) Wang, Y.; Langley, R. J.; Tamshen, K.; Harms, J.; Middleditch, M. J.; Maynard, H. D.; Jamieson, S. M. F.; Perry, J. K. Enhanced Bioactivity of a Human GHR Antagonist Generated by Solid-Phase Site-Specific PEGylation. *Biomacromolecules* **2021**, *22* (2), 299–308. https://doi.org/10.1021/acs.biomac.0c01105.

(5) Pelegri-O'Day, E. M.; Matsumoto, N. M.; Tamshen, K.; Raftery, E. D.; Lau, U. Y.; Maynard, H. D. PEG Analogs Synthesized by Ring-Opening Metathesis Polymerization for Reversible Bioconjugation. *Bioconjug. Chem.* **2018**, *29* (11), 3739–3745. https://doi.org/10.1021/acs.bioconjchem.8b00635.

(6) Kozma, G. T.; Shimizu, T.; Ishida, T.; Szebeni, J. Anti-PEG Antibodies: Properties, Formation, Testing and Role in Adverse Immune Reactions to PEGylated Nano-Biopharmaceuticals. *Adv. Drug Deliv. Rev.* **2020**, *154–155*, 163–175. https://doi.org/10.1016/j.addr.2020.07.024.

(7) Chen, B.-M.; Cheng, T.-L.; Roffler, S. R. Polyethylene Glycol Immunogenicity: Theoretical, Clinical, and Practical Aspects of Anti-Polyethylene Glycol Antibodies. *ACS Nano* **2021**, *15* (9), 14022–14048. https://doi.org/10.1021/acsnano.1c05922.

(8) Ibrahim, M.; Ramadan, E.; Elsadek, N. E.; Emam, S. E.; Shimizu, T.; Ando, H.; Ishima, Y.; Elgarhy, O. H.; Sarhan, H. A.; Hussein, A. K.; Ishida, T. Polyethylene Glycol (PEG): The Nature, Immunogenicity, and Role in the Hypersensitivity of PEGylated Products. *J. Controlled Release* **2022**, *351*, 215–230. https://doi.org/10.1016/j.jconrel.2022.09.031.

(9) Shi, D.; Beasock, D.; Fessler, A.; Szebeni, J.; Ljubimova, J. Y.; Afonin, K. A.; Dobrovolskaia, M. A. To PEGylate or Not to PEGylate: Immunological Properties of Nanomedicine's Most Popular Component, Polyethylene Glycol and Its Alternatives. *Adv. Drug Deliv. Rev.* **2022**, *180*, 114079. https://doi.org/10.1016/j.addr.2021.114079.

(10) Cox, F.; Khalib, K.; Conlon, N. PEG That Reaction: A Case Series of Allergy to Polyethylene Glycol. *J. Clin. Pharmacol.* **2021**, *61* (6), 832–835. https://doi.org/10.1002/jcph.1824.

(11) Monji, N.; Hoffman, A. S. A Novel Immunoassay System and Bioseparation Process Based on Thermal Phase Separating Polymers. *Appl. Biochem. Biotechnol.* **1987**, *14* (2), 107–120. https://doi.org/10.1007/BF02798429.

(12) Vaidya, A. A.; Lele, B. S.; Kulkarni, M. G.; Mashelkar, R. A. Thermoprecipitation of Lysozyme from Egg White Using Copolymers of N-Isopropylacrylamide and Acidic Monomers. *J. Biotechnol.* **2001**, *87* (2), 95–107. https://doi.org/10.1016/S0168-1656(00)00382-5.

(13) Vázquez-Dorbatt, V.; Tolstyka, Z. P.; Maynard, H. D. Synthesis of Aminooxy End-Functionalized pNIPAAm by RAFT Polymerization for Protein and Polysaccharide Conjugation. *Macromolecules* **2009**, *42* (20), 7650–7656. https://doi.org/10.1021/ma9013803.

(14) Jain, K.; Vedarajan, R.; Watanabe, M.; Ishikiriyama, M.; Matsumi, N. Tunable LCST Behavior of Poly(N-Isopropylacrylamide/Ionic Liquid) Copolymers. *Polym. Chem.* **2015**, *6* (38), 6819–6825. https://doi.org/10.1039/C5PY00998G.

(15) Pei, Y.; Chen, J.; Yang, L.; Shi, L.; Tao, Q.; Hui, B.; Li, J. The Effect of pH on the LCST of Poly(N-Isopropylacrylamide) and Poly(N-Isopropylacrylamide-Co-Acrylic Acid). *J. Biomater. Sci. Polym. Ed.* **2004**, *15* (5), 585–594. https://doi.org/10.1163/156856204323046852.

(16) Matsumoto, N. M.; Buchman, G. W.; Rome, L. H.; Maynard, H. D. Dual pH- and Temperature-Responsive Protein Nanoparticles. *Eur. Polym. J.* **2015**, *69*, 532–539. https://doi.org/10.1016/j.eurpolymj.2015.01.043.

(17) Gao, X.; Cao, Y.; Song, X.; Zhang, Z.; Xiao, C.; He, C.; Chen, X. pH- and Thermo-Responsive Poly(N -Isopropylacrylamide- Co -Acrylic Acid Derivative) Copolymers and Hydrogels with LCST Dependent on pH and Alkyl Side Groups. *J. Mater. Chem. B* **2013**, *1* (41), 5578–5587. https://doi.org/10.1039/C3TB20901F.

(18) McCallum, J. A.; Walker, J. R. L. Phenolic Biosynthesis during Grain Development in Wheat: Changes in Phenylalanine Ammonia-Lyase Activity and Soluble Phenolic Content. *J. Cereal Sci.* **1990**, *11* (1), 35–49. https://doi.org/10.1016/S0733-5210(09)80179-3.

(19) Udenfriend, S.; Stein, S.; Böhlen, P.; Dairman, W.; Leimgruber, W.; Weigele, M. Fluorescamine: A Reagent for Assay of Amino Acids, Peptides, Proteins, and Primary Amines in the Picomole Range. *Science* **1972**, *178* (4063), 871–872. https://doi.org/10.1126/science.178.4063.871.

(20) Zhang, A.; Barner, J.; Göessl, I.; Rabe, J. P.; Schlüter, A. D. A Covalent-Chemistry Approach to Giant Macromolecules and Their Wetting Behavior on Solid Substrates. *Angew. Chem. Int. Ed.* **2004**, *43* (39), 5185–5188. https://doi.org/10.1002/anie.200460390.

(21) Ye, J.; Narain, R. Water-Assisted Atom Transfer Radical Polymerization of N-Isopropylacrylamide: Nature of Solvent and Temperature. *J. Phys. Chem. B* **2009**, *113* (3), 676–681. https://doi.org/10.1021/jp808905s.

(22) Teodorescu, M.; Matyjaszewski, K. Atom Transfer Radical Polymerization of (Meth)Acrylamides. *Macromolecules* **1999**, *32* (15), 4826–4831. https://doi.org/10.1021/ma990175x.

(23) Fantin, M.; Isse, A. A.; Gennaro, A.; Matyjaszewski, K. Understanding the Fundamentals of Aqueous ATRP and Defining Conditions for Better Control. *Macromolecules* **2015**, *48* (19), 6862–6875. https://doi.org/10.1021/acs.macromol.5b01454.

(24) Zhang, Q.; Wilson, P.; Li, Z.; McHale, R.; Godfrey, J.; Anastasaki, A.; Waldron, C.; Haddleton, D. M. Aqueous Copper-Mediated Living Polymerization: Exploiting Rapid Disproportionation of CuBr with Me6TREN. *J. Am. Chem. Soc.* **2013**, *135* (19), 7355–7363. https://doi.org/10.1021/ja4026402.

(25) Heredia, K. L.; Bontempo, D.; Ly, T.; Byers, J. T.; Halstenberg, S.; Maynard, H. D. In Situ Preparation of Protein−"Smart" Polymer Conjugates with Retention of Bioactivity. *J. Am. Chem. Soc.* **2005**, *127* (48), 16955–16960. https://doi.org/10.1021/ja054482w.

(26) Heredero, M.; Beloqui, A. Enzyme-Polymer Conjugates for Tuning, Enhancing, and Expanding Biocatalytic Activity. *ChemBioChem* **2023**, *24* (4), e202200611. https://doi.org/10.1002/cbic.202200611.

(27) Vaidya, A. A.; Lele, B. S.; Deshmukh, M. V.; Kulkarni, M. G. Design and Evaluation of New Ligands for Lysozyme Recovery by Affinity Thermoprecipitation. *Chem. Eng. Sci.* **2001**, *56* (19), 5681–5692. https://doi.org/10.1016/S0009-2509(01)00169-5.

Chapter 5 Optimized Synthesis of Abuse-Deterrent Prodrug for Biological Studies

5.1 Introduction

The Secretary of the Department of Health and Human Services continues to declare substance abuse and overdose crisis as a Public Health Emergency.[1] Opioids were involved in over 80,000 overdose deaths in 2021, which equates to approximately 75% of all drug overdose deaths.[2] Many strategies to combat this epidemic are outlined in the FDA's Opioids Action Plan.[3] The development and use of abuse-deterrent opioid formulations is one promising strategy. According to the FDA, abuse-deterrent formulations target the known or expected routes of abuse.[4] The general categories of abuse-deterrent technology include: chemical and physical barriers, agonist/antagonist combination, inclusion of aversive substances, unconventional opioid delivery systems, and prodrugs.[5]

Our research group has been most interested in the prodrug technology for the development of abuse-deterrent formulations. We previously reported a dual-enzyme responsive peptide that released a small molecule payload upon sequential digestion by two enzymes—a digestive protease followed by trypsin.[6] It was envisioned that this modular design could be used for future drug delivery applications. We recently optimized this dual-enzyme responsive peptide platform towards an efficient abuse-deterrent opioid prodrug for oral administration. The optimized prodrug sequences were evaluated for their analgesic properties *in vivo* and were found to have a similar effect as oxycodone. The prodrug sequences were also determined to be stable to different pHs, household chemicals, and digestive enzyme kits to further confirm their ability to act as an abuse-deterrent prodrug to chemical and physical barriers. With these promising preliminary results, our next goal was to scale up the synthesis of the prodrugs to examine other biological effects of these prodrugs, such as chronic pain effects, post-operative pain effects, and sensory testing for chronic neuropathic pain. This chapter highlights the work

that was involved in scaling up the synthesis for one of the optimized prodrug sequences, BT-2-61L.

5.2 Results and Discussion

During the scaling-up process of BT-2-61L, only one major change was implemented in the synthesis. The main difference between how the prodrug was previously synthesized and in this work is outlined in Scheme 1. The initial strategy to synthesize the carboxybenzyl (Cbz) protected diamine began with a coupling between N-methylethylenediamine and ethyl trifluoroacetate followed by installation of the Cbz protecting group, then removal of the trifluoroacetate protecting group with lithium hydroxide. However, we found that a Boc-protected N-methylethylenediamine is commercially available for $2.8/g.

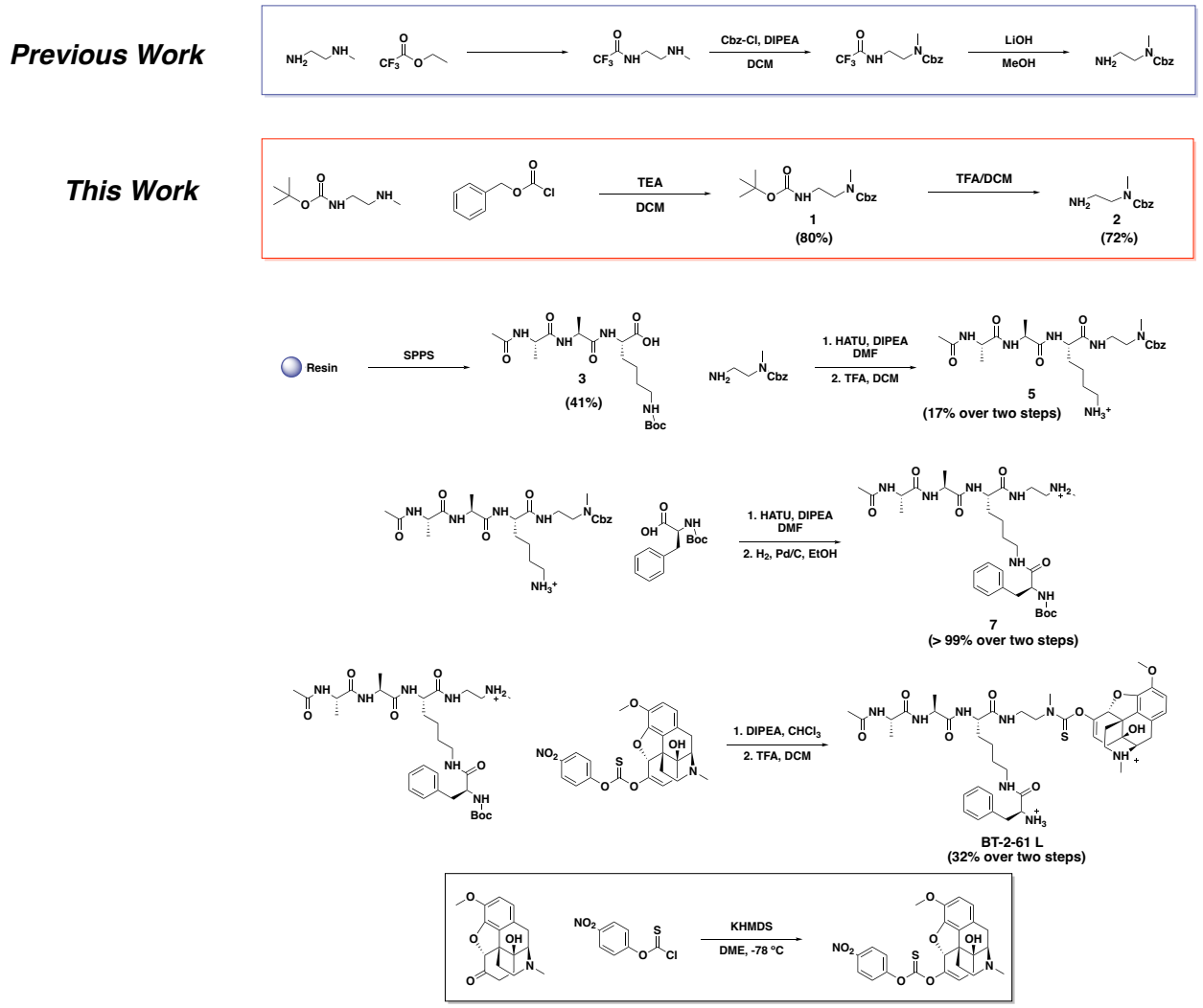

Figure 5.1 Optimized synthesis of prodrug BT-2-61 L.

This allowed for us to skip the initial coupling step and to immediately move forward to the Cbz installation to give compound **1** followed by Boc deprotection, which precipitates readily as the trifluoroacetate salt in diethyl ether as compound **2**. All subsequent steps in the synthesis of prodrug BT-2-61 L were followed as previously developed. Compound **2** was first coupled to peptide Ac-AAK (compound **3)** to afford compound **4**, which then undergone Boc-deprotection to give **5**. Compound **5** was then coupled to Boc-protected phenylalanine to yield compound **6.** Deprotection of the Cbz protecting group in **6** yielded **7**, which then allowed for the oxycodone

electrophile to be installed to give the final prodrug BT-2-61 L following the last Boc-deprotection of precursor compound **8**. It may be of interest to note that purification of each step was conducted either by reverse phase HPLC or precipitation in diethyl ether.

5.3 Conclusions

This chapter describes an optimized synthesis of prodrug BT-2 61 L, which enables for ease in scale-up. The prodrug prepared herein was given to Professor Catherine Cahill for further pain studies.

5.4 References

(1) *List of Public Health Emergency Declarations*. https://aspr.hhs.gov:443/legal/PHE/Pages/default.aspx (accessed 2023-11-29).

(2) *Drug Overdose Deaths | Drug Overdose | CDC Injury Center*. https://www.cdc.gov/drugoverdose/deaths/index.html (accessed 2023-08-16).

(3) Research, C. for D. E. and. FDA Opioids Action Plan. *FDA* **2018**.

(4) Research, C. for D. E. and. Abuse-Deterrent Opioid Analgesics. *FDA* **2021**.

(5) Litman, R. S.; Pagán, O. H.; Cicero, T. J. Abuse-Deterrent Opioid Formulations. *Anesthesiology* **2018**, *128* (5), 1015–1026. https://doi.org/10.1097/ALN.0000000000002031.

(6) Boehnke, N.; Maynard, H. D. Design of Modular Dual Enzyme-Responsive Peptides. *Pept. Sci.* **2017**, *108* (5), e23035. https://doi.org/10.1002/bip.23035.

5.5 Materials and Methods

Oxycodone was supplied by our collaborator Professor Chris Evans in the UCLA Department of Neurosciences who is licensed through the DEA. All other chemicals were used as purchased unless otherwise noted from Acros, Alfa Aesar, Sigma Aldrich, Combi-Blocks, Chem-Impex, or Fisher Scientific. All amino acids used in this study were purchased from Chem-Impex as the L-variants. Dichloromethane (DCM) was distilled over CaH_2 and stored under argon, 1,2-dimethoxyethane, methanol, acetonitrile (MeCN) and other dry solvents were dried by purging with nitrogen and passage through activated alumina columns prior to use.

5.6 Analytical Techniques

NMR spectra were obtained using either AV400 or AV500 spectrometers. ESI mass spectra were obtained using an Agilent 6530 QTOF-ESI with a 1260 Infinity LC with autosampler. Normal phase and reverse phase flash chromatography was carried out using a Biotage Isolera One Flash Purification Chromatography system. Analytical reverse phase HPLC was carried out on an Agilent 1260 Infinity II HPLC system equipped with an autosampler and a UV detector using a Poroshell 120 2.7 μm C18 120 Å column (Analytical: 2.7 μm, 4.6 x 100 mm) with monitoring at λ = 220 and 280 nm and with a flow rate of 0.8 mL/min. Preparatory reverse phase HPLC was carried out on an Agilent 1290 Infinity II high performance liquid chromatography system equipped with a UV detector using a Luna 5 μm C18 100 Å column (Preparatory: 5 μm, 250 × 21.2 mm) with monitoring at λ = 214 and 254 nm and with a flow rate of 20 mL/min.

5.7 Appendix with Supplementary Figures

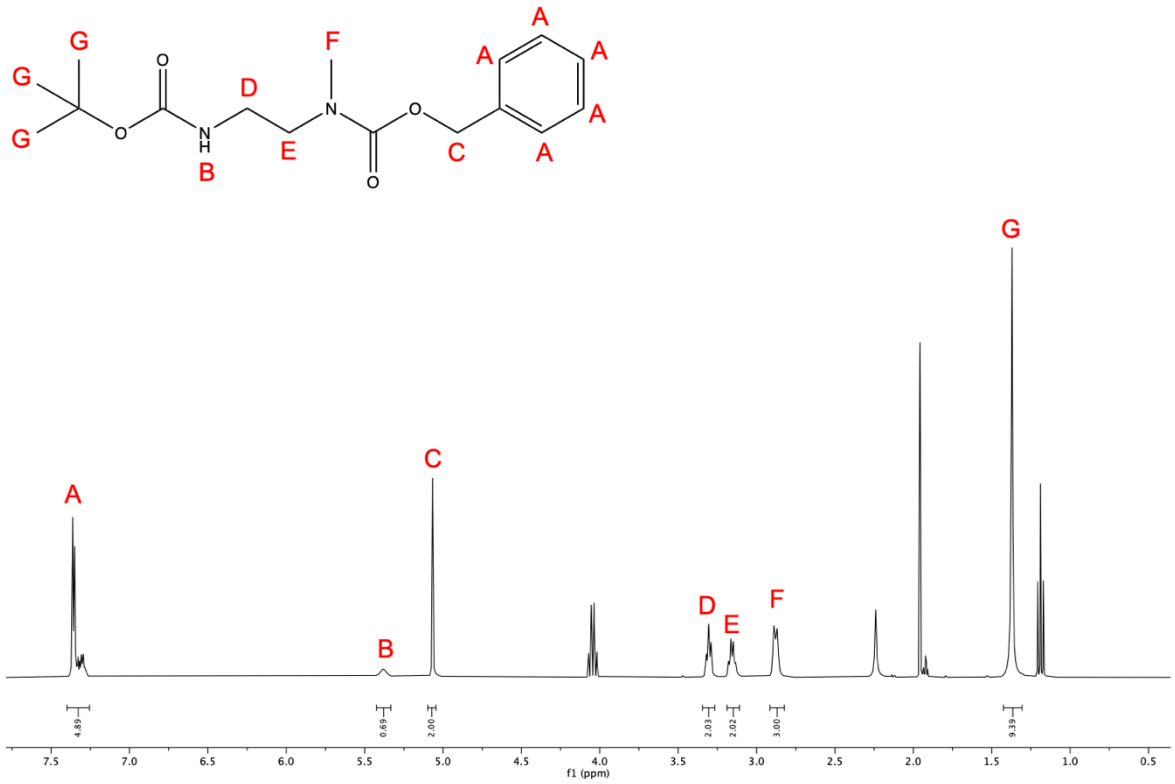

Figure S5.1 ^{1}H NMR spectrum of **1** in CD_3CN.

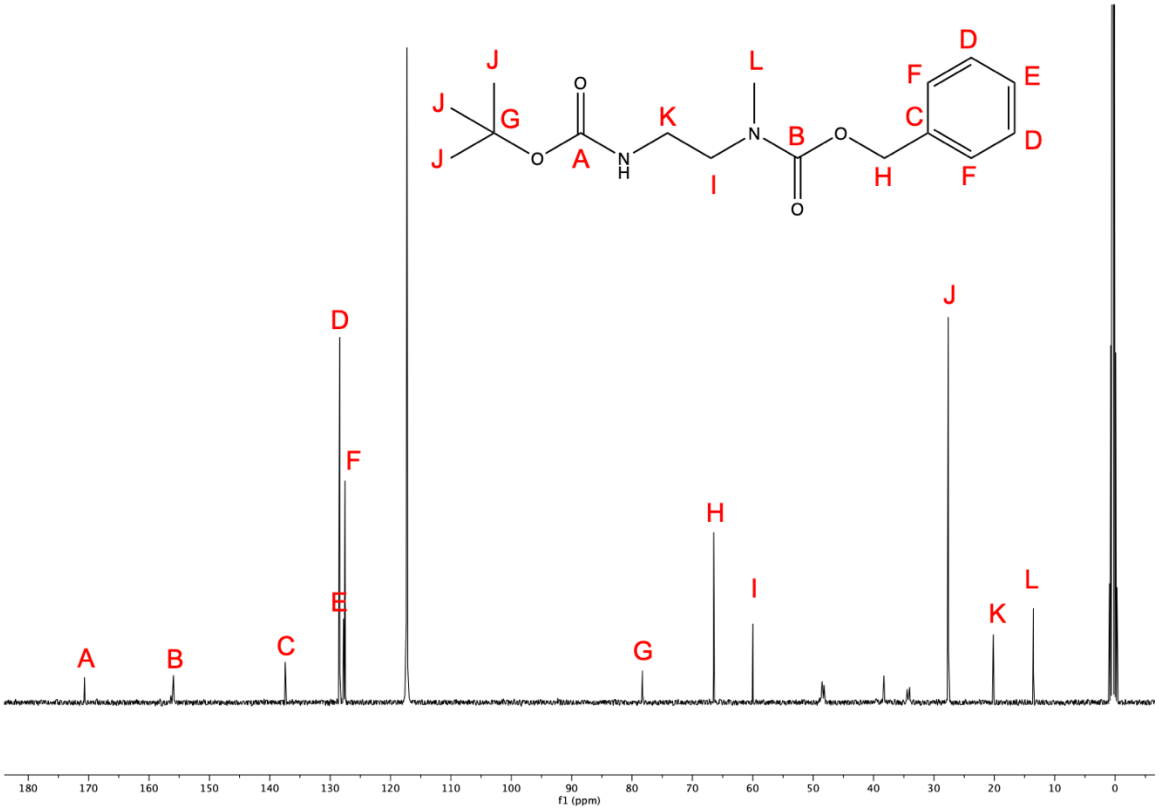

Figure S5.2 ^{13}C NMR Spectrum of **1** in CD_3CN.

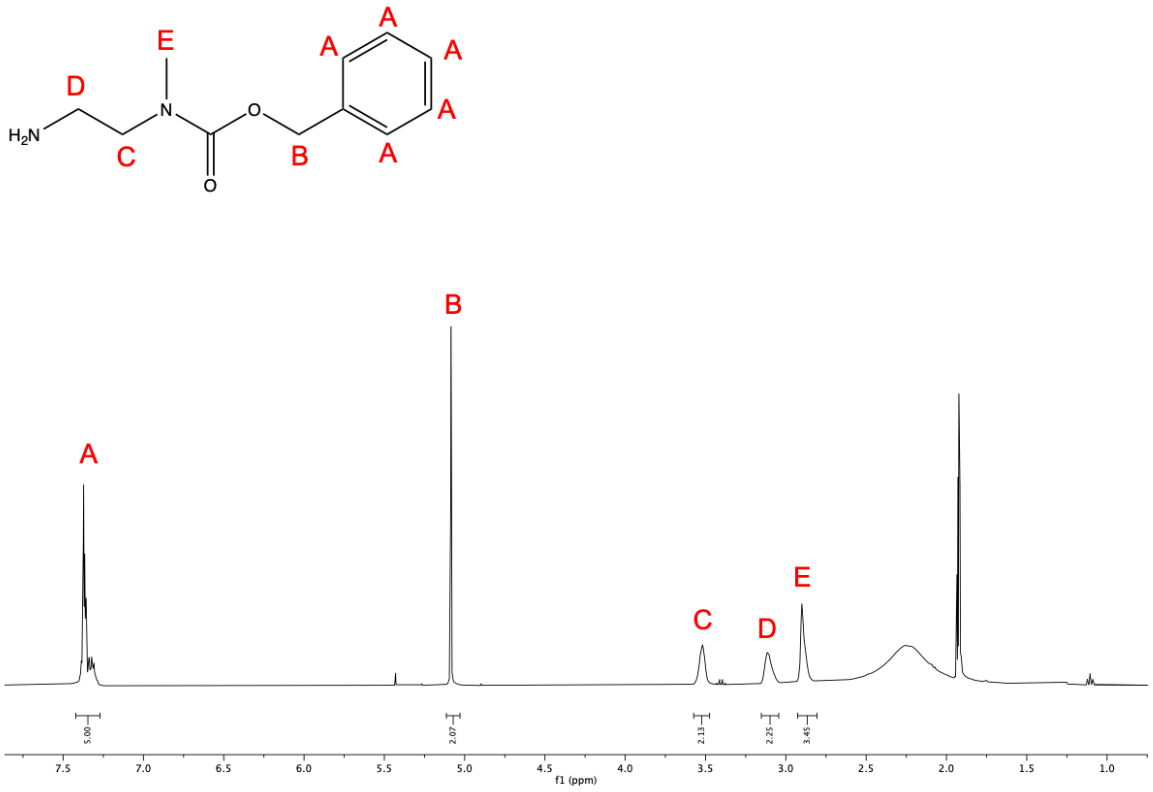

Figure S5.3 ^{1}H NMR Spectrum of **2** in CD_3CN.

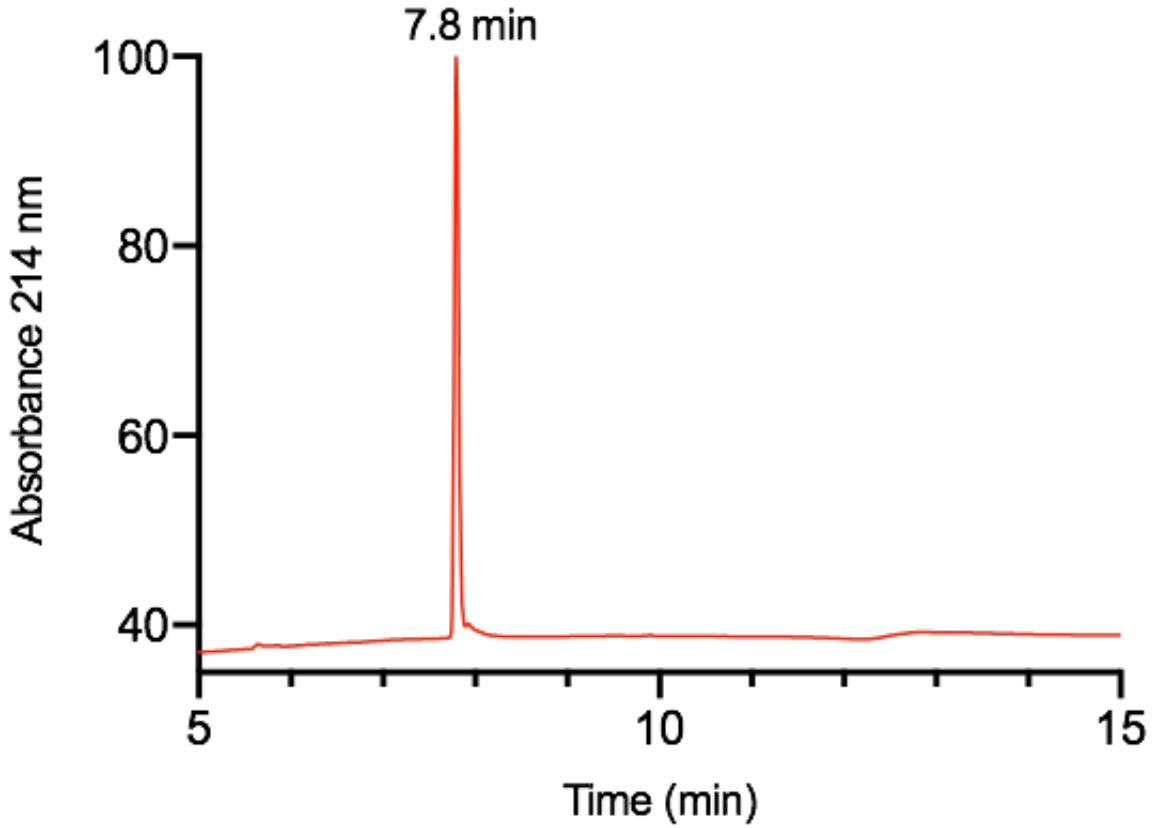

Figure S5.4 Analytical HPLC chromatogram of pure compound **4**.

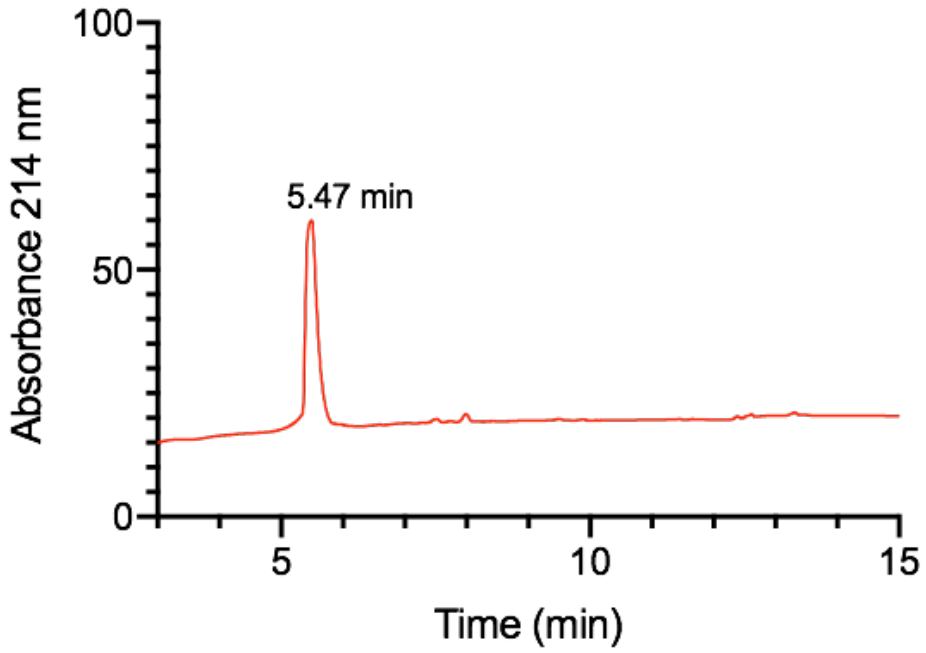

Figure S5.5 Analytical HPLC chromatogram of pure compound **5**.

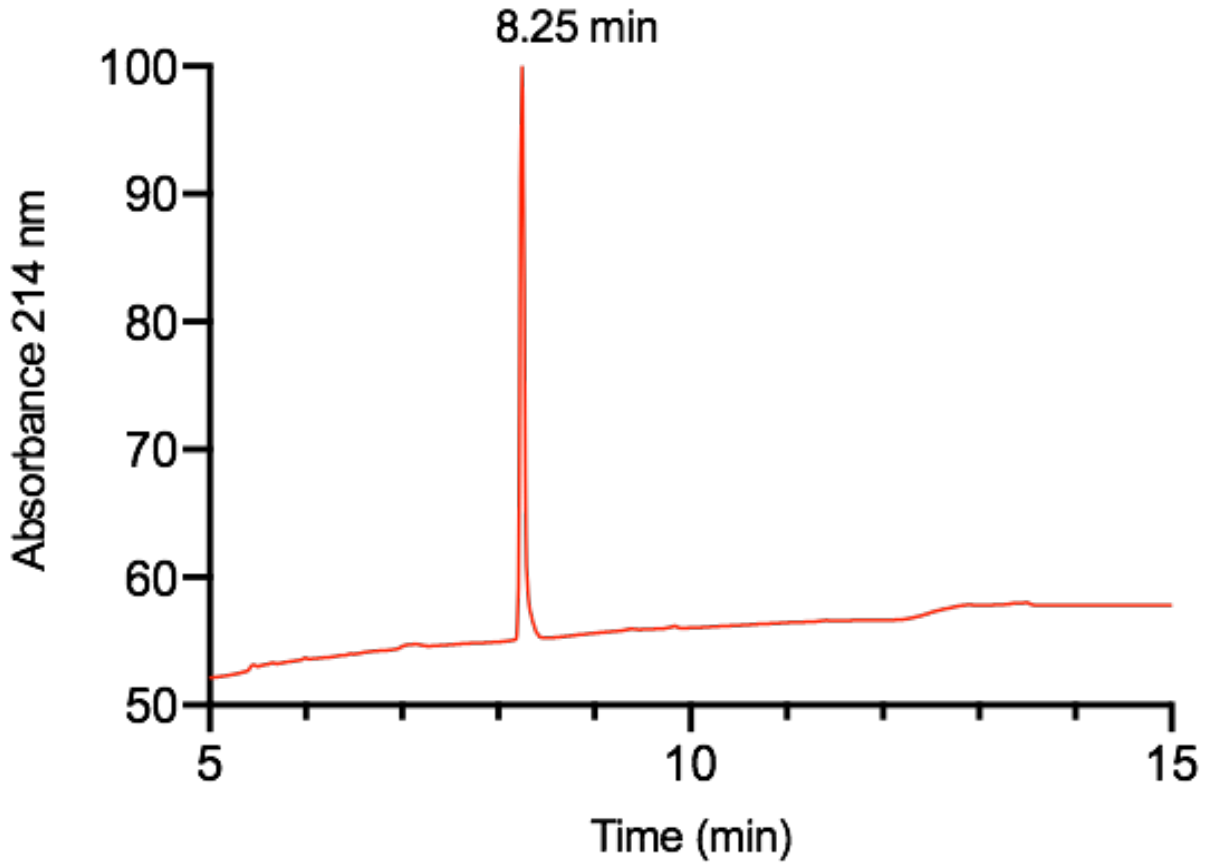

Figure S5.6 Analytical HPLC chromatogram of pure compound **6.**

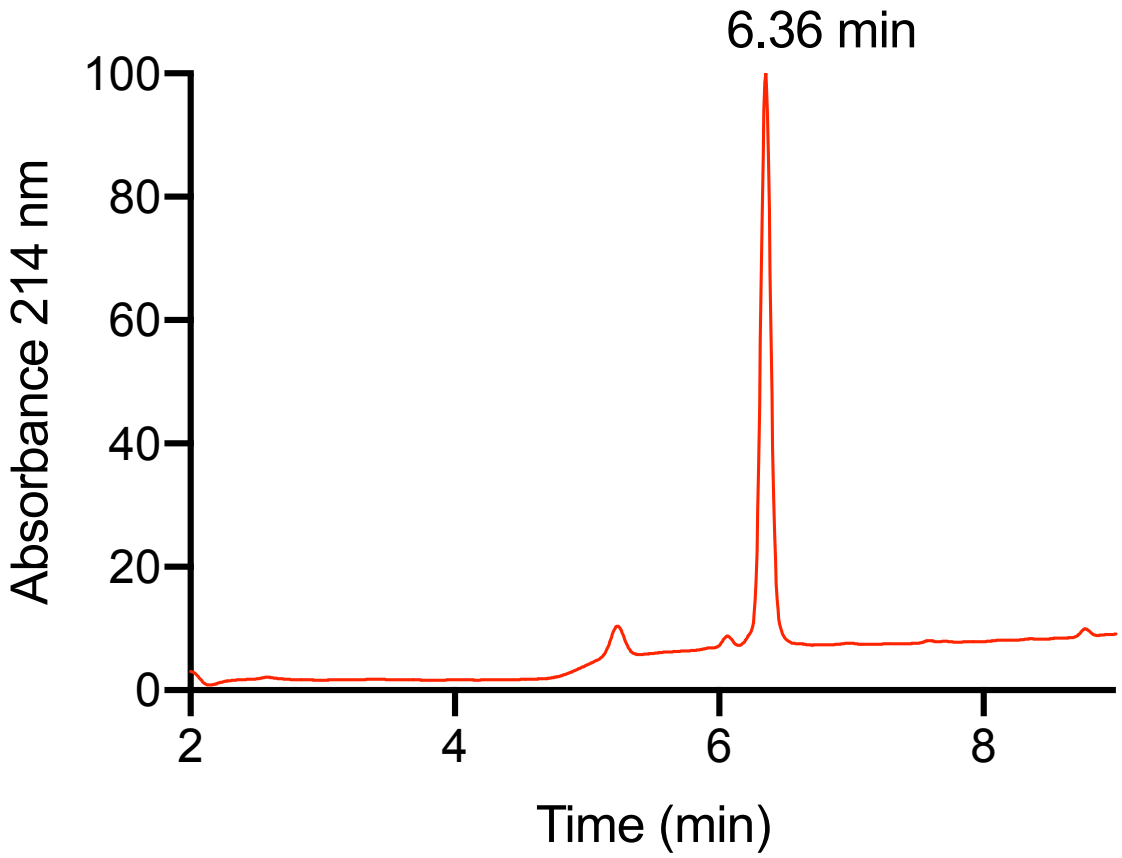

Figure S5.7 Analytical HPLC chromatogram of compound **7.**

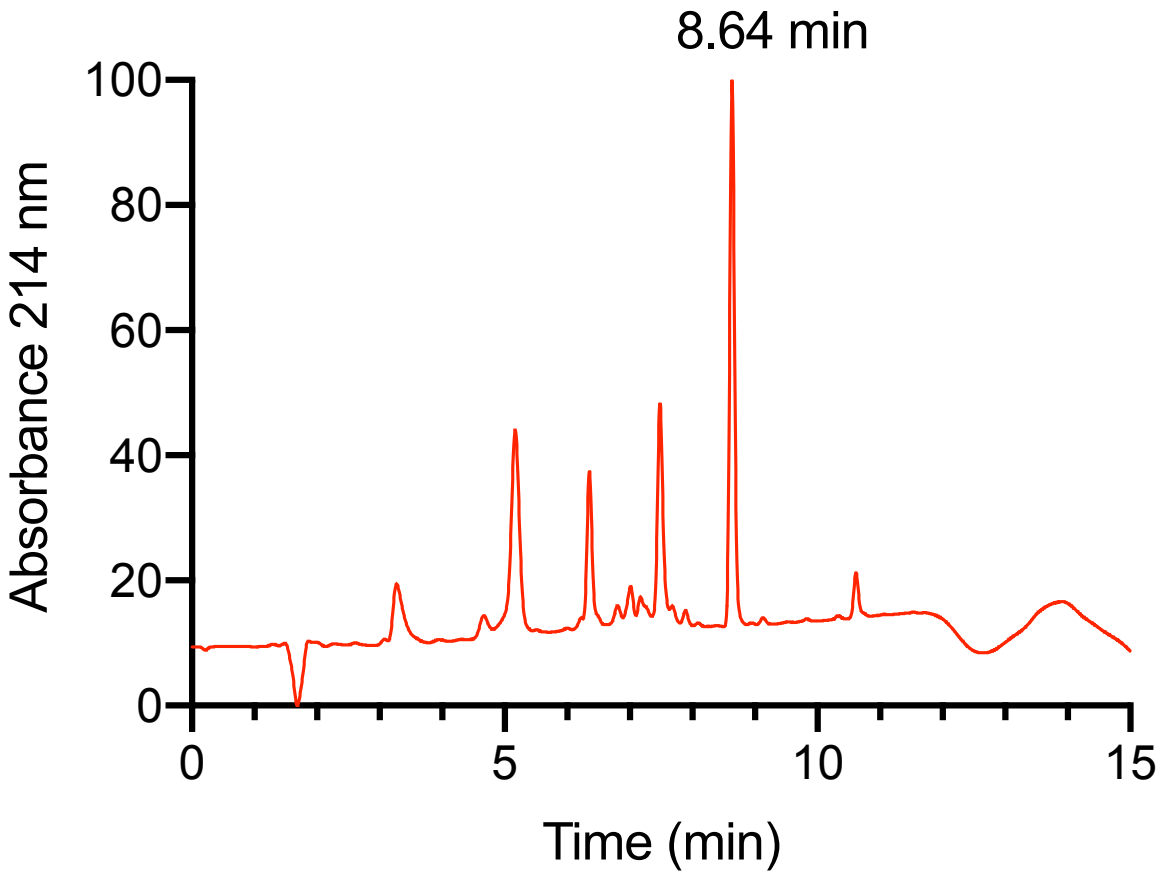

Figure S5.8 Analytical HPLC Chromatogram of compound **8.**

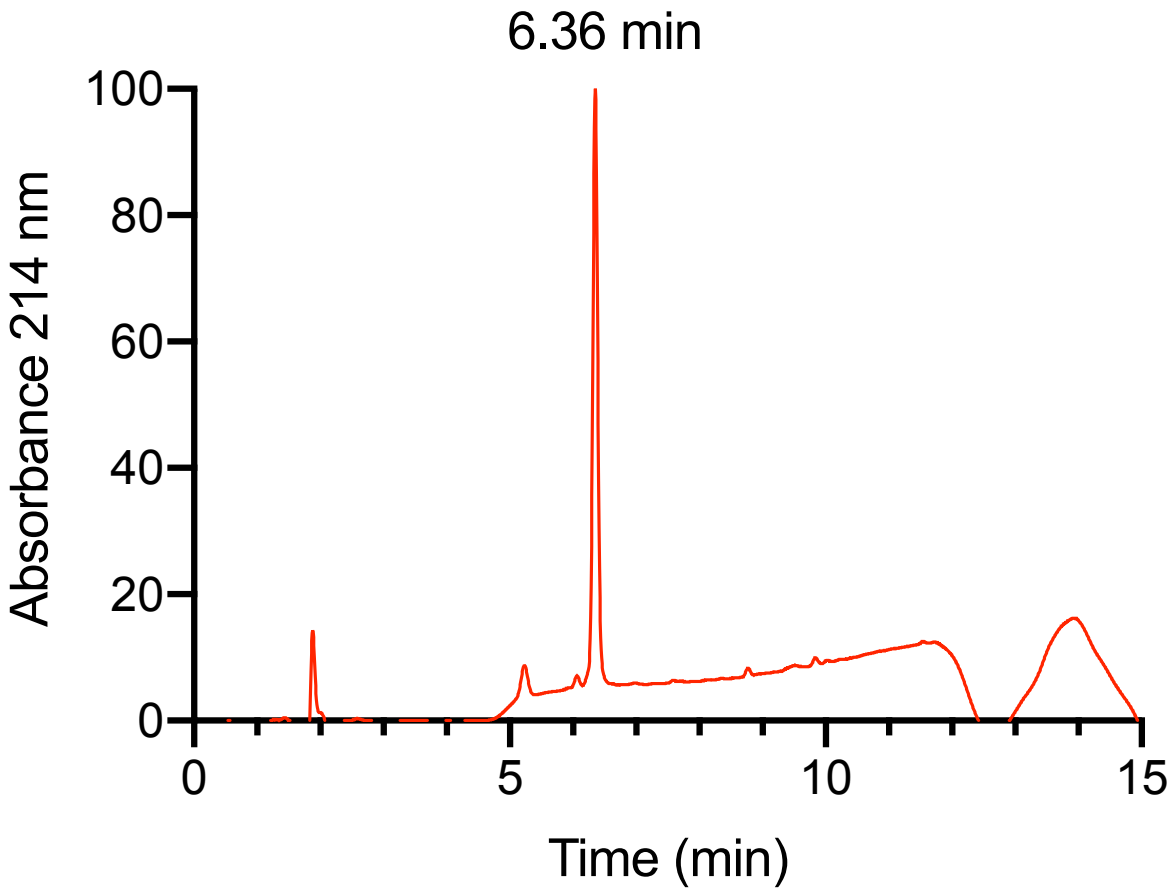

Figure S5.9 Analytical HPLC Chromatogram of pure BT-2-61 L.

5.7 Experimental and Appendix References

Synthesis of **1**

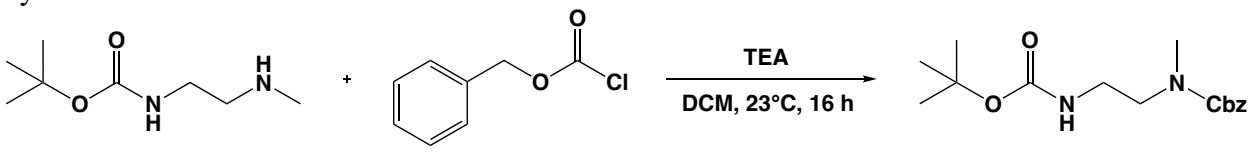

Procedure:

A two neck, 250 mL round bottom flask was charged with a stir bar and flame dried twice under vacuum with an argon cycle in between each flame dry. tert-Butyl2-(methylamino)ethylcarbamate (1.100 g, 1 Eq., 6.313 mmol) was weighed out as a yellow oil in a scintillation vial and transferred to the round bottom flask using 10 mL of anhydrous DCM. 40 mL of DCM were added to the flask, forming a pale yellow solution. Anhydrous triethylamine (1.022 g, 1.41 mL, 1.6 Eq., 10.10 mmol) was added to the reaction with no observable exotherm or color change. This was cooled to 0 ℃ under an argon atmosphere. Separately, carbooxybenzoyl chloride (Cbz-Cl) (1.131 g, 1.002 mL, 1.05 Eq., 6.629 mmol) was added to a scintillation vial and dissolved in 20 mL of anhydrous DCM. The Cbz-Cl solution was then added to the round bottom flask over a period of thirty minutes *via* syringe pump. No color change or exotherm was observed. This was left to stir under an atmosphere of static argon for 16 hours.

After 16 hours, the reaction was transferred to a separatory funnel where the organic layer was washed once with brine. The organic layer was collected, dried with anhydrous magnesium sulfate, filtered, and concentrated under vacuum. The material was further purified using a KP-Sil 100 g column with a gradient of 10-100% ethyl acetate against hexanes and a dry load technique. Fractions of pure product were concentrated under vacuum to yield **1** as yellow oil with a mass of 1.566 g (80% yield). ^{1}H NMR (400 MHz, CD_3CN) δ 7.40 – 7.26 (m, 5H), 5.38 (s, 1H), 5.07 (s, 2H), 3.31 (t, J = 6.1 Hz, 2H), 3.16 (q, J = 6.1 Hz, 2H), 2.88 (d, J = 8.4 Hz, 3H),

1.37 (s, 9H). ^{13}C NMR (101 MHz, CD_3CN) δ 170.68, 156.18, 137.44, 128.43, 127.78, 127.53, 78.27, 66.49, 59.98, 27.64, 20.17, 13.54

Synthesis of **2**

Procedure:

1 (1.5 g, 1 Eq., 4.9 mmol) was dissolved in 5 mL of DCM in a scintillation vial charged with a stir bar, creating a clear solution. TFA (3.9 g, 2.6 mL, 7 Eq., 34 mmol) was added to the solution, forming a light-yellow color with CO_2 evolution. This was stirred under ambient conditions for 15 minutes. Gas evolution continued for 3-5 minutes.

After 15 minutes, the reaction was concentrated under a stream of air to remove the TFA and DCM. Once all the solvent was removed, 20 mL of diethyl ether was added, and the vial was mixed, immediately forming a white suspension. This was cooled down and centrifuged, then the supernatant was decanted off. This material was triturated once more with diethyl ether (20 mL), and the vial was centrifuged, and the supernatant was decanted off, leaving a white solid. This was concentrated under vacuum to yield a white solid with a mass of 0.73 g (72% yield). ^{1}H NMR (400 MHz, CD_3CN) δ 7.42 – 7.27 (m, 5H), 5.09 (s, 2H), 3.52 (s, 2H), 3.11 (s, 2H), 2.90 (s, 3H).

Synthesis of Ac-AAK Peptide **(3)** From Resin

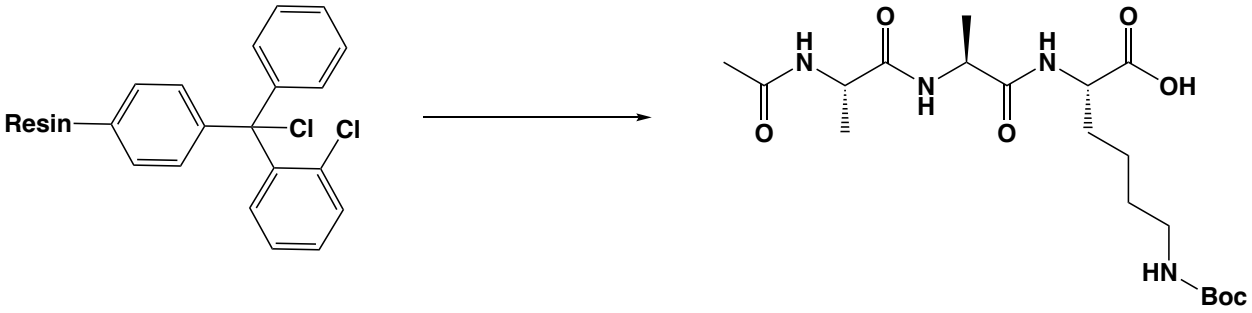

Procedure:

2.00 g (0.21 mmol/g resin) of 2-chlorityl chloride resin was swelled in DCM for one hour on the peptide shaker inside a 25 mL syringe.

Afterwards, DCM was removed from the syringe and the resin was rinsed once with DCM. Fmoc-Lys(Boc)-OH (857 mg, 3 Eq.,1.83 mmol) was dissolved in 5 mL of NMP and 5 mL of DCM, then DIPEA (473 mg, 0.638 mL, 6 Eq., 3.66 mmol) was added to the scintillation vial. This mixture was added slowly to the resin which evolved some gas (HCl). The syringe was then vented twice to remove HCl after slow manual shaking. The syringe was then put on the peptide shaker for 60 minutes.

The resin was rinsed with DCM, DMF, DCM, MeOH, and finally DCM twice. 8 mL of 20% 4-methylpiperidine in DMF was then added to the syringe and shaken for 15 minutes to remove the Fmoc protecting group. This step was repeated to ensure quantitative deprotection of the Fmoc group.

The resin was rinsed with DCM, DMF, DCM, MeOH, and finally DCM. Fmoc-Ala-OH (570 mg, 3 Eq., 1.83 mmol) and HATU (694 mg, 3 Eq.,1.83 mmol) were dissolved in 10 mL of NMP, then DIPEA (473 mg, 0.638 mL, 6 Eq., 3.66 mmol) was added to the scintillation vial. This mixture was added to the resin, which was then put on the shaker for 45 minutes. This step was repeated to ensure quantitative coupling.

The resin was rinsed with DCM, DMF, DCM, MeOH, and finally DCM. 8 mL of 20% 4-methylpiperidine in DMF was then added to the syringe and shaken for 15 minutes to remove the Fmoc protecting group. This step was repeated to ensure quantitative deprotection of the Fmoc group.

The resin was rinsed with DCM, DMF, DCM, MeOH, and finally DCM. Ac-Ala-OH (240 mg, 3 Eq., 1.83 mmol) and HATU (694 mg, 3 Eq.,1.83 mmol) were dissolved in 10 mL of NMP, then DIPEA (473 mg, 0.638 mL, 6 Eq., 3.66 mmol) was added to the scintillation vial. This mixture was added to the resin, which was then put on the shaker for 45 minutes. This step was repeated to ensure quantitative coupling.

The resin was rinsed with DCM, DMF, DCM, MeOH, and then DCM 5 times. Then, ~ 10 mL of 20% HFIP in DCM was added to the syringe and shaken for about 30 seconds. Upon addition of this solution to resin, the resin turned red. The solution of the peptide was then eluted into a 100 mL round bottom flask. This process was repeated three times to ensure complete resin cleavage. The solution was concentrated under vacuum until only a few mL of peptide solution remained. This was then precipitated into 45 mL 1:1 hexanes:diethyl ether. A white product immediately crashed out, so this was centrifuged, and the supernatant was decanted off, leaving a white solid behind. This was then transferred to a scintillation vial using 8 mL of 3:1 chloroform-methanol and concentrated under vacuum to yield a white solid with a mass of 108 mg (41% yield). ESI-MS calculated for $C_{19}H_{35}N_4O_7$ [M+H] Expected: 431.43; Observed: 431.25

Synthesis of **4**

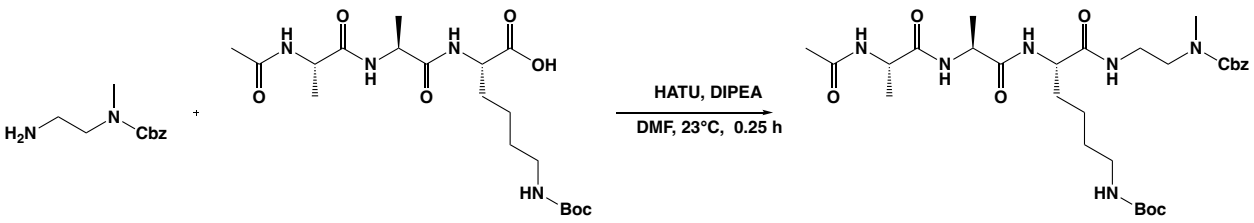

Procedure:

3 (99.75 mg, 1 Eq., 0.2317 mmol) and HATU (105.7 mg, 1.2 Eq., 0.237 mmol) were added to a 20 mL scintillation vial and dissolved in 3 mL of DMF. To this clear solution was added DIPEA (179.7 mg, 0.242 mL, 6 Eq., 1.390 mmol), which turned the solution to a yellow color. This solution was stirred for 15 minutes to activate the carboxylic acid.

After activation, benzyl **2** (2-aminoethyl)(methyl)carbamate (57.91 mg, 1.2 Eq., 0.278 mmol) was added as a solid to the scintillation vial with no observable color change or exotherm. The solution retained its yellow color and was allowed to stir at 23 ℃ for 15 minutes.

After 15 minutes, the crude reaction was analyzed by analytical HPLC to show that the product has formed (Note: previously synthesized standards of this reaction were used to compare with the crude reaction). The reaction was concentrated under vacuum, and the crude product was re-dissolved in 4 mL of 50/50 acetonitrile/water with 0.1% TFA and filtered to be purified by prep HPLC with a 1 mL injection and a gradient of 10-100% acetonitrile against water. The highlighted peak below corresponds with the fraction that was collected. These fractions were collected, concentrated under vacuum and lyophilized to yield a white solid with mass 30 mg (21% yield). ESI-MS calculated for $C_{30}H_{49}N_6O_8$ [M+H] Expected: 621.3428 Observed: 621.35.

Synthesis of **5**

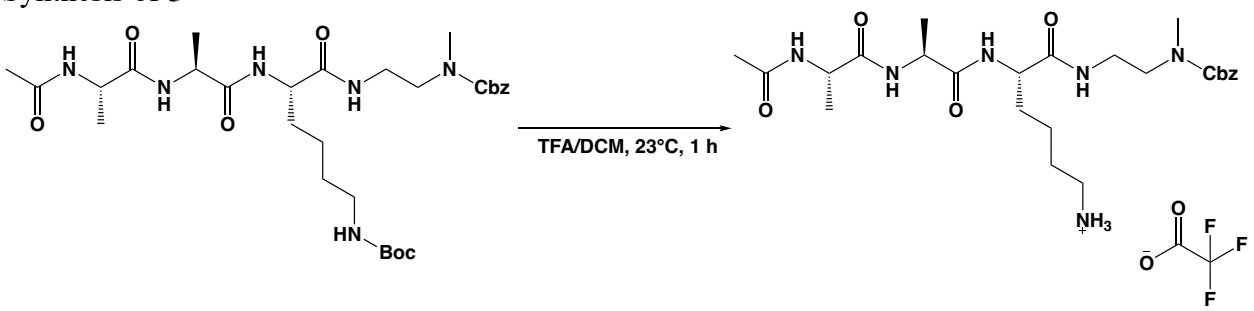

Procedure:

4 (30 mg, 1 Eq, 0.048 mmol) was dissolved in scintillation vial with 0.5 mL of 1:1 DCM/TFA, forming a pale-yellow solution. This was left to stir at 23 ℃ for one hour. After one hour, the crude reaction was concentrated under vacuum. At this point, the material was precipitated in 20 mL of cold diethyl ether, and the solution immediately became white and opaque. The scintillation vial was centrifuged, and the supernatant was decanted off. The resulting product was concentrated under vacuum to yield a white solid with a mass of 30 mg (> 99% yield). ESI-MS calculated for $C_{25}H_{40}N_6O_5$ [M+H] Expected: 521.3082; Observed: 521.32.

Synthesis of **6**

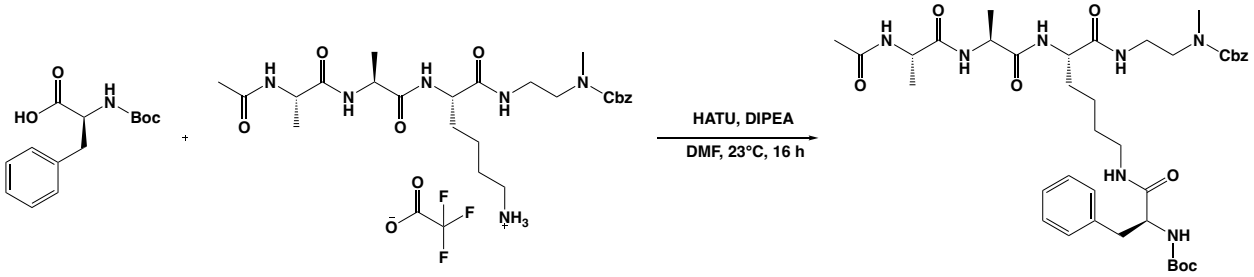

Procedure:

Boc-Phe-OH (22.9 mg, 1.5 Eq., 0.0863 mmol) and HATU (32.8 mg, 1.5 Eq., 0.0863 mmol) were added as solids to a dram vial charged with a stir bar. This was dissolved in 0.5 mL of DMF, then DIPEA (29.7 mg, 0.041 mL, 4 Eq., 0.230 mmol) was added to the flask, turning the solution a bright yellow color. This was left to stir for 15 minutes at room temperature. Separately, **5** (30.0 mg, 1 Eq., 0.0575 mmol) was dissolved in 0.5 mL of DMF then additional DIPEA (29.7 mg, 0.041 mL, 4 Eq, 0.230 mmol) was added to the flask, forming a pale-yellow solution. After 15 minutes of activation, the activated carboxylic acid solution was transferred to the amine solution and was left to stir at 23 ℃. After 16 hours, a sample of the crude mixture was analyzed by HPLC comparing to a pure product standard that was prepared previously. The concentrated crude product was then re-dissolved in 3 mL of 50/50 acetonitrile/water with 0.1% TFA and subsequently purified by prep HPLC with a 1 mL injection and a gradient of 10-100% acetonitrile against water. The highlighted peak below corresponds with the fraction that was collected. These fractions were collected, concentrated under vacuum, and lyophilized to yield a white solid with a mass of 44 mg (> 99 % yield). ESI-MS calculated for $C_{39}H_{58}N_7O_9$ [M+H] Expected: 768.4217; Observed: 768.44.

Synthesis of **7**

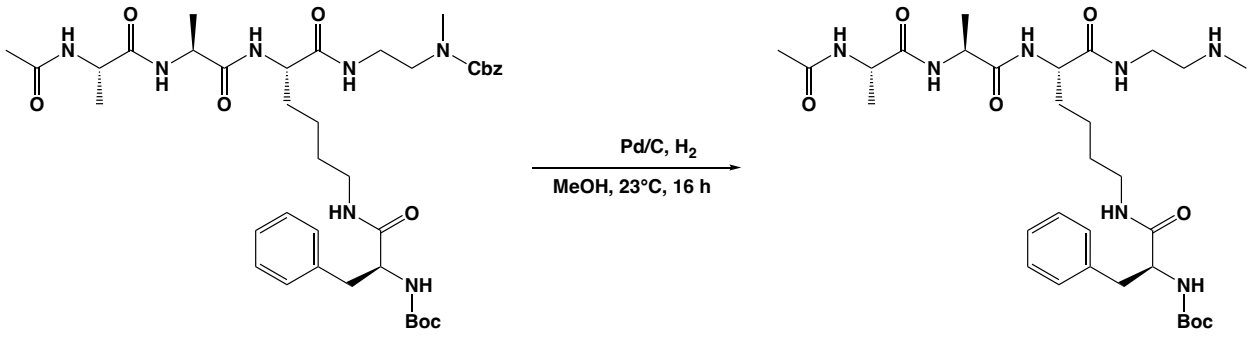

6 (44 mg, 1 Eq., 0.057 mmol) was added to a flame dried 100 mL round bottom flask charged with a stir bar and dissolved in 15 mL of methanol. To this pale-yellow solution was added palladium on carbon (3.0 mg, 0.5 Eq., 0.029 mmol, 10 wt% Pd), turning the reaction mixture black. The round bottom flask was sparged with argon for 15 minutes before putting the flask under a hydrogen atmosphere *via* H_2 balloon. The flask was sparged with an H_2 balloon until it was empty, then the balloon was refilled. The process was repeated two more times, then the balloon was refilled and left under a hydrogen atmosphere at room temperature for 16 hours. After 16 hours, a sample of the crude reaction mixture was analyzed by HPLC to determine the starting material conversion to product. At 16 hours, it appears that less than 50% of starting material was converted to product. Due to this, reaction was allowed to proceed for an additional 16 hours. At 32 hours, another sample of the crude reaction mixture was analyzed by HPLC to determine starting material conversion to product. However, only 50% conversion was observed. An additional amount of palladium on carbon (3.0 mg, 0.5 Eq., 0.029 mmol, 10 wt% Pd) was added to the solution, sparged with argon for 10 minutes, sparged with hydrogen, and subsequently left under hydrogen atmosphere for another 16 hours. At 48 hours, a sample of the crude mixture was analyzed on HPLC, which contained no residual starting material.

Palladium was removed by passing the reaction mixture through a 1 μm PTFE syringe filter. Then the solvent was removed under vacuum. The concentrated crude product was then re-dissolved in 2 mL of 50/50 acetonitrile/water with 0.1% TFA and purified by prep HPLC with a 1 mL injection and a gradient of 10-100% acetonitrile against water. The fractions containing the product were collected, concentrated under vacuum, and lyophilized to yield a white solid with a mass of 36 mg (> 99% yield). ESI-MS calculated for $C_{31}H_{52}N_7O_7$ [M+H] Expected: 634.3850; Observed: 634.40.

Synthesis of **8**

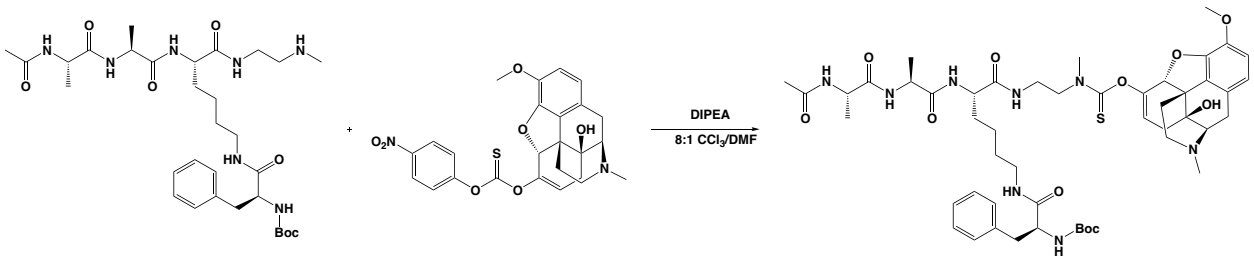

Procedure:

7 (33 mg, 1 Eq, 0.044 mmol) was added to a one neck, 25 mL round bottom flask charged with a stir bar. The peptide was dissolved in 2.5 mL of chloroform and 0.5 mL of DMF. DIPEA (57 mg, 0.077 mL, 10 Eq, 0.44 mmol) was added to the solution, keeping the color intact. This was allowed to stir at room temperature for five minutes.

Separately, a sample of O-((4R,4aS,7aR,12bS)-4a-hydroxy-9-methoxy-3-methyl-2,3,4,4a,5,7a-hexahydro-1H-4,12-methanobenzofuro[3,2-e]isoquinolin-7-yl) O-(4-nitrophenyl) carbonothioate (24 mg, 1.1 Eq, 0.049 mmol) (provided by my colleague Billy Treacy) was weighed out in a dram vial and dissolved in 1 mL of chloroform. After the five minutes was over, the electrophile was added dropwise over a minute to the peptide, forming a golden solution. The dram vial was then washed twice with 1 mL of chloroform, which was added to the round bottom flask. The reaction was allowed to stir at 23 ℃ for 16 hours.

Afterwards, the reaction was concentrated under vacuum to remove the chloroform. The solution was then precipitated into 45 mL of cold 1:1 hexanes/diethyl ether. This was centrifuged to leave a brown solid with mass of 16 mg (37% yield), which was used directly in the next step with no further purification.

Synthesis of BT-2-61L

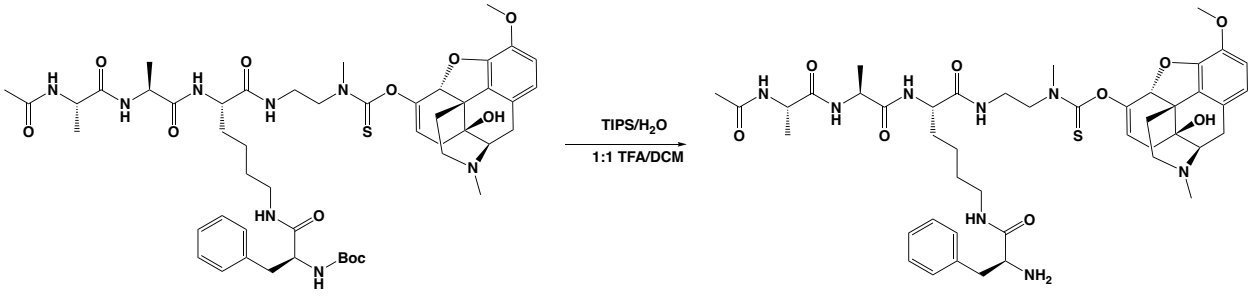

Procedure:

8 was dissolved in 10 mL of 1:1 TFA/DCM and transferred to a scintillation vial, forming a pale-yellow solution. 0.25 mL of water and 0.25 mL of TIPS were added to the vial with no discernible color change. The reaction was left to stir at 23 ℃.

After an hour, the reaction was concentrated under vacuum. The contents of the reaction were filtered through an HPLC filter and diluted with 4 mL of 1:1 acetonitrile/water with 0.1% TFA and purified by prep HPLC with a 1 mL injection and a gradient of 10-100% acetonitrile against water. The product fractions were collected, concentrated under vacuum, and lyophilized to yield a white solid mass of 15.14 mg (> 90% yield). ESI-MS calculated for $C_{45}H_{63}N_8O_9S$ [M+H] Expected: 891.44; Observed: 891.45.